NOVA SCHOOL OF SCIENCE & TECHNOLOGY

DEPARTAMENT OF CHEMISTRY

NUTRIENT REMOVAL BY A MICROALGAL-BACTERIAL CONSORTIUM AS A MEANS TO REDUCE THE AERATION DEMAND IN WASTEWATER TREATMENT

DISSERTATION SUBMITTED IN FULFILMENT OF THE REQUIREMENTS FOR THE DEGREE OF DOCTOR (PhD) IN SUSTAINABLE CHEMISTRY

VIRGÍNIA DA CONCEIÇÃO FERNANDES DE CARVALHO

Master in Biological Engineering

DOCTORAL PROGRAMME IN SUSTAINABLE CHEMISTRY

NOVA University Lisbon

September, 2021

NOVA SCHOOL OF SCIENCE & TECHNOLOGY

DEPARTAMENT OF CHEMISTRY

NUTRIENT REMOVAL BY A MICROALGAL-BACTERIAL CONSORTIUM AS A MEANS TO REDUCE THE AERATION DEMAND IN WASTEWATER TREATMENT

VIRGÍNIA DA CONCEIÇÃO FERNANDES DE CARVALHO

Master in Biological Engineering

DOCTORAL PROGRAMME IN SUSTAINABLE CHEMISTRY

NOVA University Lisbon

September, 2021

DEPARTAMENT OF CHEMISTRY

NUTRIENT REMOVAL BY A MICROALGAL-BACTERIAL CONSORTIUM AS A MEANS TO REDUCE THE AERATION DEMAND IN WASTEWATER TREATMENT

DISSERTATION SUBMITTED IN FULFILMENT OF THE REQUIREMENTS FOR THE DEGREE OF DOCTOR (PhD) IN SUSTAINABLE CHEMISTRY

VIRGÍNIA DA CONCEIÇÃO FERNANDES DE CARVALHO

Master in Biological Engineering

Adviser: Joana Costa Fradinho, Researcher, NOVA University Lisbon

Co-advisers: Maria d'Ascensão Miranda Reis, Full Professor, NOVA University Lisbon

Adrian Michael Oehmen, Senior Lecturer, The University of Queensland

Examination Committee:

Chair: Susana Filipe Barreiros
Full Professor, FCT-NOVA

Rapporteurs: Raúl Muñoz Torre
Full Professor, Universidade de Valladolid,
Albert Guisasola Canudas
Professor Agregat, Escola d´Enginyeria, Universitat Autònoma de Barcelona

Adviser: Joana Costa Fradinho
Researcher, NOVA University Lisbon

Members: José António Couto Teixeira
Full Professor, Universidade do Minho
Ana Luísa Almaça da Cruz Fernando
Associated professor, NOVA University Lisbon

DOCTORATE IN SUSTAINABLE CHEMISTRY

NOVA University Lisbon
September, 2021

NOVA SCHOOL OF SCIENCE & TECHNOLOGY

DEPARTAMENT OF CHEMISTRY

NUTRIENT REMOVAL BY A MICROALGAL-BACTERIAL CONSORTIUM AS A MEANS TO REDUCE THE AERATION DEMAND IN WASTEWATER TREATMENT

VIRGÍNIA DA CONCEIÇÃO FERNANDES DE CARVALHO

Master in Biological Engineering

Adviser: Joana Costa Fradinho, Researcher, NOVA University Lisbon

Co-advisers: Maria d'Ascensão Miranda Reis, Full Professor, NOVA University Lisbon

Adrian Michael Oehmen, Senior Lecturer, The University of Queensland

Examination Committee:

Chair: Susana Filipe Barreiros
Full Professor, FCT-NOVA

Rapporteurs: Raúl Muñoz Torre
Full Professor, Universidade de Valladolid,
Albert Guisasola Canudas
Professor Agregat, Escola d´Enginyeria, Universitat Autònoma de Barcelona

Adviser: Joana Costa Fradinho
Researcher, NOVA University Lisbon

Members: José António Couto Teixeira
Full Professor, Universidade do Minho
Ana Luísa Almaça da Cruz Fernando
Associated professor, NOVA University Lisbon

DOCTORATE IN SUSTAINABLE CHEMISTRY

NOVA University Lisbon
September, 2021

Nutrient removal by a microalgal-bacterial consortium as a means to reduce the aeration demand in wastewater treatment

Para os meus familiares e amigos
que caminharam ao meu lado
nesta aventura

ACKNOWLEDGMENTS

This thesis has been one of the most fulfilling adventure in my professional life and I am very glad that I am able to close a chapter that was not always easy. When I look back, I remember years of hard work, frustration, lots of insecurities but also fun, valuable experiences and happy memories.

Yet, I would not have made it this far without the help of several people. First, I would like to thank my supervisors Joana, Maria and Adrian for always supporting and guiding me through this period. Adrian, I really appreciate your effort to overcome the limitation of the time difference and to be always available to meet at late hours.

I cannot forget all my colleagues of Bioeng that make my days shinier, especially Elsa, Elisabete, Soraia, Paulo, Rita, Joana M., Catarina and Rafaela. A big thanks to my favorite Serbian girl, Srdjana, with whom I share endless conversations and fruitful discussions about work and life.

To my friends of "revenge of 80's", our WhatsApp group that was many times my " breath of fresh air", where our conversations and shared experiences, even with thousands of kilometers of distance, always pushed me up.

Diana, Salomé and Isabel thank you for your friendship and your words on the right moment.

Last, but not least, a big thank you to my family that always supported and helped me and will always be my safe haven.

Nothing of this would be possible without the FCT funding PD/BD/114574/2016 and NOVA University of Lisbon.

I am looking forward to new adventures in the future.

Para ser grande, sê inteiro: nada
Teu exagera ou exclui.
Sê todo em cada coisa. Põe quanto és
No mínimo que fazes.
Assim em cada lago a lua toda
Brilha, porque alta vive.

Ricardo Reis (1933)

ABSTRACT

Nutrient runoff leads to serious environmental problems, such as eutrophication, that reduces water quality and unbalances aquatic habitats. Biological treatment of wastewaters reduces the need of the use of harmful and expensive chemicals and allows the recovery and upcycling of nutrients from wastewaters, consistent with the circular economy concept. Phosphorus removal is normally performed by enhanced biological phosphorus removal systems (EBPR), while the simultaneous removal of phosphorus and nitrogen is performed using biological nutrient removal (BNR) systems. Due to the need of aeration to promote nutrient removal, this treatment method requires huge energy costs. Microalgal-bacterial consortia are a sustainable alternative to BNR systems, as they are independent of mechanical aeration since the necessary oxygen for heterotrophic bacteria is photosynthetically produced.

A sludge enriched in *Accumulibacter* was subjected to dark (anaerobic) – light (aerobic) cycles and a microalgal-bacterial consortium was selected, with a capacity to remove up to 64 mg P/L. This photosynthetic EBPR system was capable of removing high amount of phosphorus with no need of aeration and under low COD:P ratio (200:60).

To test the effect of seed sludge on the selection of the photosynthetic EBPR system, fresh activated sludge was used as a reactor inoculum that operated in the same dark (anaerobic) – light (aerobic) conditions. This start-up strategy showed that a microalgal-bacterial consortium that performs photo-EBPR could be selected independently of the seed sludge. A higher enrichment of the biomass in *Accumulibacter* is correlated with faster selection: 14 days when *Accumulibacter* sludge was inoculated as opposed to 29 days with real activated sludge.

Since wastewater treatment plants require simultaneous phosphorus and nitrogen removal, a sequencing batch reactor was operated in dark (anaerobic) – light (aerobic) – dark (anoxic) conditions to promote nitrogen removal. The selected microalgal-bacterial consortium was able to remove 25 ± 9.2 mg P/L and 38 ± 0.92 mg N/L with a COD:N:P ratio of 300:40:60. The main mechanisms of nutrient removal were phosphorus accumulation as polyphosphate by polyphosphate accumulating organisms and nitrogen removal by biomass assimilation, since 33 ± 5% of ammonia was converted to nitrate through nitrification, which was further removed by denitrification during the dark anoxic phase. Raman spectrometry showed to be a potential tool for a real-time monitoring of the photo-BNR system, offering a faster alternative to laborious standard analytical methods.

To understand the key operational parameters of the photosynthetic BNR system, a reactor was operated over 260 days, where the impact of light period duration and carbon dioxide concentration were tested. Results indicated that the nutrient removal efficiencies of the microalgal-bacterial consortium were enhanced by higher periods of light exposition, rather than higher availability of CO_2.

The photosynthetic biological nutrient removal system opens the possibility to reduce the costs of wastewater treatment and has the potential to be a more sustainable wastewater treatment alternative.

Key words: Nutrient removal; photosynthetic systems; microalgal-bacterial consortium; circular economy; energetic efficiency.

RESUMO

A libertação de efluentes com alta concentração de nutrientes gera problemas ambientais, como é o caso da eutrofização, reduzindo a qualidade da água e alterando os habitats aquáticos. O tratamento biológico de águas residuais é associado a um menor impacto ambiental, uma vez que reduz a necessidade de uso de químicos perigosos e dispendiosos e possibilita a recuperação de nutrientes das águas residuais e posterior reciclagem, respeitando o conceito de economia circular. A remoção de fósforo é normalmente feita por sistemas de remoção de fósforo melhorada (EBPR), enquanto a remoção simultânea de fósforo e azoto é feita em sistemas de remoção biológica de nutrientes (BNR). Devido às necessidades de arejamento para promover a remoção de nutrientes, este tipo de método exibe custos elevados devido ao consumo energético. Os consórcios de microalgas e bactérias são alternativas mais sustentáveis aos processos convencionais, uma vez que mostram ter grande capacidade de remoção e não tem uma dependência do arejamento mecânico, sendo o oxigénio necessário para as bactérias heterotróficas fotossinteticamente produzido pelas microalgas.

Uma lama enriquecida em *Accumulibacter* foi sujeita a ciclos de escuro (anaeróbio) - luz (aeróbio), sendo possível selecionar um consorcio de microalgas e bactérias capaz de remover até 64 mg P/L. Este EBPR fotossintético foi capaz de remover grandes concentrações de fósforo sem necessidade de arejamento e com baixa razão COD:P (200:60).

De forma a testar o efeito do inóculo na seleção do EBPR fotossintético, um reator foi inoculado com lamas ativadas frescas e operado nas mesmas condições escuro (anaeróbio) – luz (aeróbio). Esta estratégia de enriquecimento mostrou que um consorcio de microalgas e bactérias, capaz de fazer EBPR fotossintético, consegue ser selecionado independentemente do inóculo usado, contudo, quanto mais enriquecida a biomassa for em *Accumulibacter* mais rápido o processo de seleção: 14 dias quando usado lamas enriquecidas em *Accumulibacter* contra 29 dias quando usado lamas ativadas.

Uma vez que as estações de tratamento de água requerem a remoção simultânea de fósforo e azoto, o ATU foi removido do meio e o reator foi operado em condições de escuro (anaeróbio) – luz (aeróbio) – escuro (anóxico) de forma a promover a remoção de azoto. O consorcio de microalgas e bactérias selecionado foi capaz de remover 25 ± 9.2 mg P/L e 38 ± 0.92 mg N/L com uma razão COD:N:P de 300:40:60. Os principais mecanismos de remoção de nutrientes foram acumulação de polifosfato pelos organismos acumuladores de fósforo e remoção de azoto por assimilação pela biomassa, sendo que 33 ± 5% da amónia foi convertida em nitratos, via nitrificação, que foram posteriomenre removidos por desnitrificação na fase de escuro anóxica. A espectrometria de Raman mostrou ser uma ferramenta promissora para uma monitorização em *real-time* dos sistemas BNR, oferecendo uma alternativa mais rápida às análises laboratoriais convencionais.

De forma a perceber os parâmetros chave na seleção de um BNR fotossintético, um reator foi operado durante 260 dias, no qual foi testado o impacto de diferentes tempos de

exposição à luz e concentrações de dióxido de carbono. Os resultados indicaram que o tempo de exposição solar melhora a capacidade de remoção de nutrientes deste consórcio de microalgas e bactérias, mais do que o aumento da concentração de CO_2.

Os sistemas fotossintéticos de remoção biológica de nutrientes abrem a possibilidade de reduzir os custos do tratamento de águas residuais e aparentam ser uma alternativa mais sustentável.

Palavras chave: Remoção de nutrientes; sistemas fotossintéticos; consórcios de microalgas e bactérias; economia circular; eficiência energética

TABLE OF CONTENTS

LIST OF FIGURES

LIST OF TABLES

LIST OF EQUATIONS

1. INTRODUCTION

1.1. Nitrogen and Phosphorus Nutrient Pollution

Nitrogen (N) and phosphorus (P) are nutrients that can be naturally found in aquatic ecosystems, however, when in excess, they unbalance the ecosystems, triggering severe environmental problems. In particular, the discharge of waste streams with high phosphorus and nitrogen concentrations, in the form of phosphates, ammonia, nitrates or nitrites, can cause eutrophication of rivers, lakes and oceans (Dai et al., 2021; Fallahi et al., 2021).

Natural lakes and reservoirs are considered eutrophic when N and P concentrations exceed 0.2 mg/L and 0.02 mg/L, respectively (Dai et al., 2021). Eutrophication reduces water and food resources quality and deteriorate habitats by decreasing oxygen availability that fish and other aquatic species need to survive. It also unbalances the natural life environments, or even cause toxic emissions of CO_2, H_2S and CH_4 (Izadi et al., 2020; Raschke, 1993). Eutrophication mostly results from anthropogenic activities (Dalu et al., 2019; Wang et al., 2019): agriculture, by the intensive use of chemical fertilizers; animal farming, by the generation of high amount of manure; aquaculture; urban and industrial sources, by the discharge of wastewaters, and fossil fuel sources (Camargo et al., 2005; Dai et al., 2021). In the worst scenario, besides climate change and reduction of water quality and availability, pollution caused by the release of high amount of nutrients could lead to biodiversity loss and the degradation of ecosystems and human health. Furthermore, the excess of nutrients also leads to economic problems and have a negative impact on the economic activities of the regions where it occurs. (Rajaniemi et al., 2021). In addition to that, food production through modern agriculture is highly reliant on the application of fertilizers containing N and P (Yang et al., 2017). If for one hand there are benefits that results from the fertilizers use, for the other hand, the pollution provoked by ammonia and nitrate release due to agriculture in the European Union (EU27) was estimated to cost 61–215 billion per year (Gu et al., 2021; van Grinsven et al., 2018), wherebby the European Union has been facing huge financial losses due to eutrophication (Gu et al., 2021). While ammonia is mainly produced from Haber-Bosh process, a high energy dependent process, the main source of P is the phosphate rock located in mines, mainly located in Morocco and China (Wei et al., 2018). The accessibility and quality of this rocks are limited (Wei et al., 2018) and, consequently, phosphate rock has been declared

in 2014 by the European Union as a critical raw material (Rossi et al., 2018) and some projections indicate that global phosphorus reserves could be exhausted in the next century (Yang et al., 2017). Around 80% of the extracted P is used in the production of fertilizers (Cederberg, 2010; Sengupta et al., 2015).

The P and N that are consumed by animals and humans are released with the excreta and discharged into sewage systems as wastewater. In the last years, the environmental crisis has become an urgent social problem in specific areas and engaged a wide variety of stakeholders with different values and interests (Le Moal et al., 2019). Therefore, it is fundamental to optimize wastewater treatment plants (WWTP), not only by increasing the treatment efficiency, but also by adopting more sustainable approaches, where valuable resources from waste could be recycled and upcycled (Wei et al., 2018). In terms of sustainable nutrient management, the nutrient concentration in the effluent must fulfill the discharge standards, to improve water quality and reduce the economic impact of pollution. In addition, the generated sludge produced during treatment must be valorized and used for fertilizer production, for example (Dai et al., 2021; van Grinsven et al., 2018; Wei et al., 2018). In Europe, these discharge limits are regulated by the normative 91 /271 /EEC and 98/15/CE (European Commission), which limits the total P concentration in the effluent to 2 mg P/L, for a population equivalent between 10 000 and 100 000, or 1 mg P/L, for a population equivalent higher than 100 000. In the case of N, the total concentration limit was fixed to 15 mg N/L, for a population equivalent between 10 000 and 100 000, or 10 mg N/L for a population equivalent higher than 100 000.

1.2. Nutrient Removal Processes

To accompany the population growth and societal development, the wastewater sector has developed and implemented new technologies, thus increasing the efficiency of wastewater treatment (WWT). Activated sludge, probably the most used WWT technique during secondary treatment for nutrient removal, was developed in 1914 (Pell and Wörman, 2011).

Nowadays, WWT is focused on removing a wide range of pollutant, among them P and N are the frequent target compounds, since these elements contribute to eutrophication and deterioration of our natural water ecosystems. P and N removal can be performed by chemical, biological methods or by the combination of both (Pell and Wörman, 2011). The chemical and biological nutrient removal process is typically performed separately, since integrating both processes often leads to problems with optimizing each single process (Henze and Harremoës, 1990).

Chemical precipitation of P normally occurs by addition of aluminum, iron or lime precipitant, which causes the precipitation of insoluble P. Although this process shows removal efficiencies of P that could be higher than 90%, it increases the cost of treatment due to the cost of the chemical precipitants and to the increased waste sludge that needs to be disposed. Furthermore, chemical precipitation negatively impacts the forthcoming sludge treatment by

anaerobic digestion, generating less biogas and methane during the anaerobic digestion process. Moreover, it also reduces the potential of P recovery from the sludge or even the direct use of treated sludge as fertilizer (Izadi et al., 2020; Rajaniemi et al., 2021).

Ammonium ions do not easily precipitate and methods such as adsorption, air stripping, membrane separation or biological methods should be employed (Rajaniemi et al., 2021), like assimilation, nitritation/anammox (a promising but difficult process to control) or nitrification/denitrification processes (Kuypers et al., 2018). The latter is most typically employed, but requires extensive aeration for nitrification, while external organic carbon is required for heterotrophic denitrification, which can also be very dispendious (Kuypers et al., 2018). Nitrification takes place by a two-step process catalyzed by chemolithoautotrophic microorganisms. First by the oxidation of ammonia into nitrite, by ammonia oxidizing bacteria (AOB), and then nitrite into nitrate, by the nitrite oxidizing bacteria (NOB), in the presence of electron acceptor (oxygen) (Arp and Stein, 2003; Izadi et al., 2020) (**Figure 1.1**). All AOB contain *AMO* and *HAO* genes, however, some microorganisms (*Nitrospira* spp) also contains *nxr* genes and can oxidize ammonia all the way to nitrate (**Figure 1.1**) (Daims et al., 2015; Kuypers et al., 2018; van Kessel et al., 2015). Denitrification occur in anoxic conditions where nitrate is converted into nitrogen gas (N_2), if the process is complete (Kuypers et al., 2018). The first step is the nitrate reduction to nitrite that is catalyzed by either a membrane-bound nitrate reductase (*nar*) or periplasmic nitrate reductase (*nap*) genes, then, a series of reactions need to occur to obtain the final product of denitrification, N_2 (**Figure 1.1**) (Kuypers et al., 2018; Arp and Stein, 2003; Izadi et al., 2020). Conventional nitrogen removal has high cost, is energy and resource demanding and could produces nitrous oxide, contributing to global warming (Kuypers et al., 2018).

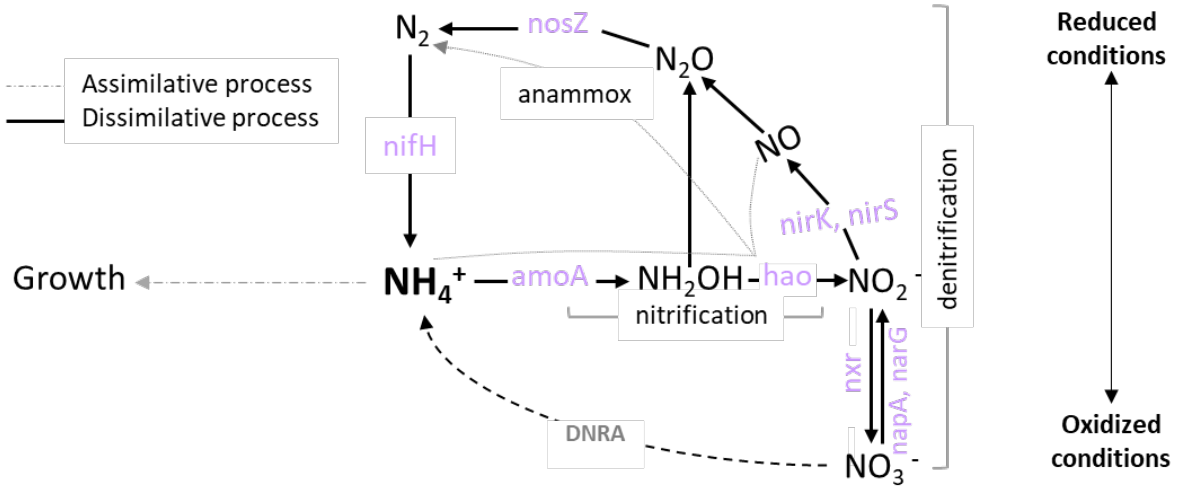

Figure 1.1 - The nitrogen cycle.
(anammox - anaerobic ammonia oxidation; DNRA - dissimilatory nitrate reduction to ammonium. The genes involved are presented in purple (Adapted fromm Levy-Booth et al., 2014)).

Phosphorus can also be removed from wastewaters by biological methods, such as enhanced biological phosphorus removal (EBPR) processes and algal systems (Bunce et al., 2018). Therefore it would be beneficial to couple N and P removal, by combining nitrification,

denitrification, and phosphorus removal in one single biological nutrient removal (BNR) system (Chen et al., 2021).

BNR processes are composed by anaerobic, aerobic and anoxic tanks, where sludge is recirculated (Izadi et al., 2021) to provide the operational conditions required to select polyphosphate accumulating organisms (PAOs), along with nitrogen removing organisms for nitrification (AOB and NOB) and denitrification (Izadi et al., 2021; Zhu et al., 2008). Overall, BNR implies the combination of biological N removal with EBPR process.

In EBPR systems, PAOs have a fundamental role, by consuming the volatile fatty acids (VFAs) in anaerobic conditions and accumulating polyhydroxyalkanoates (PHAs). The energy (ATP) for PHA accumulation is provided from glycogen and poly-phosphate (poly-P) hydrolysis, and further release of phosphate. The reducing power (NADH) needed comes from glycogen degradation and tricarboxylic acid (TCA) cycle (Oehmen et al., 2005b; Smolders et al., 1994b). During the aerobic period, P is removed from the bulk liquid, a step that requires ATP and NADH. PHA consumption and oxidative phosphorylation, a reaction oxygen dependent, provides enough ATP and NADH for P uptake, and further poly P accumulation inside the cells, glycogen replenishment and biomass growth (Oehmen et al., 2007b; Smolders et al., 1994a, 1995) (**Figure 1.2**). PAOs are known for their ability to uptake high concentrations of phosphorus, higher than the metabolic necessities for growth, accumulating the excess P as poly-P reserves. Due to the high P content, the sludge generated during the treatment process could be used for P recovery and bring economic benefits to the WWTP and environmental benefits for society (Gutierrez et al., 2020; Yang et al., 2017).

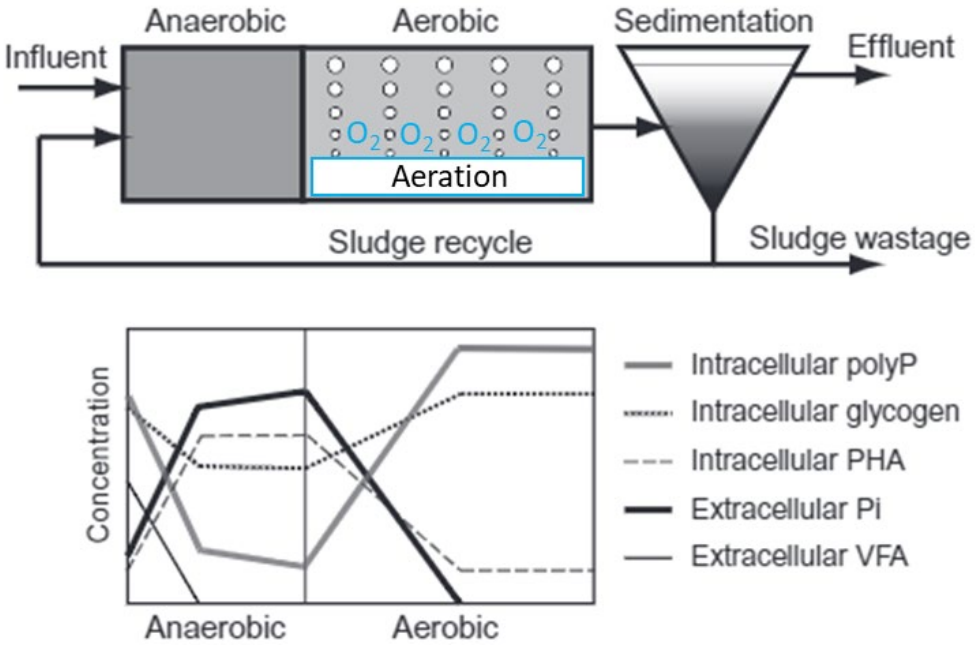

Figure 1.2 - Schematic representation of a conventional EBPR process with an anaerobic/aerobic configuration and the corresponding characteristic profile of a sludge fed with VFAs during an EBPR cycle.
(Adapted from He and Mcmahon, 2011).

PAOs phenotype includes a wide variety of bacteria that are characterized by the high capacity of P uptake, by accumulating excess P removal as poly-P. Although the proteobacteria *Candidatus* Accumulibacter, closely related to *Rhodocyclus* genus, has been assumed to be the most important PAO in EBPR systems, the Actinobacteria *Tetrasphaera* has also been shown to display an important role, contributing to P removal in EBPR systems. Actually, *Tetrasphaera* seems to be more versatile than *Accumulibacter* with regards to the range of organic carbon sources that it can consume, and could represent up to 30 % of the total bacteria in EBPR plants (Kong et al., 2005; Marques et al., 2018, 2017; Nielsen et al., 2019; Yang et al., 2017).

Tetrasphaera is able to uptake carbon sources such as glucose and amino acids anaerobically and use the accumulated polymers as an energy source for aerobic P uptake and accumulation as poly-P. It is postulated that Tetrasphaera is not able to perform PHA cycling. Furthermore, while *Accumulibacter* is known for anaerobic glycogen consumption, *Tetrasphaera* could produce or consume it, depending on the carbon source (Kristiansen et al., 2013; Marques et al., 2018, 2017; Yang et al., 2017). When fed with glucose, in anaerobic conditions, *Tetrasphaera* related microorganisms ferment glucose and glycogen is produced and stored, using the energy from poly-P release and fermentation, while during aerobic conditions, the stored glycogen is degraded to provide carbon and energy for P uptake (and poly-P formation) and for growth (Kristiansen et al., 2013). When fed with acetate, propionate and/or a mixture of amino acids, glycogen is consumed anaerobically, followed by poly-P degradation and P release, while during the aerobic phase poly-P is formed and glycogen is produced using the energy from the stored carbon (amino acids) (Marques et al., 2018, 2017; Nguyen et al., 2011).

Some classes of PAOs are capable of using nitrate (NO_3^-) or nitrite (NO_2^-) as electron acceptor in the absence of oxygen, accomplished by the use of intracellular PHAs for simultaneous removal of N and P under anoxic conditions (Izadi et al., 2021). These microorganisms are called denitrifying PAOs (dPAOs) and several studies showed the capacity of PAO microorganisms, including both *Accumulibacter* and *Tetrasphaera,* to couple N and P removal (Camejo et al., 2016; Carvalho et al., 2007; Kong et al., 2005; Lanham et al., 2018a; Marques et al., 2018; Oehmen et al., 2010; Saad et al., 2016). The advantages of such a strategy is related with a lesser need for external carbon dosing (since organic carbon is normally limited in wastewater), reduced sludge production and lower energy costs (Chen et al., 2021; Saad et al., 2016).

Besides PAOs, other microorganisms can deeply impact the effectiveness of EBPR processes (Yang et al., 2017). Glycogen accumulating organisms (GAOs) are another group of bacteria that can compete with PAOs for anaerobic VFA uptake and obtain their energy for carbon uptake solely from the hydrolysis of glycogen (Oehmen et al., 2005a). These bacteria do not store poly-P and, consequently, their existence was for years generally associated to the failure of P-removal in EBPR systems (Lopez-Vazquez et al., 2009; Oehmen et al., 2007a; Rubio-Rincón et al., 2017; Shen and Zhou, 2016). However, recent studies have shown that GAOs could have a major importance in BNR systems, since different studies on mixed PAO-

GAO cultures suggest that GAOs, rather than PAOs, use nitrate as electron acceptor (Rubio-Rincón et al., 2017). Besides that, GAOs could also be important in the overall carbon and nutrient transformations (Nielsen et al., 2019). Indeed, these findings suggested that PAOs and GAOs may have more than a competitive relationship and the presence of both microorganisms could be partially syntrophic (Nielsen et al., 2019; Rubio-Rincón et al., 2017).

Generally, in BNR systems, PAOs are responsible for P removal and anoxic denitrification (dPAOs), while autotrophic AOBs and NOBs perform nitrification in aerobic conditions and denitrifying microorganisms perform denitrification, possibly forming nitrogen gas (N_2) if the denitrification process is complete (**Figure 1.1**) (Chen et al., 2021; Rajaniemi et al., 2021; Zeng et al., 2003; Zhao et al., 2018).

The use of BNR systems for nutrient removal allows nutrient recovery from wastewaters. This recovery is fundamental to satisfy the increasing agricultural phosphorus needs and is also an integral part of the sustainable P management needed to support future global nutrient demand, contributing to a circular economy. Furthermore, nutrients captured in stabilized biosolids can be directly employed in the fields in many countries, compensating for chemical fertilizers (Winkler and Straka, 2019; Yang et al., 2017). Sewage sludges show a strong potential for nutrient recovery and upcycling but face social and environmental barriers due to the possible presence of heavy metals, organic pollutants and pathogens, depending on the source of the wastewater and its treatment, as well as the sludge treatment (Das et al., 2020; Lam et al., 2020; Moinard et al., 2021; Seleiman et al., 2020). Because of that, sewage sludge needs to face an adequate treatment before land application as fertilizer (Das et al., 2020). There have been multiple efforts to optimizing the recovery of these nutrients by anaerobic digestion, struvite (a naturally crystal of magnesium, ammonium and phosphate) precipitation, incineration and P recovery from ashes (Bora et al., 2020; Seleiman et al., 2020).

Although BNR systems can achieve good treatment efficiencies, traditional BNR processes are very dependent on aeration, which increase the cost and environmental footprint of wastewater treatment systems. The energy required for aeration can comprise 45-75% of the total energy consumption in WWTP (Awe et al., 2016; Panepinto et al., 2016; Rosso et al., 2008). Furthermore, these systems are not appropriate for the treatment of wastewaters with low carbon:nutrient ratios (Feng et al., 2021; Yuan et al., 2020). Thus, to improve WWTP efficiency and water quality, it is of great interest to enhance the existing wastewater treatment processes and develop new low-energy and high-efficient processes (Dai et al., 2021). The implementation of photosynthetic systems can positively contribute to the so needed WWTP technology development.

1.3. Photosynthetic systems for nutrient removal

Wastewater treatment should be achieved using methods that do not undermine the environmental quality and human health. Phototrophic and photosynthetic organisms are a sustainable alternative, since they present high efficiencies in nutrients and carbon assimilation from wastewaters using the energy from light (Capson-Tojo et al., 2020). In addition, the

use of phototrophic and photosynthetic processes prevent carbon and nutrient dissipation, which typically occur in chemotrophic metabolism, working as an atmospheric CO_2 sink (Capson-Tojo et al., 2020). Light driven technologies for wastewater treatment could be divided into single systems of microalgae or phototrophic bacteria and microalgal - bacterial consortiums.

Phototrophic purple bacteria (PPB), probably the microorganisms with the most diverse metabolism, use the bacteriochlorophyll pigment to obtain energy from wavelengths (infrared) complementary to those that use chlorophylls (visible) - the oxygenic organisms (Fradinho et al., 2021). The use of PPB related technology for domestic wastewater treatment has been shown to be a good option for nutrient removal (Hülsen et al., 2016, 2013; Puyol et al., 2017). PPB are able to use the energy from light to recover nutrients through assimilation during cell growth, while extra ATP availability can be used for poly-P storage. This N and P assimilation are dependent on the amount of degradable COD, particularly VFAs (Fradinho et al., 2021; Hülsen et al., 2013; Puyol et al., 2017). The main disadvantage of using these microorganisms for nutrient removal is the high carbon requirement, which results in high C:N:P ratios that are usually not found in domestic wastewaters (Hülsen et al., 2013).

Microalgae and cyanobacteria are microorganisms, which in the presence of light and water, have the capacity of CO_2 assimilation and lipids, starch or glycogen accumulation, depending on the microorganism. Microalgae can also be heterotrophic and mixotrophic, which increase their tolerance to the usually stressful conditions in photosynthetic systems used for wastewater treatment, whilst contributing with their high metabolic versatility to remove pollutants (Torres-Franco et al., 2020). Many studies have reported the feasibility of applying microalgal technology in wastewater treatment, showing nutrient removal efficiencies as high as 95% (Alcántara et al., 2015b; de Godos et al., 2010; Posadas et al., 2015b; Ji et al., 2020; Kant et al., 2021;). The use of microalgae in wastewater treatment is advantageous since besides nutrient removal, it could simultaneously produce bioenergy, including biodiesel, biohydrogen, methane and bioelectricity, and reduce CO_2 concentration in the atmosphere (Kant et al., 2021). Nevertheless, in microalgae systems, the small cell size, low biomass concentration and densities similar to water result in a low settling velocity, which limits the cost-effectiveness of biomass recovery, and creates a hurdle for the use of microalgae technologies for wastewater treatment (Alcántara et al., 2015; Fallahi et al., 2021).

Some microalgae have the capacity of luxury P uptake, which means that they are able to uptake more P than needed for growth (Anbalagan et al., 2017; Brown and Shilton, 2014; Powell et al., 2011; Solovchenko et al., 2016; Yang et al., 2017). The concept of using microalgal-bacterial consortia for wastewater treatment has been seen as a potential alternative to enhance nutrient removal from wastewater (Fallahi et al., 2021). These consortia present synergistic effects and mutual interaction, since the microalgae will consume the CO_2 released by the bacteria and produce the O_2 that heterotrophic bacteria need to grow and survive (Abinandan et al., 2018; Fallahi et al., 2021; Fatemeh et al., 2021; Luo et al., 2017; Ramanan et al., 2016). The main nutrient removal mechanism associated with microalgal-bacterial consortium is biomass assimilation, which constitutes a valuable product (Posadas et al., 2015b,

2015a; Torres-Franco et al., 2021). Moreover, the microalgal-bacterial flocs enhance the sedimentation of algae, allowing the separation of the biomass from the effluent (Fallahi et al., 2021; Kant et al., 2021). This bioflocculation by microalgae and bacteria consortiums is considered sustainable, non-toxic and an inexpensive approach for biomass and nutrient recovery (Fallahi et al., 2021). Furthermore, the biomass could be used as natural slow release fertiliser, recycling the nutrients present in the used water (Fallahi et al., 2021; Mulbry et al., 2005; Sanz-Luque et al., 2020; Wágner et al., 2021).

Various traditional (open or closed) systems and advanced microalgal-bacterial cultivation systems have been developed. High-rate algal ponds (HRAP) and waste stabilization ponds (WSP) are common technologies used for nutrient removal. HRAPs are open raceway ponds where paddle wheels are normally used to provide turbulence and enhance algal productivity, oxygen transfer and wastewater treatment. HRAP are typically shallow, with depths between 0.15 to 1 m (Sutherland et al., 2014; Wang et al., 2018), whereas, the most cost-effective relationship was found for a depth around 0.3 m (Young et al., 2017). WSP are low energy-consuming systems and mainly used for wastewater treatment in small communities (Brown and Shilton, 2014). WSP are low cost, simple to operate and provide effective wastewater treatment in terms of organic carbon and pathogen removal. However, sedimentation is generally poor, and nitrification/denitrification is typically not observed in these WWT systems. Also, the hydraulic retention time (HRT) used in HRAP (from 3 to 15 days) (Young et al., 2017; Wang et al., 2018; Posadas et al., 2015; Toledo-Cervantes et al., 2019) and in WSP (between 2 - 3 days to 2 - 3 weeks) (Abdel-Raouf et al., 2012; Camargo Valero and Mara, 2007; Ho et al., 2017; Leite et al., 2009) is higher than in conventional BNR systems, thus requiring longer operation times or increased land areas to obtain the same nutrient removal.

Although microalgal-bacterial systems have certain advantages, they have been under-implemented in comparison to conventional EBPR and BNR systems, with further research being needed to increase the technology readiness level (Yang et al., 2017). Recently, microalgae-bacteria consortia for wastewater treatment with lower HRT than the one typically used in HRAP and WSP have been developed (**Table 1.1**).

Table 1.1 - Nutrient removal efficiency in algae-bacterial systems operated with low HRT.

	COD:N:P (mg basis)	HRT (h)	Aeration	Dark Period	Removal Efficacy N	P
(Guo et al., 2021)	320:35:9	16	Yes	No	90%	97%
(Lin et al., 2019)	700:20:5	16	Yes	Yes	89%	37%
(Ji et al., 2020a)	250:25:9	n.a	No	No	100%	100%
(García et al., 2017)	176*:106:33	48	Yes	No	98%	67%
(Liu et al., 2017)	300:35:11	n.a	Yes	No	60%	35%

*total organic carbon; n.a – the HRT of these research is not clear. The authors only reveal the time of light exposition.

The last research on microalgal-bacterial for WWT, however, do not fulfill all the requirements for a more sustainable system, since they are still dependent on a high COD:Nutrient ratio and external aeration or are idealized to work under continuous light availability, a condition that does not occur in real wastewater environments. The present study aims to develop a microalgal-bacterial based system, capable of nutrient removal at low COD:N:P ratios, with no need of mechanical aeration, since microalgal are a natural oxygen providers. The proposed photosynthetic system is operated in dark and light cycles to promote the removal of P and N, by stimulating the fundamental anoxic, aerobic and anoxic conditions required for full nutrient removal.

1.4. Motivation and objective

Conventional biological wastewater treatment methods have high energy consumption and contribute towards the emission of greenhouse gases. The contribution of the sector to greenhouse gas emissions is not only related to the direct emissions of the process itself (e.g. N_2O, CH_4) but also to the high energy consumption due to intensive aeration, energy that is mainly produced from fossil fuels. The total costs in conventional WWTP related with energy consumption varies between 25 – 60%, depending on the plant dimension and localization, (Luo et al., 2019), and at least 45% of this cost are linked with aeration (Awe et al., 2016; Panepinto et al., 2016; Rosso et al., 2008). By removing the aeration necessities, the costs with wastewater treatment are, indeed, reduced.

The goal of this work was to develop a more sustainable wastewater treatment technology, based on microalgae-bacterial consortia, capable of removing high concentrations of nutrients without the need of costly aeration (**Figure 1.3**). The suggested photosynthetic technology targets the system operation under dark/light cycles, whereas in the dark period PAOs consume VFAs in anaerobic conditions and in anoxic conditions perform denitrification, with no need of organic carbon supplementation (**Figure 1.4**). In the presence of light, microalgae assimilate nutrients and consume the CO_2 produced by heterotrophic bacteria respiration and produce the O_2 necessary for bacterial growth and nutrient uptake, as described in **Figure 1.4**. Due to the bacteria and microalgae flocs, the biomass can exhibit good and fast settling characteristics, obtaining a clear supernatant, and overcoming one of the main issues of algae-based treatment, which is the difficulty in separating the biomass sludge from the clean water.

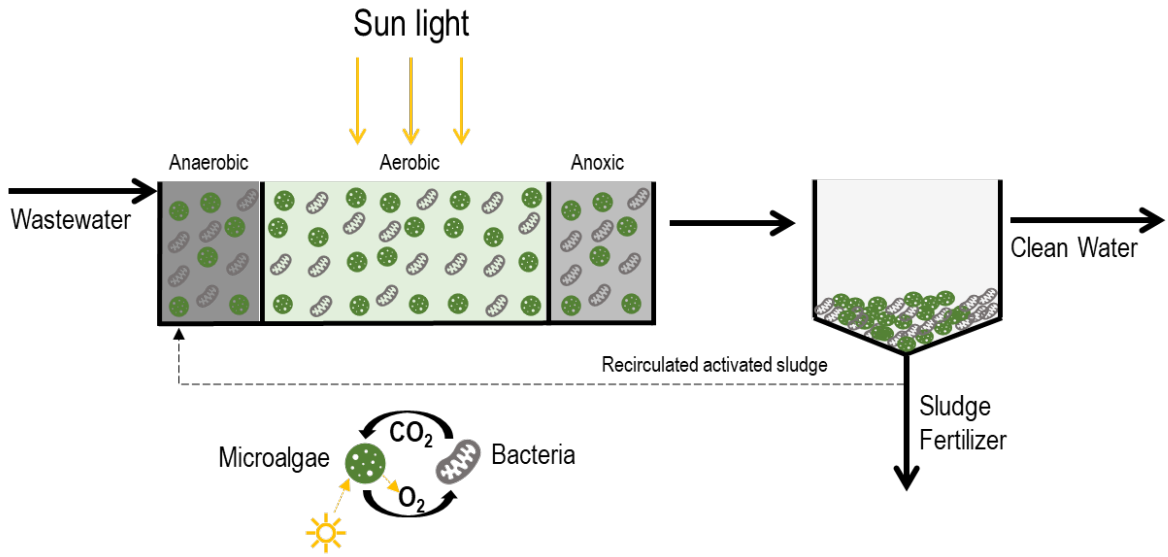

Figure 1.3 - Schematic representation of the desired system to be developed

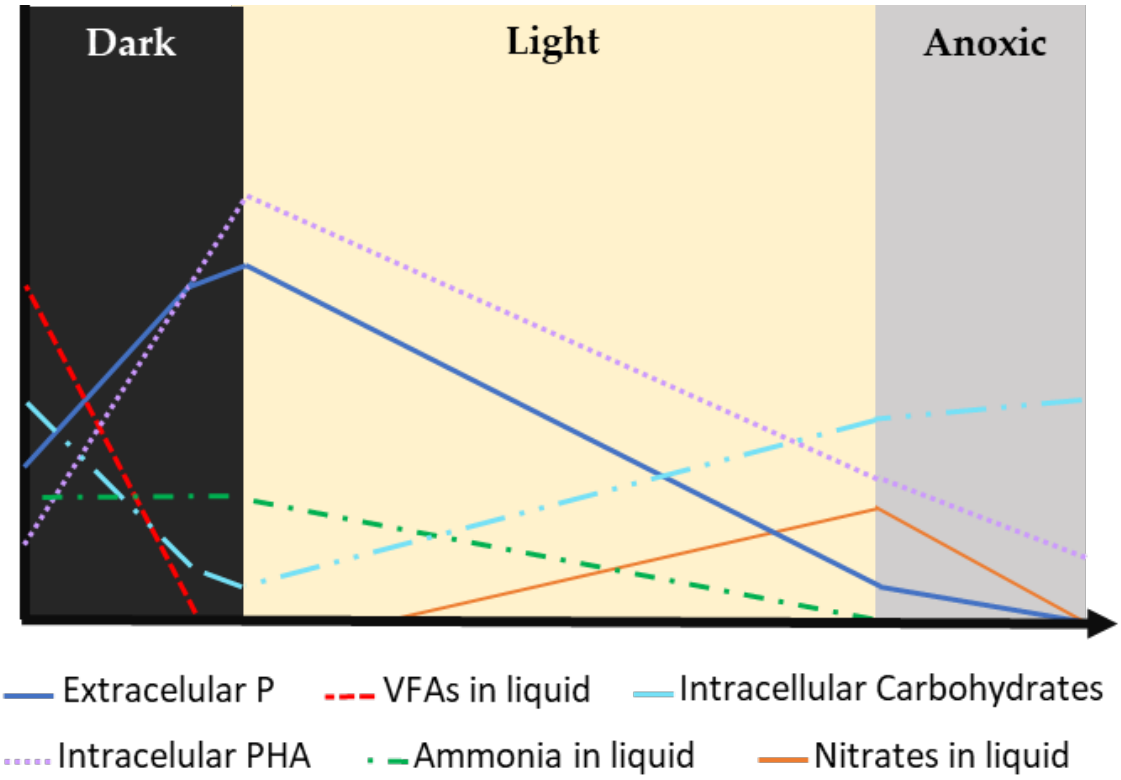

Figure 1.4 - Expected chemical transformations occurring during a photo-BNR cycle exhibited with a sludge fed by Acetate and Propionate during the anaerobic period.

1.5. Thesis outline

The organization and distribution of chapters are summarized below.

Chapter 3 describes how a microalgae-bacterial consortium, with a high capacity for P removal and with no need of mechanical aeration (photo-EBPR), could be selected in alternating dark (anaerobic)/light (aerobic) cycles. The seed sludge used for photo-EBPR selection was a biomass previously enriched in *Accumulibacter* phosphatis.

This chapter was published in an international peer reviewed scientific journal as:

Carvalho, V.C.F., Freitas, E.B., Silva, P.J., Fradinho, J.C., Reis, M.A.M., Oehmen, A., 2018. The impact of operational strategies on the performance of a photo-EBPR system. Water Res. 129, 190–198. https://doi.org/10.1016/j.watres.2017.11.010

Chapter 4 evaluates if a photo-EBPR system could be selected even if the seed sludge used is wastewater activated sludge, by studying the influence of the type of inoculum and the amount of PAOs on the time needed for photo-EBPR selection.

This chapter was published in an international peer reviewed scientific journal as:

Carvalho, V.C.F., Freitas, E.B., Fradinho, J.C., Reis, M.A.M., Oehmen, A., 2019. The effect of seed sludge on the selection of a photo-EBPR system. New Biotechnol. 49, 112–119. https://doi.org/10.1016/j.nbt.2018.10.003

Chapter 5 demonstrates that a high amount of phosphorus, ammonia and nitrate could be simultaneously removed by a microalgae-bacterial consortium in dark (anaerobic) /light (aerobic) /dark (anoxic) cycles with no need of mechanical aeration (Photo-BNR) and identified the main mechanisms involved in the nutrient removal process.

This chapter was published in an international peer reviewed scientific journal as

Carvalho, V.C.F., Kessler, M., Fradinho, J.C., Oehmen, A., Reis, M.A.M., 2021. Achieving nitrogen and phosphorus removal at low C / N ratios without aeration through a novel phototrophic process. Sci. Total Environ. 793, 148501. https://doi.org/10.1016/j.scitotenv.2021.148501

Chapter 6 evaluates the possibility of a real time photo-BNR process monitoring using Raman spectrometry, a tool that could facilitate the control of the photo-BNR systems operation.

This chapter was published in an international peer reviewed scientific journal as:

Franca, R.D.G., Carvalho, V.C.F., Fradinho, J.C., Reis, M.A.M., Lourenço, N.D., 2021. Raman Spectrometry as a Tool for an Online Control of a Phototrophic Biological Nutrient Removal Process. Appl. Sci. 11, 6600. https://doi.org/10.3390/app11146600

Chapter 7 describes how the efficiency of a photo BNR process could be optimized, and which key parameters must be controlled in order to have a stable system. This chapter supports chapter 5, by elucidating the main mechanisms involved in nutrient removal.

Chapter 8 corresponds to the Conclusions and Future work.

REFERENCES

Abdel-Raouf, N., Al-Homaidan, A.A., Ibraheem, I.B.M., 2012. Microalgae and wastewater treatment. Saudi J. Biol. Sci. 19, 257–275. https://doi.org/10.1016/j.sjbs.2012.04.005

Abinandan, S., Subashchandrabose, S.R., Venkateswarlu, K., Megharaj, M., 2018. Nutrient removal and biomass production: advances in microalgal biotechnology for wastewater treatment. Crit. Rev. Biotechnol. https://doi.org/10.1080/07388551.2018.1472066

Alcántara, C., Domínguez, J.M., García, D., Blanco, S., Pérez, R., García-Encina, P.A., Muñoz, R., 2015a. Evaluation of wastewater treatment in a novel anoxic-aerobic algal-bacterial photobioreactor with biomass recycling through carbon and nitrogen mass balances. Bioresour. Technol. 191, 173–186. https://doi.org/10.1016/j.biortech.2015.04.125

Alcántara, C., Posadas, E., Guieysse, B., Muñoz, R., 2015b. Microalgae-based Wastewater Treatment. Handb. Mar. Microalgae Biotechnol. Adv. 439–455. https://doi.org/10.1016/B978-0-12-800776-1.00029-7

Anbalagan, A., Schwede, S., Lindberg, C.F., Nehrenheim, E., 2017. Influence of iron precipitated condition and light intensity on microalgae activated sludge based wastewater remediation. Chemosphere 168, 1523–1530. https://doi.org/10.1016/j.chemosphere.2016.11.161

Arp, D.J., Stein, L.Y., 2003. Metabolism of Inorganic N Compounds by Ammonia-Oxidizing Bacteria. Crit. Rev. Biochem. Mol. Biol. 38, 471–495. https://doi.org/10.1080/10409230390267446

Awe, O.W., Liu, R., Zhao, Y., 2016. Analysis of Energy Consumption and Saving in Wastewater Treatment Plant : Case Study from Ireland. J. Water Sustain. 6, 63–76. https://doi.org/10.11912/jws.2016.6.2.63-76

Bora, R.R., Richardson, R.E., You, F., 2020. Resource recovery and waste-to-energy from wastewater sludge via thermochemical conversion technologies in support of circular economy: a comprehensive review. BMC Chem. Eng. 2, 1–16. https://doi.org/10.1186/s42480-020-00031-3

Brown, N., Shilton, A., 2014. Luxury uptake of phosphorus by microalgae in waste stabilisation ponds: Current understanding and future direction. Rev. Environ. Sci. Biotechnol. 13, 321–328. https://doi.org/10.1007/s11157-014-9337-3

Bunce, J.T., Ndam, E., Ofiteru, I.D., Moore, A., Graham, D.W., 2018. A review of phosphorus removal technologies and their applicability to small-scale domestic wastewater treatment systems. Front. Environ. Sci. https://doi.org/10.3389/fenvs.2018.00008

Camargo, J.A., Alonso, Á., De La Puente, M., 2005. Eutrophication downstream from small reservoirs in mountain rivers of Central Spain. Water Res. 39, 3376–3384. https://doi.org/10.1016/j.watres.2005.05.048

Camargo Valero, M.A., Mara, D.D., 2007. Nitrogen removal via ammonia volatilization in maturation ponds. Water Sci. Technol. 55, 87–92. https://doi.org/10.2166/wst.2007.349

Camejo, P.Y., Owen, B.R., Martirano, J., Ma, J., Kapoor, V., Santo Domingo, J., McMahon, K.D.,

Noguera, D.R., 2016. Candidatus Accumulibacter phosphatis clades enriched under cyclic anaerobic and microaerobic conditions simultaneously use different electron acceptors. Water Res. 102, 125–137. https://doi.org/10.1016/j.watres.2016.06.033

Capson-Tojo, G., Batstone, D.J., Grassino, M., Vlaeminck, S.E., Puyol, D., Verstraete, W., Kleerebezem, R., Oehmen, A., Ghimire, A., Pikaar, I., Lema, J.M., Hülsen, T., 2020. Purple phototrophic bacteria for resource recovery: Challenges and opportunities. Biotechnol. Adv. 43, 107567. https://doi.org/10.1016/j.biotechadv.2020.107567

Carvalho, G., Lemos, P.C., Oehmen, A., Reis, M.A.M., 2007. Denitrifying phosphorus removal : Linking the process performance with the microbial community structure 41, 4383–4396. https://doi.org/10.1016/j.watres.2007.06.065

Cederberg, C., 2010. Improving nutrient management in agriculture to reduce eutrophication, acidification and climate change, Environmental Assessment and Management in the Food Industry. Woodhead Publishing Limited. https://doi.org/10.1533/9780857090225.1.3

Chen, H., Zhou, W., Zhu, S., Liu, F., Qin, L., 2021. Biological nitrogen and phosphorus removal by a phosphorus-accumulating bacteria Acinetobacter sp . strain C-13 with the ability of heterotrophic nitrification – aerobic denitrification. Bioresour. Technol. 322, 124507. https://doi.org/10.1016/j.biortech.2020.124507

Dai, H., Han, T., Sun, T., Zhu, H., Wang, X., Lu, X., 2021. Nitrous oxide emission during denitrifying phosphorus removal process: A review on the mechanisms and influencing factors. J. Environ. Manage. 278, 111561. https://doi.org/10.1016/j.jenvman.2020.111561

Daims, H., Lebedeva, E. V., Pjevac, P., Han, P., Herbold, C., Albertsen, M., Jehmlich, N., Palatinszky, M., Vierheilig, J., Bulaev, A., Kirkegaard, R.H., Von Bergen, M., Rattei, T., Bendinger, B., Nielsen, P.H., Wagner, M., 2015. Complete nitrification by Nitrospira bacteria. Nature 528, 504–509. https://doi.org/10.1038/nature16461

Dalu, T., Wasserman, R.J., Magoro, M.L., Froneman, P.W., Weyl, O.L.F., 2019. River nutrient water and sediment measurements inform on nutrient retention, with implications for eutrophication. Sci. Total Environ. 684, 296–302. https://doi.org/10.1016/j.scitotenv.2019.05.167

Das, P., Khan, S., AbdulQuadir, M., Thaher, M., Waqas, M., Easa, A., Attia, E.S.M., Al-Jabri, H., 2020. Energy recovery and nutrients recycling from municipal sewage sludge. Sci. Total Environ. 715, 136775. https://doi.org/10.1016/j.scitotenv.2020.136775

de Godos, I., Blanco, S., García-Encina, P.A., Becares, E., Muñoz, R., 2010. Influence of flue gas sparging on the performance of high rate algae ponds treating agro-industrial wastewaters. J. Hazard. Mater. 179, 1049–1054. https://doi.org/10.1016/j.jhazmat.2010.03.112

Dobbeleers, T., Caluwé, M., Dockx, L., Daens, D., D'aes, J., Dries, J., 2020. Biological nutrient removal from slaughterhouse wastewater via nitritation/denitritation using granular sludge: an onsite pilot demonstration. J. Chem. Technol. Biotechnol. 95, 111–122. https://doi.org/10.1002/jctb.6212

European Commission, 2021. Paris Agreement [WWW Document]. URL

https://ec.europa.eu/clima/policies/international/negotiations/paris_en (accessed 7.7.21).
European Commission, n.d. Urban Waste Water Directive [WWW Document]. Urban Waste Water Dir. URL https://ec.europa.eu/environment/water/water-urbanwaste/legislation/directive_en.htm (accessed 6.1.21).
Fallahi, A., Rezvani, F., Asgharnejad, H., Khorshidi Nazloo, E., Hajinajaf, N., Higgins, B., 2021. Interactions of microalgae-bacteria consortia for nutrient removal from wastewater: A review. Chemosphere 272, 129878. https://doi.org/10.1016/j.chemosphere.2021.129878
Fatemeh, S., Hennige, S., Willoughby, N., Adeloye, A., Gutierrez, T., 2021. Integrating micro-algae into wastewater treatment : A review. Sci. Total Environ. 752, 142168. https://doi.org/10.1016/j.scitotenv.2020.142168
Feng, X., Bao, X., Che, L., Wu, Q., 2021. Enhance biological nitrogen and phosphorus removal in wastewater treatment process by adding food waste fermentation liquid as external carbon source. Biochem. Eng. J. 165, 107811. https://doi.org/10.1016/j.bej.2020.107811
Fradinho, J., Allegue, L.D., Ventura, M., Puyol, D., 2021. Up-scale challenges on biopolymer production from waste streams by Purple Phototrophic Bacteria mixed cultures: A critical review. Bioresour. Technol. https://doi.org/10.1016/j.biortech.2021.124820
García, D., Alcántara, C., Blanco, S., Pérez, R., Bolado, S., Muñoz, R., 2017. Enhanced carbon, nitrogen and phosphorus removal from domestic wastewater in a novel anoxic-aerobic photobioreactor coupled with biogas upgrading. Chem. Eng. J. 313, 424–434. https://doi.org/10.1016/j.cej.2016.12.054
Gu, B., van Grinsven, H.J.M., Lam, S.K., Oenema, O., Sutton, M.A., Mosier, A., Chen, D., 2021. A Credit System to Solve Agricultural Nitrogen Pollution. Innov. 2, 100079. https://doi.org/10.1016/j.xinn.2021.100079
Guo, D., Zhang, X., Shi, Y., Cui, B., Fan, J., Ji, B., Yuan, J., 2021. Microalgal-bacterial granular sludge process outperformed aerobic granular sludge process in municipal wastewater treatment with less carbon dioxide emissions. Environ. Sci. Pollut. Res. 28, 13616–13623. https://doi.org/10.1007/s11356-020-11565-7
Gutierrez, F., Kinney, K.A., Katz, L.E., 2020. Phosphorus speciation in municipal wastewater solids and implications for phosphorus recovery. Environ. Eng. Sci. 37, 316–327. https://doi.org/10.1089/ees.2019.0360
He, S., Mcmahon, K.D., 2011. Microbiology of "Candidatus Accumulibacter" in activated sludge. Microb. Biotechnol. https://doi.org/10.1111/j.1751-7915.2011.00248.x
Henze, M., Harremoës, P., 1990. Chemical-Biological Nutrient Removal The HYPRO Concept, in: Hahn, H.H., Klute, R. (Eds.), Chemical Water and Wastewater Treatment. Springer Berlin Heidelberg, Berlim, pp. 499–510. https://doi.org/https://doi.org/10.1007/978-3-642-76093-8_33
Ho, L.T., Van Echelpoel, W., Goethals, P.L.M., 2017. Design of waste stabilization pond systems: A review. Water Res. 123, 236–248. https://doi.org/10.1016/j.watres.2017.06.071
Hülsen, T., Barry, E.M., Lu, Y., Puyol, D., Keller, J., Damien, J., 2016. Domestic wastewater treatment with purple phototrophic bacteria using a novel continuous photo anaerobic membrane bioreacto. Water Res. 100, 486–495.

https://doi.org/10.1016/j.watres.2016.04.061
Hülsen, T., Batstone, D.J., Keller, J., 2013. Phototrophic bacteria for nutrient recovery from domestic wastewater. Water Res. 50, 18–26. https://doi.org/10.1016/j.watres.2013.10.051
Izadi, Parnian, Izadi, Parin, Eldyasti, A., 2021. Enhancement of simultaneous nitrogen and phosphorus removal using intermittent aeration mechanism. J. Environ. Sci. 109, 1–14. https://doi.org/10.1016/j.jes.2021.02.026
Izadi, Parnian, Izadi, Parin, Eldyasti, A., 2020. Design, operation and technology configurations for enhanced biological phosphorus removal (EBPR) process: a review, Reviews in Environmental Science and Biotechnology. Springer Netherlands. https://doi.org/10.1007/s11157-020-09538-w
Ji, B., Zhang, M., Gu, J., Ma, Y., Liu, Y., 2020. A self-sustaining synergetic microalgal-bacterial granular sludge process towards energy-efficient and environmentally sustainable municipal wastewater treatment. Water Res. 179, 115884. https://doi.org/10.1016/j.watres.2020.115884
Kant, S., Mehariya, S., Kant, R., Kumar, Manu, Pugazhendhi, A., Kumar, Mukesh, Atabani, A.E., Kumar, G., Kim, W., Seo, S., Yang, Y., 2021. Wastewater based microalgal biorefinery for bioenergy production : Progress and challenges. Sci. Total Environ. 751, 141599. https://doi.org/10.1016/j.scitotenv.2020.141599
Kong, Y., Nielsen, J.L., Nielsen, P.H., 2005. Identity and ecophysiology of uncultured actinobacterial polyphosphate-accumulating organisms in full-scale enhanced biological phosphorus removal plants. Appl. Environ. Microbiol. 71, 4076–4085. https://doi.org/10.1128/AEM.71.7.4076-4085.2005
Kristiansen, R., Thi, H., Nguyen, T., Saunders, A.M., Lund Nielsen, J., Wimmer, R., Le, V.Q., Mcilroy, S.J., Petrovski, S., Seviour, R.J., Calteau, A., Lehmann Nielsen, K., Nielsen, P.H.H., Nguyen, H.T.T., Saunders, A.M., Nielsen, J.L., Wimmer, R., Le, V.Q., Mcilroy, S.J., Petrovski, S., Seviour, R.J., Calteau, A., Nielsen, K.L., Nielsen, P.H.H., 2013. A metabolic model for members of the genus Tetrasphaera involved in enhanced biological phosphorus removal. ISME J. 7, 543–554. https://doi.org/10.1038/ismej.2012.136
Kuypers, M.M.M., Marchant, H.K., Kartal, B., 2018. The microbial nitrogen-cycling network. Nat. Rev. Microbiol. 16, 263–276. https://doi.org/10.1038/nrmicro.2018.9
Lam, K.L., Zlatanović, L., van der Hoek, J.P., 2020. Life cycle assessment of nutrient recycling from wastewater: A critical review. Water Res. 173. https://doi.org/10.1016/j.watres.2020.115519
Lanham, A.B., Oehmen, A., Carvalho, G., Saunders, A.M., Nielsen, P.H., Reis, M.A.M., 2018. Denitrification activity of polyphosphate accumulating organisms (PAOs) in full-scale wastewater treatment plants. Water Sci. Technol. 78, 2449–2458. https://doi.org/10.2166/wst.2018.517
Le Moal, M., Gascuel-Odoux, C., Ménesguen, A., Souchon, Y., Étrillard, C., Levain, A., Moatar, F., Pannard, A., Souchu, P., Lefebvre, A., Pinay, G., 2019. Eutrophication: A new wine in an old bottle? Sci. Total Environ. 651, 1–11. https://doi.org/10.1016/j.scitotenv.2018.09.139
Leite, V.D., Athayde, G.B., de Sousa, J.T., Lopes, W.S., Henrique, I.N., 2009. Treatment of

domestic wastewater in shallow waste stabilization ponds for agricultural irrigation reuse. J. Urban Environ. Eng. 3, 58–62. https://doi.org/10.4090/juee.2009.v3n2.058062

Levy-Booth, D.J., Prescott, C.E., Grayston, S.J., 2014. Microbial functional genes involved in nitrogen fixation, nitrification and denitrification in forest ecosystems. Soil Biol. Biochem. 75, 11–25. https://doi.org/10.1016/j.soilbio.2014.03.021

Lin, C., Cao, P., Xu, X., Ye, B., 2019. Algal-bacterial symbiosis system treating high-load printing and dyeing wastewater in continuous-flow reactors under natural light. Water (Switzerland) 11. https://doi.org/10.3390/w11030469

Liu, L., Fan, H., Liu, Y., Liu, C., Huang, X., 2017. Development of algae-bacteria granular consortia in photo-sequencing batch reactor. Bioresour. Technol. 232, 64–71. https://doi.org/10.1016/j.biortech.2017.02.025

Lopez-Vazquez, C.M., Oehmen, A., Hooijmans, C.M., Brdjanovic, D., Gijzen, H.J., Yuan, Z., van Loosdrecht, M.C.M., 2009. Modeling the PAO-GAO competition: Effects of carbon source, pH and temperature. Water Res. 43, 450–462. https://doi.org/10.1016/j.watres.2008.10.032

Luo, L., Dzakpasu, M., Yang, B., Zhang, W., Yang, Y., Wang, X.C., 2019. A novel index of total oxygen demand for the comprehensive evaluation of energy consumption for urban wastewater treatment. Appl. Energy 236, 253–261. https://doi.org/10.1016/j.apenergy.2018.11.101

Luo, Y., Le-Clech, P., Henderson, R.K., 2017. Simultaneous microalgae cultivation and wastewater treatment in submerged membrane photobioreactors: A review. Algal Res. 24, 425–437. https://doi.org/10.1016/j.algal.2016.10.026

Marques, R., Ribera-Guardia, A., Santos, J., Carvalho, G., Reis, M.A.M., Pijuan, M., Oehmen, A., 2018. Denitrifying capabilities of Tetrasphaera and their contribution towards nitrous oxide production in enhanced biological phosphorus removal processes. Water Res. 137, 262–272. https://doi.org/10.1016/j.watres.2018.03.010

Marques, R., Santos, J., Nguyen, H., Carvalho, G., Noronha, J.P., Nielsen, P.H., Reis, M.A.M., Oehmen, A., 2017. Metabolism and ecological niche of Tetrasphaera and Ca. Accumulibacter in enhanced biological phosphorus removal. Water Res. 122, 159–171. https://doi.org/10.1016/j.watres.2017.04.072

Moinard, V., Levavasseur, F., Houot, S., 2021. Current and potential recycling of exogenous organic matter as fertilizers and amendments in a French peri-urban territory. Resour. Conserv. Recycl. https://doi.org/10.1016/j.resconrec.2021.105523

Mulbry, W., Westhead, E.K., Pizarro, C., Sikora, L., 2005. Recycling of manure nutrients: Use of algal biomass from dairy manure treatment as a slow release fertilizer. Bioresour. Technol. 96, 451–458. https://doi.org/10.1016/j.biortech.2004.05.026

Nguyen, H.T.T., Le, V.Q., Hansen, A.A., Nielsen, J.L., Nielsen, P.H., 2011. High diversity and abundance of putative polyphosphate-accumulating Tetrasphaera-related bacteria in activated sludge systems. FEMS Microbiol. Ecol. 76, 256–267. https://doi.org/10.1111/j.1574-6941.2011.01049.x

Nielsen, P.H., McIlroy, S.J., Albertsen, M., Nierychlo, M., 2019. Re-evaluating the

microbiology of the enhanced biological phosphorus removal process. Curr. Opin. Biotechnol. 57, 111–118. https://doi.org/10.1016/j.copbio.2019.03.008

Oehmen, A., Carvalho, G., Freitas, F., Reis, M.A.M., 2010. Assessing the abundance and activity of denitrifying polyphosphate accumulating organisms through molecular and chemical techniques. Water Sci. Technol. 61, 2061–2068. https://doi.org/10.2166/wst.2010.976

Oehmen, A., Lemos, P.C., Carvalho, G., Yuan, Z., Keller, J., Blackall, L.L., Reis, M.A.M., 2007a. Advances in enhanced biological phosphorus removal: From micro to macro scale. Water Res. 41, 2271–2300. https://doi.org/10.1016/j.watres.2007.02.030

Oehmen, A., Yuan, Z., Blackall, L.L., Keller, J., 2005a. Comparison of acetate and propionate uptake by polyphosphate accumulating organisms and glycogen accumulating organisms. Biotechnol. Bioeng. 91, 162–168. https://doi.org/10.1002/bit.20500

Oehmen, A., Zeng, R.J., Keller, J., Yuan, Z., 2007b. Modeling the Aerobic Metabolism of Polyphosphate-Accumulating Organisms Enriched with Propionate as a Carbon Source. Water Environ. Res. 79, 2477–2486. https://doi.org/https://doi.org/10.1002/j.1554-7531.2007.tb00347.x

Oehmen, A., Zeng, R.J., Yuan, Z., 2005b. Anaerobic Metabolism of Propionate by Polyphosphate-Accumulating Organisms in Enhanced Biological Phosphorus Removal Systems. https://doi.org/10.1002/bit.20480

Panepinto, D., Fiore, S., Zappone, M., Genon, G., Meucci, L., 2016. Evaluation of the energy efficiency of a large wastewater treatment plant in Italy. Appl. Energy 161, 404–411. https://doi.org/10.1016/j.apenergy.2015.10.027

Pell, M., Wörman, A., 2011. Biological Wastewater Treatment Systems, Second Edi. ed, Comprehensive Biotechnology, Second Edition. Elsevier B.V. https://doi.org/10.1016/B978-0-08-088504-9.00381-0

Posadas, E., Morales, M. del M., Gomez, C., Acién, F.G., Muñoz, R., 2015a. Influence of pH and CO_2 source on the performance of microalgae-based secondary domestic wastewater treatment in outdoors pilot raceways. Chem. Eng. J. 265, 239–248. https://doi.org/10.1016/j.cej.2014.12.059

Posadas, E., Muñoz, A., García-González, M.C., Muñoz, R., García-Encina, P.A., 2015b. A case study of a pilot high rate algal pond for the treatment of fish farm and domestic wastewaters. J. Chem. Technol. Biotechnol. 90, 1094–1101. https://doi.org/10.1002/jctb.4417

Powell, N., Shilton, A.N., Pratt, S., Chisti, Y., 2011. Luxury uptake of phosphorus by microalgae in waste stabilization ponds. Environ. Sci. Technol. 63, 704–709. https://doi.org/10.1021/es703118s

Puyol, D., Batstone, D.J., Hülsen, T., Astals, S., Peces, M., Krömer, J.O., 2017. Resource recovery from wastewater by biological technologies: Opportunities, challenges, and prospects. Front. Microbiol. 7. https://doi.org/10.3389/fmicb.2016.02106

Rajaniemi, K., Hu, T., Nurmesniemi, Emma-Tuulia Tuomikosk, Sari Lassi, U., 2021. Phosphate and Ammonium Removal from Water through Electrochemical and Chemical

Precipitation of Struvite. Processes 9. https://doi.org/https://doi.org/10.3390/pr9010150

Ramanan, R., Kim, B.H., Cho, D.H., Oh, H.M., Kim, H.S., 2016. Algae-bacteria interactions: Evolution, ecology and emerging applications. Biotechnol. Adv. 34, 14–29. https://doi.org/10.1016/j.biotechadv.2015.12.003

Raschke, R.L., 1993. Guidelines for Assessing and Predicting Eutrophication Status of Small Southeastern Piedmont Impoundments.

Rossi, L., Reuna, S., Fred, T., Heinonen, M., 2018. RAVITA Technology – new innovation for combined phosphorus and nitrogen recovery. Water Sci. Technol. 78, 2511–2517. https://doi.org/10.2166/wst.2019.011

Rosso, D., Larson, L.E., Stenstrom, M.K., 2008. Aeration of large-scale municipal wastewater treatment plants : state of the art 973–979. https://doi.org/10.2166/wst.2008.218

Rubio-Rincón, F.J., Lopez-Vazquez, C.M., Welles, L., van Loosdrecht, M.C.M., Brdjanovic, D., 2017. Cooperation between Candidatus Competibacter and Candidatus Accumulibacter clade I, in denitrification and phosphate removal processes. Water Res. 120, 156–164. https://doi.org/10.1016/j.watres.2017.05.001

Saad, S.A., Welles, L., Abbas, B., Lopez-Vazquez, C.M., van Loosdrecht, M.C.M., Brdjanovic, D., 2016. Denitrification of nitrate and nitrite by 'Candidatus Accumulibacter phosphatis' clade IC. Water Res. 105, 97–109. https://doi.org/10.1016/j.watres.2016.08.061

Sanz-Luque, E., Bhaya, D., Grossman, A.R., 2020. Polyphosphate: A Multifunctional Metabolite in Cyanobacteria and Algae. Front. Plant Sci. 11, 1–21. https://doi.org/10.3389/fpls.2020.00938

Seleiman, M.F., Santanen, A., Mäkelä, P.S.A., 2020. Recycling sludge on cropland as fertilizer – Advantages and risks. Resour. Conserv. Recycl. 155, 104647. https://doi.org/10.1016/j.resconrec.2019.104647

Sengupta, S., Nawaz, T., Beaudry, J., 2015. Nitrogen and Phosphorus Recovery from Wastewater. Curr. Pollut. Reports 1, 155–166. https://doi.org/10.1007/s40726-015-0013-1

Shen, N., Zhou, Y., 2016. Enhanced biological phosphorus removal with different carbon sources. Appl. Microbiol. Biotechnol. 100, 4735–4745. https://doi.org/10.1007/s00253-016-7518-4

Smolders, G.J.F., Meij, J. Van Der, Loosdrecht, M.C.M. Van, 1994a. Stoichiometric Model of the Aerobic Metabolism of the Biological Phosphorus Removal Process 44, 837–848.

Smolders, G.J.F., van der Meij, J., van Loosdrecht, M.C.M., Heijnen, J.J., 1995. A structured metabolic model for the anaerobic and aerobic stoichiometry of the biological phosphorus removal process. Biotechnology and Bioengineering. Biotechnol. Bioeng. 47, 277–287.

Smolders, G.J.F., van der Meij, J., van Loosdrecht, M.C.M., Heijnen, J.J., 1994b. Model of the anaerobic metabolism of the biological phosphorus removal process: Stoichiometry and pH influence. Biotechnol. Bioeng. 43, 461–470. https://doi.org/10.1002/bit.260430605

Solovchenko, A., Verschoor, A.M., Jablonowski, N.D., Nedbal, L., 2016. Phosphorus from wastewater to crops : An alternative path involving microalgae 34, 550–564. https://doi.org/10.1016/j.biotechadv.2016.01.002

Sutherland, D.L., Turnbull, M.H., Craggs, R.J., 2014. Increased pond depth improves algal productivity and nutrient removal in wastewater treatment high rate algal ponds. Water Res. 53, 271–281. https://doi.org/10.1016/j.watres.2014.01.025

Toledo-Cervantes, A., Posadas, E., Bertol, I., Turiel, S., Alcoceba, A., Muñoz, R., 2019. Assessing the influence of the hydraulic retention time and carbon/nitrogen ratio on urban wastewater treatment in a new anoxic-aerobic algal-bacterial photobioreactor configuration. Algal Res. 44, 101672. https://doi.org/10.1016/j.algal.2019.101672

Torres-Franco, A., Passos, F., Figueredo, C., Mota, C., Muñoz, R., 2020. Current advances in microalgae-based treatment of high-strength wastewaters: challenges and opportunities to enhance wastewater treatment performance. Rev. Environ. Sci. Biotechnol. 8. https://doi.org/10.1007/s11157-020-09556-8

Torres-Franco, A.F., Zuluaga, M., Hernández-Roldán, D., Leroy-Freitas, D., Sepúlveda-Muñoz, C.A., Blanco, S., Mota, C.R., Muñoz, R., 2021. Assessment of the performance of an anoxic-aerobic microalgal-bacterial system treating digestate. Chemosphere 270. https://doi.org/10.1016/j.chemosphere.2020.129437

United Nations for Climate Change, n.d. Key aspects of the Paris Agreement [WWW Document]. URL https://unfccc.int/process-and-meetings/the-paris-agreement/the-paris-agreement/key-aspects-of-the-paris-agreement (accessed 6.8.21).

van Grinsven, H.J.M., van Dam, J.D., Lesschen, J.P., Timmers, M.H.G., Velthof, G.L., Lassaletta, L., 2018. Reducing external costs of nitrogen pollution by relocation of pig production between regions in the European Union. Reg. Environ. Chang. 19, 1829. https://doi.org/10.1007/s10113-019-01497-5

van Kessel, M.A.H.J., Speth;, D.R., Albertsen;, M., Nielsen;, P.H., den Camp;, H.J.M.O., Kartal;, B., Jetten;, M.S.M., Lücker, S., 2015. Complete nitrification by a single microorganism. Nature 1–17. https://doi.org/10.1038/nature16459

Wágner, D.S., Cazzaniga, C., Steidl, M., Dechesne, A., Valverde-Pérez, B., Plósz, B.G., 2021. Optimal influent N-to-P ratio for stable microalgal cultivation in water treatment and nutrient recovery. Chemosphere 262. https://doi.org/10.1016/j.chemosphere.2020.127939

Wang, J., Fu, Z., Qiao, H., Liu, F., 2019. Assessment of eutrophication and water quality in the estuarine area of Lake Wuli, Lake Taihu, China. Sci. Total Environ. 650, 1392–1402. https://doi.org/10.1016/j.scitotenv.2018.09.137

Wang, M., Keeley, R., Zalivina, N., Halfhide, T., Scott, K., Zhang, Q., van der Steen, P., Ergas, S.J., 2018. Advances in algal-prokaryotic wastewater treatment: A review of nitrogen transformations, reactor configurations and molecular tools. J. Environ. Manage. 217, 845–857. https://doi.org/10.1016/j.jenvman.2018.04.021

Wei, S.P., van Rossum, F., van de Pol, G.J., Winkler, M.K.H., 2018. Recovery of phosphorus and nitrogen from human urine by struvite precipitation, air stripping and acid scrubbing: A pilot study. Chemosphere 212, 1030–1037. https://doi.org/10.1016/j.chemosphere.2018.08.154

Winkler, M.K., Straka, L., 2019. New directions in biological nitrogen removal and recovery from wastewater. Curr. Opin. Biotechnol. 57, 50–55.

https://doi.org/10.1016/j.copbio.2018.12.007

Xie, C., Zhao, J., Tang, J., Xu, J., Lin, X., Xu, X., 2011. The phosphorus fractions and alkaline phosphatase activities in sludge. Bioresour. Technol. 102, 2455–2461. https://doi.org/10.1016/j.biortech.2010.11.011

Yang, Y., Shi, X., Ballent, W., Mayer, B.K., 2017. Biological Phosphorus Recovery: Review of Current Progress and Future Needs. Water Environ. Res. 89, 2122–2135. https://doi.org/10.2175/106143017x15054988926424

Young, P., Taylor, M., Fallowfield, H.J., 2017. Mini-review: high rate algal ponds, flexible systems for sustainable wastewater treatment. World J. Microbiol. Biotechnol. 33, 0. https://doi.org/10.1007/s11274-017-2282-x

Yuan, C., Wang, B., Peng, Y., Li, X., Zhang, Q., Hu, T., 2020. Enhanced nutrient removal of simultaneous partial nitrification , denitrification and phosphorus removal (SPNDPR) in a single-stage anaerobic / micro-aerobic sequencing batch reactor for treating real sewage with low carbon / nitrogen. Chemosphere 257, 127097. https://doi.org/10.1016/j.chemosphere.2020.127097

Zeng, R.J., Lemaire, R., Yuan, Z., Keller, J., 2003. Simultaneous nitrification, denitrification, and phosphorus removal in a lab-scale sequencing batch reactor. Biotechnol. Bioeng. 84, 170–178. https://doi.org/10.1002/bit.10744

Zhao, J., Wang, X., Li, X., Jia, S., Peng, Y., 2018. Combining partial nitrification and post endogenous denitrification in an EBPR system for deep-level nutrient removal from low carbon/nitrogen (C/N) domestic wastewater. Chemosphere 210, 19–28. https://doi.org/10.1016/j.chemosphere.2018.06.135

Zhu, G., Peng, Y., Li, B., Guo, J., Yang, Q., Wang, S., 2008. Biological removal of nitrogen from wastewater. Rev. Environ. Contam. Toxicol. 192, 159–195. https://doi.org/10.1007/978-0-387-71724-1_5

2. MATERIALS AND METHODS

2.1. Reactor Set-up

The main reactor used for studying the photo-EBPR and photo-BNR processes was a 3.8 L acrylic reactor with an internal halogen lamp (**Figure 2.1**), stirred at, approximately, 700 rpm with a magnetic stirrer. Light intensity was adjusted to the requirements of each specific experiment as referred in each chapter. Temperature was controlled at 20 ± 4 ˚C, using a thermostat bath, and pH was measured using an analog sensor (Mettler Toledo, LLC, Columbus, OH, USA) and controlled using a P&I control at 7.5 ± 0.1 (Hanna Instruments, Limena, Italy). O_2 and CO_2 concentration was measured over all the reactor operation using analog electrodes (Mettler Toledo, LLC, Columbus, OH, USA). The reactor data was acquired using the Bio CTR software (Mário Eusébio, FCT/NOVA, Lisbon, Portugal). Feed composition and reactor operation conditions are presented in each chapter since these conditions have changed over the developed work.

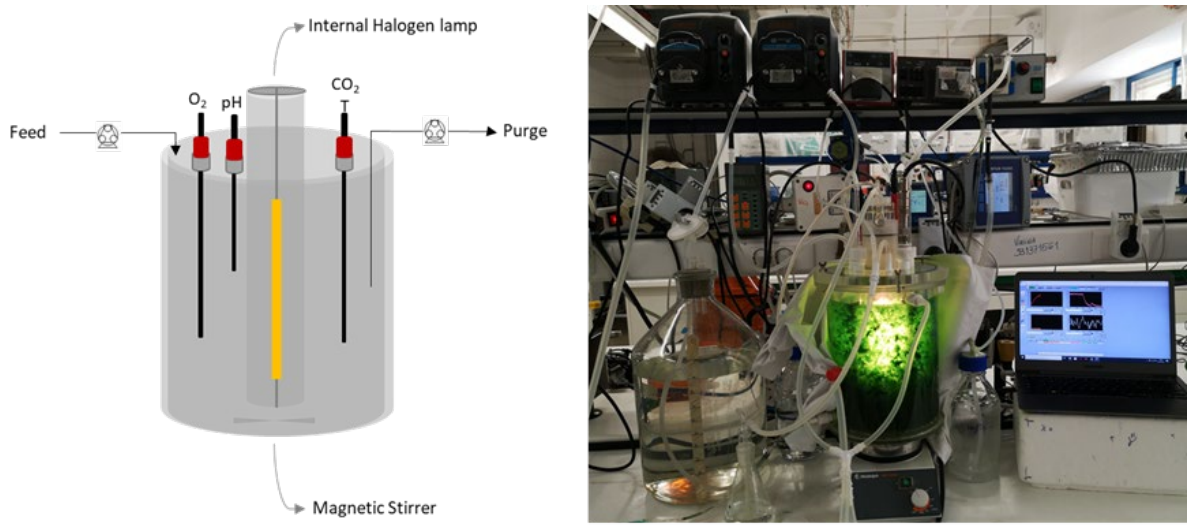

Figure 2.1.- Reactor and setup configuration used in most of the experiments.

2.2. Analytical methods

Acetate and propionate were determined by high-performance liquid chromatography (HPLC), using a VWR Hitachi Chromaster with a Biorad Aminex HPX-87H 300x7.8 MM column and a DAD detector. 0.01 N sulfuric acid was used as eluent, with an elution rate of 0.5 mL/min and an operating temperature of 30º C.

Phosphate and ammonia concentrations were determined by colorimetric methods implemented in a flow segmented analyser (Skalar 5100, Skalar Analytical, The Netherlands). For the cell poly-phosphate content, an acid digestion of a sample was performed with 0.3 M H_2SO_4 and 400 mg of $K_2S_2O_8$ and analyzed using the flow segmented analyzer. PHAs were determined by gas chromatography (GC) using the method described by Lanham et al. (2013), using a Bruker 430-GC gas chromatograph equipped with a FID detector and a Restek column (60m, 0.53mm internal diameter, 1 μM df, crossbond). For carbohydrates determination, an acid digestion, described by Lanham et al. 2012 with 0.9 M HCL was made during 3 hours and the supernatant was analyzed by HPLC with a VARIAN Metacarb 87H column and a Merck Differential Refractometer RI-71 detector. 0.01 N sulfuric acid was used as eluent, with an elution rate of 0.5 mL/min and an operating temperature of 30º C. Total suspended solids (TSS) and volatile suspended solids (VSS) were calculated according to standard methods (APHA/AWWA/1995). The light intensity provided by the halogen lamp was measured using a LI-COR light meter (LI-250 A), equipped with a pyranometer sensor LI-200 SA.

To determine the culture chlorophyll and bacteriochlorophyll content, pigments extraction was performed using the biomass pellet of a sample. To extract the pigments, ethanol (95% V/V) was added to the biomass pellet, vortexed and incubated overnight at room temperature and in dark conditions. Pigments quantification method is described in each chapter.

2.3. Calculation of Kinetic and Stoichiometric parameters

Phosphate release (Prelease in mg P/L) was calculated as the difference between the phosphorus concentration in the end of the dark (anaerobic) phase and the phosphorus concentration in the beginning of the dark (anaerobic) phase. Total phosphate uptake (P uptake total in mg P/L) was calculated as the difference between the phosphorus concentration in the end of the light phase and the phosphorus concentration in the end of dark (anaerobic). Phosphate uptake in the light period (P uptake light in mg P/L) was calculated as the difference between the phosphorus concentration in the end of the light period before air supply and the phosphorus concentration in the beginning of the light period. Phosphate uptake in the light period in the presence of air (Puptake light + air in mg P/L) was calculated as the difference between the phosphorus concentration in the beginning and the end of the aeration period. Phosphate uptake in the dark (anoxic) period (in mg P/L) was calculated as the difference between the phosphorus concentration in the end of light phase and the end of the dark anoxic period. P net removal (in mg P/L), in **chapter 3** and in **chapter 4**, was calculated as the difference of phosphorus concentration in the end and the beginning of the 8h cycle. To determine

the cell poly-P content, the supernatant phosphate concentration was subtracted from the total phosphate concentration obtained by sample digestion.

Removal efficiency (%), in **chapter 3** and in **chapter 4,** is the difference between the phosphorus concentration in the end of the dark phase and in the end of the cycle, dividing by the phosphorus concentration in the end of the dark phase. Active biomass (X) was calculated by subtracting PHA and total carbohydrates from VSS. The yield of P uptake per PHA consumed ($Y_{P/PHA}$ in P mmol /C mmol) was calculated by dividing the P uptake by the PHA consumed at the determined period. The specific P release rate (qr in mg P/mg X.h), the specific P uptake rates (q_u in mg P/mg X.h) were determined by adjusting a linear regression line to the experimental concentrations determined along the different periods of the cycle and dividing the slope by the average of the concentration of the active biomass (X) during the cycle. For the specific P release rate (mg P/L.h), linear regression was made in the period of P release during the dark phase. For specific P total uptake rate, linear regression was made in the period of 4 hours of light. For specific P light uptake rate, linear regression was made in the period of light with no air. For specific P light and air uptake rate linear regression was made in the period of light and air.

Ammonia consumption (in mg N/L) was calculated as the difference between the ammonia concentration in the beginning and end of the light period. Nitrate removal (in mg N /L) was calculated as the difference between the nitrate concentration in the end of the light and in the end of anoxic phase.

P and N global removal or efficiency (%), in **chapter 5** and in **chapter 7,** were calculated considering the concentrations in the influent and in the effluent.

CO_2 production (in mg C/L) during the dark anaerobic and anoxic phases was calculated as the difference between CO_2 concentration in the end and the beginning of the respective phase. Similarly, CO_2 consumption (in mg C/L) during the light phase was calculated as the difference between the CO_2 concentrations at the beginning and end of this phase. Net CO_2 (in mg C/L) was calculated as the difference between the CO_2 consumed during the light and the CO_2 produced during the dark anaerobic and anoxic phase. Aqueous Carbon dioxide was measured with a CO_2 sensor and then the concentrations were readjusted considering the pH of the reactor, taking into account the equations of CO_2 equilibrium in water and their respective constants according to Henry's Law, using the following equations (K=0.0017M; Ka_1=4.47E^{-7}M; Ka_2=4.69E^{-11}M) :

$$H^+ = 10^{pH} \quad \textbf{Equation 2.1}$$

$$\alpha_{H_2CO_3} = \frac{[H^+]^2}{[H^+]^2+[H^+]K_{a1}+K_{a1}K_{a2}} \quad \textbf{Equation 2.2}$$

$$\alpha_{HCO_3^-} = \frac{[H^+]K_{a1}}{[H^+]^2+[H^+]K_{a1}+K_{a1}K_{a2}} \quad \textbf{Equation 2.3}$$

$$[CO_2]_{total} = [CO_2]_{aq} + \frac{\propto HCO_3^-[CO_2]_{aq} + \propto HCO_3^- K[CO_2]_{aq}}{\propto H_2CO_3} \quad \textbf{Equation 2.4}$$

Sludge volume index (SVI) was measured inside the reactor in the end of the cycle, after 15 min of settling, and was calculated according the following equation (Pierce et al., 1998).

$$SVI(\frac{mL}{g\ TSS}) = \frac{\frac{Volume\ of\ sedimented\ biomass\ (mL)}{Volume\ of\ reactor\ liquor\ (L)}}{TSS\ (\frac{g}{L})} \quad \textbf{Equation 2.5}$$

2.4. Microbiological Analysis

Phylogenetic analysis of the bacterial community was done through Fluorescence in situ hybridization (FISH) as previously described by Amann 1995a, on fixed samples with 4% paraformaldehyde or ethanol, according to Nielsen et al., 2009. The oligonucleotide probes used were the fluorescein isothiocyanate (FITC)-labelled EUBmix (EUB338, EUB338II, EUB338III) for all bacteria, applied with the cyanine 3 (Cy3)-labelled probes: ALF969 (Oehmen et al., 2006), BET42a, GAM42a (Manz et al., 1992) and DELTA495 (Lücker et al., 2007) for the major proteobacterial groups of Alphaproteobacteria, Betaproteobacteria, Gammaproteobacteria and Deltaproteobacteria, respectively; PAOmix (PAO651, PAO462, PAO846) for *Candidatus* Accumulibacter phosphatis; Acc-I-444 which targets type I *Accumulibacter* PAOs and Acc-II-444 for *Accumulibacter* PAOs type II; CPB_654 for *Candidatus* Competibacter phosphatis; Prop207 for *Ca*. *Propionivibrio aalborgensis* (Albertsen et al., 2016);. Tet1-126, Tet2-892, Tet2-147 and Tet3-654 for *Tetrasphaera*. Grb for *Rhodobacter* & *Roseobacter* and RHC439 for *Rhodocyclus*; Rhodo2 for *Rhodospirillum* (Sanguin et al., 2006); Rhodopseud for *Rhodopseudomonas* (Demanèche et al., 2008); ACR915 for Archaea; Nso1225 for ammonia oxidizing bacteria (AOBs) (*Nitrosomonadaceae*; *Nitrosomonadales*); and NIT3 (*Nitrobacter* spp.) and Ntspa662 *(Nitrospira* spp.) for nitrite oxidizing bacteria (NOBs); TFOmix (TFO_DF218, TFO_DF618 (Wong et al. 2004)) for *Defluviicoccus vanus* cluster I and SuperDFmix (a mixture of TFOmix, with DFmix (DF988 +DF1020 (Meyer et al. 2006)) and DF198 (Nittami et al. 2009)) *for Defluviicoccus vanus* cluster I, II and III, respectively. More details are available at probeBase 2016. Negative controls consisted of biomass samples with no probes added. To observe both bacterial and photosynthetic populations, fresh and fixed biomass samples were visualized using a Zeiss Imager D2 epifluorescence microscope (Germany), at 1000 X amplification. To visualize intracellular poly-P granules, Loeffler's Methylene Blue staining was performed according to (Murray, RGE, Doetsch, RN, Robinow, 1994).

Samples for DNA extraction were taken and centrifuged at 10.000g for 3 min. DNA was extracted and the V1–3 region of the 16s rRNA gene was sequenced by Illumina Technology through the company DNASense (Aalborg, Denmark).

REFERENCES

Albertsen, M., McIlroy, S.J., Stokholm-Bjerregaard, M., Karst, S.M., Nielsen, P.H., 2016. "Candidatus Propionivibrio aalborgensis": A novel glycogen accumulating organism abundant in full-scale enhanced biological phosphorus removal plants. Front. Microbiol. 7, 1–17. https://doi.org/10.3389/fmicb.2016.01033

Amann, R.I., 1995. In situ identification of micro-organisms by whole cell hybridization with rRNA-targeted nucleic acid probes, in: Akkermans, A.D.L., Van Elsas, J.D., De Bruijn, F.J. (Eds.), Molecular Microbial Ecology Manual. Springer Netherlands, Dordrecht, pp. 331–345. https://doi.org/10.1007/978-94-011-0351-0_23

APHA/AWWA/WEF, 2012. Standard Methods for the Examination of Water and Wastewater. Stand. Methods.

Demanèche, S., Sanguin, H., Poté, J., Navarro, E., Bernillon, D., Mavingui, P., Wildi, W., Vogel, T.M., Simonet, P., 2008. Antibiotic-resistant soil bacteria in transgenic Antibiotic-resistant soil bacteria in transgenic plant fields. PNAS 105, 3957–3962. https://doi.org/10.1073/pnas.0800072105

Lanham, A.B., Ricardo, A.R., Albuquerque, M.G.E., Pardelha, F., Carvalheira, M., Coma, M., Fradinho, J., Carvalho, G., Oehmen, A., Reis, M.A.M., 2013. Determination of the extraction kinetics for the quantification of polyhydroxyalkanoate monomers in mixed microbial systems. Process Biochem. 48, 1626–1634. https://doi.org/10.1016/j.procbio.2013.07.023

Lanham, A.B., Ricardo, A.R., Coma, M., Fradinho, J., Carvalheira, M., Oehmen, A., Carvalho, G., Reis, M.A.M., 2012. Optimisation of glycogen quantification in mixed microbial cultures. Bioresour. Technol. 118, 518–525. https://doi.org/10.1016/j.biortech.2012.05.087

Lücker, S., Steger, D., Urup, K., Macgregor, B.J., Wagner, M., Loy, A., 2007. Improved 16S rRNA-targeted probe set for analysis of sulfate-reducing bacteria by fluorescence in situ hybridization 69, 523–528. https://doi.org/10.1016/j.mimet.2007.02.00

Oehmen, A., Zeng, R.J., Saunders, A.M., Blackall, L.L., 2006. Anaerobic and aerobic metabolism of glycogen- accumulating organisms selected with propionate as the sole carbon source 2767–2778. https://doi.org/10.1099/mic.0.28065-0

Manz, W., Amann, R., Ludwig, W., Wagner, M., 1992. Phylogenetic Oligodeoxynucleotide Probes for the Major Subclasses of Proteobacteria : Problems and Solutions. Syst. Appl. Microbiol. 15, 593–600. https://doi.org/10.1016/S0723-2020(11)80121-9

Meyer, R.L., Saunders, A.M., Blackall, L.L., 2006. Putative glycogen-accumulating organisms belonging to the Alphaproteobacteria identified through rRNA-based stable isotope probing. Microbiology 152, 419–429

Murray, RGE, Doetsch, RN, Robinow, C., 1994. Determinative and cytological light microscopy. Methods Gen. Mol. Bacteriol. 21–41.

Nielson, P.H., Daim, H., Lemmer, H., 2009. FISH Handbook for Biological Wastewater Treatment: Identification and quantification of microorganisms in activated sludge and

biofilms by FISH, IWA Publishing. IWA Publishing Company, London.

Nittami, T., McIlroy, S., Seviour, E.M., Schroeder, S., Seviour, R.J., 2009. Candidatus Monilibacter spp., common bulking filaments in activated sludge, are members of Cluster III Defluviicoccus. Syst. Appl. Microbiol. 32, 480–489

Sanguin, H., Herrera, A., Oger-desfeux, C., Dechesne, A., Simonet, P., Navarro, E., Vogel, T.M., Moënne-loccoz, Y., Nesme, X., Grundmann, G.L., 2006. Development and validation of a prototype 16S rRNA- based taxonomic microarray for Alphaproteobacteria 8, 289–307. https://doi.org/10.1111/j.1462-2920.2005.00895.x

Wong, M.T., Tan, F.M., Ng, W.J., Liu, W.T., 2004. Identification and occurrence of tetrad-forming Alphaproteobacteria in anaerobic-aerobic activated sludge processes. Microbiology 150, 3741–3748. https://doi.org/10.1099/mic.0.27291-0

3.

THE IMPACT OF OPERATIONAL STRATEGIES ON THE PERFORMANCE OF A PHOTO-EBPR SYSTEM

SUMMARY: A novel Phototrophic - Enhanced Biological Phosphorus Removal (Photo-EBPR) system, consisting of a consortium of photosynthetic organisms and polyphosphate accumulating organisms (PAOs), was studied in this work. A sequencing batch reactor was fed with a mixture of acetate and propionate (75%-25%) and subjected to dark/light cycles in order to select a photo-EBPR system containing PAOs and photo-synthetic organisms, the latter likely providers of oxygen to the system. The results from the selection period (stage 1) showed that the photo-EBPR culture was capable of performing P release in the dark and P uptake in the presence of light, under limited oxygen concentrations. During the optimization period, the aeration period, which was initially provided at the end of the light phase, was gradually reduced until a non-aerated system was achieved, while the light intensity was increased. After optimization of the operational conditions, the selected consortium of photosynthetic organisms/PAOs showed high capacity of P removal in the light phase in the absence of air or other electron acceptor. A net P removal of 34 ± 3 mg P/L was achieved, with a volumetric P removal rate of 15 ± 2 mg P/L.h, and 79 ± 8 % of P removal from the system. Also, in limiting oxygen conditions, the P uptake rate was independent of the PHA consumption, which demonstrates that the organisms obtained energy for P removal from light. These results indicated that a photo-EBPR system can be a potential solution for P removal with low COD/P ratios and in the absence of air, prospecting the use of natural sunlight as illumination, which would reduce the costs of EBPR operation regarding aeration.

Key words: Enhanced biological phosphorus removal (EBPR); Polyphosphate accumulating organisms (PAOs); Photosynthetic organisms; Phototrophs; Low energy.

Published as: Carvalho, V.C.F., Freitas, E.B., Silva, P.J., Fradinho, J.C., Reis, M.A.M., Oehmen, A., 2018. The impact of operational strategies on the performance of a photo-EBPR system. Water Res. 129, 190–198. https://doi.org/10.1016/j.watres.2017.11.010

3.1. Introduction

Phosphorus (P) is an element with vast applications in the chemical and food industry, and particularly in the agronomical field, (Cordell et al., 2009). However, despite P reserves being limited, its utilization is continuously increasing. For this reason P can be frequently found in water streams (agricultural and industrial) in concentrations susceptible of causing eutrophication and unbalanced ecosystems (Cai et al., 2013). Therefore, it is crucial to treat the P containing streams and, ideally, to simultaneously recover this element and reuse it, for example as fertilizer.

Enhanced biological phosphorus removal (EBPR) is a sustainable process used to remove P from wastewaters (WW), in which polyphosphate accumulating organisms (PAOs) and glycogen accumulating organisms (GAOs) compete for the limited supply of organic carbon sources, namely, volatile fatty acids (VFAs) (Carvalheira et al. 2014a). The process relies on a specific group of bacteria – PAOs – that take up phosphate from WW in excess of their requirements, under sequential anaerobic and aerobic periods (Yuan et al., 2012). In the anaerobic period, PAOs are able to hydrolyze intracellularly stored polyphosphate (Poly-P) and glycogen, producing energy and reducing power to take up VFAs and convert them into intracellular polyhydroxyalkanoates (PHAs). In the aerobic period, PAOs oxidize the PHA, obtaining energy for replenishing glycogen levels, for growth, and P uptake. In PAOs, this P uptake is higher than the P released anaerobically, leading to a net P removal from WW by concentrating it in the sludge and subsequent sludge wastage (Oehmen et al., 2004).

EBPR is a well-known system, with thoroughly optimized operational parameters, but nevertheless, requires aeration. Of the several factors that contribute towards operational costs in wastewater treatment plants (WWTP), aeration requirements are the most substantial. With the goal of aeration reduction, a new photosynthetic enhanced biological phosphorous removal system (photo-EBPR) is proposed making use of a consortium culture composed by oxygen evolving photosynthetic organisms (like microalgae, cyanobacteria) and bacteria (PAOs), in which the photosynthetic organisms can use light to produce the oxygen necessary for the system operation. The novel photo-EBPR configuration presented in this study is based on sequential dark and light cycles, where in the dark phase (with no oxygen production by photosynthetic organisms) the system will be anaerobic and PAOs will take up VFAs and convert them into PHA using the energy from poly-P and glycogen hydrolysis. In the light phase, photosynthetic organisms will use the light to produce ATP while generating oxygen that can be used by PAOs to oxidize PHA and obtain ATP for P uptake.

It is known that microalgae can grow rapidly and thrive in stringent but illuminated conditions. They require phosphorus for growth since it is an essential element for cellular constituents such as phospholipids, nucleotides and nucleic acids. Nevertheless, under certain conditions, microalgae can be triggered to take up much more phosphorus than that necessary for growth. This additional phosphorus uptake can be stored as polyphosphate, which can then be used by the cell as an internal resource when the external phosphorus concentration

is growth limiting. With this feature, algae can positively contribute towards P removal from wastewaters (Brown and Shilton, 2014).

The biotreatment of wastewater with algae to remove nutrients such as nitrogen and phosphorus and to provide oxygen for aerobic bacteria was proposed over 50 years ago by Oswald and Gotaas (1957) (Abdel-Raouf et al., 2012). Nevertheless, the use of a PAO-algae consortium to remove P via a photo-EBPR process has not previously been demonstrated or studied.

This work intends to demonstrate the possibility of selecting an microalgal-bacterial consortium that accumulates high phosphorus levels by applying dark/light periods in a strategy analogous to conventional EBPR operation (anaerobic/aerobic periods). During the 10 months of system operation, the COD concentration was gradually increased, sodium carbonate was introduced, the light intensity was changed and air was gradually removed. Also, this work evaluates the capacity of this new operating strategy in leading to a photosynthetic system with increased P removal capacity.

3.2. Materials and Methods

3.2.1. Photo-EBPR reactor

A sequencing batch reactor (SBR), with a working volume of 3.8 L was inoculated with sludge from an EBPR reactor, already enriched in PAOs (*Accumulibacter* phosphatis) and operated according to Carvalheira et al. (2014a) with a sludge retention time (SRT) of 12 days.

The SBR was subjected to transient illumination, provided by an internal halogen lamp (200W). It was operated in 8 h cycles, with 3 h dark, 4 h light and 1h of idle period. The idle period included settling time (30 minutes), the removal of supernatant and the beginning of argon sparging 10 minutes before the beginning of the next cycle. Argon was also continuously sparged during the dark phase to assure this phase was operated under anaerobic conditions. The reactor was fed in the beginning of the dark phase with 1.8 L of synthetic medium and was operated with a hydraulic retention time (HRT) of 16 h. The culture selection stage started with a light intensity of 328 W/m^2 (average of light intensity in Portugal during the year) (Gschwind et al., 2006), an SRT of 20 days (biomass was purged in the light phase, before air supply) and a chemical oxygen demand (COD) of 60 mg/L in the feed, where the carbon source was a mixture of acetate and propionate (75% / 25% of COD) to guarantee the proliferation of PAOs over GAOs (Lopez-Vazquez et al., 2009) . During this selection stage, air was supplied in the last two hours of the light phase to ensure that the cultures were not limited by oxygen (Table 1). The synthetic medium fed to the reactor was composed by 75 % (v/v) of a phosphate solution (253 mg/L of K_2HPO_4 and 154 mg/L of KH_2PO_4) and 25 % (v/v) of carbon medium with a concentration per litre of: 0.4 g $C_2H_3O_2Na.3H_2O$; 41 μL $C_3H_6O_2$; 0.59 g NH_4Cl; 0.95 g $MgSO_4.7H_2O$; 0.44 g $CaCl_2.2H_2O$; 11.7 mg allyl-N thiourea (ATU) to prevent nitrification; 31.7 mg ethylene-diaminetetraacetic (EDTA) and 3.17 mL of a micronutrients solution, with a concentration per litre of: 1.5 g $FeCl_3.6H_2O$; 0.15 g H_3BO_3; 0.03 g $CuSO_4.5H_2O$;

0.18 g KI; 0.12 g $MnCl_2.4H_2O$; 0.06 g $Na_2MoO.2H_2O$; 0.12 g $ZnSO_4.7H_2O$ and 0.15 g $CoCl_2.6H_2O$. EDTA is used to prevent the precipitation of salts, like Ca^{2+} and PO_4^{3-} present in the media.

3.2.2. Optimization of operational conditions

After the culture selection stage, the operational conditions of the SBR were optimized (**Table 3.1**). To increase the CO_2 concentration, Na_2CO_3 was fed every cycle, 5 minutes before the light period began. Other parameters like SRT, COD load, light intensity, time of aeration and settling time were also adjusted during the optimization stages.

Table 3.1 - Photo-EBPR operational conditions over the 233 days of experimental study

Description	Stage	Experimental period (d)	SRT (d)	Feed concentration of COD (mg/L)	Light intensity (W/m^2)	Time of aeration in Light period (h)	Inorganic carbon addition (mg C/L)	Settling time (min)
Culture Selection	1	105	20	60-160	328	2	0	45
Optimization of operational conditions	2	42	10	160	328	1.5	30	45
	3	48	10	200	328	1.5	30	30
	4	28	10	200	600	1.5	30	30
	5	10	10	200	600	0	30	30

3.2.3. Chlorophyll quantification

The chlorophyll concentration was calculated according to Lichtenthaler (1987), using the following equation: $C_{a+b}(\mu g/mL) = 5.24A_{664.2} + 22.24A_{648.6}$, where C_{a+b} accounts for the concentration of both chlorophyll *a* and *b*, while A is the supernatant absorbance at the indicated wavelength.

3.3. Results and discussion

3.3.1. Results

3.3.1.1 Photo-EBPR culture selection (Stage 1)

The culture selection period (stage 1) started with a feed concentration of 60 mg P/L and a COD concentration of 60 mg/L (**Figure 3.1**,**Figure 3.2**). Three sequential phases were imposed to the reactor: dark anaerobic; light without external air supply and light with aeration.

During dark, VFA uptake was immediately sustained by both phosphate release and carbohydrates consumption, with concomitant PHA production (**Figure 3.1-A**). During the light phase, phosphate was only taken up during the aerated period with PHAs being consumed and carbohydrates replenished.

COD was gradually increased from 60 to 160 mg COD/L in the feed and by day 7 (**Figure 3.1-B**), and more distinctively by day 14 (**Figure 3.1-C**), the culture could already take up some phosphate during the light period with no aeration. With the increase of the COD from 60 to 160 mg COD/L in the feed, the amount of phosphate uptake increased, reaching more than 30 mg P/L of net P removal.

The presence of light stimulated the growth of photosynthetic microorganisms, like algae and cyanobacteria. This is possible since the reactor inoculum was a mixed culture and as such, already contained photosynthetic organisms, even if in a marginal amount.

Since the results from the selection stage indicated that the reactor could perform EBPR, it was necessary to understand which are the optimal conditions for the photo-EBPR operation. Thus, 4 different optimization stages were carried out.

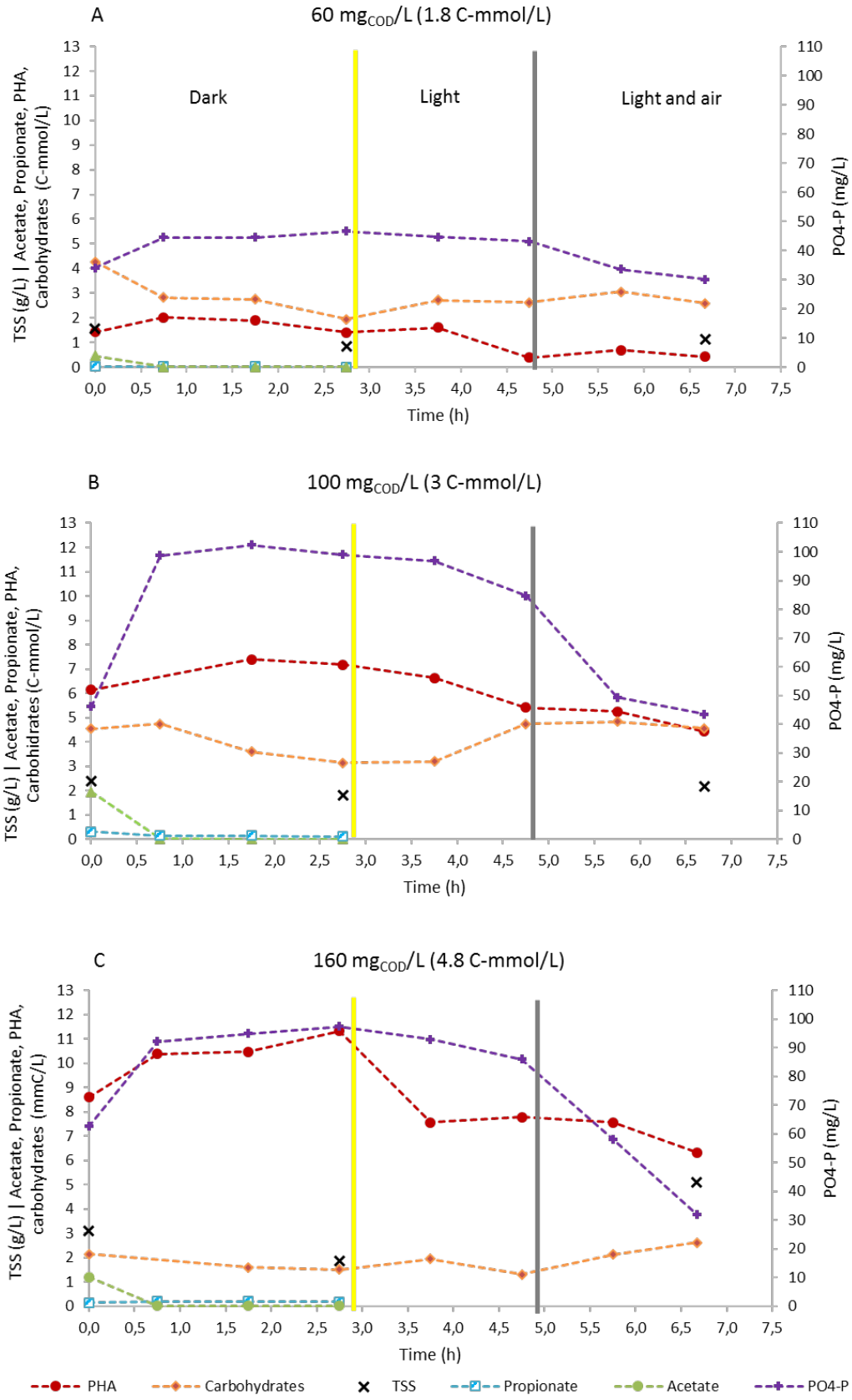

Figure 3.1 - Profile of phosphate, TSS and carbon transformations in the reactor during stage 1 (SRT: 20 d; Light Intensity 328 W/m2; Air: 2 h; no external inorganic carbon). A – 60 mg COD/L; B – 100 mg COD/L; C – 160 mg COD/L

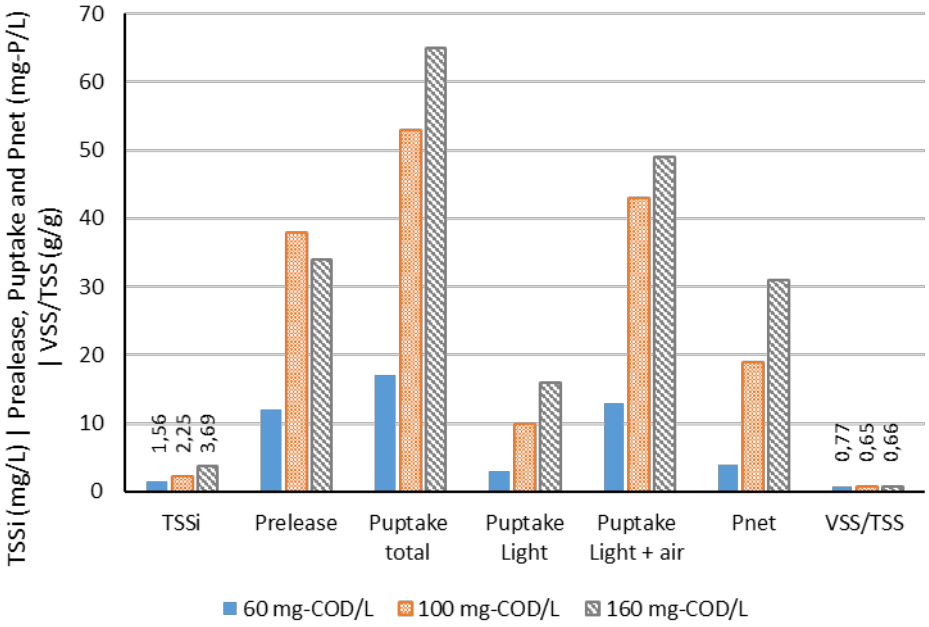

Figure 3.2 - TSS and phosphorus parameters of the reactor during stage 1 (SRT: 20 d; Light Intensity 328 W/m2; Air: 2h; no external inorganic carbon)

3.3.1.2 Process optimization

The process optimization was divided in 4 stages (stage 1 corresponds to the selection phase): in stage 2, the system was supplemented with Na_2CO_3, SRT was decreased from 20 to 10 days and aeration time was also reduced from 2h to 1h30min; in stage 3 COD was increased from 160 mg/L to 200 mg/L in the feed; in stage 4 light intensity was increased to 600 W/m^2 and in stage 5 external aeration was completely removed (**Table 3.1**).

The changes made in stage 2 led to an increase of the P release during the dark phase from 34 ± 4 mg P/L observed in stage 1 to 57 ± 2 mg P/L in stage 2, while maintaining high levels for total P uptake of 85 ± 1 mg P/L in all the light phase (**Figure 3.3-A**) and P net removals of 27 ± 5 mg P/L (**Figure 3.3-A**; **Table 3.2**). This increase in P release should not be directly caused by the addition of Na_2CO_3 - since this was only added five minutes before the beginning of light phase - but be most likely due to the increase of PHA accumulation and consumption during the dark and light phases, respectively, leading to higher P storage during the light phase and higher P release in the dark phase. Interestingly, a 2.5 fold increase of the P uptake, from 16 ± 6 mg P/L to 40 ± 6 mg P/L, was observed in the non-aerated light phase, resulting in 47 % of P being removed in this phase. Despite the enhanced P removal during the non-aerated light phase only a small amount of PHA was consumed (ΔPHA = 1.08 ± 0.4 mmol C/L) resulting in a yield of P removal per PHA consumed ($Y_{P/PHA}$) of 1.37 ± 0.54 mmol P/mmol C. As practically no PHA was consumed during this period, it can be hypothesized that P uptake was mainly done by photosynthetic microorganisms. Regarding the aerated light phase, once the air was turned on, PHA consumption increased (ΔPHA = 1.51 ± 0.23 mmol C/L) and $Y_{P/PHA}$ was 0.58 ± 0.03 mmol P/ mmol C, 2 times lower than in the non-aerated light phase (**Table 3.2**).

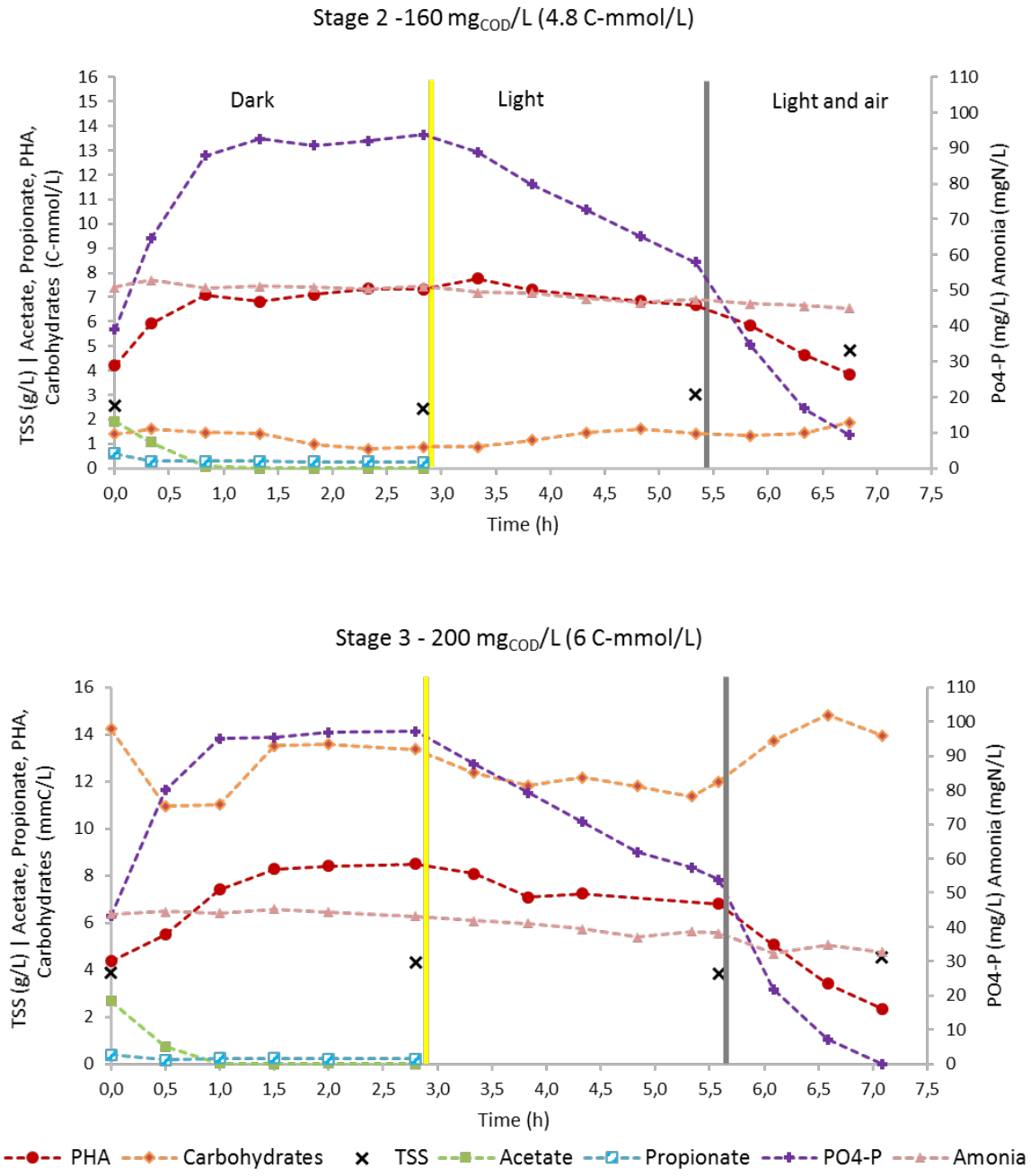

Figure 3.3 - Profile of P and carbon transformation in the reactor during stage 2 and 3.
a) Stage 2 - 160 mg COD/L in the feed and b) stage 3 - 200 mg COD/L in the feed. Other conditions: SRT: 10 d; HRT: 16 h; Light Intensity 328 W/m2; Air: 1.5 h; external inorganic carbon.

Table 3.2 - Stoichiometric and kinetic parameters for the photo-EBPR during stage 2, 3, 4 e 5.

		Stage	2[a]	3 [b]	4 [c]	5[a]
Dark phase		$P_{release}$	57 (2)	53 (15)	32 (10)	30 (2)
		q_r	32 (8)	24 (6)	20 (12)	23 (1)
		TSS_i	2.24 (0.47)	3.79 (0.45)	4.21 (0.82)	3.39 (0.23)
		$Y_{PHA/VFAs}$	1.28 (0.20)	1.72 (0.33)	1.34 (0.23)	1.12 (0.19)
		$Y_{P/VFAs}$	0.75 (0.01)	0.45 (0.14)	0.55 (0.39)	0.23 (0.01)
		$Y_{Gly/VFAs}$	0.26 (0.03)	0.20 (0.09)	0.71 (0.56)	0.34 (0.21)
Light phase	Non – aerated	P_{uptake}	40 (6)	52 (13)	54 (13)	64 (5)
		q_u	6 (2)	8 (3)	7 (1)	6 (0)
		ΔPHA	1.08(0.40)	2.22 (0.71)	6.78 (1.14)	8.04 (1.46)
	Aerated	P_{uptake}	53 (5)	43 (17)	22 (2)	n/a
		q_u	15 (4)	11 (3)	5 (2)	n/a
		ΔPHA	1.51 (0.23)	5.36 (1.36)	1.21 (0.02)	n/a
	Total	P_{uptake}	85 (1)	94 (4)	76 (11)	64 (5)
		q_u	10 (1)	9 (1)	7 (1)	6 (0)
		Pnet	27 (5)	41 (17)	43 (17)	34 (3)
		VSS/TSS	0.71 (0.01)	0.68 (0.01)	0.69 (0.02)	0.80 (0.02)

$P_{release}$, P_{uptake}, Pnet and P final in mg-P/L; VSS/TSS in g/g; TSS_i in g/L; q_r, q_u in mg-P/mg-X.h; ΔPHA in C-mmolC/L

a- Average of 2 cycles; b - Average of 4 cycles; c - Average of 3 cycles.

Stage 2: Light intensity=328 W/m²; time of air =1.5 h; settling time = 45 min and 160 mg-COD/L in the feed

Stage 3: Light intensity=328 W/m²; time of air =1.5 h; settling time = 30 min and 200 mg-COD/L in the feed

Stage 4: Light intensity=600 W/m²; time of air =1.5 h; settling time = 30 min and 200 mg-COD/L in the feed

Stage 5: Light intensity=600 W/m²; no air; settling time = 30 min and 200 mg-COD/L in the feed

Given the improved P uptake rates (total, light and light with air) observed during stage 2, COD was increased from 160 to 200 mg/L in the feed (stage 3) (**Figure 3.3-B**). As a consequence of higher carbon availability, the biomass concentration increased and a higher total P uptake (94 ± 4 mg P/L) was observed, resulting, in comparison with stage 2, in a lower effluent P concentration during stage 3, with a net P removal above 40 mg P/L (**Table 3.2**). Another implication of the COD increase was an augmentation of the net PHA production during the dark period from 2.79 ± 0.47 mmol C/L in stage 2 to 6.59 ± 1.74 mmol C/L in stage 3. Also, in comparison to stage 2, a two-fold increase on PHA consumption (ΔPHA = 2.22 ± 0.71 mmol C/L) in the non-aerated light period and a three-fold increase (ΔPHA = 5.36 ± 1.36 mmol C/L) in the period with aeration was observed in stage 3 (**Table 3.2**). Nevertheless, from stage 2 to 3, no significant change was observed in all specific P release/uptake rates (q_r, q_u).

It is known that the algae activity is influenced by light, usually leading to more oxygen production with increased light intensities (Muñoz and Guieysse, 2006). In stage 4 the light intensity of the system was increased from 328 to 600 W/m², to mimic a summer day in Portugal. The higher light intensity resulted in an increase of biomass concentration from 3.79 g TSS/L in stage 3 to 4.21 g TSS/L in stage 4 (**Table 3.2**). However, the most evident changes

occurred during the light phase, namely a constant P uptake and a much higher PHA consumption in the non-aerated period (ΔPHA = 6.78 ± 1.14 mmol C/L), resulting in a $Y_{P/PHA}$ of 0.22 ± 0.10 mmol P/mmol C in the first 1.5 hours of the light period. The PHA stopped to be consumed after 1.5 hours of light (with no air) even when the air was turned on. The specific P uptake rates were similar in the non-aerated and aerated light period (q_u= 7 ± 1 mg P/mg X.h and q_u=5 ± 2 mg P/mg X.h, respectively). The VSS/TSS ratio was similar in stage 3 (0.68 ±0.01) and stage 4 (0.69 ±0.01) (**Table 3.2**).

One of the main goals of this study was to operate a photo-EBPR system that did not require aeration, but instead, could use light to produce enough oxygen to drive phosphorus removal by the microbial community. The results from the light phase in stage 4 (**Figure 3.4-A**) suggested that P could be removed without external aeration. However, the impact of eliminating the aeration phase in terms of process capacity and culture performance had to be assessed. Therefore, in the next step air supply was totally removed. The results showed that the removal of air did not substantially affect the net P removal and the specific P release/uptake values (**Figure 3.4-B; Table 3.2**). In fact, despite the decrease in the biomass concentration (4.34 ± 0.86 to 3.24 ± 0.05 g TSS/L), a net P removal of 34 ± 3 mg P/L was achieved, the specific P release rate was maintained and the specific P uptake rate (q_u= 6 ± 0 mg P/mg X.h) was similar as the one obtained in stage 4 (**Table 3.2**). Moreover, the P uptake was constant throughout the entire light phase, as observed in stage 4. However, in stage 5, two distinct PHA profiles can be clearly observed, with a relatively high PHA consumption in the first 1.5 hour period corresponding to a $Y_{P/PHA}$ of 0.16 ±0.03 P-mol/C-mol and a period with very low PHA consumption in the last 2.5 hours of the cycle associated with a continuous P removal, with a $Y_{P/PHA}$ of 1.22 ±0.06 mmol P/mmol C.

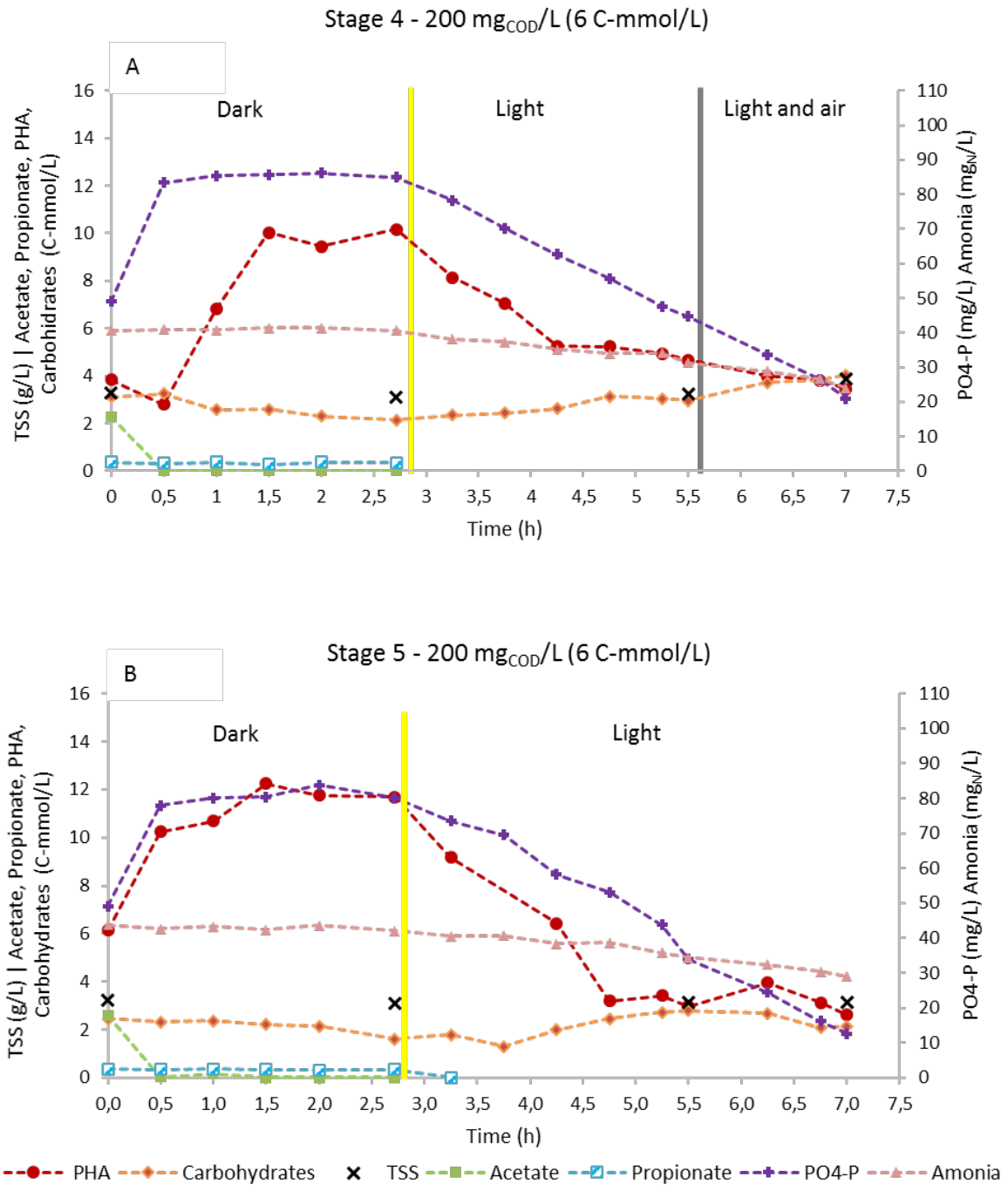

Figure 3.4 - Profile of P and carbon transformation in the reactor during stage 4 and 5.
a) stage 4 - SRT: 10 d; HRT:16 h; Light Intensity 600 W/m2; Air: 1.5 h; external inorganic carbon and b) stage 5 - SRT: 10 d; HRT:16 h; Light Intensity 600 W/m2; No Air; external inorganic carbon.

Microbial characterization by FISH analysis (**Table 3.3**) showed an increase of the abundance of PAOs from stage 1 to stage 5 and more GAO organisms were found in stage 5 (showed by the application of CPB_654 probe). Also, a steady increase of the presence of photosynthetic organisms was observed throughout the experimental work (**Figure 3.5**) with a co-dominance shared with PAOs by stage 5 (**Table 3.3**). However, despite the increase in GAO abundance, PAOs were still the dominant bacterial population present in the biomass (**Table 3.3**).

Table 3.3 - FISH results for the evaluation of the microbial population during the selection and optimization of the photo-EBPR system.

Stage \ Probe	PAOmix (PAOs)	CPB_654 (GAOs)	SuperDFmix (TFOmix + DFmix + DF198)	TFOmix	Prop207
Stage 1 (60 COD/L)	++	+	+-	-	-
Stage 1 (160 COD/L)	+++	++	-	-	-
Stage 3	+++	+ -	+ - -	-	-
Stage 5	+++	++	+ - -	-	-

(–) non present; (+ – –) almost non-existent; (+ –) present; (+) abundant; (++) very abundant; (+++) dominant.

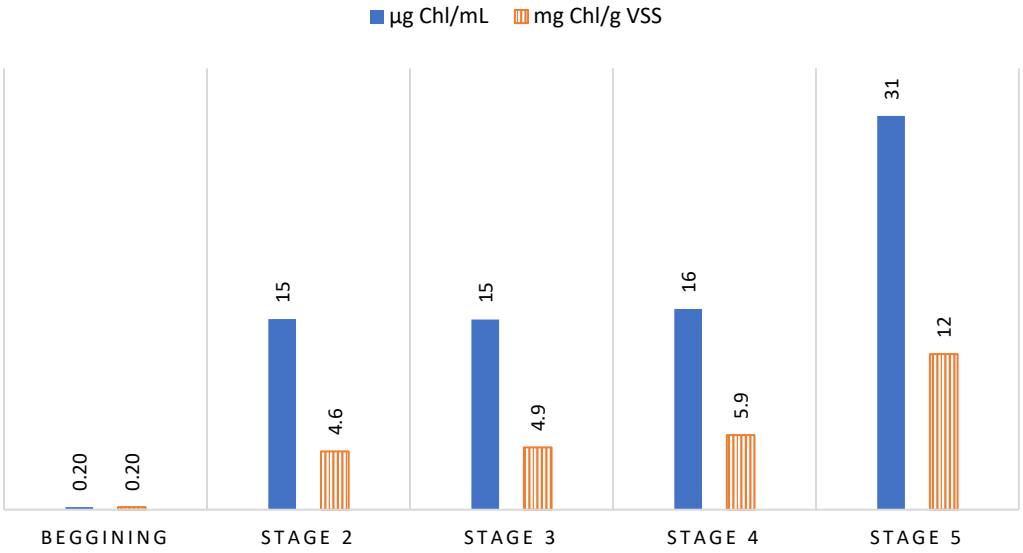

Figure 3.5 - Profile of chlorophyll concentration during the five stages of the photo-EBPR operation.

The evolution of the photosynthetic organism's presence in the reactor could be followed through the sludge chlorophyll content (**Figure 3.5**). Results show an increase of the chlorophyll content along the reactor operation, from the residual value of 0.20 mg Chl/g VSS presented at the beginning of the reactor operation up to 12 mg Chl/g VSS at stage 5 (**Figure 3.5**). In stage 2 and 3, with a light intensity of 328 W/m^2, similar concentrations of chlorophylls were found 4.6 and 4.9 mg Chl/g VSS, respectively. The increase of light intensity in stage 4, led only to a small increase of the chlorophyll concentration to 5.9 mg Chl/g VSS. However, when external aeration was removed in stage 5, and the culture became dependent on light as energy source, the chlorophyll concentration more than doubled, to 12 mg Chl/g VSS, indicating the intensification of the amount of the photosynthetic microorganisms present in the photo-EBPR culture.

3.3.2. Discussion

3.3.2.1 Process optimization

The results presented above showed that the photo-EBPR system is an effective option for P removal using light instead of aeration. To obtain such a system, adequate conditions must be applied in order to select a photo-EBPR culture.

Interestingly, the new EBPR system selected in this work shows a different trend in the correlation between PHA and P as compared with the traditional EBPR process. In photo-EBPR, oxygen availability seems to be the trigger factor for PHA consumption, but not for P removal.

By sequentially analyzing the results from stage 2 up to stage 5 it is likely that in stage 2 and 3, the culture was subjected to oxygen limiting conditions during the non-aerated light phase (**Figure 3.6**). As a result, PHA consumption was low during the non-aerated period and the observed P removal was likely due to the activity of photosynthetic organisms (**Figure 3.4**). When aeration commenced, the culture had the availability of both oxygen and light, which led to an increase of the P uptake rate since the culture could obtain energy from light and from PHA oxidation.

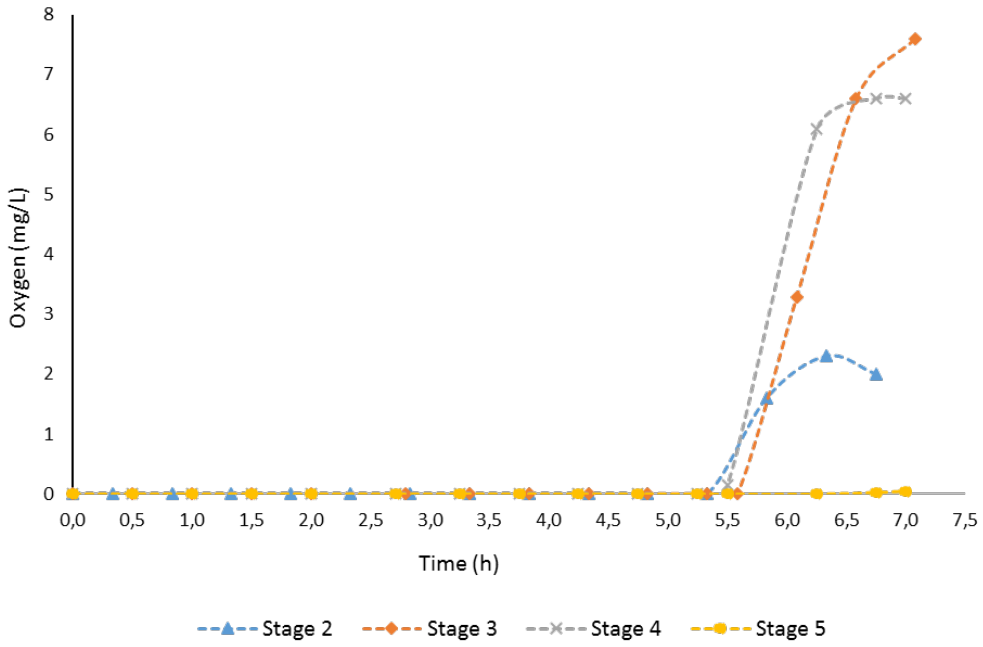

Figure 3.6 - Profile of Oxygen concentration during the cycle in stage 2, stage 3, stage 4 and stage 5.

In stage 4, the light intensity of the system was increased, likely stimulating the oxygen production by algae/cyanobacteria, although not enough to increase the dissolved oxygen concentration in the light phase (**Figure 3.6**). Nevertheless, the increased auto-oxygenation of the system appeared to shift the PHA consumption to the early hours of the light phase. However, the P uptake rate remained constant throughout the entire light phase. This indicates that while PHA consumption was dependent on oxygen availability, the P uptake was neither

dependent on PHA consumption, nor on the oxygen availability per se, since the presence of aeration in the last hours of stage 4 cycles (**Figure 3.6**) had no impact on the P uptake rate. This was more clearly confirmed in stage 5 where aeration was completely removed and the P uptake rate was still constant during the entire light phase, independently of PHA consumption.

It is clear that P uptake is independent of PHA consumption in stage 4 and 5. It can be hypothesized that when the auto-oxygenation of the system increased, microorganisms (likely PAOs) could consume PHA in the first 1.5 hours of the light phase, but under oxygen limited conditions. It is possible that under such conditions, the energy requirement for maintenance may be higher than under a fully oxygenated system, a possibility also suggested by the results of Carvalheira et al. 2014c when traditional PAO systems were operated under limited oxygen conditions (0.1-0.3 mg O_2/L). If this is the case, then the energy generated during PHA consumption could meet the energy requirements for growth, glycogen replenishment and maintenance, but not for phosphate uptake. Also, since FISH results indicate a bacterial dominance by PAOs, and in the dark phase the PHA accumulation was associated with P release, it can be speculated that PAOs may have other means to get energy to take up P during the light phase that does not depend on PHA consumption. Indeed, the presence of a photosynthetic population evidently capable of taking up P in the presence of light suggests that the PHA consumption was not necessarily the dominant mechanism leading to P removal. This is confirmed by the $Y_{P/PHA}$ obtained in this study that ranged from 0.81±0.21 to 1.37±0.54 P-mol/C-mol in certain periods of the light phase, which are much higher than the values of 0.41 P-mol/C-mol estimated by the model of Smolders et al. (1994) in traditional PAO systems. This seems to indicate that energy for P uptake during limited oxygen concentration levels was obtained from light. Future work will focus on clarifying this matter, as well as ascertain which organisms are responsible for P uptake and through which mechanisms is the P preferentially removed.

Another interesting observation is that the increase of light intensity from stages 2-3 to stages 4-5 did not lead to an increase of the P uptake rate during the non-aerated light periods (**Table 3.2**). This suggests that at stage 2 and 3 the photosynthetic organisms were already being operated under light saturating conditions regarding their P uptake capacity. Finally, this work indicates that by the end of stage 5 the mixed culture system was indeed capable of an enhanced P removal in transient illuminated conditions without the need of aeration. Regarding the final quality of the effluent, P concentrations in stage 5 were over the limit discharge levels. It should be referred, however, that this system was operated with an influent with a very low COD/P ratio (3.3 mg COD/ mg P) and a P concentration in the feed of 60 mg P/L. Despite these demanding conditions, the culture was in fact capable of a net P removal of 34 ± 3 mg P/L.

3.3.2.2 Impacts of the study

The use of a photobioreactor for the treatment of wastewaters containing carbon and P was shown to be possible with a significant reduction/elimination of the oxygen supply,

which might have a significant impact on operational costs in a WWTP. On the other hand, CO_2 was likely consumed in the system by photosynthetic organisms and its supplementation as Na_2CO_3 increased the global P removal. This brings a further asset to the proposed photo-EBPR system, since it can potentially serve to sequester CO_2 emissions from off-gas.

Comparing the results obtained in this study with the ones obtained in some recent studies on EBPR performance, it is possible to conclude that the proposed photo-EBPR culture achieved higher net P removal with lower COD/P ratios. In stage 5, the net P removal obtained was 34 mg/L with a COD/P ratio of 100/30, while Carvalheira et al. (2014a) and Carvalheira et al. (2014b) only obtained 20 mg/L of net P removal with a COD/P ratio of 100/10. A recent study from Valverde-Pérez et al. (2016), using real wastewaters in laboratory tests, obtained a net P removal of 10 mg/L with a COD/P ratio of 100/5, while comparing with results obtained in full-scale WWTPs with EBPR systems, López-Vázquez et al. (2008) indicated a net P removal of 10.4 mg/L with a COD/P ratio of 100/10. These results show that in the Photo-EBPR system much less carbon is required to remove the same amount of P. Broughton et al. (2008) estimated that the limit of influent COD/P ratio to be 100/7.7 for a conventional industrial EBPR wastewater treatment system. Considering that >30 ppm of P could be removed from a feed containing 200 mg COD, our results show that this photo-EBPR system can achieve COD/P ratios approximately half of that achieved by a conventional EBPR system. The results show the ability of the photo-EBPR system to treat effluents with low carbon concentration and high P amount, which can occur in agricultural wastewaters (Cai et al., 2013).

Several studies focused on P removal in wastewater stabilization pounds (WSP) (Vendramelli et al. 2016), (Leite et al., 2009) (Powell et al., 2009),(Powell et al., 2011)) showed P removal between 0 and 15 mg/L by these systems (with high HRT and SRT), which was less than what was obtained in this study. High P influent concentrations of 30 mg/L were tested by Powell et al. 2009, however, in a 25 days test, they could not remove all the phosphorus fed to the system, while in the present work, with 60 mg P/L in the influent, 79 ± 8 % of the P was removed in just 4h.

Like the present photo-EBPR process, wastewater treatment in WSP requires large land space, as more than one pond with a high HRT is normally needed, and the effluent is commonly only used as water for irrigation, as it does not meet the discharge limits. Using the photo-EBPR system, some of these limitations of the WSP could be overcome, as the natural diurnal cycle would permit wastewater treatment in one single reactor: during the night, no oxygen is produced by algae, so, the system is anaerobic and the COD is degraded; during the day, oxygen will be produced and nutrients will be removed, either by photosynthetic organisms and/or by other bacteria. The low HRT of the photo-EBPR system – 16 hours – and the good quality effluent, would allow efficient treatment of the wastewaters, enabling the discharge of the effluent to natural water bodies and the application of the sludge as fertilizer. In order to effectively operate this photo-EBPR system at large-scale, a different process design would be required as compared to WSPs, a design that would maximize the contact between the natural sunlight and the mixed liquor.

Photo-EBPR systems can potentially be operated as stand-alone processes with natural sunlight and no aeration, or combined in phases with aeration periods to remove high levels of P with low COD/P ratios (e.g. industrial wastewaters). It can be applied to wastewater treatment plants using the final P rich sludge (**Figure 3.7**) as fertilizer or recovering the phosphorus for further reutilization. Although this system requires more available space, to intensify the light capture, and being situated in places with good solar exposition, the photo – EBPR system has low maintenance requirements as it is a low cost (i.e. no aeration requirements) and simple process to operate.

Figure 3.7 - Picture of the reactor in the end of the selection phase (stage 1): a- reactor during light phase; b-reactor during settling phase.

3.4. Conclusions

This study demonstrates that a photo-EBPR culture can be selected under transient illuminated conditions with no need of aeration. Results indicate the development of a photosynthetic organisms/PAO consortium capable of P release/uptake cycles with a net P removal over 30 mg P/L. The uncoupling of P uptake from the PHA consumption, as well as the constant P uptake rate, independently of oxygen availability, suggests that the selected microorganisms are able to obtain ATP for P uptake using light. Thus, the photo-EBPR system can be applied for the treatment of effluents with low COD/P ratios (lower than the values required for traditional EBPR systems), with the addition that aeration can be minimized/removed, leading to costs reduction. Future studies will focus on improving the effluent P quality and operating the system under natural illumination conditions, while further elucidating P uptake mechanisms.

REFERENCES

Abdel-Raouf, N., Al-Homaidan, A.A. & Ibraheem, I.B.M., 2012. Microalgae and wastewater treatment. Saudi Journal of Biological Sciences, 19(3), 257–275. Available at: http://dx.doi.org/10.1016/j.sjbs.2012.04.005.

Albertsen, M., Mcllroy, S.J., Stokholm-Bjerregaard, M., Karst, S.M., Nielsen, P.H., 2016. "Candidatus Propionivibrio aalborgensis": A novel glycogen accumulating organism abundant in full-scale enhanced biological phosphorus removal plants. Frontiers in Microbiology, 7(JUL), pp.1–17.

Amann RI. 1995a. In situ identification of microorganisms by whole cell hybridization with rRNA-targeted nucleic acid probes. – Bookmetrix Analysis. In F. Akermans, A., van Elsas, J., de Bruijn, ed. Molecular Microbial Ecology Manual. Springer Netherlands, 1–15.

Amann, R.I. Binder, B.J., Olson, R.J., Chisholm, S.W., Devereux, R., Stahl, D.A, 1990b. Combination of 16S rRNA-Targeted Oligonucleotide Probes with Flow Cytometry for Analyzing Mixed Microbial Populations. Applied and Environmental Microbiology, 56(6), 1919–1925.

Brown, N. & Shilton, A., 2014. Luxury uptake of phosphorus by microalgae in waste stabilisation ponds: Current understanding and future direction. Reviews in Environmental Science and Biotechnology, 13(3), 321–328.

Broughton, A., Pratt, S., Shilton, A., 2008. Enhanced biological phosphorus removal for high-strength wastewater with a low rbCOD:P ratio. Bioresource Technology 99 (5), 1236-1241.

Cai, T., Park, S.Y. & Li, Y., 2013. Nutrient recovery from wastewater streams by microalgae: Status and prospects. Renewable and Sustainable Energy Reviews, 19, 360–369. Available at: http://dx.doi.org/10.1016/j.rser.2012.11.030.

Carvalheira, M., Oehmen, A., Carvalho, G. & Reis, M., 2014c. Survival strategies of polyphosphate accumulating organisms and glycogen accumulating organisms under conditions of low organic loading. Bioresource Technology, 172, 290–296. Available at: http://linkinghub.elsevier.com/retrieve/pii/S0960852414013108.

Carvalheira, M., Oehmen, A., Carvalho, G. & Reis, M.A.M., 2014a. The effect of substrate competition on the metabolism of polyphosphate accumulating organisms (PAOs). Water Research, 64, 149–159.

Carvalheira, M., Oehmen, A., Carvalho, G., Eusébio, M.A.M., 2014b. The impact of aeration on the competition between polyphosphate accumulating organisms and glycogen accumulating organisms. Water Research, 66, 296–307.

Cordell, D., Drangert, J.O. & White, S., 2009. The story of phosphorus: Global food security and food for thought. Global Environmental Change, 19(2), 292–305.

Crocetti, G.R., Hugenholtz, P., Bond, P.L., Schuler, A., Keller, J., Jenkins, D., Blackall, L.L., 2000. Identification of polyphosphate-accumulating organisms and design of 16SrRNA-

directed probes for their detection and quantitation. Applied and Environmental Microbiology, 66(3), 1175–1182.

Daims, H., Bruhl, A., Amann, R., Schleifer, K.H., Wagner, M., 1999. The domain-specific probe EUB338 is insufficient for the detection of all Bacteria: development and evaluation of a more comprehensive probe set. Systematic and applied microbiology, 22(3), 434–44. Available at: http://www.sciencedirect.com/science/article/pii/S0723202099800538.

Gschwind, B., Ménard, L., Albuisson, M., Wald, L., 2006. Converting a successful research project into a sustainable service: the case of the SoDa Web service. Environ. Modell. Softw. 21, 1555e1561. Available at: http://www.soda-is.com/eng/index.html.

Leite, V.D., Junior, G.B.A., Sousa, J. T., Lopes, W.S.,Henrique, I.N., 2009. Treatment of domestic wastewater in shallow waste stabilization ponds for agricultural irrigation reuse. Journal of Urban and Environmental Engineering, 3(2), 58–62.

Lichtenthaler, H., K., 1987. Chlorophylls and carotenoids: Pigments of photosynthetic biomembranes. Methods in Enzymologym, 148, 350-382.Lopez-Vazquez, C.M., Oehmen, A., Yuan, Z., Loosdrecht, M.C., 2009. Modeling the PAO-GAO competition: Effects of carbon source, pH and temperature. Water Research, 43(2), 450–462.

López-Vázquez, Carlos M. Hooijmans, C.M., Brdjanovic, D., Gijzen, H J., Loosdrecht, M. C., 2008. Factors affecting the microbial populations at full-scale enhanced biological phosphorus removal (EBPR) wastewater treatment plants in The Netherlands. Water Research, 42(10–11), 2349–2360.

Mata, T.M., Martins, A.A. & Caetano, N.S., 2010. Microalgae for biodiesel production and other applications: A review. Renewable and Sustainable Energy Reviews, 14(1), 217–232.

Meyer, R.L., Saunders, A.M., Blackall, L.L. 2006. Putative glycogen-accumulating organisms belonging to the Alphaproteobacteria identified through rRNA-based stable isotope probing. Microbiology, 152, 419-29.

Mcilroy, S.J., Nittami, T., Kanai, E., Fukuda, J., Saunders, A.M., Nielsen, P.H., 2015. Re-appraisal of the phylogeny and fluorescence in situ hybridization probes for the analysis of the Competibacteraceae in wastewater treatment systems. Environmental Microbiology Reports, 7(2), 166–174.

Muñoz, R. & Guieysse, B., 2006. Algal-bacterial processes for the treatment of hazardous contaminants: A review. Water Research, 40(15), 2799–2815.

Nelson, David L., Lehninger, Albert L., Cox Michael M., "Photosynthesis: harvesting light energy" in Lehninger Principles of Biochemistry., 2008. W.H. Freeman and Company, New York, 742-764.Nittami, T., Mcllroy, S., Seviour E.M., Schroeder, S., Seviour, R.J., 2009. Candidatus Monilibacter spp., common bulking filaments in activated sludge, are members of Cluster III Defluviicoccus. Systematic and Applied Microbiology, 32(7), 480–489. Available at: http://dx.doi.org/10.1016/j.syapm.2009.07.003.

Oehmen, A., Yuan, Z., Blackall, L.L., Keller, J., 2004. Short-term effects of carbon source on the competition of polyphosphate accumulating organsisms and glycogen accumulating organisms. Water Science and Technology, 50(10), 139–144.

Powell, N., Shilton, A., Pratt, S., Chiti,Y., 2008. Luxury uptake of phosphorus by microalgae in waste stabilization ponds. Environmental Science and Technology, 42(16), pp.5958–5962.

Powell, N.,Shilton, A., Chisti, Y., Pratt, S., 2009. Towards a luxury uptake process via microalgae - Defining the polyphosphate dynamics. Water Research, 43(17), 4207–4213. Available at: http://dx.doi.org/10.1016/j.watres.2009.06.011.

Smolders, G. J. F., van der Meij, J., van Loosdrecht, M. C. M., & Heijnen, J. J. (1994). Model of the anaerobic metabolism of the biological phosphorus removal process: Stoichiometry and pH influence. Biotechnology and Bioengineering, 43(6), 461–470.

Valverde-Pérez, B., Wágner, D. S., Lóránt, B., Gülay, A., Smets, B.F., Plósz, B. G., 2016. Short-sludge age EBPR process - Microbial and biochemical process characterisation during reactor start-up and operation. Water Research, 104, 320–329.

Vendramelli, R.A., Vijay, S. & Yuan, Q., 2016. Phosphorus Removal Mechanisms in a Facultative Wastewater Stabilization Pond. Water, Air, & Soil Pollution, 227(11), 417. Available at: http://link.springer.com/10.1007/s11270-016-3130-6.

Wong, M.T., Tan, F.M., Ng, W.J., Liu, W.T., 2004. Identification and occurrence of tetrad-forming Alphaproteobacteria in anaerobic-aerobic activated sludge processes. Microbiology, 150(11), 3741–3748.

Yuan, Z., Pratt, S. & Batstone, D.J., 2012. Phosphorus recovery from wastewater through microbial processes. Current Opinion in Biotechnology, 23(6), 878–883. Available at: http://dx.doi.org/10.1016/j.copbio.2012.08.001.

4.
THE EFFECT OF SEED SLUDGE ON THE SELECTION OF A PHOTO-EBPR SYSTEM

SUMMARY: The Phototrophic – Enhanced biological phosphorus removal system (photo-EBPR) was recently proposed as an alternative photosynthetic process for conventional phosphorus removal. Previous work showed the possibility of obtaining a photo-EBPR system starting from a culture already enriched in polyphosphate accumulating organisms (PAOs). The present work evaluated whether the same could be achieved starting from conventional activated sludge. Therefore, a sequencing batch reactor inoculated with sludge from a wastewater treatment plant (WWTP), was fed with a mixture of acetate and propionate (75%:25%) and subjected to dark/light cycles to select a photo-EBPR system, containing PAOs and photosynthetic organisms, the oxygen providers for the system. The obtained results showed that it is possible to obtain a photo-EBPR system starting from a WWTP sludge, although the process is slower than when started with a sludge already enriched in PAOs. At the end of 29 days of operation time, the system could remove 60 ± 2 mg P/L of phosphorus in the light period, from which 13 ± 1 mg P/L was removed during the phase without external air supply. These results indicate that a photo-EBPR system can be obtained independently of the seed sludge initially used, provided that a suitable operating strategy is implemented, i.e., by imposing conditions that favour the growth and coexistence of PAOs and photosynthetic microorganisms.

Keywords: Photo-Enhanced biological phosphorus removal; Polyphosphate accumulating organisms; Photosynthetic organisms; Low energy.

Published as: Carvalho, V.C.F., Freitas, E.B., Fradinho, J.C., Reis, M.A.M., Oehmen, A., 2019. The effect of seed sludge on the selection of a photo-EBPR system. N. Biotechnol. 49, 112–119. https://doi.org/10.1016/j.nbt.2018.10.003

4.1. Introduction

P is an element with vast applications in agriculture and industry, but which can negatively impact the environment when released. Reserves of P are limited, making it crucial to treat P rich wastewater streams, preferably through processes that allow P recovery and reutilization, to promote the circular economy and an environmentally friendly P cycle (Cai et al., 2013).

One of the options for treatment of P-rich wastewater streams is the enhanced biological phosphorus removal (EBPR) system, which requires intensive aeration and thus increased operational costs (Rosso et al., 2008). With the aim of reducing the aeration dependence of EBPR processes, a new phototrophic-enhanced biological phosphorus removal (photo-EBPR) process was recently proposed (Carvalho et al., 2018). The photo-EBPR system is composed of a consortium of polyphosphate (poly-P) accumulating organisms (PAOs) and photosynthetic microorganisms (algae, cyanobacteria and others) operated under dark/light cycles. During the dark anaerobic period, glycogen is hydrolyzed and poly-P is degraded (P release), producing the necessary energy for volatile fatty acids consumption and accumulation as polyhydroxyalkanoates (PHA). During the light phase, photosynthetic microorganisms produce the necessary oxygen and, consequently, PHA is consumed, providing energy and carbon for the regeneration of poly-P and glycogen pools (Carvalho et al., 2018; Smolders et al., 1994b, 1994a). In addition, photosynthetic microorganisms can have an important role in P removal (Brown and Shilton, 2014).

The first results obtained in **chapter 3** demonstrated that the photo-EBPR system is capable of treating streams with high P concentration (60 mg P/L) without need of external aeration. This high P removal capacity, combined with low-cost operation, makes the system competitive when compared with the traditional EBPR systems. In the same chapter, it was shown that it is possible to obtain a photo-EBPR system using as inoculum a sludge already enriched in *Candidatus* Accumulibacter phosphatis. These organisms are well known for their capacity for high P uptake in conventional EBPR systems. However, it is important to clarify if the establishment of a photo-EBPR system can also occur starting from a seed sludge which has not been enriched in PAOs.

The aim of this study was to determine if it is possible to select a photo-EBPR system using ordinary activated sludge from a conventional WWTP as seed sludge and compare the results obtained previously. Selecting a photo-EBPR culture directly from activated sludge could simplify the start-up and facilitate the implementation of photo-EBPR systems.

4.2. Materials and Methods

4.2.1 Photo-EBPR reactors

A sequencing batch reactor (SBR), with a working volume of 4.4 L, was inoculated with sludge from an aerobic tank from a WWTP in Lisbon, Portugal, and subjected to transient

illumination, provided by an internal halogen lamp (200W) with a light intensity of 328 W/m^2 (average of light intensity in Portugal during the year) (Gschwind, B., Ménard, L., Albuisson, M., Wald, 2006). It was operated in 8 h cycles, with 3h dark, 4h light and 1h of idle period. The idle period included settling time (30 min), the purge of supernatant and argon sparging 10 min before the beginning of the next cycle. To guarantee the anaerobic conditions of the dark phase, argon was continuously sparged. The SBR was fed in the beginning of the dark phase with 2.2 L of synthetic medium and was operated with a hydraulic retention time (HRT) of 16 h and a sludge retention time (SRT) of 20 d (biomass was purged in the light phase, before air supply). The study started with the reactor being operated with a phosphorus concentration and a chemical oxygen demand (COD), both of 60 mg/L in the feed, where the carbon source was a mixture of acetate and propionate (75% / 25% of COD) to guarantee the proliferation of PAOs over GAOs (Lopez-Vazquez et al., 2009) . Air was supplied in the last 2 h of the light phase to ensure that the culture was not limited by O_2. The synthetic medium feed was composed of 75% (v/v) of a phosphate solution (253 mg/L of K_2HPO_4 and 154 mg/L of KH_2PO_4) and 25% (v/v) of carbon medium with a concentration per L of: 0.4 g sodium acetate trihydrate; 41 µL propionic acid; 0.59 g NH_4Cl; 0.95 g $MgSO_4.7H_2O$; 0.44 g $CaCl_2.2H_2O$; 11.7 mg allyl-N thiourea (ATU) to prevent nitrification; 31.7 mg ethylene-diaminetetraacetic (EDTA) to prevent salt precipitation and 3.17 mL of a micronutrients solution, with a concentration per L of: 1.5 g $FeCl_3.6H_2O$; 0.15 g H_3BO_3; 0.03 g $CuSO_4.5H_2O$; 0.18 g KI; 0.12 g $MnCl_2.4H_2O$; 0.06 g $Na_2MoO.2H_2O$; 0.12 g $ZnSO_4.7H_2O$ and 0.15 g $CoCl_2.6H_2O$. Over the 29 days of operation, the COD was increased from 60 to 160 mg/L (**Table 4.1**).

Table 4.1 - Profile of COD increase during the 29 days of the experimental trial.

COD in feed (mg/L)	60	100	160
Operation days	1-7	8-14	15-29

4.2.1. Chlorophyll quantification

The chlorophyll concentration was calculated according to Lichtenthaler (1987), using the following equation: $C_{a+b}(\mu g/mL) = 5.24A_{664.2} + 22.24A_{648.6}$, where C_{a+b} accounts for the concentration of both chlorophyll *a* and *b*, while A is the supernatant absorbance at the indicated wavelength.

4.3. Results and Discussion

4.3.1. Photo-EBPR culture selection strategy

In order to understand the effect of the seed sludge in the selection of a photo-EBPR system, this study started with an inoculum of activated sludge from an aerobic tank from a WWTP (Beirolas, Lisbon). The WWTP is a conventional activated sludge plant located in Lisbon, with the capacity to treat a population size of 213.510 equivalent inhabitants, corresponding to an average daily flow of 54.500 m^3/day ("Águas do Tejo Atlântico. Statistics for Beirolas

WWTP," 2018). The culture selection period started with an initial P concentration of 60 mg P/L and a small COD feed concentration of just 60 mg/L, in order to restrict the organic carbon uptake to the dark anaerobic phase.

Results show that in the first cycle with 60 mg/L of COD, the culture could not carry out EBPR despite VFAs being totally consumed during the dark phase (**Figure 4.1-A**). This suggests that the sludge from the WWTP was not enriched in PAOs and therefore not capable of immediately performing P release/uptake cycles. However, since VFAs were completely consumed in the dark period, COD in the feed was increased to 100 mg/L and, after 7 d selection, the SBR started performing EBPR (**Figure 4.1-B**). The VFAs were fully taken up and converted to PHA during the dark phase, while carbohydrates were degraded and P was released. During the light phase, P was taken up (at a higher efficiency during the aerated period), PHA was consumed and carbohydrate levels were replenished (**Figure 4.1-B**). Over time, algae began to grow as a consequence of the transient illuminated cycles. This was possible since the reactor inoculum was a mixed culture and, as such, already contained photosynthetic organisms, albeit a marginal amount. At this stage, the culture could already take up some P (10 mg P/L) during the light period with no aeration, a feature that may have resulted from the O_2 availability from algae or direct P uptake by algae. Nevertheless, higher P uptake (22 mg P/L) occurred in the presence of air (**Figure 4.1-B;Figure 4.2**), suggesting that during the light phase with no aeration, the O2 produced by the photosynthetic microorganisms was insufficient and limited the amount of P uptake.

When COD was increased to 160 mg/L, by day 15, (**Figure 4.1-C**), P release (47 ± 4 mg P/L) and total P uptake (60 ± 2 mg P/L) also increased (**Figure 4.2**), probably due to the higher PHA availability. The higher carbon availability in the dark phase enabled more PHA accumulation and during the light phase the energy for P uptake by PAOs was obtained through PHA consumption. When more PHA is available, more P can be taken up by PAOs. However, we cannot ignore the possibility that the increase of photosynthetic microorganisms, as well as leading to a gradual oxygenation of the system, may have also contributed to the P removal.

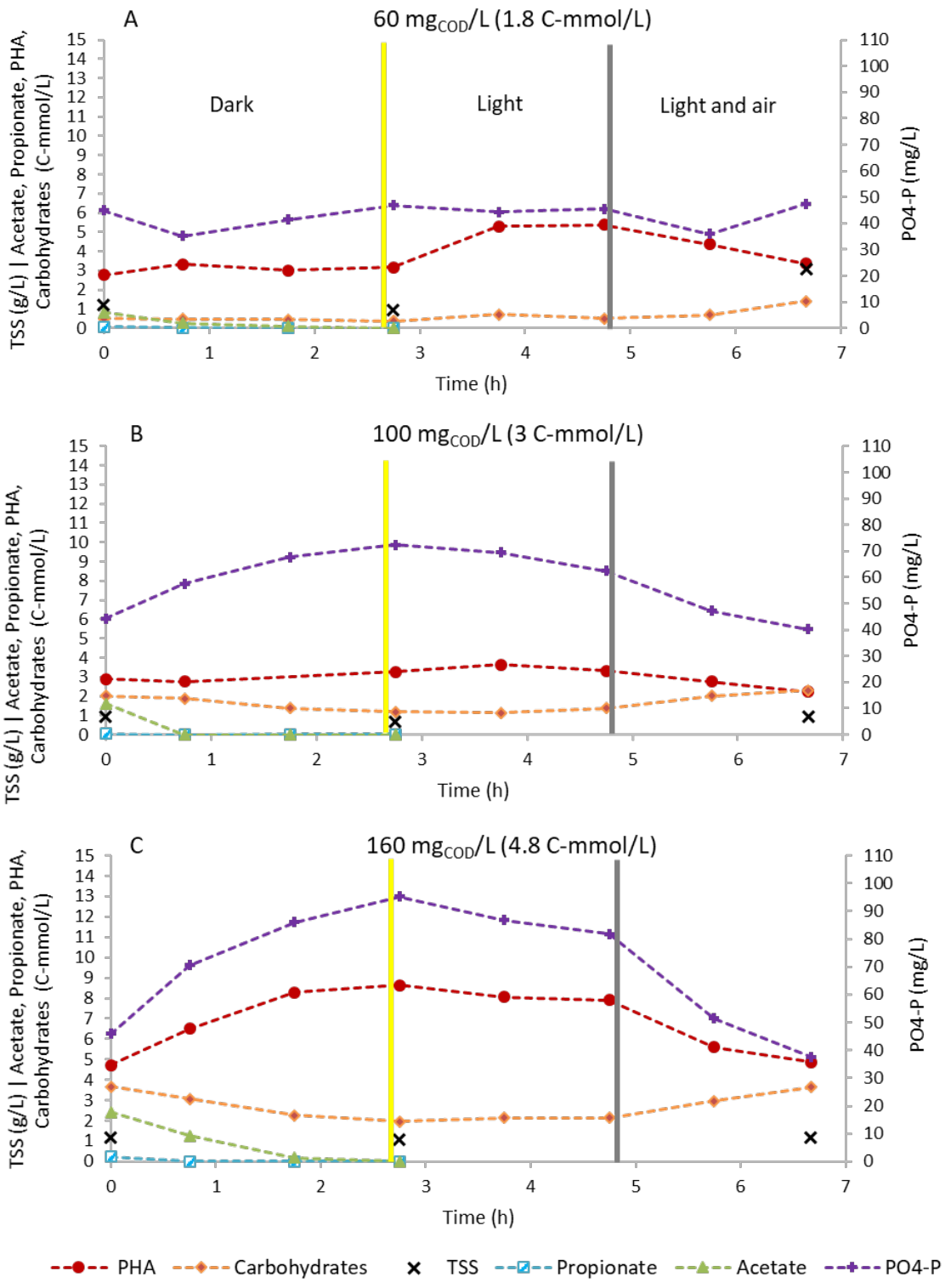

Figure 4.1 - Profile of P and carbon transformation during SBR operation.
A – CODfeed= 60 mg/L; B – CODfeed= 100 mg/L and C – CODfeed= 160 mg/L.

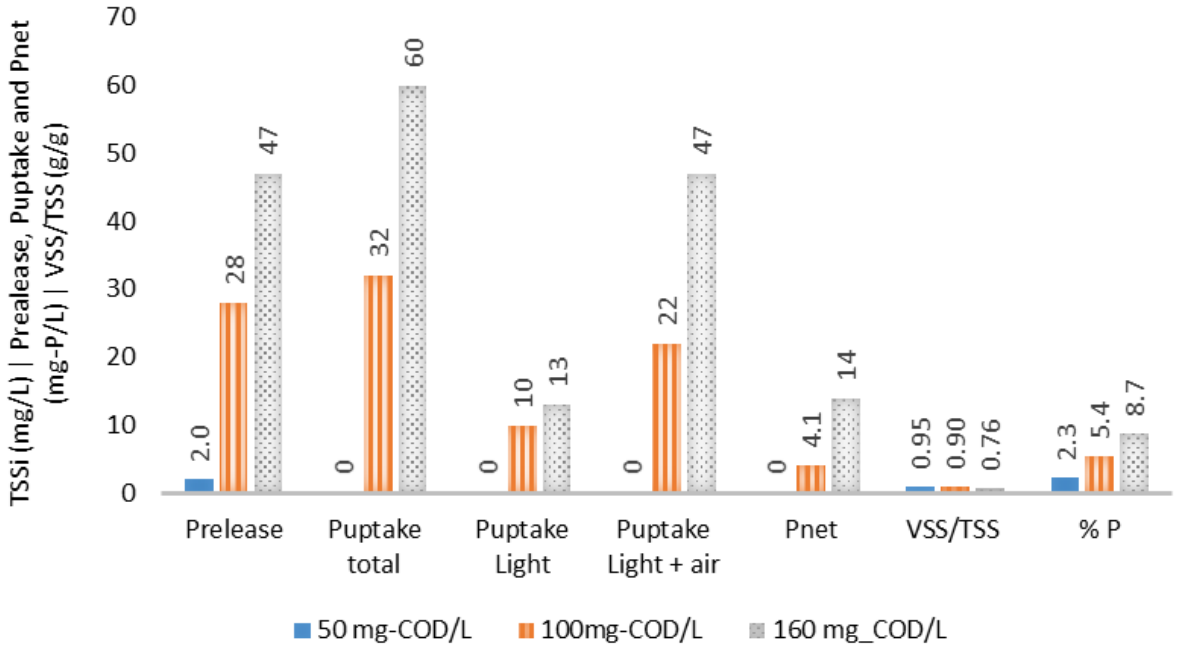

Figure 4.2 - TSS and phosphorous parameters obtained during the SBR operation time.

The P uptake in the light period with no aeration also increased with selection time, from 0 to 13 ± 1 mg P/L, associated with photosynthetic microorganisms' growth and the increase in the quantity of PAOs (**Table 4.2**) similarly to that described in Carvalho et al., 2018. The increase of photosynthetic microorganisms was monitored by microscope observation and confirmed by chlorophyll extraction and quantification (**Figure 4.3**). The results confirmed the increase in the amount of the photosynthetic microorganisms during the photo-EBPR selection period and supported the hypothesis of increased phototrophic O_2 production during the illumination period without external aeration. The amount of poly-P was also monitored during the SBR operation time, with Loeffler's Methylene Blue staining. Typical PAO aggregates were observed, with the intracellular vesicles of poly-P stained in pink-purple due to the high content in poly-P, which accumulates as intracellular granules (**Figure 4.4**).

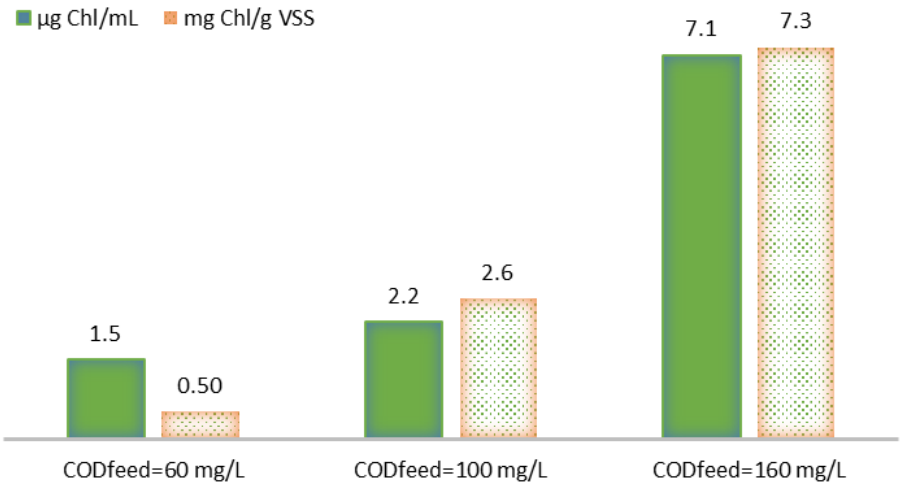

Figure 4.3 - Chlorophyll concentration during the SBR operation time.

Table 4.2 - FISH analysis from the evolution of the photo-EBPR culture.

	ALF969 (Alphaproteobacteria)	**BET42a** (Betaproteobacteria)	**GAM42a** (Gammaproteobacteria)	**Delta495** (Deltaproteobacteria)	**PAOmix** (PAOs)	**CPB_654** (Competibacter)	**Prop 207** (Propionivibrio)	**G Rb** (Rhodobacter and Roseobacter)	**Rhodo2** (Rhodospirillum)	**Rhodopseud** (Rhodopseudomonas)	**SuperDFmix** (Defluviicoccus vanus cluster I, II, III)	**TFOmix** (Defluviicoccus vanus cluster I)
COD_{feed}= 60 mg/L	+-	+	+	+--	+	+-	-	+	+--	+--	-	-
COD_{feed}= 160 mg/L	+--	++	++	+--	++	++	-	+-	-	+--	+	-

(–) non present; (+ – –) almost non-existent; (+ –) present; (+) abundant; (++) very abundant; (+++) dominant.

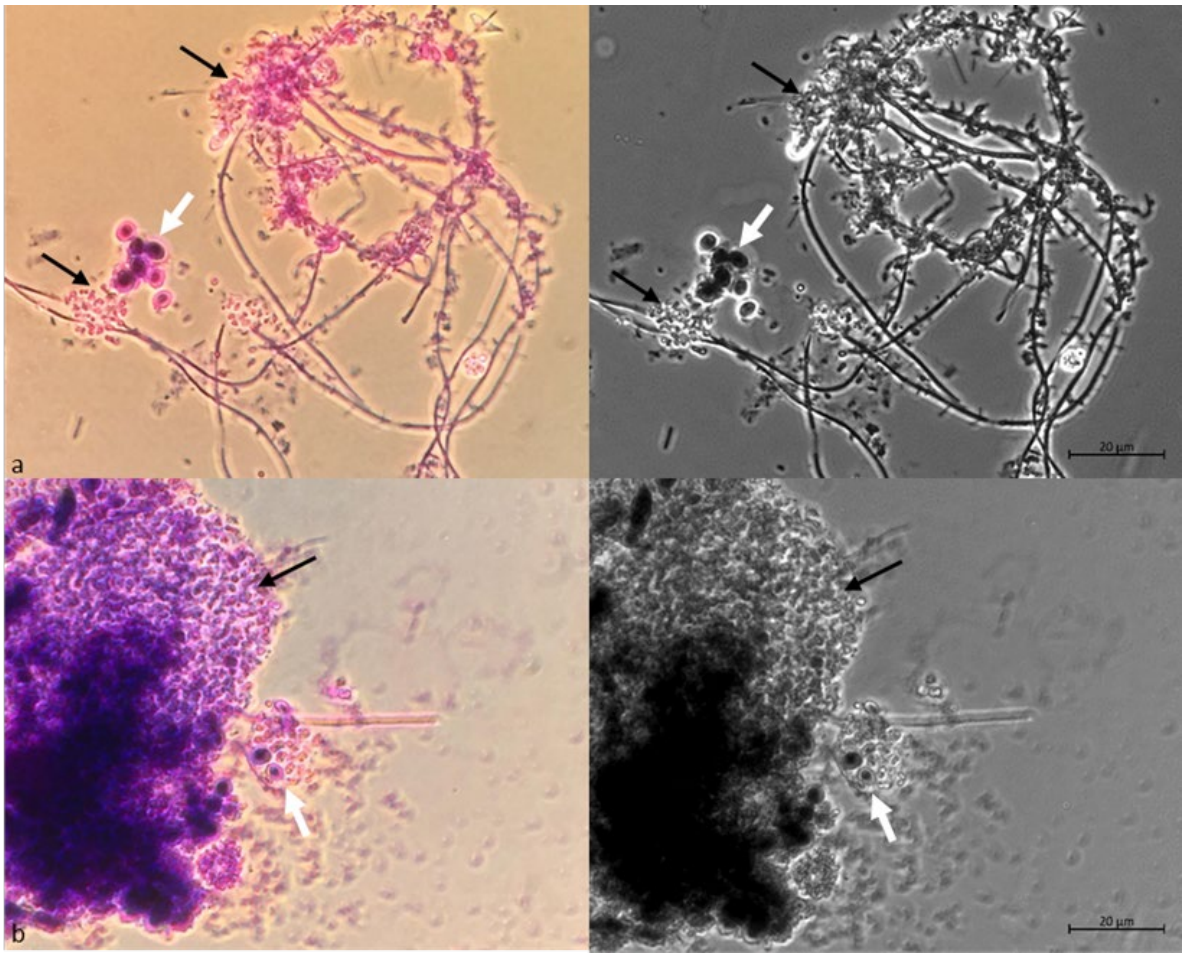

Figure 4.4 - Loeffler's methylene blue staining of the biomass during SBR operation, at 1000 X, brightfield. a) CODfeed= 60 mg/L; b) CODfeed= 160 mg/L. Black arrows show the poly-P accumulating bacteria that stains in pink/purple. White arrows show algae. The scale bar for all panels is 20 µm.

The percentage of P in the sludge increased from 2.3 % to 8.7 % during the selection time, proving the increased capacity of the system to accumulate P, and thus, its ability to perform EBPR (**Figure 4.2**). The VSS/TSS ratio obtained at the end of the selection period was similar during both selection strategies (**Table 4.3**), indicating the same P sludge content, when compared with the results obtained with a sludge enriched in PAOs in **chapter 3** (Carvalho et al., 2018). The P removal efficiency increased from 0 at the beginning of operation to 67% ± 9 for a COD of 160 mg/L, contributing to the increase of the net P removal up to 14 ± 7 mg P/L (**Figure 4.2**). However, this value was lower than that previously observed in **chapter 3** (Carvalho et al. 2018) at the same COD concentration, where a net P removal of 30 mg P/L was obtained (**Table 4.3**). However, the active biomass obtained in this study (0.97 ± 0.36 g/L) was less than half that in **chapter 3** (2.26 ± 0.21 g/L), indicating a similar specific net P removal achieved (**Table 4.3**). It was also clear that the selection period was faster in **chapter 3**, which took 14 days to reach a photo-EBPR system, against the 29 days needed with a sludge from a WWTP (**Table 4.3**). Nevertheless, despite requiring a longer selection period, it was indeed possible to start from an activated sludge seed and obtain a culture enriched in a consortium

of PAOs and photosynthetic organisms, with an exhibited ability to remove P in the absence of air.

FISH results (**Table 4.2**) confirmed the increase in amount of *Candidatus* Accumulibacter phosphatis (PAO mix probe) (**Figure 4.5**) in the sludge and showed a decrease in that of *Rhodobacter* and *Roseobacter* (GRb probe) and *Rhodospirillum* (Rhodo2 probe) (**Figure 4.6**). However, the amount of glycogen accumulating organisms (GAOs) (CPB_654 and SuperDFMix probes) was higher in the last step of the selection of the photo-EBPR process, due to the increased time with higher O_2 availability in the system, as suggested previously (Carvalheira et al., 2014). GAOs use glycogen as their primary energy source for anaerobic VFA uptake and do not perform anaerobic P release or aerobic P uptake. Therefore, they do not contribute towards P removal in EBPR systems and even compete with PAOs for the carbon source. Thus, it is important to follow closely the presence of GAOs in EBPR systems (Oehmen et al., 2007a). Comparing the amount of PAOs at the end of the selection stage of the photo-EBPR process in both studies, it is evident that the photo-EBPR sludge became more enriched in PAOs when the seed sludge was already selected with *Candidatus* Accumulibacter phosphatis. However, the quantity of GAOs was the same, whether starting with sludge from a WWTP or from an EBPR reactor (**Table 4.2**).

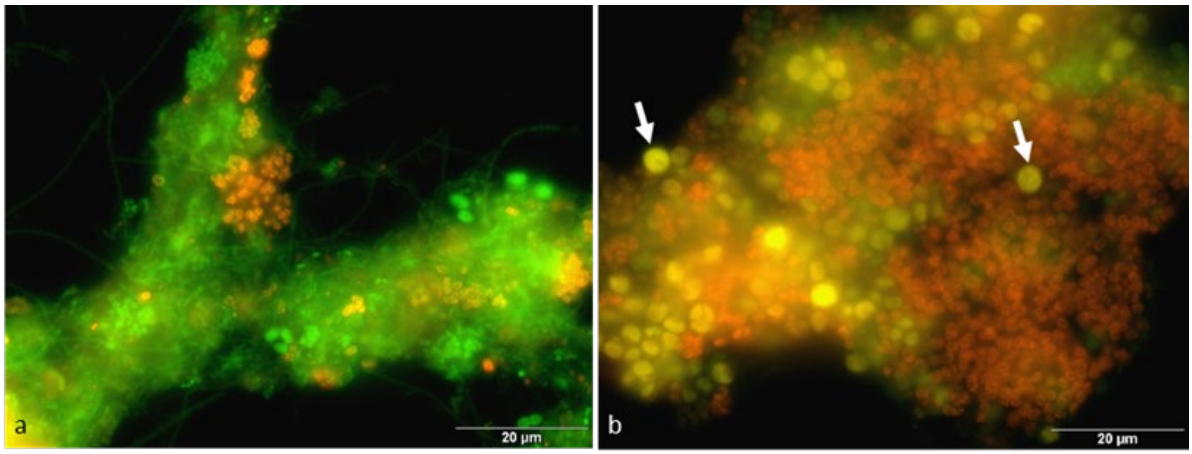

Figure 4.5 - FISH images of biomass samples taken during SBR operation, at 1000 X.
a) COD_{feed}= 60 mg/L; b) COD_{feed}= 160 mg/L. The images show bacteria hybridized with FITC EUBmix probe (green) and Cy3-labelled PAOmix (red). White arrows show algae not stained with any fluorochrome, but with yellowish color corresponding to their autofluorescence (b). The scale bars for all panels are 20 µm.

Table 4.3 - Comparison of the results obtained in the end of the selection period of the photo-EBPR obtained in the present work with the results obtained in **chapter 3** (Carvalho et al., 2018).

	$P_{release}$ (mg P/L)	P_{Uptake} (mg P/L)			X(g/L)	P net (mg P/L)	VSS/TSS	Initial chlorophyll concentration		Final chlorophyll concentration		Fish		Time of selection (days)
	Dark	Light	Light and air	Total				µg Chl/mL	mg Chl/g VSS	µg Chl/mL	mg Chl/g VSS	PAOmix	CPB_654	
Present work (Seed sludge from a WWTP)	47 ± 4	13 ± 1	47 ± 4	60 ± 2	0.97 ± 0.36	14 ± 7	0.76 ± 0.13	1.5	0.50	7.1	7.3	++	++	29
Chapter 3 Carvalho et al. (2018) (seed sludge enriched in *Accumulibacter* phosphatis)	34 ± 2	16 ± 6	49 ± 8	65 ± 1	2.26 ± 0.21	31 ± 0	0.66 ± 0.01	0.20	0.20	15	4.6	+++	++	14

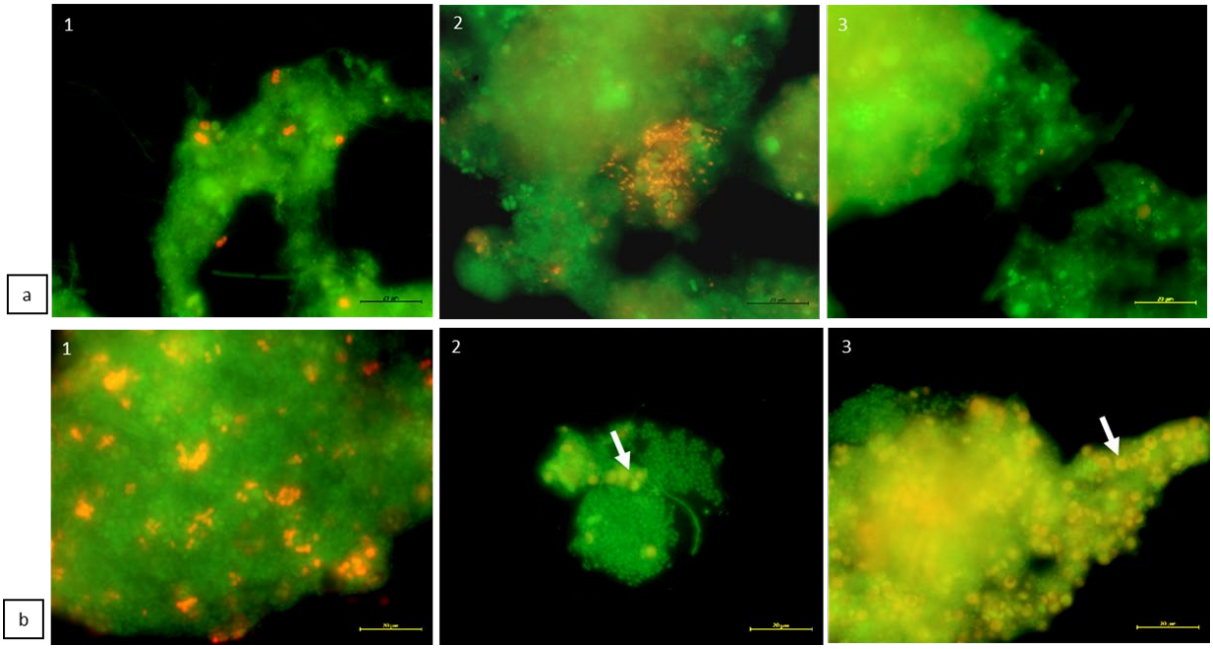

Figure 4.6 - FISH images of biomass samples taken during SBR operation, at 1000 X.
a) COD_{feed}= 60 mg/L; b) COD_{feed}= 160 mg/L. The images show bacteria hybridized with FITC EUBmix probe (green) and Cy3-labelled probes: 1) CPB_654 (red) for *Competibacter*; 2) GRb (red) for *Rhodobacter*/*Roseobacter*; 3) Rhodo 2 (red) for *Rhodospirillum*. White arrows show algae not stained with any fluorochrome, but with yellowish color corresponding to their autofluorescence. The scale bars for all panels are 20 μm.

The results suggest that the selection of the photo-EBPR could be easily achieved using sludge from a conventional WWTP by providing the right conditions, with no requirement for a first step selection in PAOs, saving time and decreasing the operation costs. This means that either in waste stabilization ponds (WSP) or in conventional WWTPs that do not perform EBPR, the photo-EBPR system could be implemented starting from sludge available on site. In the first case, and as discussed previously in **chapter 3** (Carvalho et al., 2018), the natural diurnal cycle would permit wastewater treatment in a single reactor: during the night, no O_2 is produced by algae, so the system is anaerobic and the COD is degraded, while during the day, O_2 will be produced and nutrients removed, either by photosynthetic organisms and/or by other bacteria. To implement the photo-EBPR system in WWTPs, the conventional EBPR operation could be adapted: one dark reactor could be designated for the anaerobic phase (occurring during night and day) and the illuminated/aerobic phase could take place in a second reactor. Effluent from the illuminated reactor could be recirculated to the dark reactor and differences in HRT between phases could be compensated, (1) during the day by the different volume of the reactors, and (2) during the night by allocating an equalization tank upstream or downstream of the anaerobic reactor (a strategy and reactor configuration to be defined in future studies).

The illuminated reactor requires a design that maximizes contact between natural sunlight and the mixed liquor. To intensify light capture, the photo-EBPR system needs more space compared to conventional EBPR, as well as being situated in locations with good solar

exposure. However, these two requirements can be met in WWTPs located in large city surroundings, as well as small towns and villages in rural areas where space is not a constraint for WWTPs and where wastewater is sometimes treated in WSP or high-rate algae pounds (HRAP) using algal-bacterial consortia. The photo-EBPR system could be an appropriate solution for these cases as it can optimize phosphorous removal combined with low-cost operation (no aeration needed) and low maintenance requirements.

Future tests will investigate whether the O_2 produced by phototrophs could also be used for N removal by nitrification/denitrification processes. Due to the low DO concentrations observed in the photo-EBPR process, an increase in O_2 level may be necessary considering the lower O_2 affinity (i.e. higher K_{O2} value) of nitrifiers as compared to PAOs (Carvalheira et al., 2014a; Henze et al., 2015) . Nevertheless, low DO opens the possibility of P removal in combination with simultaneous nitrification and denitrification (Zeng et al., 2003). In addition, it could promote the activity of denitrifying P removal in this process to further save the often-limiting carbon sources for denitrification. N removal would be a further asset for the photo-EBPR system in addition to P removal and recovery.

4.4. Conclusions

The present study indicates that conventional activated sludge can be enriched in PAOs and photosynthetic organisms capable of performing photosynthetic EBPR. Although the culture selection process was slower in comparison with cultures already enriched in PAOs (**chapter 3**) (Carvalho et al., 2018), activated sludge is widely available and a photo-EBPR system can be readily implemented without the need of a seed sludge previously enriched in PAOs. This start-up simplification can facilitate the implementation of photo-EBPR systems in WWTPs that currently do not perform EBPR and where there is no direct access to a sludge enriched in PAOs. The implementation of photo-EBPR systems will allow energy savings by eliminating the intensive aeration that increases operation costs in conventional EBPR.

REFERENCES

Águas do Tejo Atlântico. Statistics for Beirolas WWTP [WWW Document], 2018. URL https://www.aguasdotejoatlantico.adp.pt/content/beirolas (accessed 1.3.18).

Albertsen, M., McIlroy, S.J., Stokholm-Bjerregaard, M., Karst, S.M., Nielsen, P.H., 2016. "Candidatus Propionivibrio aalborgensis": A novel glycogen accumulating organism abundant in full-scale enhanced biological phosphorus removal plants. Front. Microbiol. 7, 1–17. https://doi.org/10.3389/fmicb.2016.01033

Amann, R.I., 1995. In situ identification of micro-organisms by whole cell hybridization with rRNA-targeted nucleic acid probes, in: Akkermans, A.D.L., Van Elsas, J.D., De Bruijn, F.J. (Eds.), Molecular Microbial Ecology Manual. Springer Netherlands, Dordrecht, pp. 331–345. https://doi.org/10.1007/978-94-011-0351-0_23

Amann, R.I., Binder, B.J., Olson, R.J., Chisholm, S.W., Devereux, R., Stahl, D.A., 1990. oligonucleotide probes with flow cytometry for analyzing mixed microbial populations . Combination of 16S rRNA-Targeted Oligonucleotide Probes with Flow Cytometry for Analyzing Mixed Microbial Populations. Appl. Environ. Microbiol. 56, 1919–1925. https://doi.org/10.1111/j.1469-8137.2004.01066.x

Brown, N., Shilton, A., 2014. Luxury uptake of phosphorus by microalgae in waste stabilisation ponds: Current understanding and future direction. Rev. Environ. Sci. Biotechnol. 13, 321–328. https://doi.org/10.1007/s11157-014-9337-3

Cai, T., Park, S.Y., Li, Y., 2013. Nutrient recovery from wastewater streams by microalgae: Status and prospects. Renew. Sustain. Energy Rev. 19, 360–369. https://doi.org/10.1016/j.rser.2012.11.030

Carvalheira, Mónica, Oehmen, A., Carvalho, G., Eusébio, M., Reis, M.A.M., 2014. The impact of aeration on the competition between polyphosphate accumulating organisms and glycogen accumulating organisms. Water Res. 66, 296–307. https://doi.org/10.1016/j.watres.2014.08.033

Carvalheira, M., Oehmen, A., Carvalho, G., Reis, M., 2014. Survival strategies of polyphosphate accumulating organisms and glycogen accumulating organisms under conditions of low organic loading. Bioresour. Technol. 172, 290–296. https://doi.org/10.1016/j.biortech.2014.09.059

Carvalho, V.C.F., Freitas, E.B., Silva, P.J., Fradinho, J.C., Reis, M.A.M., Oehmen, A., 2018. The impact of operational strategies on the performance of a photo-EBPR system. Water Res. 129, 190–198. https://doi.org/10.1016/j.watres.2017.11.010

Crocetti, G.R., Hugenholtz, P., Bond, P.L., Schuler, A.J., Keller, J., Jenkins, D., Blackall, L.L., 2000. Identification of polyphosphate-accumulating organisms and design of 16SrRNA-directed probes for their detection and quantitation. Appl. Environ. Microbiol. 66, 1175–1182. https://doi.org/10.1128/AEM.66.3.1175-1182.2000.Updated

Daims, H., Brühl, a, Amann, R., Schleifer, K.H., Wagner, M., 1999. The domain-specific probe EUB338 is insufficient for the detection of all Bacteria: development and evaluation of a

more comprehensive probe set. Syst. Appl. Microbiol. 22, 434–44. https://doi.org/10.1016/S0723-2020(99)80053-8

Demanèche, S., Sanguin, H., Poté, J., Navarro, E., Bernillon, D., Mavingui, P., Wildi, W., Vogel, T.M., Simonet, P., 2008. Antibiotic-resistant soil bacteria in transgenic Antibiotic-resistant soil bacteria in transgenic plant fields. PNAS 105, 3957–3962. https://doi.org/10.1073/pnas.0800072105

Giuliano, L., Domenico, M. De, Domenico, E. De Höfle, M.., Yakimov, M.M., 1999. Identification of Culturable Oligotrophic Bacteria within Ligurian Sea by 16S rRNA Sequencing and Probing 77–78.

Gschwind, B., Ménard, L., Albuisson, M., Wald, L., 2006. Converting a successful research project into a sustainable service: the case of the SoDa Web service. Environ. Modell. Softw. 21, 1555e1561.

Henze, M., Gujer, W., Mino, T., van Loosedrecht, M., 2015. Activated Sludge Models ASM1, ASM2, ASM2d and ASM3. Water Intell. Online 5, 9781780402369–9781780402369. https://doi.org/10.2166/9781780402369

Lopez-Vazquez, C.M., Oehmen, A., Hooijmans, C.M., Brdjanovic, D., Gijzen, H.J., Yuan, Z., van Loosdrecht, M.C.M., 2009. Modeling the PAO-GAO competition: Effects of carbon source, pH and temperature. Water Res. 43, 450–462. https://doi.org/10.1016/j.watres.2008.10.032

Lücker, S., Steger, D., Urup, K., Macgregor, B.J., Wagner, M., Loy, A., 2007. Improved 16S rRNA-targeted probe set for analysis of sulfate-reducing bacteria by fluorescence in situ hybridization 69, 523–528. https://doi.org/10.1016/j.mimet.2007.02.009

Manz, W., Amann, R., Ludwig, W., Wagner, M., 1992. Phylogenetic Oligodeoxynucleotide Probes for the Major Subclasses of Proteobacteria : Problems and Solutions. Syst. Appl. Microbiol. 15, 593–600. https://doi.org/10.1016/S0723-2020(11)80121-9

Mcilroy, S.J., Nittami, T., Kanai, E., Fukuda, J., Saunders, A.M., Nielsen, P.H., 2015. Re-appraisal of the phylogeny and fluorescence in situ hybridization probes for the analysis of the Competibacteraceae in wastewater treatment systems. Environ. Microbiol. Rep. 7, 166–174. https://doi.org/10.1111/1758-2229.12215

Meyer, R.L., Saunders, A.M., Blackall, L.L., 2006. Putative glycogen-accumulating organisms belonging to the Alphaproteobacteria identified through rRNA-based stable isotope probing. Microbiology 152, 419–429. https://doi.org/10.1099/mic.0.28445-0

Murray, RGE, Doetsch, RN, Robinow, C., 1994. Determinative and cytological light microscopy. Methods Gen. Mol. Bacteriol. 21–41.

Nielson, P.H., Daim, H., Lemmer, H., 2009. FISH Handbook for Biological Wastewater Treatment: Identification and quantification of microorganisms in activated sludge and biofilms by FISH, IWA Publishing. IWA Publishing Company, London.

Nittami, T., McIlroy, S., Seviour, E.M., Schroeder, S., Seviour, R.J., 2009. Candidatus Monilibacter spp., common bulking filaments in activated sludge, are members of Cluster III Defluviicoccus. Syst. Appl. Microbiol. 32, 480–489. https://doi.org/10.1016/j.syapm.2009.07.003

Oehmen, A., Lemos, P.C., Carvalho, G., Yuan, Z., Keller, J., Blackall, L.L., Reis, M.A.M., 2007. Advances in enhanced biological phosphorus removal: From micro to macro scale. Water Res. 41, 2271–2300. https://doi.org/10.1016/j.watres.2007.02.030

Oehmen, A., Zeng, R.J., Saunders, A.M., Blackall, L.L., 2006. Anaerobic and aerobic metabolism of glycogen- accumulating organisms selected with propionate as the sole carbon source 2767–2778. https://doi.org/10.1099/mic.0.28065-0

Rosso, D., Larson, L.E., Stenstrom, M.K., 2008. Aeration of large-scale municipal wastewater treatment plants : state of the art 973–979. https://doi.org/10.2166/wst.2008.218

Sanguin, H., Herrera, A., Oger-desfeux, C., Dechesne, A., Simonet, P., Navarro, E., Vogel, T.M., Moënne-loccoz, Y., Nesme, X., Grundmann, G.L., 2006. Development and validation of a prototype 16S rRNA- based taxonomic microarray for Alphaproteobacteria 8, 289–307. https://doi.org/10.1111/j.1462-2920.2005.00895.x

Smolders, G.J.F., Meij, J. Van Der, Loosdrecht, M.C.M. Van, 1994a. Stoichiometric Model of the Aerobic Metabolism of the Biological Phosphorus Removal Process 44, 837–848.

Smolders, G.J.F., van der Meij, J., van Loosdrecht, M.C.M., Heijnen, J.J., 1994b. Model of the anaerobic metabolism of the biological phosphorus removal process: Stoichiometry and pH influence. Biotechnol. Bioeng. 43, 461–470. https://doi.org/10.1002/bit.260430605

Wong, M.T., Tan, F.M., Ng, W.J., Liu, W.T., 2004. Identification and occurrence of tetrad-forming Alphaproteobacteria in anaerobic-aerobic activated sludge processes. Microbiology 150, 3741–3748. https://doi.org/10.1099/mic.0.27291-0

Zeng, R.J., Lemaire, R., Yuan, Z., Keller, J., 2003. Simultaneous nitrification, denitrification, and phosphorus removal in a lab-scale sequencing batch reactor. Biotechnol. Bioeng. 84, 170–178. https://doi.org/10.1002/bit.10744

5.

ACHIEVING NITROGEN AND PHOSPHORUS REMOVAL AT LOW C/N RATIOS WITHOUT AERATION THROUGH A NOVEL PHOTOTROPHIC PROCESS

SUMMARY: Conventional wastewater treatment technologies for biological nutrient removal (BNR) are highly dependent on aeration for oxygen supply, which represents a major operational cost of the process. Recently, phototrophic enhanced biological phosphorus removal (photo-EBPR) has been suggested as an alternative system for phosphorus removal, based on a consortium of photosynthetic microorganisms and chemotrophic bacteria, eliminating the need for costly aeration. However, wastewater treatment plants must couple nitrogen and phosphorus removal to achieve discharge limits. For this reason, a new microalgae-bacterial based system for phosphorus and nitrogen removal is proposed in this work. The photo-BNR system studied here consists of a sequencing batch reactor operated with dark anaerobic, light aerobic, dark anoxic and idle periods, to allow both N and P removal. Results of the study show that the photo-BNR system was able to remove 100 % of the 38 ± 0.92 mg N/L of ammonia fed to the reactor and 94 ± 3% of the total nitrogen (Influent COD:N ratio of 300:40, similar to domestic wastewater). Moreover, an average of 25 ± 9.2 mg P/L was simultaneously removed in the photo-BNR tests, representing the P removal capacity of this system, which exceeds the level of P removal required from typical domestic wastewater. Full ammonia removal was achieved during the light phase, with 67 ± 5% of this ammonia being assimilated by the microbial culture and the remaining 33 ± 5% being converted into nitrate. The assimilated P corresponded to 2.8 ± 0.23 mg P /L, which only represented, approximately, 1/9 of the P removal capacity of the system. Half of the nitrified ammonia was subsequently denitrified during the dark anoxic phase (50 ± 24%). Overall, the photo-BNR system represents the first treatment alternative for N and P from domestic wastewater with no need of mechanical aeration or supplemental carbon addition, representing an alternative low-energy technology of interest.

Keywords: Biological nutrients removal (BNR); Polyphosphate accumulating organisms (PAOs); Microalgae-Bacterial Consortium; Nitrogen removal; No aeration; Greenhouse gases (GHG).

Published as: Carvalho, V.C.F., Kessler, M., Fradinho, J.C., Oehmen, A., Reis, M.A.M., 2021. Achieving nitrogen and phosphorus removal at low C / N ratios without aeration through a novel phototrophic process. Sci. Total Environ. 793, 148501. https://doi.org/10.1016/j.scitotenv.2021.148501

5.1. Introduction

Population growth and consequent rapid urbanization, intensive agricultural practices and industrial expansion are increasing environmental and water pollution, either through the release of streams with excessive nitrogen (N) and/or phosphorus (P) concentrations, or through the excessive use of fertilizers (Taziki et al., 2015). Exceeding N and P discharge limits into natural water courses can lead to eutrophication, disturbing the balance of aquatic ecosystems.

Nowadays, the most common process implemented in wastewater treatment plants (WWTP) for N & P removal is biological nutrient removal (BNR), typically through sequential zones in activated sludge systems: anaerobic for carbon uptake and P release; anoxic for heterotrophic denitrification and some P uptake (Mandel et al., 2019); and aerobic for nitrification and P uptake. Such BNR systems require intensive oxygen (O_2) supply, often accounting for approximately 60% of WWTP energy costs (Rosso et al., 2008).

One potential solution to decrease aeration energy costs is through phototrophic anoxygenic bacteria and microalgae systems (Capson-Tojo et al., 2020; Hülsen et al., 2013).

Previous studies have already demonstrated that algal-bacterial consortia for wastewater treatment can achieve better nutrient removal efficiency than bacteria or algal systems by themselves. Also, the algal-bacterial agglomerates reduce the biomass harvesting costs in comparison to algal systems (Liu et al., 2017; Muñoz et al., 2005). The algal-bacterial interaction plays an important role in nutrient removal since there is a synergistic relationship between them (Taziki et al., 2015). This green technology reduces oxygenation costs, when compared with activated sludge systems, and improves nutrients recovery, when compared with anaerobic digestion technologies in WWTPs (Muñoz and Guieysse, 2006; Toledo-Cervantes et al., 2019). Microalgae produce the oxygen for bacteria and fixate the CO_2 released from bacterial metabolism, while using inorganic nutrients for growth (Jia and Yuan, 2016). Microalgae are a group of microorganisms capable of fast growth and strong adaptability in wastewater, that have the ability for nutrients removal. The use of microalgae for nitrogen removal is advantageous since inorganic nitrogen is assimilated by microalgae for biomass production and ammonium and nitrate can be removed highly efficiently (Lv et al., 2019).

High rate algal ponds (HRAP) is a widely used technology to achieve nutrient removal, however, it normally exhibits low sedimentation characteristics and the low hydraulic and sludge retention time (HRT and SRT) applied does not allow the growth of nitrifying bacterial communities (Toledo-Cervantes et al., 2019). Additionally, the short sludge retention time (SRT) limits nitrification in wastewaters with low C/N ratios (de Godos et al., 2014) and a low C/N ratio could inhibit nitrogen removal by organic carbon limitation (Toledo-Cervantes et al., 2019). Moreover, denitrification has been rarely reported in HRAPs (García et al., 2006; Godos et al., 2009; Toledo-Cervantes et al., 2019), and there exists demand for new photosynthetic technologies capable of efficient nutrient removal. Rada-Ariza et al., (2019) showed that it was possible to achieve nitrogen removal in a microalgal-bacterial reactor with more than 94% of ammonium and more than 70% of total nitrogen removal. However, the COD/N ratio

was more than 17, which is almost 3 times higher than that usually found in municipal wastewaters (Henze et al., 2008), implying a high demand of supplemental COD.

The interest in algal-bacterial consortiums for wastewater treatment has been rising. Guo et al. (2021) and Ji et al. (2020) reported microalgal – bacterial consortiums with good nutrient removal efficiency, however, challenges with these processes include the need to either provide mechanical aeration (Guo et al. 2021) or provide continuous illumination (Ji et al. 2020), which is also costly. A system incorporating both dark and light periods could be potentially more adaptable towards the utilization of direct sunlight to provide illumination. These current challenges motivated the current study, whereby the objectives were to obtain a microalgal/bacterial process capable of removing N and P, in dark/light cycles at low HRT (allowing higher influent wastewater flowrates per reactor volume), without mechanical aeration and at COD/N ratios consistent with that of domestic wastewater, to minimize the need for external COD dosage.

A promising new system, called phototrophic enhanced biological phosphorus removal (photo-EBPR), composed of a consortium of microalgae and bacteria, with no need of mechanical aeration and with good capacity for P removal, was proposed by Carvalho et al., (2018) in **chapter 3**. The photo-EBPR system was operated with dark-light cycles, mimicking conventional anaerobic-aerobic EBPR cycles and also enriching for polyphosphate accumulating organisms (PAOs), mainly *Accumulibacter* Phosphatis, at a low COD/P ratio of 3.3 and an HRT of 16h. Nevertheless, this system had not been designed to achieve combined N and P removal, thus a primary objective of this study was to adapt the photo-EBPR process towards enhancing N removal, particularly through incorporating nitrification and denitrification that augment the N removal achieved through assimilation during biomass growth. The engineering challenge was to achieve such a process without mechanical aeration or external COD addition.

In this work, the photo-EBPR system was improved and a new photosynthetic system for simultaneous P and N removal (photo-BNR), at low HRT (< 1 day) and with no need of external aeration, in order to treat a wastewater stream with a COD:N ratio of 7.5, similar to a municipal wastewater (Henze et al., 2008). To evaluate the P removal capacity of the integrated system, P was fed in excess of what is normally found in WWTPs. It is expected that during the light period, microalgae consume CO_2 and produce oxygen both for PAOs and nitrifiers and, simultaneously, assimilate P and ammonia for growth. Since both nitrifiers and microalgae are CO_2 dependent, the capacity of the photo-BNR process for CO_2 mitigation is potentially higher when compared with photo-EBPR. An anoxic dark period was added to the photo-EBPR system, placed after the light period, to allow denitrification to occur. During the dark anoxic period, since no external carbon source is added to the reactor, denitrifying PAOs (dPAOs) are expected to perform denitrification by using up the anaerobically stored PHA. Due to the interaction between microalgae and bacteria, cells can aggregate as flocs more readily and settle very fast, resulting in a solids-free effluent and, thus, solving one of the main problems when using microalgae for WW treatment. The goal with this photo-BNR process is to remove aeration requirements for biological nutrient removal and mitigate CO_2

without the need for costly external COD dosing, thereby reducing the operational costs and ecological footprint of the WWTP. In addition, this work investigates the metabolism of how phosphorus and nitrogen removal is achieved in the microalgae-bacterial consortium, since the different metabolic capacities of bacteria and microalgae influence the nutrient removal capacity of the system.

5.2. Materials and methods

5.2.1. Operation of the SBR

An SBR with a working volume of 2 L was operated with 8 h cycles (**Table 5.1**) and operated with a hydraulic retention time (HRT) of 16 h and a sludge retention time (SRT) of 18 days. The synthetic medium, fed in the beginning of each cycle, was composed of 75 % (v/v) of a phosphate solution (253 mg/L of K_2HPO_4 and 154 mg/L of KH_2PO_4) and 25 % (v/v) of carbon and nitrogen medium with a concentration per litre of: 0.64 g $C_2H_3O_2Na.3H_2O$; 68 µL $C_3H_6O_2$; 0.59 g NH_4Cl; 0.95 g $MgSO_4.7H_2O$; 0.44 g $CaCl_2.2H_2O$; 11.7 mg allyl-N thiourea (ATU, only added during the stages of PAO enrichment (stage 1 – 3) to prevent nitrification); 31.7 mg ethylene-diaminetetraacetic (EDTA) to prevent salts precipitation and 3.17 mL of a micronutrients solution, with a concentration per litre of: 1.5 g $FeCl_3.6H_2O$; 0.15 g H_3BO_3; 0.03 g $CuSO_4.5H_2O$; 0.18 g KI; 0.12 g $MnCl_2.4H_2O$; 0.06 g $Na_2MoO.2H_2O$; 0.12 g $ZnSO_4.7H_2O$ and 0.15 g $CoCl_2.6H_2O$. The carbon media contained volatile fatty acids (VFAs) at a ratio of 75% acetate and 25% propionate, to promote PAO enrichment (Carvalheira et al., 2014b). Anaerobic, aerobic, anoxic and idle periods were stirred with a magnetic stirrer at a constant rate of 700 rpm. At the end of the anoxic period, the culture was settled and decanted, with 1 L of supernatant being removed. During the following idle period, argon was bubbled to ensure anaerobic conditions before the next cycle. The reactor was inoculated with wastewater sludge from the aerobic tank of a WWTP located in Lisbon (Beirolas, Portugal). The selection of this photo-BNR system comprised 4 different stages (**Table 5.1**). First, for 43 days, stage 1, a selection of a conventional EBPR system was performed through alternating anaerobic and aerobic periods in dark conditions. Along stage 1, the COD concentration in the feed was increased from 100 mg/L to 300 mg/L, to ensure sufficient carbon to augment the PAO population. The selection of the photo-EBPR system (stage 2 and 3) was initiated by providing light to the system in order to promote the growth of photosynthetic organisms. During stage 2, which corresponds to the transition period from conventional EBPR to photo-EBPR, air was supplied during only the last 2h of illumination. When microalgae produced, per se, enough oxygen for the system (meaning that besides the oxygen consumed by the bacteria, it could be measured inside the reactor at concentrations around 1 mg O_2/L), aeration was removed for stage 3 and the SBR was operated in dark (anaerobic) and light (aerobic) cycles (**Table 5.1**). Illumination was supplied by external Osram halogen lamps (two lamps of 40 W and one of 60W), providing an intensity of 99 W/m^2 on the reactor surface, which corresponds to 4.5 W/L, a similar volumetric light intensity as used in (Carvalho et al., 2019, 2018). This light intensity

was chosen to simulate the sun irradiance levels that occur during the summer in Portugal summer day (Gschwind et al., 2006) . In stage 3, sodium carbonate (Na_2CO_3) was fed at the end of the dark anaerobic period (6 mg C/L) as a supplemental inorganic carbon source for autotrophic microorganisms (**Table 5.1**, Stage 3). Stage 4 targeted both P and N removal (**Table 5.1**) and, for this reason, Allylthiourea (ATU), which inhibits nitrification, was removed from the feed. Additionally, the reactor cycle was adjusted to include a dark period after the light phase to promote denitrification and the concentration of Na_2CO_3 inside the reactor was increased to 10 mg C /L at stage 4b (**Table 5.1**). Throughout the reactor operation, argon was sparged during the dark anaerobic phase and during the last 40 minutes of the dark anoxic phase. In stage 4, the settling time and carbon dioxide (CO_2) concentration were adjusted (**Table 5.1**) to increase the efficiency of both P and N removal. After these adjustments, the media was fed at a COD:CO_2:N:P (in mg) of 300:20:40:60, which implies a ratio of 15:1:2:3.

5.2.2. Chlorophyll and bacteriochlorophyll quantification

The chlorophyll and bacteriochlorophyll concentration was calculated according to Ritchie (2018) using the equations for pigments extraction with 100% ethanol.

Table 5.1 - Different stages of SBR operation.

Selection period		Reactor cycle conditions							
		Anaerobic	Aerobic	Anoxic	Setting	Idle	ATU	COD_{feed} (mg/L)	Na_2CO_3 (mg-C/L)*
Stage 1 day 1 – day 43	EBPR selection	Dark: 3h	Dark Air: 4h	-	0.5h	0.5h	Yes	100 – 300	-
Stage 2 day 44 – day 52	Transition phase from EBPR to photo-EBPR	Dark: 3h	Light: 4h (2h with air)	-	0.5h	0.5h	Yes	300	-
Stage 3 day 53 – day 73	Photo-EBPR (P removal)	Dark: 3h	Light: 4h	-	0.5h	0.5h	Yes	300	6
Stage 4 a day 74 – day 94	Transition period from photo-EBPR to photo-BNR	Dark: 1.5h	Light: 4.5 h	Dark: 1 h	0.5h	0.5h	No	300	6
Stage 4 b day 95 – day 128	Photo-BNR (nitrification/denitrification)	Dark: 1.75h	Light: 3.75 h	Dark: 1.75 h	0.25h	0.5h	No	300	10

(*theoretical concentration inside the reactor).

5.3. Results and discussion

The SBR operated in this study was first enriched for PAOs in a conventional EBPR process, then transitioned towards a photo-EBPR system, then into a photo-EBPR system with nitrification, and finally a photo-BNR system, for simultaneous nitrogen and phosphorus removal. The rationale for this strategy was to select the main important microorganisms for each step of the reactor operation and guarantee the presence of microorganisms that can assure efficient nitrogen and phosphorus removal.

5.3.1 SBR Acclimatization and Biomass Selection

During the first 43 days (**Figure 5.1**), the reactor was operated with anaerobic – aerobic cycles, in order to promote the growth of PAOs through conventional EBPR. During stage 1, the specific P uptake rate increased from 1.7 to 5.6 mg P/gX.h, on days 1 and 37, respectively. This increase was correlated with the selection of *Accumulibacter* PAOs (**Table 5.2**). Thus, conventional EBPR operation with PAO enrichment was successfully achieved.

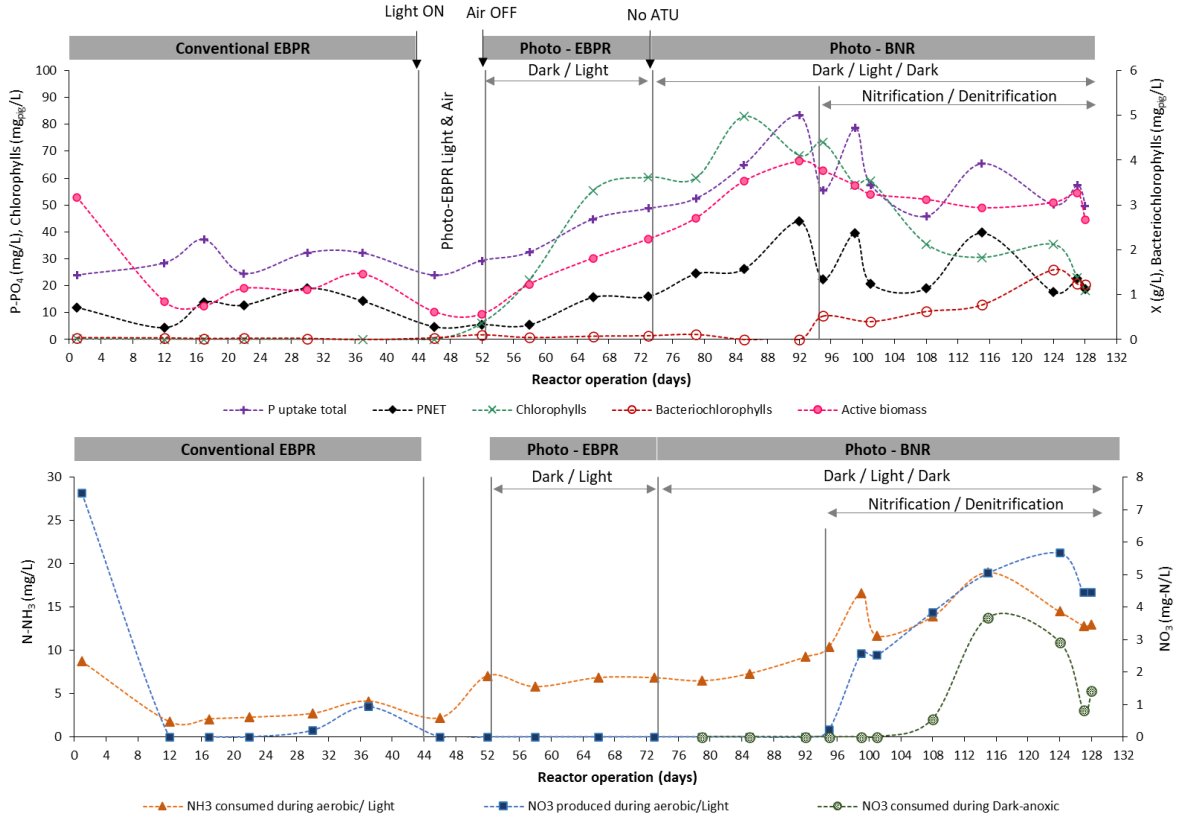

Figure 5.1- SBR performance over the 128 days of operation.
Selection of a conventional EBPR during the first 43 days (stage1); Transition period of photo-EBPR selection with light and air, between days 44 and 52 (stage 2); operation of a conventional photo-EBPR with ATU to prevent nitrification between day 53 to 73 (Stage 3); transition period of a photo-EBPR to a photo-BNR system capable of ammonia consumption only from day 74 until day 94 (stage 4a); operation of a photo-BNR system (N and P removal) from day 95 to day 128 (stage 4b) (Table 1).

Table 5.2 - FISH results during reactor operation.

Stage	Probe / Day	PAOmix	ACC-I-444	ACC-II-444	CPB_654	Super Dfmix	Nso 1225	Ntspa 662	NIT3	G Rb	ARC915
1	1	(+)	(+ -)	(+)	(+)	(+ -)	(+)	(+)	(-)	(-)	(+)
	30	(+ +)	Not analyzed	Not analyzed	(+ + +)	(+)	Not analyzed	(+)	(-)	(+)	(++)
2	52	(+ +)	Not analyzed	Not analyzed	(+)	(-)	Not analyzed	(-)	(-)	(+ -)	(++)
3	73	(+ + +)	(+ + +)	(+)	(+)	(-)	(-)	(-)	(-)	(-)	(++)
4b	115	(+ + +)	(+ + +)	(+ +)	(+)	(-)	(-)	(-)	(-)	(-)	(+)
	128	(+ + +)	(+ +)	(+ + +)	(+ +)	(-)	(-)	(-)	(-)	(-)	(+)

(-) non-existent; (+-) almost non-existent; (+) present; (++) abundant; (+++) dominant. Probes: PAOmix (PAO651, PAO462, PAO846) for *Candidatus* Accumulibacter phosphatis; Acc-I-444 which targets type I Accumulibacter PAOs and Acc-II-444 for Accumulibacter PAOs type II; CPB_654 for *Candidatus* Competibacter phosphatis; GRb for *Rhodobacter* and *Roseobacter*; SuperDFmix for *Defluviicoccus*; Nso1225 for AOBs; NIT3 and Ntspa662 for NOBs; ACR915 for Archaea.

During stage 2 (**Figure 5.1**), between days 44 and 52, which corresponds to the transition into a photo-EBPR system, the reactor was operated in dark – light periods but air was supplied in the last 2 hours of the light period to guarantee the presence of oxygen for PAOs until microalgae were adequately enriched (Carvalho et al., 2018). Chlorophylls started to be detected between days 46 and 52 (**Figure 5.1**), indicating the growth of microalgae and other photosynthetic microorganisms. On day 52, total P uptake was similar to day 37 (**Figure 5.1**), but with a decrease in the active biomass concentration, thus the specific P uptake rate increased. The P content of the biomass increased from 5.3 % (g P/g TSS) on day 37 up to 15 % on day 52, indicating that the selected biomass was efficient in P accumulation. This agreed well with the further selection of *Accumulibacter* PAOs in the biomass, as shown by FISH analysis (**Table 5.2**, day 52). At the end of stage 2 (day 52) more than 50% of the P removal occurred in the nonaerated light period (~17 mg P/L) and the remainder occurred in the period of light and air (~13 mg P/L). After day 52, the SBR started to be operated in dark – light cycles without aeration (Stage 3), in the so called photo-EBPR system (see also Carvalho et al., 2018) (**Figure 5.1**). During stage 3 of photo-EBPR operation, between day 53 and 73, the net P removal (P_{net}) increased almost 3 times, from 5.6 to 16 mg P/L (**Figure 5.1**). However, the specific P uptake rate decreased when compared to day 52 (**Table 5.3**), likely due to the increase of microalgae in the biomass, showed by the increase of chlorophyl concentration (**Figure 5.1**, stage 3), which typically exhibit a lower specific P uptake capacity as compared to PAOs like *Accumulibacter* (Carvalho et al., 2018).

Table 5.3 - Kinetic parameters obtained on stage 3 and stage 4 of the SBR operation.

Period			Stage 3		Stage 4b		
			AVG Value[1]	Day 73	AVG Value[2]	Day 115	Day 128
Dark	P release	mg P/L	30 ± 2.9	33	31 ± 3.8	26	31
		mg P/g*X*.h	6.2 ± 1.9	4.5	7.3 ± 0.76	6.6	8.3
Light	P uptake	mg P/L	42 ± 8.5	49	51 ± 7.5	61	45
		mg P/g*X*.h	7.6 ± 2.8	5.7	5.6 ± 0.80	5.7	6.7
	NH_4 uptake	mg N/L	6.5 ± 0.61	6.8	15 ± 2.9	19	13
		mg N/g*X*.h	1.2 ± 0.45	0.78	1.7 ± 0.43	1.8	2.3
	NO_3 formation	mg N/L	0	0	4.9 ± 0.58	5.1	4.5
		mg N/g*X*.h	0	0	0.72 ± 0.19	0.56	0.97
Dark-Anoxic	P uptake	mg P/L	n.a	n.a	4.1 ± 1.3	4.3	2.4
		mg P/g*X*.h	n.a	n.a	1.4 ± 0.5	0.93	2.0
	NO_3 consuption	mg N/L	n.a	n.a	2.2 ± 1.3	3.7	1.5
		mg N/g*X*.h	n.a	n.a	0.80 ± 0.22	0.85	1.0
P_{net}*		mg P/L	12 ± 6	16	25 ± 10	40	19
		mg P/g*X*.	7.8 ± 3.8	7.0	10 ± 3.1	14	11
CO_{2net}		mg C/L	n.a	7.7	5.8 ± 3.2	8.5	2.5
		mg C/g*X*	n.a	3.4	2.2 ± 0.98	3.0	1.2

Results are presented as the average ± standard deviation of the results obtained during cycle monitoring at each stage of operation.[1]average of 3 cycles (CO_2 sensor was started to be used after day 66); [2]average of 4 cycles; n.a. - not applicable.

*P net corresponds to the difference between the final and the initial P concentration in the reactor.

An example of the typical photo-EBPR operation profile is shown in **Figure 5.2** for Day 73 (stage 3), which indicates that during the dark phase, VFAs were consumed in 0.5 hours and P release was 33 mg P/L, with PHA production (**Table 5.3**, **Figure 5.2**). CO_2 was mainly produced during the VFAs consumption and PHA production (**Figure 5.2**), which corroborate with the metabolic models for EBPR systems suggested by Smolders et al. (1994) and Oehmen et al. (2005). The increase of CO_2 concentration in the last sample of the dark phase, at 2.7 h of the cycle (**Figure 5.2**), is due to the Na_2CO_3 supplementation that occurred before the light phase in stage 3.

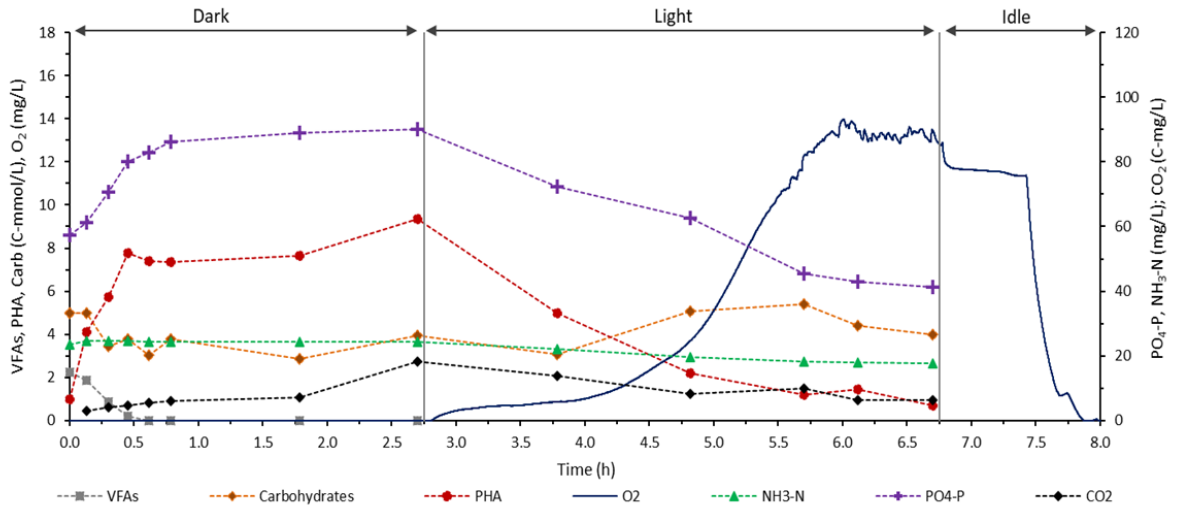

Figure 5.2 - Photo-EBPR cycle profile on operation day 73 in dark (anaerobic) – light (aerobic) cycle – Stage 3.

During the first 3 h of the light phase, P removal was associated with PHA consumption, however, after PHA reached residual levels, the P uptake rate decreased by a factor of 3 to 1.9 mg P/g*X*.h. Biomass enriched in *Accumulibacter* PAOs is known for never using all of their PHA reserves, slowly metabolising low PHA levels in standard EBPR processes (Carvalheira et al., 2014). It was also clear (**Figure 5.2**) that glycogen levels were replenished while PHA levels were high enough for both carbohydrate production and P uptake. When PHA consumption ceased, glycogen production ceased as well and was then consumed, likely due to metabolic energy requirements for cell maintenance. Aerobic glycogen consumption after PHA reaches residual levels was already observed in PAOs by Lopez et al., (2006), Lanham et al., (2013) and Carvalheira et al., (2014).

The results suggest that the P uptake was mainly carried out by *Accumulibacter* related PAO, and accumulated as poly-P, while PHA is available. On the other hand, after PHA reaches residual levels, P removal is mainly carried out by microalgae/ photosynthetic microorganisms, or other PAOs that are not PHA dependent (Lanham et al., 2013). Microalgae and cyanobacteria both use P for growth and, in addition, cyanobacteria can accumulate it as internal poly-P granules, contributing to excess P removal beyond growth requirements (Brown and Shilton, 2014; Carvalho et al., 2018; Powell et al., 2011).

The oxygen levels in stage 3 reached almost 14 mg/L, showing that the oxygen produced by microalgae was higher than the culture requirement. Supersaturation of dissolved oxygen (i.e. beyond the oxygen saturation point found from aeration) is regularly encountered in closed microalgal photoreactors (de Godos et al., 2014; Muñoz and Guieysse, 2006), since the mass-liquid transfer coefficient is low (Camacho Rubio et al., 1999) and the oxygen is not effectively stripped from the reactor (Kazbar et al., 2019).

Regarding the ammonia consumption, 6.8 mg N/L was consumed, most likely for cell growth since no NO_3 was produced (**Figure 5.2**), as nitrification was inhibited during this stage by the presence of ATU in the medium (NO_2 was also analysed and never detected; data not shown).

The CO_2 results indicated that on day 73, more carbon dioxide was consumed than produced, which means that the photo-EBPR system goes beyond a carbon-neutral system. In fact, it enables negative CO_2 emissions (**Figure 5.2**), since it can mitigate not only the CO_2 generated by the PAOs, both in anaerobic and aerobic phases, but also the extra CO_2 supplemented to the reactor. This feature of the photo-EBPR system opens the possibility of not only treating wastewater and recovering P, but also to sequester CO_2 from flue gases, reducing the concentrations of this greenhouse gas, decreasing the atmospheric pollution levels and contributing for a better air quality

5.3.2 Photo-BNR Operation

The next stage was the conversion of the photo-EBPR system to a photo-BNR system. ATU, which was fed to the reactor to prevent nitrification, was removed in the beginning of stage 4 (4a) and a dark period was added after the light aerobic period to implement anoxic conditions (**Table 5.1**). From day 74 until day 94, the Na_2CO_3 fed to the reactor targeted a concentration of 6 mg C/L inside the reactor and during this period, the ammonia consumption was not higher than 9.2 mg N/L (**Figure 5.1**) and no NO_3 was formed, probably because nitrifying bacteria were limited by CO_2 concentration. Both ammonia oxidizing organisms (AOBs) and nitrite oxidizing organisms (NOBs) need CO_2 for growth (de Godos et al., 2014; Santos et al., 2020). In addition, microalgae compete for the CO_2 with AOBs and NOBs, so when it is not available, AOBs and NOBs cannot proliferate. To promote nitrifying bacteria growth, from day 95 on (beginning of Stage 4b), the Na_2CO_3 concentration inside the reactor was increased to 10 mg C/L, and by day 99, ammonia consumption increased to 17 mg N/L with a production of 2.6 mg N/L of nitrates (**Figure 5.1**). However, no NO_3 was consumed during the dark/anoxic phase until day 108 (**Figure 5.1**), since the reactor still contained oxygen from the previous light phase and never achieved the required anoxic conditions for NO_3 consumption.

Between day 95 and day 108 (stage 4b), the illumination time was reduced in order to decrease the oxygen concentration in the end of the light phase (**Table 5.1**). Oxygen concentration is a crucial parameter to control. Its production needs to be enough for PHA oxidation, glycogen production and P uptake by PAOs, but also for AOBs and NOBs activity. However, oxygen should not reach high levels, otherwise anoxic conditions are difficult to reach in the following dark/anoxic period and then, denitrification cannot occur. The dark/anoxic period at the end of the cycle was also increased and argon was sparged in the last half hour of the dark/anoxic period to ensure that no oxygen remained in the reactor, allowing more time for denitrification. The implemented alterations in the reactor cycle promoted anoxic conditions and, consequently, nitrification and denitrification started to occur in the photo-BNR system.

By days 115 (**Figure 5.3-a**) and 128 (**Figure 5.3-b**) the culture presented a similar dark phase profile, where VFAs were consumed during the first hour of the dark phase, with P release, PHA and CO_2 production and carbohydrates consumption (**Table 5.3**). Ammonia was fully removed during the light phase, with at least 27 % of the ammonia being converted

into nitrate on day 115 and 34% on day 128 (**Table 5.3**,**Figure 5.4**). This ammonia removal could be the result of heterotrophic organisms (PAOs, GAOs or others), photosynthetic organisms' activity, ammonia oxidizing bacteria (AOB) activity, that converts ammonia into nitrite, and nitrite oxidizing bacteria (NOB) activity or/and by phototrophic nitrite oxidation (Kuypers et al., 2018). The nitrogen removal mechanisms are discussed in **section 5.3.3**.

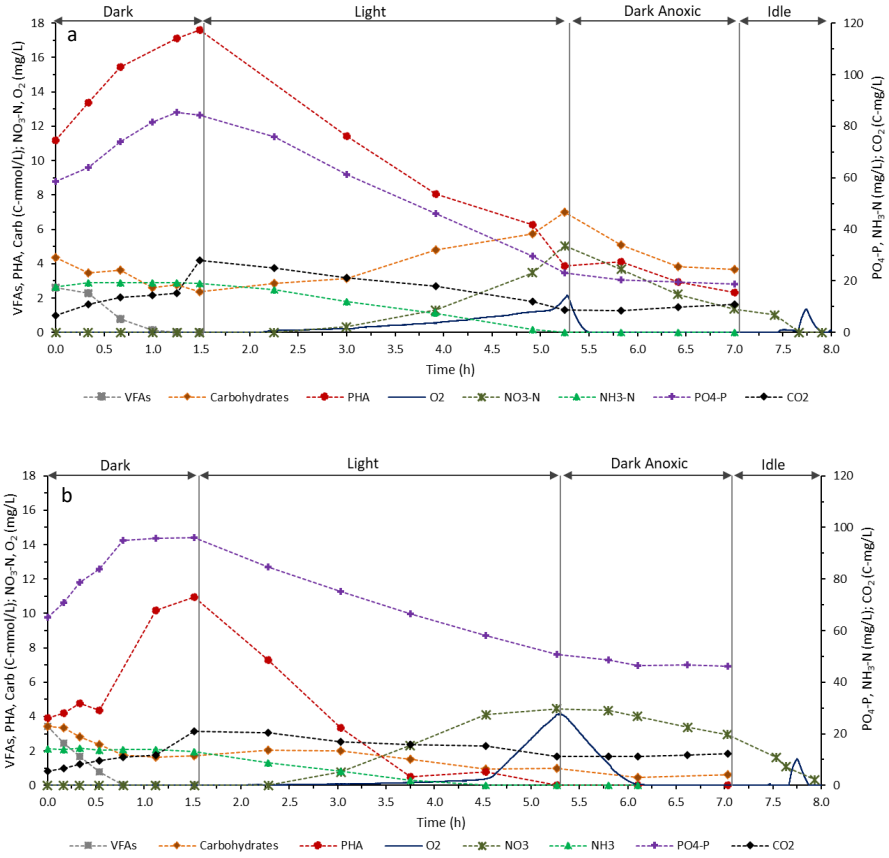

Figure 5.3 - Cycle profile of the Photo-BNR system operation in dark (anaerobic) – light (aerobic) – dark (anoxic) cycle during stage 4b.
a)day 115, b) day 128.

The main differences of the photo-BNR cycle between day 115 and 128 was the PHA content and O_2 concentration, where PHA was completely consumed in the light phase and greater oxygen accumulated on day 128, leading to less anoxic denitrification and lower P removal (**Figure 5.3-b**). During the light period of day 128, PHA reached undetectable levels in the first 2.2 h, however, P removal continued at the same rate, even after PHA became undetectable. Since P was being removed independently of the PHA presence, photosynthetic organisms could contribute towards P uptake, as seen also in **chapter 2** and **3** (Carvalho et al. (2018, 2019)). However, it is possible that after PHA achieved undetectable levels, P uptake may have been possible with the energy from glycogen hydrolysis, as carbohydrates were consumed during this period (the same trend was also observed on day 124 and 127 (**Figure 5.4**).

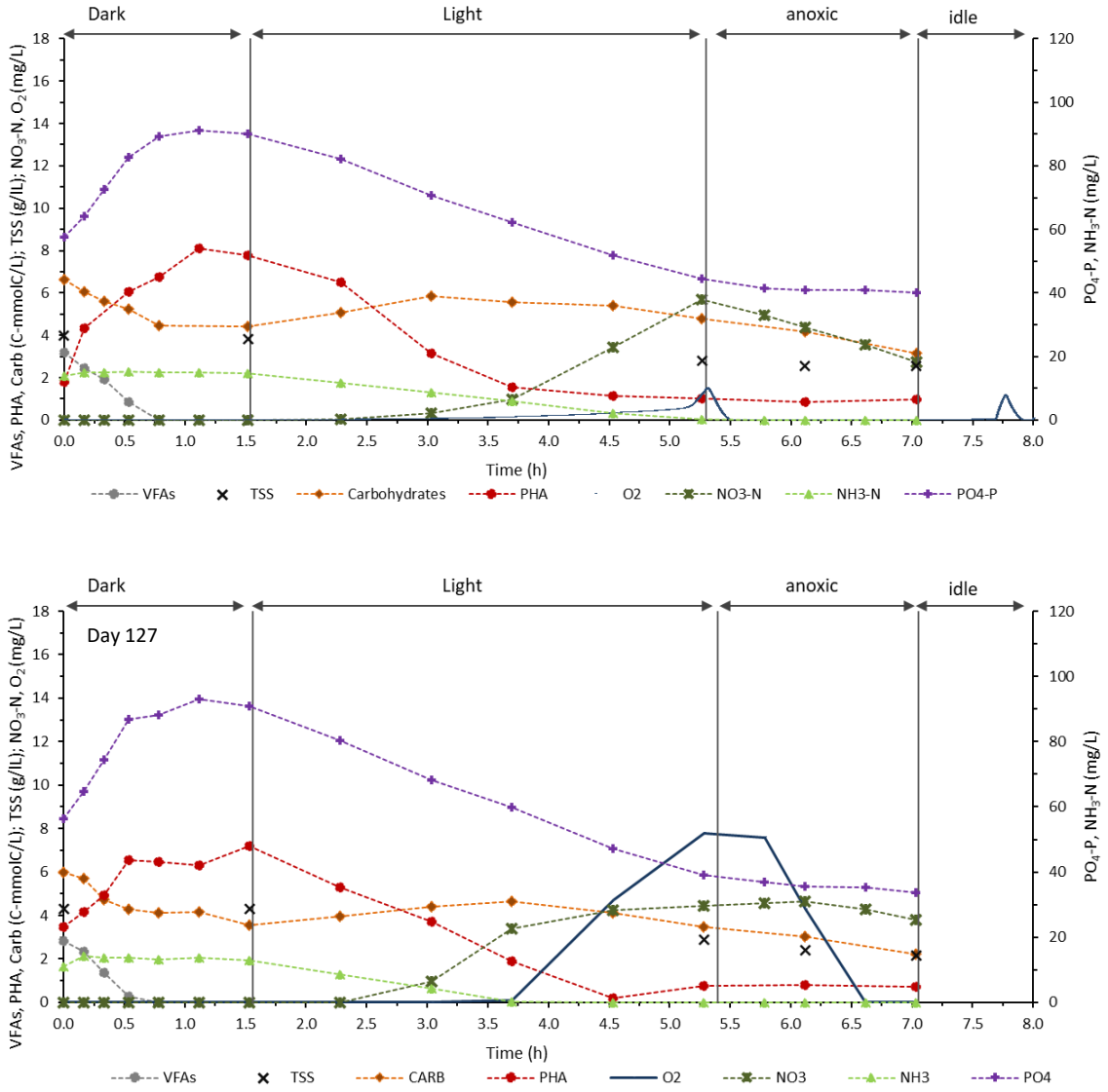

Figure 5.4 - Daily kinetic on day 124 and day 127 (Stage 4b).

During the dark phase, after illumination, of day 115 (**Figure 5.3-a**) oxygen levels reached zero, and during this dark-anoxic phase, 3.7 mg N/L of NO_3 was removed (73 % of total NO_3) in parallel with PHA and glycogen consumption. This carbohydrates consumption during the dark-anoxic phase can be due to microalgae fermenting their starch reserves (Arias et al., 2018; Atteia et al., 2013) possibly originating a variety of end products, including acetate, and others carbon compounds. It is possible that starch fermentation contributes towards fulfilling the COD demand of denitrification. However, PHA consumption and P removal also accompanied denitrification, supporting PAO activity. Since in dark anoxic conditions, microalgae do not typically perform nitrate removal (Hellebust and Ahmad, 1989; Lv et al., 2019; Sanz-Luque et al., 2015; Taziki et al., 2015), the results suggest that NO_3 consumption could be mainly attributable to dPAOs and/or dGAOs (Lanham et al., 2018b; Santos et al., 2020) in the photo-BNR system. It should be noted that nitrite was never observed to accumulate during photo-BNR operation. This is consistent with conventional activated sludge operation,

where AOB oxidation of ammonia to nitrate is typically the rate-limiting step as compared to nitrite oxidation to nitrate by NOBs (see **section 5.3.3**). Also, the NO_3 that remained after the anoxic phase was typically consumed in the settling/decant and idle phases, and thus did not enter into the anaerobic phase. This minimised COD loss to denitrification anaerobically, maximising the COD that could be taken up by PAOs, which is an important issue in EBPR. On day 128, the NO_3 consumption during dark anoxic period occurred without P uptake, suggesting that the culture was not capable of restoring its poly-P storage pools in the absence of PHA and glycogen. In this case, nitrate reduction can be attributed to a side population within the photo-EBPR system (Rincón et al., 2019) who are not PHA dependent. In addition, glycogen levels were very low, since it started to be consumed in the light phase, which can influence the photo-BNR process.

During photo-BNR operation, the net CO_2 consumption was 5.8 ± 3.2 mg C/L (**Table 5.3**), indicating that the photo-BNR system was able to mitigate the CO_2 produced by the bacterial (or other microorganisms) metabolism plus the extra CO_2 that was fed to the reactor.

The photo-BNR could remove 100 % of the ammonia (40 mg N/L), 94 ± 3 % of total N with a capacity of nitrate removal of 50 ± 24% (**Figure 5.5**). The total net P removal was 25 ± 9.2 mg P/L, which was lower than that obtained in Carvalho et al., (2018) but still much larger than the typical P concentrations found in domestic WW, while net CO_2 consumption was achieved. In addition, the sludge settling capacity was good, since with only 15 minutes of settling a clean effluent was discharged (**Figure A.1**). The photo-BNR is thus a process option of interest to achieve environmentally sustainable nutrient removal.

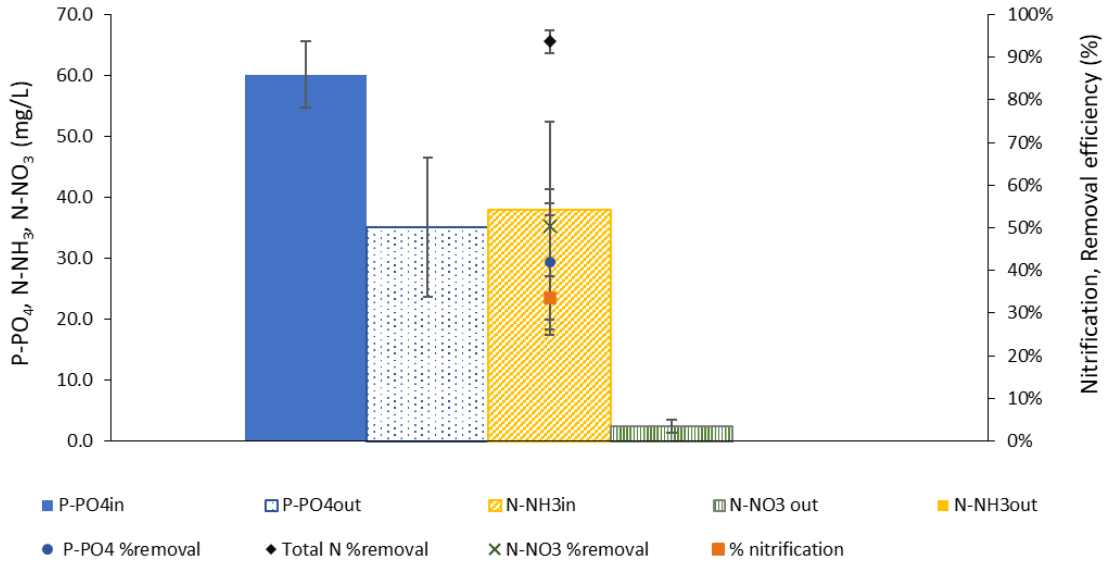

Figure 5.5 - Average removal efficiencies of N and P of 4 cycles (days 115, 124, 127 and 128) during stage 4b of photo-BNR operation.
Concentrations of phosphorus and ammonia in the influent corresponds to the experimental concentration of the feed.

5.3.3. Microbial community assessment and nutrient removal mechanisms in photo-BNR

The main mechanism of P removal in the photo-BNR process can be attributed to P uptake by PAOs, accumulated as Poly-P (**Figure 5.6**). FISH results (**Table 5.2)** indicated that the presence of *Accumulibacter* PAOs increased during reactor (**Figure 5.7**) selection and they were the dominant chemotrophic microorganisms present in the biomass, from day 73 on. FISH results and sequencing results (**Table 5.2, Table 5.4**) are not consistent about the abundance of PAOs microorganisms, since sequencing analysis do not indicates *Accumulibacter* within the 20 most abundant species in the biomass of the photo-BNR system. Similar discrepancies occurred in other studies regarding PAOs abundance (Albertsen et al., 2016; Rubio-Rincón et al., 2019; Valverde-Pérez et al., 2016). The abundance of GAOs (CPB_654 probe) increased by day 128, which correlates well with the reduced P removal, comparing with day 115. Sequencing results (**Table 5.4**) corroborate FISH data regarding the increase of GAOs, perhaps due to the increase of oxygen availability (Carvalheira et al., 2014a). The role of the microalgae (or other photosynthetic microorganisms) on P removal cannot be ignored, since on day 128 P uptake continued after PHA depletion. Sequencing results for microalgae indicate that the main microalgae present in the end of the photo-BNR operation, on day 128, was from class *Chlorophyceae* (OUT_2) (**Table 5.5**).

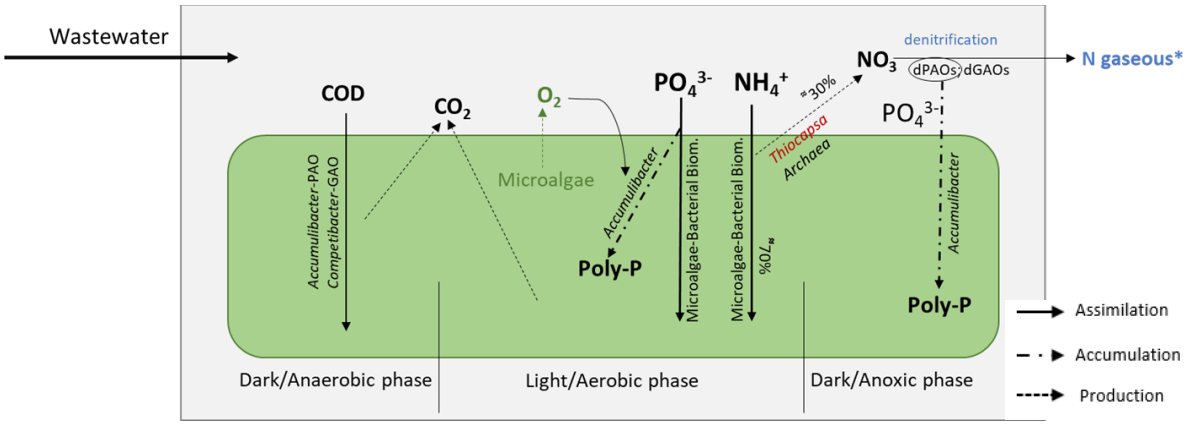

Figure 5.6 - Diagram of the nutrient removal mechanisms in the photo-BNR process.
Green color corresponds to the microbial biomass from the photo-BNR.
*N gaseous emissions were not measured.

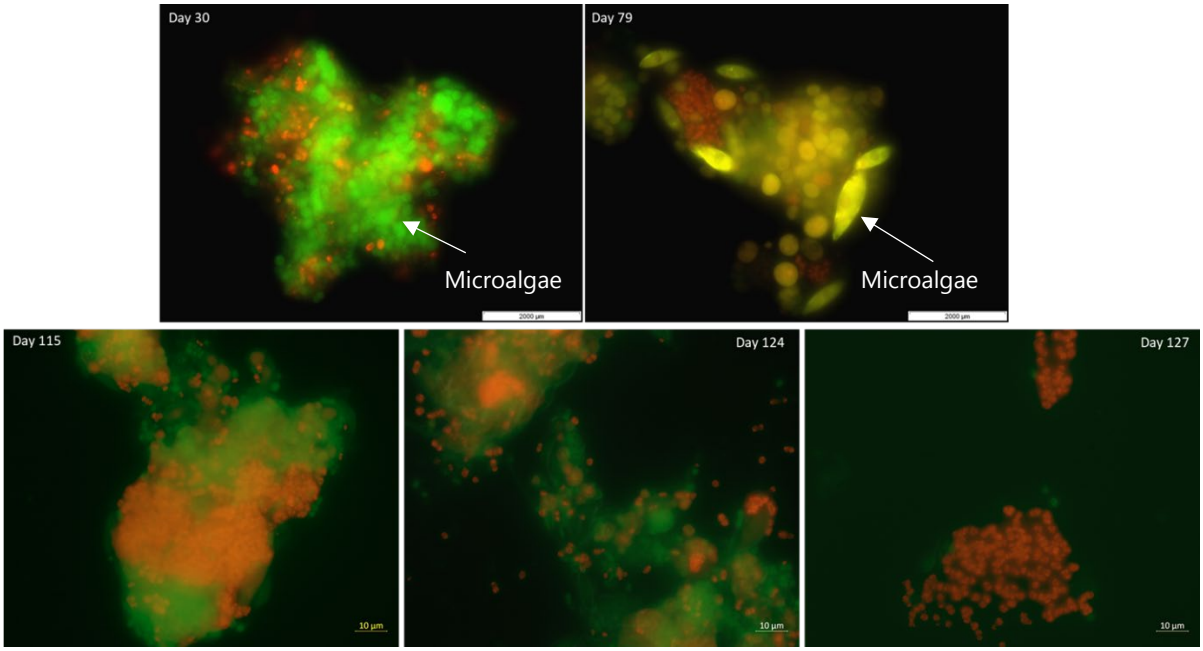

Figure 5.7 - Fish Images of PAOmix probe.
FITC labeled (green) for EUBmix probe (all bacteria) and Cy3 (red) for PAO mix probe. The intense green colour on day 30 is due to autflorescence of green algae (round shape).

Table 5.4 - 20 most abundant prokaryotic species, obtained from DNA sequencing, in the photo-BNR process.

Day 1	Day 73	Day 115	Day 128	
0	0	30.9	36.9	(C) Gammaproteobacteria; (G) Thiocapsa
0.5	17.7	16.9	20.9	(C) Gammaproteobacteria; (F) Competibacteraceae; (G) CPB_S18
0	42.6	5.8	6	(P) Cyanobacteria; (C) Choloroplast _OTU_7
0	0	21.7	9.2	(P) Cyanobacteria; (C) Cyanobacteria; (F) Familyl_OTU_11
27.5	0	0	0	(C) Acidimicrobiia; (G) Candidatus Microthrix
1	9.9	0	0	(C) Actinobacteria; (G) Nocardioides
10.9	0	0	0	(C) Actinobacteria; (G) Tetrasphaera
0	6.7	1.4	1.6	(C) Alphaproteobacteria; (F) Hyphomonadaceae_OTU_14
0	1.2	4.3	3.5	(P) Cyanobacteria; (C) Choloroplast _OTU_21
0.3	2.5	2.3	1.7	(C) Gammaproteobacteria; (G) Candidatus Competibacter
2.5	0.4	1.4	1.9	(C) Alphaproteobacteria; (G) Rhodobacter
0	1.4	1.7	1.9	(C) Gammaproteobacteria; (G) CPB_P15
0.8	1.4	0.7	0.6	(C) Alphaproteobacteria; (G) Mesorhizobium
0	1.5	0.8	1.1	(P) Cyanobacteria; (C) Choloroplast _OTU_68
0	2.3	0.5	0.4	(K) Unassigned_OTU_57
0.1	0.3	1.2	1.6	(C) Alphaproteobacteria; (G) Meganema
3.2	0	0	0	(P) Saccharibacteria; (G) SBR2113
2.9	0	0	0	(C) Anaerolineae; (F) Anaerolineaceae_OTU_44
0	0.3	0.9	1.6	(C) Gammaproteobacteria; (G) Lysobacter
2.7	0	0	0	(C) Actinobacteria; (G) Mycobacterium

(K – Kingdom; P – Phylum; C – Class; O – Order; F – Family; G- Genus).

Table 5.5 - 10 more abundant Eukaryotic species (algae), obtained from DNA sequencing, during the photo-BNR.

Day 128	
61.1	(P) Chlorophyta; (C) Chlorophyceae_OTU2
19.5	(P) Chlorophyta; (C) Trebouxiophyceae_OTU3
6.4	(P) Chlorophyta; (C) Chlorophyceae_OTU5
4.2	(P) Rozellomycota; (G) LKM11
3.1	(C) Chlorophyceae (O) Sphaeropleales
1.5	(P) Chlorophyta; (C) Chlorophyceae_OTU8
1.3	(P) Chytridiomycota; (C) Chytridiomycetes
0.9	(C) Trebouxiophyceae; (O) Chlorellales
0.5	(P) Chlorophyta;; (C) Trebouxiophyceae_OTU23
0.3	(P) Chlorophyta; (C) Chlorophyceae_OTU53

(P – Phylum; C – Class; O – order; F – Family; G- Genus)

The results obtained during this study indicate that ammonia is mainly removed by assimilation both by bacterial and algal biomass (**Figure 5.6**). The contribution of NH_3 volatilization to nitrogen removal can be considered negligible since pH was controlled at 7.5 and volatilization of NH_3 is reported to occur at pH higher than 8.5 (Camargo Valero and Mara, 2010, 2007). Assimilation was described to be one of the main mechanisms for N removal in HRAPs by de Godos et al., (2010) and Posadas et al., (2015). However, Rada-Ariza et al. (2019) and Wang et al. (2015) reported that nitrification/denitrification was the main removal mechanism of N in microalgal-bacteria photoreactor for nitrogen removal. Since AOBs and NOBs were not detected by FISH or sequencing, it can be hypothesized that *Thiocapsa,* highly represented on the photo-BNR on day 115 and 128 (**Table 5.4**), could contribute towards nitrite oxidation into nitrate (**Figure 5.6**). *Thiocapsa* species are widely distributed purple bacteria (**Figure 5.8**) capable of photoautotrophic growth on a variety of common inorganic electron acceptors, and, consequently, can oxidize nitrite anaerobically under illuminated conditions (Griffin et al., 2007; Hemp et al., 2016; Imhoff and Caumette, 2015; Kuypers et al., 2018; Schott et al., 2010). *Thiocapsa* also may enable the sequential reduction of NO to N_2, since it presents both nitric oxide reductase ($NO \rightarrow N_2O$) and nitrous oxide reductase ($N_2O \rightarrow N_2$) (Hemp et al., 2016). In addition other organisms, like Archaea (**Table 5.2**), could be responsible for ammonia oxidation to nitrite as recently shown by (Kuypers et al., 2018). Since the detection of AOBs and NOBs at very low levels is difficult by sequencing, further research will be needed to ascertain if the microorganisms here proposed were efectively the ones responsible for nitrification.

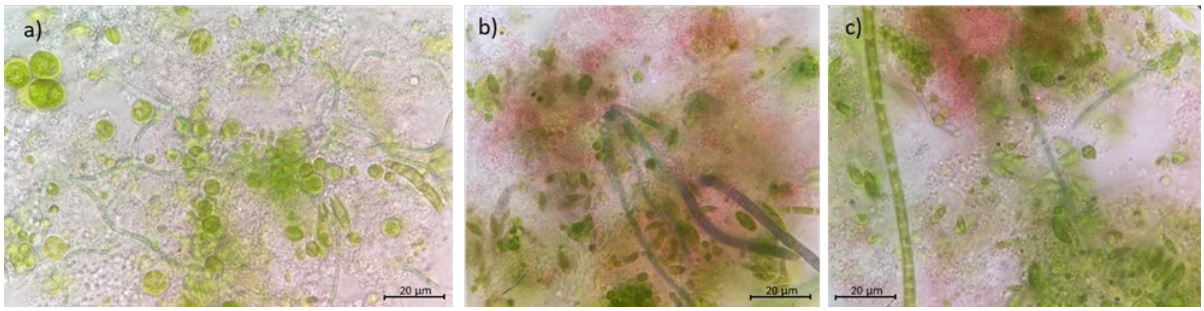

Figure 5.8 - Microscopic image of the photo-BNR sludge on day a) 59, b) 122 and c) 123.
Red biomass indicates the presence of purple bacteria, like Thiocapsa. Microalgae and Cyanobacteria appear in green color and Accumulibacter or other heterotrophic bacteria are in white.

5.4. Implications of the photo-BNR system

The first big advantage of the use of a photo-BNR system is the reduction of operation costs. The largest energy demand at a conventional WWTP is for aeration (Awe et al., 2016) and the cost of aeration can range between 45- 75% of the total energy consumption of a WWTP (Luo et al., 2019; Panepinto et al., 2016; Rosso et al., 2008). By removing the need of aeration, at least 50% of energetic costs could be reduced when using microalgae-bacteria consortia. Furthermore, since denitrification in photo-BNR does not depend on external organic carbon addition, the cost of chemical addition is reduced. Also, the direct use of sunlight does not require extra energy costs for illumination, however, a backup aerator could be employed when light availability is not enough for efficient photosynthesis. In terms of WWTP facilities, the tanks should be shallow and could demand a higher land availability, however, it is expected that the capital costs are similar as HRAP systems.

In addition to P and N removal, the system has the capacity for negative CO_2 emissions, due to the combination of microalgae and nitrifying bacteria activity that fixate atmospheric CO_2 and consume the CO_2 produced during the respiratory metabolism of heterotrophic bacteria. At a WWTP, excess CO_2 could be obtained during biogas cleaning for example, where methane gas is recovered following CO_2 separation. For this reason, the photo-BNR system can be a viable option for decreasing CO_2 emissions of a WWTP, as typically this separated CO_2 is emitted and not valorised. Moreover, the CO_2 generated during the biological treatment process would also be less as compared to a typical aerobic WWTP process, lowering further the greenhouse gas footprint of the plant.

However, the photo-BNR process is a more complex system with inter-dependent interactions between distinct bacterial groups, which implies a closer control of key parameters. From the data obtained in the present study, one of these parameters is the PHA availability. The PHA depletion earlier in the light phase reduced the energy available for P uptake, forcing glycogen consumption. When the anoxic phase started, PHA and glycogen were unavailable, limiting P uptake and denitrification. Therefore, future work should address the PHA consumption during aerobic phase, to allow higher PHA availability during the dark-anoxic phase and improve nitrate removal.

Another adjustment that the photo-BNR configuration requires is to optimise the duration of dark/light/dark-anoxic periods, in order to improve P and N removal during the light phase and to guarantee the total consumption of NO_3 during the dark-anoxic period. This last condition is very important to prevent nitrate presence during the dark feed phase, which would favour the growth of ordinary heterotrophic denitrifying organisms and deteriorate the P removal capacity of the photo-BNR system. Moreover, further studies are required to adjust the cycle length and/or operational reactor configuration to allow the photo-EBPR system implementation in outdoor conditions with diurnal illumination. Another key parameter that needs to be controlled, is oxygen concentration during the light phase which is directly dependent on the hours of light and CO_2 availability. Thus, CO_2 concentration is also a crucial parameter to control.

It is worth noting that the SRT could affect the efficiency of the photo-BNR operation. SRT not only affects population growth and selection, and thus nutrient removal efficiency, but also oxygen production by microalgae. The survival of ammonia and nitrite oxidizing microorganisms is SRT dependent and different SRT could lead to changes in nitrogen removal mechanisms. Higher SRT could lead to high biomass concentration inside the reactor and influence the microalgae-bacterial floc size, increasing nutrient removal (Zhang et al., 2021). On the other hand, excessive biomass concentration can limit photosynthesis due to the shadowing effects (González-Camejo et al., 2019). In future work, it is fundamental to test the impact of different SRT on culture selection nutrient, removal mechanism/efficiency and on biomass concentration which are related to oxygen production by microalgae.

Comparing the results obtained in the present work with nutrient removal in other photosynthetic systems, it is possible to conclude that the photo-BNR system is a more complete and efficient system that allows simultaneous removal of nitrogen, phosphorus and carbon, up to 40 mg N/L, 35 mg P/L and 300 mg COD/L, respectively. Studies about HRAP show that it is an efficient technology for carbon removal but presents some weaknesses in nutrient removal capacity. Godos et al. (2009) showed that in HRAP, using real WW, it is possible to remove up to 224 mg N /L of ammonia and achieve a COD removal higher than 2000 mg COD/L, but with an HRT of 10 days. However, phosphorus removal was not observed and nitrate was produced, resulting in an effluent with a high concentration of nitrate up to 99 mg N/L. Toledo-Cervantes et al. (2019), observed COD removal around 500 mg COD/L in an HRAP with a HRT of 4 days, with a maximum ammonium removal of 25 mg N /L and phosphorus and nitrate removal around 5 mg P /L and 3 mg N /L, respectively. Hülsen et al. (2016) showed that Phototrophic Purple Bacteria (PPB) systems, using real WW and an average HRT of 12h, have an ammonium removal capacity of 40 mg N /L and phosphorus removal around 6.5 mg P /L, but with the requirement of COD supplementation beyond that contained in the wastewater influent. Further research on photo-BNR should implicate the use of real wastewaters to address the impact of carbon feed composition on system stability and microbial population dynamics.

Although ammonia removal capacity in the mentioned studies is in the range of the photo-BNR system (40 mg N /L), less phosphorus removal capacity is observed in HRAP, WSP and other PPB systems. In addition, most of these systems required higher HRT when compared to the photo-BNR, requiring more time for nutrient removal. These results indicate that the photo-BNR is a potentially attractive alternative for nutrient removal for domestic wastewaters.

Overall, the operation of the photo-BNR process for P and N removal can be advantageous to conventional wastewater treatment, since it contributes to operational cost reduction, greenhouse gas mitigation (CO_2), and production of a sludge rich in P and N that can potentially be directly used as a fertilizer.

5.5 Conclusions

The results of this study show that effective COD, N and P removal can be simultaneously achieved in a photo-BNR system. This reduces WWTP operational costs, since no aeration is required and external COD addition can also be reduced or eliminated. The photo-BNR was able to remove 25 ± 9.2 mg P/L of phosphorus, which although only corresponds to 42 ± 17 % of the influent concentration, it is higher than the concentrations normally found in municipal wastewaters. The ammonia removal capacity was 40 mg N/L (100%), mainly by assimilation and nitrification (up to 39 %). dPAOs or dGAOs play an important role in the denitrification process, allowing a total nitrogen removal higher than 90%. The overall capacity of the photo-BNR process for nitrogen removal was 94 ± 3 %. The selected system opens the possibility of a low-cost treatment, with no need of aeration, where CO_2 mitigation can be integrated with wastewater treatment and the use of the microalgae-bacterial biomass as a fertilizer can generate extra revenue.

REFERENCES

Albertsen, M., McIlroy, S.J., Stokholm-Bjerregaard, M., Karst, S.M., Nielsen, P.H., 2016. "Candidatus Propionivibrio aalborgensis": A novel glycogen accumulating organism abundant in full-scale enhanced biological phosphorus removal plants. Front. Microbiol. 7, 1–17. https://doi.org/10.3389/fmicb.2016.01033

Amann, R.I., 1995. In situ identification of micro-organisms by whole cell hybridization with rRNA-targeted nucleic acid probes, in: Akkermans, A.D.L., Van Elsas, J.D., De Bruijn, F.J. (Eds.), Molecular Microbial Ecology Manual. Springer Netherlands, Dordrecht, pp. 331–345. https://doi.org/10.1007/978-94-011-0351-0_23

APHA/AWWA/WEF, 2012. Standard Methods for the Examination of Water and Wastewater. Stand. Methods.

Arias, D.M., Fradinho, J.C., Uggetti, E., García, J., Oehmen, A., Reis, M.A.M., 2018. Polymer accumulation in mixed cyanobacterial cultures selected under the feast and famine strategy. Algal Res. 33, 99–108. https://doi.org/10.1016/j.algal.2018.04.027

Atteia, A., Van Lis, R., Tielens, A.G.M., Martin, W.F., 2013. Anaerobic energy metabolism in unicellular photosynthetic eukaryotes. Biochim. Biophys. Acta - Bioenerg. 1827, 210–223. https://doi.org/10.1016/j.bbabio.2012.08.002

Awe, O.W., Liu, R., Zhao, Y., 2016. Analysis of Energy Consumption and Saving in Wastewater Treatment Plant : Case Study from Ireland. J. Water Sustain. 6, 63–76. https://doi.org/10.11912/jws.2016.6.2.63-76

Brown, N., Shilton, A., 2014. Luxury uptake of phosphorus by microalgae in waste stabilisation ponds: Current understanding and future direction. Rev. Environ. Sci. Biotechnol. 13, 321–328. https://doi.org/10.1007/s11157-014-9337-3

Camacho Rubio, F., Acién Fernández, F.G., Sánchez Pérez, J.A., García Camacho, F., Molina Grima, E., 1999. Prediction of dissolved oxygen and carbon dioxide concentration profiles in tubular photobioreactors for microalgal culture. Biotechnol. Bioeng. 62, 71–86. https://doi.org/10.1002/(SICI)1097-0290(19990105)62:1<71::AID-BIT9>3.0.CO;2-T

Camargo Valero, M.A., Mara, D.D., 2010. Ammonia volatilisation in waste stabilisation ponds: A cascade of misinterpretations? Water Sci. Technol. 61, 555–561. https://doi.org/10.2166/wst.2010.856

Camargo Valero, M.A., Mara, D.D., 2007. Nitrogen removal via ammonia volatilization in maturation ponds. Water Sci. Technol. 55, 87–92. https://doi.org/10.2166/wst.2007.349

Capson-Tojo, G., Batstone, D.J., Grassino, M., Vlaeminck, S.E., Puyol, D., Verstraete, W., Kleerebezem, R., Oehmen, A., Ghimire, A., Pikaar, I., Lema, J.M., Hülsen, T., 2020. Purple phototrophic bacteria for resource recovery: Challenges and opportunities. Biotechnol. Adv. 43, 107567. https://doi.org/10.1016/j.biotechadv.2020.107567

Carvalheira, Mónica, Oehmen, A., Carvalho, G., Eusébio, M., Reis, M.A.M., 2014a. The impact of aeration on the competition between polyphosphate accumulating organisms and glycogen accumulating organisms. Water Res. 66, 296–307.

https://doi.org/10.1016/j.watres.2014.08.033

Carvalheira, M., Oehmen, A., Carvalho, G., Reis, M., 2014. Survival strategies of polyphosphate accumulating organisms and glycogen accumulating organisms under conditions of low organic loading. Bioresour. Technol. 172, 290–296. https://doi.org/10.1016/j.biortech.2014.09.059

Carvalheira, Mónica, Oehmen, A., Carvalho, G., Reis, M.A.M., 2014b. The effect of substrate competition on the metabolism of polyphosphate accumulating organisms (PAOs). Water Res. 64, 149–159. https://doi.org/10.1016/j.watres.2014.07.004

Carvalho, V.C.F., Freitas, E.B., Fradinho, J.C., Reis, M.A.M., Oehmen, A., 2019. The effect of seed sludge on the selection of a photo-EBPR system. N. Biotechnol. 49, 112–119. https://doi.org/10.1016/j.nbt.2018.10.003

Carvalho, V.C.F., Freitas, E.B., Silva, P.J., Fradinho, J.C., Reis, M.A.M., Oehmen, A., 2018. The impact of operational strategies on the performance of a photo-EBPR system. Water Res. 129, 190–198. https://doi.org/10.1016/j.watres.2017.11.010

de Godos, I., Blanco, S., García-Encina, P.A., Becares, E., Muñoz, R., 2010. Influence of flue gas sparging on the performance of high rate algae ponds treating agro-industrial wastewaters. J. Hazard. Mater. 179, 1049–1054. https://doi.org/10.1016/j.jhazmat.2010.03.112

de Godos, I., Vargas, V.A., Guzmán, H.O., Soto, R., García, B., García, P.A., Muñoz, R., 2014. Assessing carbon and nitrogen removal in a novel anoxic-aerobic cyanobacterial-bacterial photobioreactor configuration with enhanced biomass sedimentation. Water Res. 61, 77–85. https://doi.org/10.1016/j.watres.2014.04.050

García, J., Green, B.F., Lundquist, T., Mujeriego, R., Hernández-Mariné, M., Oswald, W.J., 2006. Long term diurnal variations in contaminant removal in high rate ponds treating urban wastewater. Bioresour. Technol. 97, 1709–1715. https://doi.org/10.1016/j.biortech.2005.07.019

Godos, I. de, Blanco, S., García-Encina, P.A., Becares, E., Muñoz, R., 2009. Long-term operation of high rate algal ponds for the bioremediation of piggery wastewaters at high loading rates. Bioresour. Technol. 100, 4332–4339. https://doi.org/10.1016/j.biortech.2009.04.016

Griffin, B.M., Schott, J., Schink, B., 2007. Nitrite, an Electron Donor for Anoxygenic Photosynthesis. https://doi.org/10.1126/science.1139478

Gschwind, B., Ménard, L., Albuisson, M., Wald, L., 2006. Converting a successful research project into a sustainable service: the case of the SoDa Web service. Environ. Modell. Softw. 21, 1555e1561.

Guo, D., Zhang, X., Shi, Y., Cui, B., Fan, J., Ji, B., Yuan, J., 2021. Microalgal-bacterial granular sludge process outperformed aerobic granular sludge process in municipal wastewater treatment with less carbon dioxide emissions. Environ. Sci. Pollut. Res. 28, 13616–13623. https://doi.org/10.1007/s11356-020-11565-7

Hellebust, J.A., Ahmad, I., 1989. Regulation of Nitrogen Assimilation in Green Microalgae. Biol. Oceanogr. 6, 241–255. https://doi.org/https://doi.org/10.1080/01965581.1988.10749529

Hemp, J., Lücker, S., Schott, J., Pace, L.A., Johnson, J.E., Schink, B., Daims, H., Fischer, W.W., 2016. Genomics of a phototrophic nitrite oxidizer: Insights into the evolution of photosynthesis and nitrification. ISME J. 10, 2669–2678. https://doi.org/10.1038/ismej.2016.56

Henze, M., van Loosdrecht, M.C.M., Ekama, G.A., Brdjanovic, D., 2008. Biological Wastewater Treatment: Principles, Modeling and Design. IWA Publishing, London. https://doi.org/10.2166/9781780408613

Hülsen, T., Barry, E.M., Lu, Y., Puyol, D., Keller, J., Damien, J., 2016. Domestic wastewater treatment with purple phototrophic bacteria using a novel continuous photo anaerobic membrane bioreacto. Water Res. 100, 486–495. https://doi.org/10.1016/j.watres.2016.04.061

Hülsen, T., Batstone, D.J., Keller, J., 2013. Phototrophic bacteria for nutrient recovery from domestic wastewater. Water Res. 50, 18–26. https://doi.org/10.1016/j.watres.2013.10.051

Imhoff, J.F., Caumette, P., 2015. Thiocapsa . Bergey's Man. Syst. Archaea Bact. 1–8. https://doi.org/10.1002/9781118960608.gbm01116

Ji, B., Zhang, M., Gu, J., Ma, Y., Liu, Y., 2020. A self-sustaining synergetic microalgal-bacterial granular sludge process towards energy-efficient and environmentally sustainable municipal wastewater treatment. Water Res. 179, 115884. https://doi.org/10.1016/j.watres.2020.115884

Jia, H., Yuan, Q., 2016. Removal of nitrogen from wastewater using microalgae and microalgae – bacteria consortia Removal of nitrogen from wastewater using microalgae and microalgae – bacteria consortia. Cogent Environ. Sci. 31. https://doi.org/10.1080/23311843.2016.1275089

Kazbar, A., Cogne, G., Urbain, B., Marec, H., Le-Gouic, B., Tallec, J., Takache, H., Ismail, A., Pruvost, J., 2019. Effect of dissolved oxygen concentration on microalgal culture in photobioreactors. Algal Res. 39, 101432. https://doi.org/10.1016/j.algal.2019.101432

Kuypers, M.M.M., Marchant, H.K., Kartal, B., 2018. The microbial nitrogen-cycling network. Nat. Rev. Microbiol. 16, 263–276. https://doi.org/10.1038/nrmicro.2018.9

Lanham, A.B., Oehmen, A., Carvalho, G., Saunders, A.M., Nielsen, P.H., Reis, M.A.M., 2018. Denitrification activity of polyphosphate accumulating organisms (PAOs) in full-scale wastewater treatment plants. Water Sci. Technol. 78, 2449–2458. https://doi.org/10.2166/wst.2018.517

Lanham, A.B., Oehmen, A., Saunders, A.M., Carvalho, G., Nielsen, P.H., Reis, M.A.M., 2013a. Metabolic versatility in full-scale wastewater treatment plants performing enhanced biological phosphorus removal. Water Res. 47, 7032–7041. https://doi.org/10.1016/j.watres.2013.08.042

Lanham, A.B., Ricardo, A.R., Albuquerque, M.G.E., Pardelha, F., Carvalheira, M., Coma, M., Fradinho, J., Carvalho, G., Oehmen, A., Reis, M.A.M., 2013b. Determination of the extraction kinetics for the quantification of polyhydroxyalkanoate monomers in mixed microbial systems. Process Biochem. 48, 1626–1634. https://doi.org/10.1016/j.procbio.2013.07.023

Lanham, A.B., Ricardo, A.R., Coma, M., Fradinho, J., Carvalheira, M., Oehmen, A., Carvalho, G., Reis, M.A.M., 2012. Optimisation of glycogen quantification in mixed microbial cultures. Bioresour. Technol. 118, 518–525. https://doi.org/10.1016/j.biortech.2012.05.087

Liu, L., Fan, H., Liu, Y., Liu, C., Huang, X., 2017. Development of algae-bacteria granular consortia in photo-sequencing batch reactor. Bioresour. Technol. 232, 64–71. https://doi.org/10.1016/j.biortech.2017.02.025

Lopez, C., Pons, M.N., Morgenroth, E., 2006. Endogenous processes during long-term starvation in activated sludge performing enhanced biological phosphorus removal. Water Res. 40, 1519–1530. https://doi.org/10.1016/j.watres.2006.01.040

Lv, J., Wang, X., Feng, J., Liu, Q., Nan, F., Jiao, X., Xie, S., 2019. Comparison of growth characteristics and nitrogen removal capacity of five species of green algae. J. Appl. Phycol. 31, 409–421. https://doi.org/10.1007/s10811-018-1542-y

Mandel, A., Zekker, I., Jaagura, M., Tenno, T., 2019. Enhancement of anoxic phosphorus uptake of denitrifying phosphorus removal process by biomass adaption. Int. J. Environ. Sci. Technol. 16, 5965–5978. https://doi.org/10.1007/s13762-018-02194-2

Muñoz, R., Guieysse, B., 2006. Algal-bacterial processes for the treatment of hazardous contaminants: A review. Water Res. 40, 2799–2815. https://doi.org/10.1016/j.watres.2006.06.011

Muñoz, R., Jacinto, M., Guieysse, B., Mattiasson, B., 2005. Combined carbon and nitrogen removal from acetonitrile using algal-bacterial bioreactors. Appl. Microbiol. Biotechnol. 67, 699–707. https://doi.org/10.1007/s00253-004-1811-3

Nielson, P.H., Daim, H., Lemmer, H., 2009. FISH Handbook for Biological Wastewater Treatment: Identification and quantification of microorganisms in activated sludge and biofilms by FISH, IWA Publishing. IWA Publishing Company, London.

Oehmen, A., Zeng, R.J., Yuan, Z., 2005. Anaerobic Metabolism of Propionate by Polyphosphate-Accumulating Organisms in Enhanced Biological Phosphorus Removal Systems. https://doi.org/10.1002/bit.20480

Panepinto, D., Fiore, S., Zappone, M., Genon, G., Meucci, L., 2016. Evaluation of the energy efficiency of a large wastewater treatment plant in Italy. Appl. Energy 161, 404–411. https://doi.org/10.1016/j.apenergy.2015.10.027

Posadas, E., Muñoz, A., García-González, M.C., Muñoz, R., García-Encina, P.A., 2015. A case study of a pilot high rate algal pond for the treatment of fish farm and domestic wastewaters. J. Chem. Technol. Biotechnol. 90, 1094–1101. https://doi.org/10.1002/jctb.4417

Powell, N., Shilton, A.N., Pratt, S., Chisti, Y., 2011. Luxury uptake of phosphorus by microalgae in waste stabilization ponds. Environ. Sci. Technol. 63, 704–709. https://doi.org/10.1021/es703118s

Rada-Ariza, A.M., Fredy, D., Lopez-Vazquez, C.M., Van der Steen, N.P., Lens, P.N.L., 2019. Ammonium removal mechanisms in a microalgal-bacterial sequencing-batch photobioreactor at different solids retention times. Algal Res. 39, 101468. https://doi.org/10.1016/j.algal.2019.101468

Ritchie, R.J., 2018. Measurement of chlorophylls a and b and bacteriochlorophyll a in organisms from hypereutrophic auxinic waters. J. Appl. Phycol. 30, 3075–3087. https://doi.org/10.1007/s10811-018-1431-4

Rosso, D., Larson, L.E., Stenstrom, M.K., 2008. Aeration of large-scale municipal wastewater treatment plants : state of the art 973–979. https://doi.org/10.2166/wst.2008.218

Rubio-Rincón, F. J., Weissbrodt, D.G., Lopez-Vazquez, C.M., Welles, L., Abbas, B., Albertsen, M., Nielsen, P.H., van Loosdrecht, M.C.M., Brdjanovic, D., 2019. "Candidatus Accumulibacter delftensis": A clade IC novel polyphosphate-accumulating organism without denitrifying activity on nitrate. Water Res. 161, 136–151. https://doi.org/10.1016/j.watres.2019.03.053

Rubio-Rincón, Francisco J., Welles, L., Lopez-Vazquez, C.M., Abbas, B., Van Loosdrecht, M.C.M., Brdjanovic, D., 2019. Effect of lactate on the microbial community and process performance of an EBPR system. Front. Microbiol. 10, 1–11. https://doi.org/10.3389/fmicb.2019.00125

Santos, J.M.M., Rieger, L., Lanham, A.B., Carvalheira, M., Reis, M.A.M., Oehmen, A., 2020. A novel metabolic-ASM model for full-scale biological nutrient removal systems. Water Res. 171. https://doi.org/10.1016/j.watres.2019.115373

Sanz-Luque, E., Chamizo-Ampudia, A., Llamas, A., Galvan, A., Fernandez, E., 2015. Understanding nitrate assimilation and its regulation in microalgae. Front. Plant Sci. 6. https://doi.org/10.3389/fpls.2015.00899

Schott, J., Griffin, B.M., Schink, B., 2010. Anaerobic phototrophic nitrite oxidation by Thiocapsa sp. strain KS1 and Rhodopseudomonas sp. strain LQ17. Microbiology 156, 2428–2437. https://doi.org/10.1099/mic.0.036004-0

Smolders, G.J.F., van der Meij, J., van Loosdrecht, M.C.M., Heijnen, J.J., 1994. Model of the anaerobic metabolism of the biological phosphorus removal process: Stoichiometry and pH influence. Biotechnol. Bioeng. 43, 461–470. https://doi.org/10.1002/bit.260430605

Taziki, M., Ahmadzadeh, H., A. Murry, M., R. Lyon, S., 2015. Nitrate and Nitrite Removal from Wastewater using Algae. Curr. Biotechnol. 4, 426–440. https://doi.org/10.2174/2211550104666150828193607

Toledo-Cervantes, A., Posadas, E., Bertol, I., Turiel, S., Alcoceba, A., Muñoz, R., 2019. Assessing the influence of the hydraulic retention time and carbon/nitrogen ratio on urban wastewater treatment in a new anoxic-aerobic algal-bacterial photobioreactor configuration. Algal Res. 44, 101672. https://doi.org/10.1016/j.algal.2019.101672

Valverde-Pérez, B., Wágner, D.S., Lóránt, B., Gülay, A., Smets, B.F., Plósz, B.G., 2016. Short-sludge age EBPR process – Microbial and biochemical process characterisation during reactor start-up and operation. Water Res. 104, 320–329. https://doi.org/10.1016/j.watres.2016.08.026

Wang, M., Yang, H., Ergas, S.J., van der Steen, P., 2015. A novel shortcut nitrogen removal process using an algal-bacterial consortium in a photo-sequencing batch reactor (PSBR). Water Res. 87, 38–48. https://doi.org/10.1016/j.watres.2015.09.016

6.

RAMAN SPECTROMETRY AS A TOOL FOR AN ONLINE CONTROL OF A PHOTO-TROPHIC BIOLOGICAL NUTRIENT REMOVAL PROCESS

SUMMARY: Real-time bioprocess monitoring is crucial for efficient operation and effective bioprocess control. Aiming to develop an online monitoring strategy for facilitating optimization, fault detection and decision-making during wastewater treatment in a photo-biological nutrient removal (photo-BNR) process, this study investigated the application of Raman spectroscopy for quantification of total organic content (TOC), volatile fatty acids (VFA), carbon dioxide (CO_2), ammonia (NH_3), nitrate (NO_3), phosphate (PO_4), total phosphorus (total P), polyhydroxyalkanoates (PHA), total carbohydrates, total and volatile suspended solids (TSS and VSS, respectively). Specifically, partial least squares (PLS) regression models were developed to predict these parameters based on Raman spectra and evaluated based on a full cross-validation. Through optimization of spectral pre-processing, Raman shift regions and latent variables, 8 out of the 11 parameters that were investigated – namely, TOC, VFA, CO_2, NO_3, total P, PHA, TSS and VSS - could be predicted with good quality by the respective Raman-based PLS calibration models, as shown by the high coefficient of determination (R^2>90.0%) and residual prediction deviation (RPD>5.0), and relatively low root mean square error of cross-validation. This study showed for the first time the high potential of Raman spectroscopy for online monitoring of TOC, VFA, CO_2, NO_3, total P, PHA, TSS and VSS in a photo-BNR reactor.

Keywords: Microalgal-bacterial consortium; Biological wastewater treatment; Photo-biological nutrient removal reactor; Raman spectroscopy; Real-time monitoring.

Published as: Franca, R.D.G., Carvalho, V.C.F., Fradinho, J.C., Reis, M.A.M., Lourenço, N.D., 2021. Raman Spectrometry as a Tool for an Online Control of a Phototrophic Biological Nutrient Removal Process. Appl. Sci. 11. 6600. https://doi.org/10.3390/app11146600

Authors Contribution: Virginia Carvalho operated the photosynthetic bioreactors, took the samples and performed the analysis for process performance evaluation; Rita Franca carried

out the RAMAN spectrometry analysis, since data refinement, models development and validation. Maria Reis, Joana Fradinho and Nídia Lourenço supervised all the work.

6.1. Introduction

Demographic expansion and the improvement of life standards around the world led to rapid urbanization, intensive agricultural practices and industrial expansion. Consequently, environmental and water pollution increased, either through the release of waste streams with high concentrations of carbon, nitrogen (N) and/or phosphorus (P), or through the excessive use of fertilizers (Taziki et al., 2015). Exceeding N and P discharge limits into natural water reserves can lead to eutrophication, perturbing the equilibrium of aquatic ecosystems (Izadi et al., 2020). Improving the ecological status of water sources is a growing concern for many nations, in particular regarding the reduction of N and P concentrations during wastewater treatment (Fatemeh et al., 2021)

The technologies currently applied for N and P removal in wastewater treatment plants (WWTPs) are highly oxygen (O_2) and/or chemical-dependent, which not only increases the operation costs of wastewater treatment, but also has a negative impact on the environment, due to the high greenhouse gas emissions that occur both during the wastewater treatment process and energy production for aeration. Biological nutrient removal (BNR) is the most common process implemented for simultaneous P and N removal, typically through sequential zones in activated sludge systems: anaerobic for carbon uptake and P release; anoxic for heterotrophic denitrification and P uptake; and aerobic for nitrification and P uptake. Such BNR systems require intensive O_2 supply, often accounting for approximately 60% of WWTPs energy costs (Rosso et al., 2008; Luo et al., 2019).

The use of phototrophic anoxygenic bacteria or microalgae systems for wastewater treatment is a good alternative to decrease aeration energy costs in WWTPs (Fatemeh et al., 2021; Capson-Tojo et al., 2020; Hülsen et al., 2013; Winkler and Straka, 2019). Furthermore, microalgal-bacterial consortia can achieve higher nutrient removal efficiencies than bacterial or microalgal systems alone and with reduced oxygenation costs. In fact, microalgae not only perform nutrient removal but also consume the carbon dioxide (CO_2) produced by bacteria, while producing, through photosynthesis, the O_2 required for system oxygenation and heterotrophic bacterial growth (Fatemeh et al., 2021). In addition, higher nutrient recovery can be achieved when compared with anaerobic technologies in WWTPs (Muñoz and Guieysse 2006; Toledo-Cervantes et al., 2019), and the good settling properties of the microalgal-bacterial flocs reduces the biomass harvesting costs associated to microalgal systems (Liu et al., 2017; Munõz et al., 2005). In **chapter 3** and **4**, a photo-enhanced biological phosphorus removal (photo-EBPR) system composed of a consortium of microalgae and bacteria demonstrated a good capacity for P removal at a low chemical oxygen demand (COD) to P ratio (COD/P) and without external aeration requirements. The photo-EBPR system was operated with dark-

light cycles, simulating conventional anaerobic-aerobic EBPR cycles, resulting in a culture enriched with polyphosphate accumulating organisms (PAOs) and microalgae (Carvalho et al., 2018; Carvalho et al., 2019).

In the current chapter, a photo-BNR system combining P and N removal was operated and monitored as described in **chapter 5** (Carvalho et al., 2021). In photo-BNR systems, volatile fatty acids (VFA), or other organic carbon sources, are consumed during the dark period. During the light period, microalgae consume CO_2 and produce O_2 to be used by PAOs and nitrifiers. Furthermore, PAOs will store excess P as polyphosphate, while nitrifiers oxidize ammonia to nitrate. Since both nitrifiers and microalgae are CO_2 dependent, the CO_2 mitigation ability of the photo-BNR process is potentially higher than other BNR processes. An anoxic dark period is added after the light period, to allow denitrification to occur. During the dark anoxic period, when no external carbon source is added, denitrifying PAOs are expected to perform denitrification by using the anaerobically stored polyhydroxyalkanoates (PHA). The main mechanisms of nutrient removal observed in the photo-BNR were ammonia assimilation by the microbial biomass, phosphorus accumulation as poly-P by PAOs, and nitrate removal by denitrification. Due to the interaction between microalgae and bacteria, cells can aggregate as flocs more easily and settle very fast, resulting in a solids-free effluent and, thus, solving one of the main problems of using microalgae for wastewater treatment. The goal of the photo-BNR process is to remove BNR aeration requirements and mitigate CO_2 without the need for costly external COD dosing, thus reducing the operational costs and ecological footprint of the WWTP (Carvalho et al., 2021)

Real-time bioprocess monitoring is of crucial importance for efficient operation and effective bioprocess control (Lourenço et al., 2012). In contrast with offline, retrospective and time-consuming reference analytical methods, which do not provide a real-time knowledge of process performance, the use of fast, non-destructive, robust and sensitive online spectroscopy probes, in combination with chemometrics, have great potential for real-time monitoring of key bioprocess parameters, significantly reducing the time required for bioprocess control and optimization (Veloso & Ferreira, 2017). Raman spectroscopy can provide a wide range of information, from molecular structure to chemical environment, being among the most interesting spectroscopic-based techniques reported for online monitoring of microbiological processes (Veloso & Ferreira, 2017). In fact, in addition to representing a rapid, eco-friendly and economic alternative to reference analytical methods (e.g. chromatography), Raman spectroscopy is particularly suitable for in situ quantitative monitoring of multiple component bioprocesses, owing to the incorporation of fiber optic-based probes, as well as due to its insensitivity to water (Barra et al., 2021). Nevertheless, applications of online bioprocess monitoring and control using Raman spectroscopy coupled with chemometrics are still scarce. Examples include nitrate and nitrite monitoring in a wastewater treatment bioreactor (Ianoul et al., 2002), real-time prediction of glucose concentration during microalgae cultivation in a photobioreactor (Paudel et al., 2015) and during mammalian cell cultivations (Kozma et al., 2017),

as well as monitoring of substrates and products during bacterial and yeast fermentation processes (Lourenço et al., 2012; Veloso & Ferreira, 2017), especially for pharmaceutical industrial application (Claßen et al., 2016; Esmonde-White et al., 2016).

In this context, the application of Raman spectroscopy for online monitoring of a photo-BNR is of outmost interest, facilitating optimization, fault detection and decision-making during the wastewater treatment process. Specifically, real-time knowledge on key-parameters such as NH_3, nitrate (NO_3), phosphate (PO_4), total organic content (TOC), VFA and CO_2 can be crucial for optimizing nutrient and carbon removal, namely by controlling the CO_2 dosing and the time length of the anaerobic (dark), aerobic (light) and anoxic periods. In addition to PO_4, polyphosphate (poly-P), or total P (which allow a more direct monitoring and control of the P removal performance), PHA and carbohydrates are key functionally relevant intracellular polymers also involved in the EBPR process, their real-time quantification significantly contributing for understanding the dynamics and optimizing the nutrient removal process. Moreover, monitoring cell growth by following the total suspended solids (TSS) and volatile suspended solids (VSS) by Raman spectroscopy would also provide important information on the system performance, such as, for example, the light availability per biomass concentration, a parameter that can affect photosynthesis efficiency (Foladori et al., 2019).

Micro-Raman spectroscopy has been used for simultaneous identification and quantification of the intracellular polymers poly-P, poly(3-hydroxybutyrate) (PHB) and glycogen in individual microbial cells from complex environmental samples, characterizing their distribution among conventional EBPR microbial populations (Majed & Gu, 2010; Li et al., 2018). Recent studies further developed Raman microscopy-based quantitative approaches to assess the structural dynamics and storage states of these relevant intracellular polymers, crucial for fundamental understanding of the EBPR process (Guo et al., 2019; Fernando et al., 2019). In addition, Raman microscopy was shown to identify and quantify poly-P in microalgal cells, specifically Chlorella vulgaris (Moudříková et al., 2016). However, Raman microscopy is not suitable for online measurements and although Raman spectroscopy has been suggested as a fast and efficient tool for process control of PHB bioproduction through qualitative and quantitative in situ monitoring of intracellular PHB content in *Cupriavidus necator* H16 cultures (Samek et al., 2016), its application for real-time monitoring in mixed microbial bioprocesses is limited and has never been demonstrated for a photo-BNR system.

Unlike Raman microscopy, where specific Raman peaks can be used to follow the associated biomolecules, Raman spectra acquired through an immersion probe in a complex environmental ecosystem, such as a photo-BNR reactor, are very complex, including a large amount of data. Therefore, Raman spectroscopy needs to be combined with chemometric tools to extract the relevant information from the spectral data and develop quantitative mathematical models that will ultimately allow real-time predictions of the system properties and concentration of various analytes based on new, in line, fast and non-destructive spectroscopic measurements.

The present study aimed to develop a Raman-based monitoring strategy for the real-time prediction of several key parameters of a photo-BNR reactor for process control and optimization. Therefore, Raman spectra were acquired at-line, directly from mixed liquor samples harvested from a lab-scale photo-BNR reactor, and partial least squares (PLS) calibration models were developed to predict the concentration of TOC, VFA, CO_2, NH_3, NO_3, PO_4, total P, PHA, carbohydrates, TSS and VSS in the mixed liquid. The capacity of the calibration models to predict the reference data measured by standard analytical methods was evaluated by a full cross-validation procedure.

6.2. Materials and methods

6.2.1. Reactor operation and sampling

An acrylic sequencing batch reactor (SBR) with a working volume of 2 L was inoculated with wastewater sludge from the aerobic tank of a WWTP located in Lisbon (Beirolas, Portugal). The SBR was fed with a synthetic domestic wastewater and operated for 128 days in 8-h cycles, comprising subsequent periods of anaerobic (dark), aerobic (light) and anoxic phases for 7 hours, followed by 1 hour for settling and withdrawal as described in **Chapter 5**. Mixed liquor samples were harvested from the SBR during 7 hours of each reactor cycle, along the selected treatment cycles (13 samples per cycle, as example in **Figure B.1**) and used for both at-line Raman spectra acquisition and offline quantification of TOC, CO_2, VFA, CO_2, NH_3, NO_3, PO_4, total P, PHA, glycogen, TSS and VSS through reference analytical methods as described in **Chapter 2**. Total P, TSS and VSS were only determined on samples collected at specific timepoints. Four SBR cycles were selected for this study, corresponding to the SBR operation days 73 (cycle A; samples 1-13), 79 (cycle B; samples 14-26), 85 (cycle C; samples 27-39) and 101 (cycle D; samples 40-52). Specifically, the duration of the anaerobic/aerobic/anoxic phases were 3 h/4 h/0 h on cycle A, 1.5 h/2.5 h/3 h on cycles B and C, and 1.5 h/3.5 h/2 h on cycle D. The quantification of all parameters was performed in the four selected cycles, except for TOC, which was only measured on cycle A.

6.2.2. Raman spectroscopic method

Raman spectra of 2 mL mixed liquor samples were acquired directly after collection and without pre-treatment using a fiber coupled Raman probe (RPB Raman probe, InPhotonics) routed to a modular spectrometer (Ocean Optics QE65 Pro), and a 785 nm excitation laser (RGBLase LLc, USA) with 500 mW output. The Raman probe used was a non-immersible anodized aluminium probe with a stainless-steel tip and focused light with a working distance of 7.5 mm. Thermo-electric cooling was applied in the spectrometer with a detector set point of -10ºC. Each spectrum was obtained in the Raman shift range from 2677.68 to -62.34 cm^{-1}, with a 3.69 cm^{-1}/pixel linear dispersion, corresponding to 1044 data points. Raman spectroscopy analysis was performed at-line directly on the mixed liquor samples, without any pre-treatment, in order to mimic online measurements. One scan was performed for each sample.

A 5 sec integration time was applied during spectral acquisitions on cycles A, B and C, and an integration time of 200 msec was used on samples from cycle D to avoid signal oversaturation. The acquired spectra correspond to the first basic measurements in a lab-scale photo-BNR. In real systems, overlaying fluorescence is an expected interference and this aspect will be focused on a future work.

6.2.3. Chemometric analysis

PLS calibration models were developed based on Raman spectra of mixed liquor samples (Raman spectroscopic method) and on respective standard measurements of the selected parameters (reference analytical method). Commercial OPUS Quant2 software, version 8.2.28 (Bruker Optik GmbH, Germany), was used for spectral data pre-processing and chemometric PLS calibration model development for each selected parameter.

Raman spectral pre-processing is crucial to remove undesired systematic variations in the spectral data that are unrelated to the analytical information, consequently degrading the predictive ability of a calibration model. To extract the spectral information related to each one of the parameters considered, the corresponding PLS calibration models were optimized in terms of spectral range, pre-processing method and number of factors or latent variables (LV) employed, a maximum of 10 LV being considered.

Optimization of calibration models was performed using the OPUS Quant2 optimization tool, which evaluates the combination of different data pre-processing strategies with various spectral ranges, resulting in more than 1000 tested combinations (Ludwig et al., 2019). Specifically, a Raman shift region defined by the user is divided into 10 equal subregions and the best combination of subregions is iteratively searched by the optimization tool. Mean-centering was applied as default in every pre-processing strategy, in addition to the eleven default pre-processing strategies, which include no further spectral data pre-processing, constant offset elimination, straight line subtraction (SLS), vector normalization (standard normal variate; SNV), minimum-maximum (Min-Max) normalization, multiplicative scatter correction (MSC), first derivative (1st Der) and second derivatives (17 smoothing points used as default), as well as the combined methods 1st Der + SLS, 1st Der + SNV and 1st Der + MSC.

A full cross-validation (leave-one-out) procedure was adopted to determine the optimal number of LV, based on the minimum value obtained for the root mean square error of cross-validation (RMSECV). The prediction performance and accuracy of the PLS models were evaluated based on the coefficient of determination of cross-validation (R^2_{CV}), the RMSECV, and the residual prediction deviation of cross-validation (RPD_{CV}). Specifically, the RPD value indicates whether a PLS model has insufficient prediction quality (RPD<2.5) or if it can be used as a rough screening method (2.5<RDP<3), as a good screening method (3<RPD<5), as a quality control method (5<RPD<8) or as an excellent method for analytical tasks (RPD>8) (Mendes et al., 2020). Bias was also considered, corresponding to the systematic averaged deviation between the predicted and the reference values. Overall, robust, reliable, and unbiased calibration models are characterized by combining low values of RMSECV, high R^2_{CV} and RPD_{CV}, a bias value close to zero, as well as a low number of LV in order to avoid the overfitting of the

model. Depending on the studied parameter, some samples were excluded from the calibration set during PLS model development, either in case of no detectable amounts of the analyte in a sample (null concentration determined by the reference method) or when the associated measurement was considered an outlier based on the Mahalanobis distance. The spectra of samples containing null concentration of a parameter were not included in the PLS model in order to avoid an imbalanced calibration model focused on the concentration region around zero, instead of the concentration range of interest for each parameter. Since NO_2 was not detectable in any of the analyzed samples, PLS models were not developed for this parameter.

6.3. Results and Discussion

6.3.1. Development of PLS calibration models

To study the possibility of using Raman spectroscopy as a monitoring tool in a photo-BNR wastewater treatment process, Raman spectra were acquired from mixed liquor samples harvested along four selected SBR cycles (13 samples/cycle), as described in **section 6.2.1**. Although each spectrum was obtained in the Raman shift range from 2677.68 to -62.34 cm^{-1}, the region below 200 cm^{-1} corresponded to spectral noise, not being considered in the development of PLS models. The most intense peaks in the Raman spectra were observed within the range 2000-1000 cm^{-1}, as observed in the raw Raman spectra of all samples used in this study (**Figure 6.1**). Nevertheless, it was difficult to make direct peak attributions through visual inspection due to overlapping vibrational modes of different constituents in such complex samples, confirming the need for multivariate analysis methods such as PLS regression.

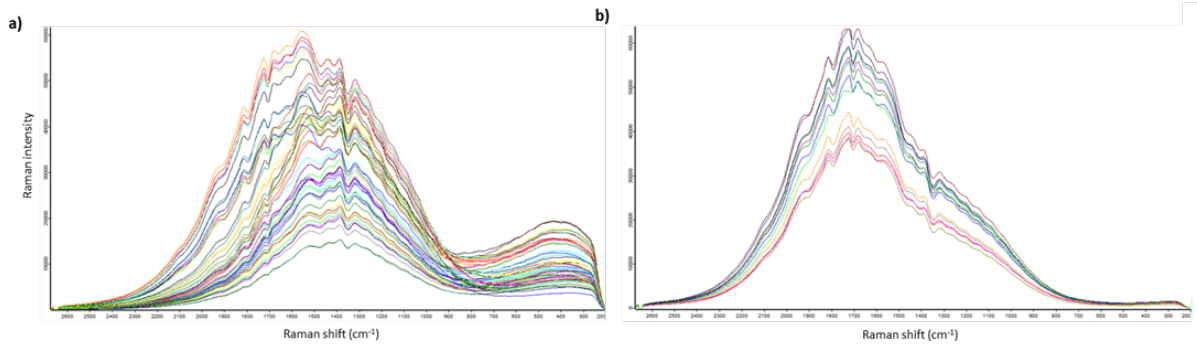

Figure 6.1- Raw Raman spectra of mixed liquor samples harvested from the SBR.
a) cycles A, B and C (samples 1-39; 5-sec integration time), and b) cycle D (samples 40-52; 200-msec integration time).

To extract relevant spectral information, PLS model optimization was carried out by testing different spectra pre-processing strategies in combination with various spectral regions using the OPUS software, as described in **section 6.2.3**. Proper selection of spectral ranges is essential to avoid that bands of interfering components are accounted by the PLS algorithm, consequently deteriorating the quality of the model. The main spectral truncations used as input for this optimization process included the total spectral range without the noise

region (2677.68-200 cm^{-1}) and two spectral truncations covering the most peak-concentrated areas of the spectra (2000-200 cm^{-1} and 2000-1000 cm^{-1}). In addition, aiming for a more refined search of relevant spectral data, different spectral regions were considered for each parameter, according to Raman shift attributions described in the literature (Movasaghi et al., 2007). Specifically, distinct regions within the Raman shift range 1200-600 cm^{-1} were considered in the development of models for PO_4 and poly-P for comprising P-O-P and PO_2^- stretching vibrations (Li et al., 2018; Guo et al., 2019; Fernando et al., 2019; Moudříková et al., 2016; Movasaghi et al., 2007; Ma et al., 2020; Majed et al., 2020), whereas the 1450-1200 cm^{-1} range was tested for modelling CO_2 (Kobayashi et al., 2012). Similarly, region 1600-1350 cm^{-1} was tested for NH_3 models owing to the N-H in plane deformation reported within this range (Movasaghi et al., 2007), while 1100-1000 cm^{-1} range was tested for NO_3 models due to symmetric N-O stretching vibrations (Ianoul et al., 2002). Moreover, 1800-400 cm^{-1} and 1200-800 cm^{-1} were studied during the construction of PLS models for VFA due to characteristic C-C, C=O, C-H, CH_2 and CH_3 bands (Majed &Gu, 2010; Li et al., 2018; Fernando et al., 2019; Jost et al., 2017; Izumi et al., 2010), and the regions 1800-1700 cm^{-1} + 1000-800 cm^{-1} + 500-400 cm^{-1} were specifically tested in PHA modelling for comprising previously associated Raman shifts (Majed & Gu, 2010; Guo et al., 2019; Jost et al., 2017; Izumi et al., 2010; De Gelder et al., 2008),. Finally, the Raman shifts 500-450 cm^{-1} + 1200-800 cm^{-1} were used to build calibration models for carbohydrates owing to their specific association with glycogen (Majed & Gu, 2010; Li et al., 2018; Movasaghi et al., 2007).

6.3.2. Evaluation of PLS calibration models

The models developed for each parameter were evaluated mostly based on the RMSECV and R2CV, while still considering the calibration parameters, i.e. root mean square error of calibration (RMSEC) and coefficient of determination of calibration (R2Cal). **Table 6.1** presents the optimized pre-processing strategy, spectral region and number of LV used in the final PLS models selected for each studied parameter, along with the respective calibration and cross-validation statistical results. These calibration models are graphically represented in **Figure 6.2**, which depicts the regression line that correlates the analytically measured values of each calibration sample with the corresponding values predicted by the calibration model. Overall, it was possible to establish a good relation between Raman spectral data and the concentration of all the studied parameters. This was denoted by the very high R^2_{Cal} (> 99.3%) and prediction deviation of calibration (RPD_{Cal} > 11.6), and by the relatively low RMSEC values registered for almost all parameters (**Table 6.1**), except for NH_3, which presented slightly less favourable calibration results (R^2_{Cal} = 96.2%; RPD_{Cal} = 5.2). These statistical results reflect the data represented in **Figure 6.2**, where the calibration points very well fit the regression line for each parameter, with more scattered data points around the regression line being exceptionally observed in the NH_3 model.

Table 6.1 - Raman-PLS models developed for each studied parameter, within the indicated concentration range.

					Calibration			Cross-validation			
Parameter	**n**	**Range**	**Spectral regions (cm^{-1})**	**Pre-processing [a]**	**LV**	**R^2_{Cal} (%)**	**RMSEC [b]**	**RPD_{Cal}**	**R^2_{CV} (%)**	**RMSECV [b]**	**RPD_{CV}**	**Bias**
Carbohydrates	28	2.8 - 8.3 mmolC L^{-1}	1200.0 - 1159.5 999.4 - 959.0 920.3 - 878.0 839.4 - 798.9	n.a.p.	7	99.4	0.15	12.5	88.2	0.53	2.9	-0.012
CO_2	33	3.0 - 16.7 g L^{-1}	1450.3 - 1398.8 1374.8 - 1297.6	MSC	8	99.8	0.16	21.9	90.0	0.96	3.2	0.063
NH_3	37	17.2 - 26.5 mgN L^{-1}	2677.7 - 1685.8 1439.2 - 1189.0 944.2 - 199.0	1st Der + MSC	8	96.2	0.72	5.2	65.5	1.89	1.7	-0.018
NO_3	6	0.3 - 3.3 mgN L^{-1}	1080.4 - 1069.4	n.a.p	3	99.6	0.14	14.9	97.7	0.18	6.7	-0.028
PHA	24	0.7 - 12.8 mmolC L^{-1}	1001.3 - 898.2 850.4 - 798.9 491.6 - 464.0	1st Der + SNV	9	99.9	0.12	37.6	95.9	0.71	5.0	-0.011
PO_4	36	32.2 - 99.6 mgP L^{-1}	1030.7 - 940.6 670.1 - 579.9	n.a.p.	8	99.4	1.95	13.1	70.0	12.10	1.8	0.364
TOC	13	17.4 - 43.2 ppm	1501.8 - 1349.1 1051.0 - 898.2 751.0 - 598.3	COE	5	99.5	0.76	13.6	96.7	1.38	5.5	0.070
Total P	11	0.1 - 0.4 g L^{-1}	1179.8 - 1168.7 1159.5 - 1139.3	1st Der + MSC	9	100.0	0.00	323.0	99.0	0.01	10.3	0.001
TSS	13	2.7 - 5.8 g L^{-1}	1801.8 - 1698.7 1601.2 - 1500.0 1100.7 - 999.4	SNV	5	99.9	0.03	34.2	97.5	0.14	6.3	-0.003
VFA	8	0.1 - 2.7 mmolC L^{-1}	1934.2 - 1685.8 944.2 - 694.0	n.a.p.	4	99.5	0.10	13.9	95.4	0.18	4.7	0.027
VSS	13	2.1 - 4.5 g L^{-1}	1901.1 - 1500.0 1400.6 - 1299.4 1100.7 - 999.4	Min-Max	5	99.3	0.08	11.6	93.9	0.17	4.1	-0.019

Total carbohydrates, carbon dioxide (CO_2), ammonia (NH_3), nitrate (NO_3), polyhydroxyalkanoates (PHA), phosphate (PO_4), total organic content (TOC), total phosphorus (total P), total suspended solids (TSS), volatile fatty acids (VFA), and volatile suspended solids (VSS). For each parameter, the optimized pre-processing strategy, spectral regions, and number of latent variables (LV) used in the selected model are indicated, along with the respective statistical results from the calibration (coefficient of determination of calibration, R^2_{Cal}; root mean square error of calibration, RMSEC; residual prediction deviation of calibration, RPD_{Cal}) and the full (leave-one-out) cross-validation (coefficient of determination of cross-validation, R^2_{CV}; root mean square error of cross-validation, RMSECV; residual prediction deviation of cross-validation, RPD_{CV}; Bias) obtained during the prediction of the indicated parameters. The number of samples included in the calibration set (n) of each calibration model is indicated for each parameter.

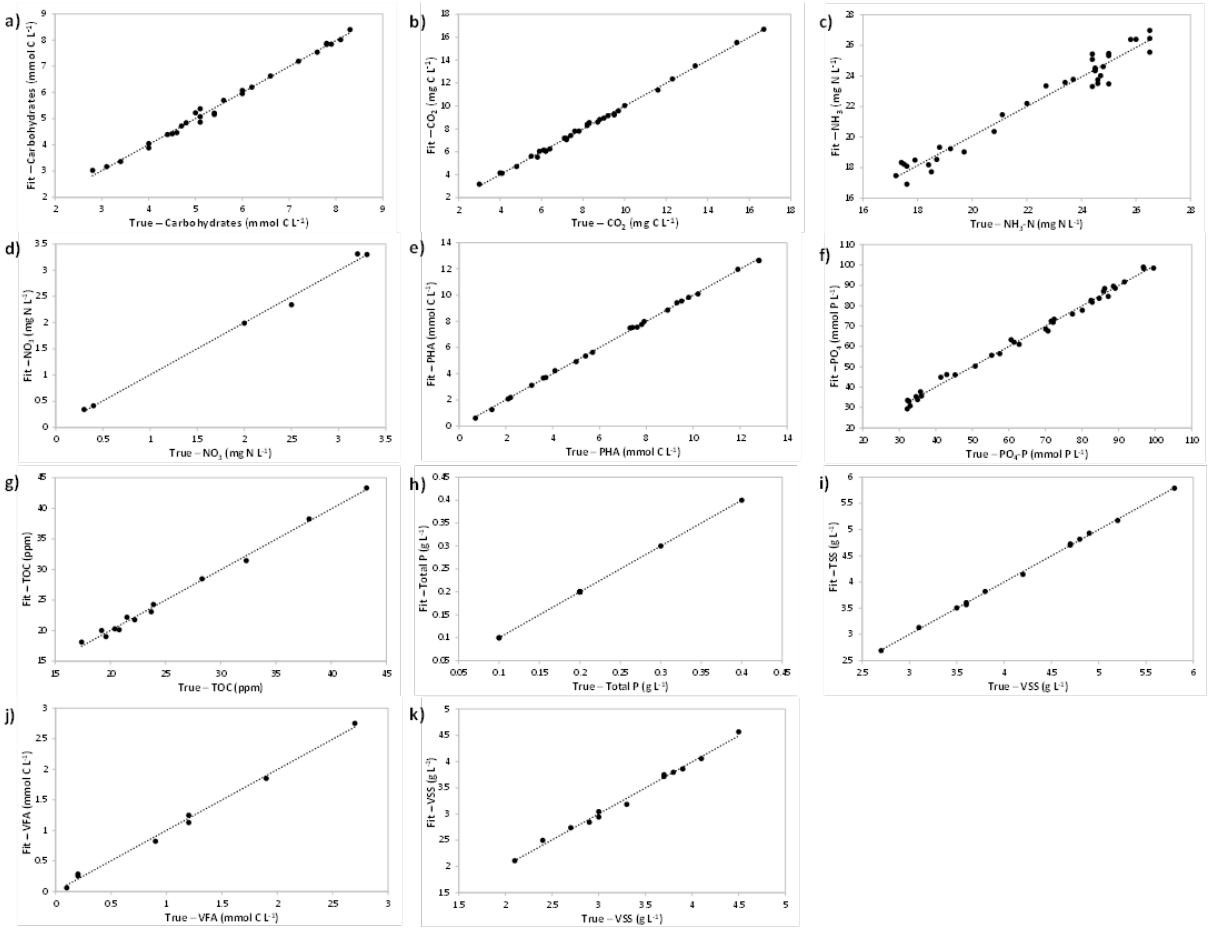

Figure 6.2 - Representation of the Raman-PLS calibration models.
Developed for a) total carbohydrates, b) carbon dioxide (CO_2), c) ammonia (NH_3), d) nitrate (NO_3), e) polyhydroxyalkanoates (PHA), f) phosphate (PO_4), g) total organic content (TOC), h) total phosphorus (total P), i) total suspended solids (TSS), j) volatile fatty acids (VFA), and k) volatile suspended solids (VSS).
The dotted line represents the calibration regression line that correlates the analytical values (True) of each calibration sample with the corresponding values fitted by the Raman-PLS calibration model (Fit). The pre-processing strategy, spectral regions, and number of latent variables used in the development of each model are indicated in Table 1, along with the statistical calibration results.

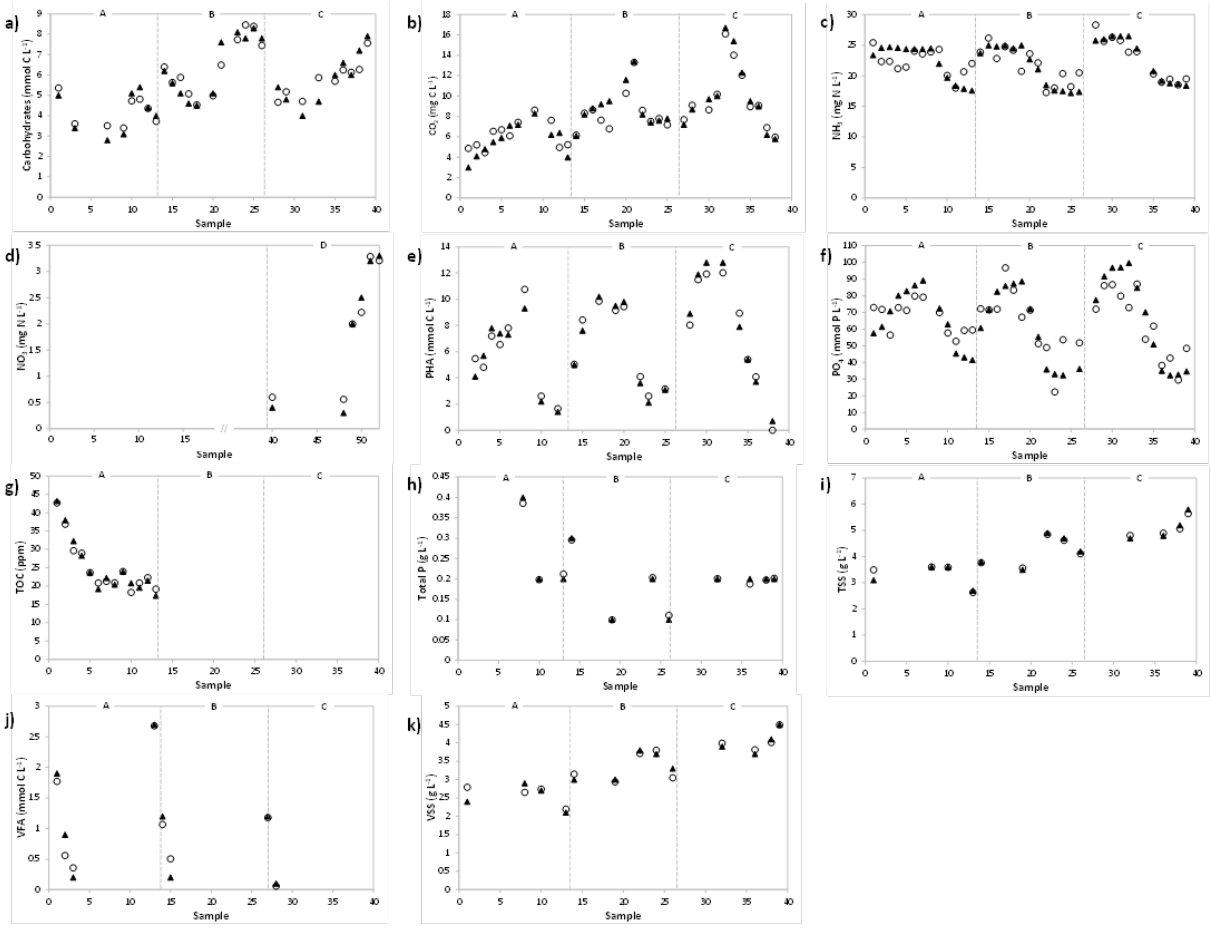

Figure 6.3 - Representation of the prediction capabilities of the Raman-PLS models.
Developed for a) total carbohydrates, b) carbon dioxide (CO_2), c) ammonia (NH_3), **d)** nitrate (NO_3), **e)** polyhydroxyalkanoates (PHA), **f)** phosphate (PO_4), **g)** total organic content (TOC), **h)** total phosphorus (total P), **i)** total suspended solids (TSS), **j)** volatile fatty acids (VFA), and **k)** volatile suspended solids (VSS). For each parameter and calibration sample, the analytical values measured by reference methods (▲) are represented along with the corresponding parameter values predicted by the respective cross-validation model (○). The pre-processing strategy, spectral regions, and number of latent variables used in the development of the PLS models are indicated in Table 1, for each studied parameter, along with the statistical cross-validation results. Vertical dashed lines separate the sample sets from each studied cycle, corresponding to the SBR operational days 73 (cycle A; samples 1-13), 79 (cycle B; samples 14-26), 85 (cycle C; samples 27-39) and 101 (cycle D; samples 40-52).

Regarding the prediction performance of these calibration models, the excellent statistical results (R2CV > 90.0%; RPDCV > 3.2) obtained for TOC, VFA, CO_2, NO_3, Total P, PHA, TSS and VSS (**Table 6.1**) indicate that these parameters can be quantified with good quality through the respective Raman-based PLS models. On the other hand, the models developed for the prediction of PO_4, NH_3 and carbohydrates did not perform as well, according to their lower cross-validation quality parameters, i.e. R2 < 90% and RPDCV < 3.0. Overall, the RMSECV values are higher than the corresponding RMSEC, but the determined bias values were close to zero for all parameters, except for PO_4 (Bias = 0.364; **Table 6.1**). The cross-validation outcome, which represents the performance of each PLS model to predict the concentrations of the respective parameter, is graphically illustrated in **Figure 6.3**, where the reference analytical values measured for each sample are plotted together with the corresponding values predicted by a full cross-validation (leave-one-out) procedure. In addition, **Figure 6.1** allows to observe each parameter's profile and the trend of predicted values along the SBR cycles. Overall, the analytical data for each parameter (**Figure 6.3**) followed the expected profile along the photo-BNR reactor cycles, i.e. the decrease in VFA and carbohydrates concentration values, in parallel with the increase of PHA and PO_4 concentrations along the anaerobic phase; followed by the decrease in NH_3, PO_4 and PHA concentrations, along with the increase in NO_3 concentration (nitrification) and poly-P and glycogen contents in the subsequent aerobic phase.

The parameter predictions based on Raman spectra in **Figure 6.2** and **Figure 6.3** correspond to single measurements and there is only one parameter prediction for each spectrum. Repetitions of spectra acquisition were not performed since the biological reactions continued to occur in each sample after collection from the bioreactor. Thus, variations were expected to occur between those repetitions over a short period of time. However, the continuous monitoring during a long period allows the generation of continuous data and reveals the reproducibility of the monitored system.

Despite the procedures to minimize the noise in the calibration data set (simple pre-processing, spectral region selection and outlier removal), for some parameters, the low number of samples available and the low diversity of analytical values might have contributed to PLS model overfitting. In order to minimize this effect, a full cross-validation procedure was used for PLS model development. However, an external validation using an independent test set is required to evaluate de the degree of overfitting of the developed PLS models by comparing the performance of the test set with that of the calibration set

6.3.3. Nitrate (NO_3)

NO_3 was not detected on cycles A, B and C, because denitrification was only occurring on cycle D (**Figure 6.3-d**), leading to a very small number of calibration samples available for developing the Raman-based PLS model to predict NO_3 concentrations. Nevertheless, the reference values were broadly spanned through the investigated concentration range (0.3-3.3 mgN L^{-1}; **Figure 6.3-d**), allowing to obtain predictions of NO_3 concentration with high accuracy (RMSECV = 97.7% and RPD_{CV} = 6.7) simply requiring three LV and the mean centering of the spectral data (no additional pre-processing needed) in the 1080.4-1069.4 cm^{-1} range (**Table 6.1**). In fact, according to the UV resonance Raman spectra of nitrate solutions, symmetric N−O stretching vibrations have been reported to produce strong bands at 1044 cm^{-1} for NO_3 (Ianoul et al., 2002). The possibility of implementing Raman based real-time monitoring of NO_3 in a photo-BNR reactor would contribute to control denitrification efficiency, by adapting the length of the anoxic phase, for example, and, consequently, guaranteeing that no NO_3 is present when organic carbon is fed. The simultaneous presence of NO_3 and organic carbon promotes the growth of heterotrophic denitrifying organisms, which compete for carbon with PAOs and lead to photo-BNR failure over the time (Izadi et al., 2020; Valverde Perez, 2015).

6.3.4 Ammonia (NH_3)

The best model obtained for monitoring NH_3 concentration involved eight LV and used the 1st Der + MSC as pre-processing method in three spectral regions (**Table 6.1**), one of which (1439.2-1189.0 cm^{-1}) comprising Raman shifts previously attributed to N-H in plane deformation (1400 and 1425 cm^{-1}), and part of a band associated with NH_3 (1550-1428 cm^{-1}) (Movasaghi et al., 2007). Despite the promising calibration parameters (R^2_{Cal} = 96.2% and RMSEC = 0.72 mgN L^{-1}), the low R^2_{CV} and RDP_{CV} values of 65.5% and 1.7, respectively, and the substantial RMSECV (1.89 mgN L^{-1}) obtained imply that this model has a poor prediction capacity, being unable to extract the relevant information from the spectral data. This is evidenced by the scattering of data points around the regression line (**Figure 6.2-c**) and the discrepancy between the measured and predicted NH_3 concentration values for some of the samples (**Figure 6.3-c**). Yet, no further samples were excluded from the data set, as no clear outliers were detected. The significantly better calibration results in comparison to cross-validation suggest that a higher number of samples should be used for PLS model development in order to represent the whole NH_3 concentration range under study. Accordingly, is it possible that the prediction accuracy of the PLS model could be improved by including more samples to equally cover the total NH_3 concentration range. In fact, real-time knowledge on the NH_3 concentration in a photo-BNR reactor would allow the assessment of its nutrient removal capacity and the adaptation of the operational conditions when the treatment efficiency would not meet the discharge requirements.

6.3.5 Phosphate (PO_4) and total phosphorus (Total P)

Regarding PO_4, PLS model optimization led to the selection of a spectral region comprising a Raman shift specific for ν1 vibration domain of the PO_4 group, *i.e.* 960 cm^{-1} (Ma et al., 2020). Similarly to the model developed for NH_3, the cross-validation results obtained for the PO_4 model in the 32.2-99.6 mgP L^{-1} range (R^2_{CV} = 70.0%; RMSEC = 12.10 mgP L^{-1}; **Figure 6.3-f**) were significantly worse than the calibration statistics (R^2_{Cal} = 99.4%; RMSEC = 1.95 mgP L^{-1}). Accordingly, the RPD_{CV} of 1.7 confirmed the insufficient prediction quality of the model. In contrast, the PLS model developed for estimating total P concentrations presented an excellent prediction performance (**Figure 6.3-h**), as evidenced by the cross-validation results, *i.e.* R^2_{CV} = 99.0% and RPD_{CV} = 10.3 (**Table 6.1**). In fact, the RMSEC and RMSECV values (0.0 and 0.01 g L^{-1}) were very similar denoting a good calibration model for the P concentration range from 0.1 to 0.4 g L^{-1}, as illustrated in **Figure 6.3-h**). The spectral data pre-processing involved the application of 1st Der + MSC in the regions 1179.8-1168.7 cm^{-1} + 1159.5-1139.3 cm^{-1}, which are in accordance with the PO_2 stretching vibrations band reported to occur around 1175-1168 cm^{-1} (Majed & Gu ,2010) and 1163-1130 (Guo et al., 2019) and used to quantify the intracellular poly-P content (Majed & Gu, 2010; Li et al., 2018; Guo et al., 2019; Fernando et al., 2019; Mendes et al., 2020; Ma et al., 2020). However, this model required nine LV, which is a relatively high number of factors, eventually leading to overfitting of data. Future work is needed to confirm the prediction capacity of this potentially relevant model, by performing external validation tests. Accurate real-time monitoring of total P would significantly improve the capacity to understand which is the main mechanism of P removal in the photo-BNR process, and thus evaluate the possibility of using the excess sludge as fertilizer, since high P amounts in the biomass indicate high accumulation as poly-P.

6.3.6 Total carbohydrates and polyhydroxyalkanoates (PHA)

Most studies using Raman as a monitoring tool for PHA production have focused on intracellular polymer content, composition and degree of crystallinity (Jost et al., 2017). The most prominent contributions of PHB to a bacterial Raman spectrum were associated with a peak at around 1734 cm^{-1} (De Gelder et al., 2008). Furthermore, studies using commercial co-polymers of poly(3-hydroxybutyrate-*co*-3-hydroxyvalerate) (PHBV) identified specific Raman bands associated with 3-hydroxyvalerate (3HV) (Jost et al., 2017) and quantified the molar fraction of 3HV in polyester solutions and molten polyester films based on specific Raman peaks (Izumi et al., 2010). Subsequently, Raman spectroscopy has been suggested as a potentially fast and efficient tool for process control of PHB bioproduction through qualitative and quantitative *in situ* monitoring of intracellular PHB content in biomass, specifically in *Cupriavidus necator* H16 cultures (Samek et al., 2016).

In the context of wastewater treatment in a photo-BNR reactor, online monitoring of intracellular polymers such as PHA and glycogen (accounted as part of the total carbohydrates), which are involved in the P removal process, is relevant to assess if nutrient removal is limited

by low concentration of the biopolymers and to optimize this process. The Raman region located at 1200-800 cm^{-1} has been reported to be mainly dominated by polysaccharide peaks, and the spectral region between 1288 and 987 cm^{-1} was previously used to develop a Raman-based PLS model for carbohydrates in powdered milk samples (Moros et al., 2007). Accordingly, optimization of the PLS models for total carbohydrates in the present study led to the selection of spectral regions within the 1200-800 cm^{-1} range (**Table 6.1**), which include some of the peaks characteristic of glycogen vibrations (484-478, 860-840, 944-937, 1087-1048, 1131, 1383-1333, and 1460 cm^{-1}) (Majed & Gu, 2010).

The glycogen skeletal deformation band (484-478 cm^{-1}) was not accounted in the carbohydrates model, probably due to overlapping peak positions between PHA and glycogen in this region (Majed et al., 2020). In fact, the optimized PLS model for PHA included the 484-478 cm^{-1} band within the selected spectral regions, *i.e.* 491.6-464.0 cm^{-1} + 850.4-798.9 cm^{-1} + 1001.3-898.2 cm^{-1} (**Table 6.1**). The selection of these spectral regions is in accordance with two of the most prominent bands reported in the Raman spectra of PHB and PHBV: 433 and 860-840 cm^{-1}, assigned to δ(C-C) skeletal deformations and ν(C-C) skeletal stretches, respectively (Majed & Gu, 2010)

Despite the excellent calibration statistical results obtained in both models (R^2_{Cal} and RMSEC of 99.4% and 0.15 mmolC L^{-1} for total carbohydrates, and 99.9% and 0.12 mmolC L^{-1} for PHA, respectively), good cross-validation performance was only reached in the PHA model (R^2_{CV} = 95.9%, RPD_{CV} = 5.0; **Figure 6.3-e**), while only satisfactory results were obtained in the model developed for total carbohydrates (R^2_{CV} = 88.2%, RPD_{CV} = 2.9; **Figure 6.3-a**). Overall, the predicted values follow the measured values along the SBR treatment cycles, as represented in **Figure 6.3-a**) and e) for total carbohydrates and PHA, respectively. Nevertheless, according to the respective RPD values, the PLS model constructed for PHA prediction could be used as a good screening method within the 0.7-12.8 mmolC L^{-1} concentration range, while the one for total carbohydrates can only be considered as a rough screening method for concentration values within 2.8-8.3 mmol C L^{-1}(Mendes et al., 2020). In light of the labor-intensive, complex and time-consuming protocols involved in the analytical methods used to measure PHA and total carbohydrates (involving biomass digestions, GC and HPLC analysis, respectively), the application of Raman spectroscopy as a fast, direct and not destructive monitoring tool would enable timely decisions regarding process control and optimization.

6.3.7 Volatile fatty acids (VFA) and total organic carbon (TOC)

Modelling VFA concentration was based on the spectral regions 944.2-694.0 cm^{-1} and 1934.2-1685.8 cm^{-1} (**Table 6.1**) which include ν(C-C) skeletal stretches (860-840 cm^{-1}) (Jost et al., 2017) and c(C=O) stretching vibrations (1725-1750 cm^{-1}) (Majed & Gu, 2010; Jost et al., 2017; Izumi et al., 2010), respectively. By applying mean centering alone as pre-processing, this model yielded very good cross-validation results in the VFA concentration range from 0.1 to 2.7 mmolC L^{-1} (RMSECV = 0.18 mmolC L^{-1}, R^2_{CV} = 95.4% and RPD_{CV} = 4.7; **Figure 6.3-j**). Contrarily to the time-consuming analytical method used for assessing VFA concentration

(HPLC), Raman spectroscopy has the potential to deliver much faster information about the reactor performance.

Regarding the final model selected for predicting TOC concentration, the spectral regions used in the model span over a large range of the Raman spectrum (from 1500 to 600 cm^{-1};**Table 6.1**). In fact, important regions for the vibrations associated with organic matter are expected to involve a wide spectral range, including aliphatic C-H stretching, vibrations related to carboxylic groups, aromatic groups, carboxylate groups and protein amide (Ludwig et al., 2019). Although TOC measurements were only available for one of the studied cycles, a good correlation between the reference analytical data and the pre-processed (constant offset elimination), selected Raman spectral regions could be obtained by using five LV, as indicated by the calibration results (R^2_{Cal} = 99.5%, RMSEC = 0.76 ppm, RPD_{Cal} = 13.6;**Table 6.1**). Moreover, the cross-validation was successful (R^2_{CV} = 96.7%; RPD_{CV} = 5.5), the reference TOC profile within the 17.4-43.2 ppm range being very well predicted by the Raman-based PLS model (**Figure 6.3-g**).

Real-time information on the concentration of VFA and TOC can help in preventing the presence of organic carbon during the light aerobic period of the SBR cycles. The presence of organic carbon during the light aerobic period promotes the growth of heterotrophic phototrophic purple bacteria and ordinary aerobic heterotrophs, which consequently, reduces the efficiency of the photo-BNR, since PAOs accumulate more P (Hülsen et al., 2013).

6.3.8 Total suspended solids (TSS) and volatile suspended solids (VSS)

As expected, the spectral regions used by the PLS models for estimating TSS and VSS are very similar, covering related regions within the 2000-1000 cm^{-1} range (**Table 6.1**). Despite the application of different normalization methods as pre-processing (SNV for TSS versus Min-Max normalization for VSS), both models were constructed based on five LV and the statistical calibration and cross-validation results were comparable, the TSS performing slightly better (RMSECV and RPD_{CV} of 97.5% and 6.3 for TSS versus 93.9% and 4.1 for VSS, **Figure 6.3-i** and **Figure 6.3-k**, respectively).

6.3.9 Carbon dioxide (CO_2)

The CO_2 concentration model used two short regions of Raman shifts (1450.3-1398.8 cm^{-1} + 1374.8-1297.6 cm^{-1}), which comprise two peaks attributed to vibrational modes of CO_2, specifically 1388 cm^{-1} and 1285 cm^{-1} (Kobayashi et al., 2012). The spectral pre-processing involved MSC, and cross-validation revealed a good prediction accuracy within a large CO_2 concentration range (3.0-16.7 g L^{-1}), as indicated by the cross-validation results (R^2_{CV} = 90.0%, RMSECV of 0.96 g L^{-1}; RPD_{CV} = 3.2;**Table 6.1**). In fact, **Figure 6.3-b** shows excellent correlations between Raman spectroscopy and reference analysis, highlighting Raman spectroscopy as a potentially useful tool for providing real-time information on the CO_2 concentration. Real-time knowledge on the CO_2 level in a photo-BNR reactor is essential for understanding if photosynthesis, and thus oxygen production by microalgae, is limited by inorganic carbon availability and, when it happens, to increase the CO_2 feed to the system. Comparing to regular CO_2

sensors, this can be advantageous because no further correction, based on pH, is necessary to know the real CO_2 concentration, reducing the delay time and improving the overall nutrient removal efficiency of the photo-BNR.

6.4 Conclusions

This study showed that Raman spectroscopy, allied with PLS, is a very promising tool for monitoring the concentration of TOC, VFA, CO_2, NO_3, total P, PHA, TSS and VSS in a photo-BNR reactor in real-time. This was shown by the high R^2_{CV} and RPDcv values obtained for these parameters: 96.7% and 5.5 for TOC, 95.4% and 4.7 for VFA, 90.0% and 3.2 for CO_2, 97.7% and 6.7 for NO_3, 99.0% and 10.3 for Total P, 95.9% and 5.0 for PHA, 97.5% and 6.3 for TSS, 93.9% and 4.1 for VSS, respectively. Regarding NH_3, PO_4 and total carbohydrates, the prediction accuracy of the respective Raman-based PLS models (R^2_{CV} and RPDcv of 65.5% and 1.7 for NH_3, 70.0% and 1.8 for PO_4; 88.2% and 2.9 for total carbohydrates, respectively) could possibly be improved by including more samples in the calibration set.

The performance of the PLS calibration models was evaluated by a full cross-validation procedure and can be further assessed by an external validation using additional samples that were not included in model development (external test set). After external validation, the models can then be used for predicting the concentration of the different parameters simply based on the Raman spectral data, minimizing the need for performing extensive off-line analyses. Although the external validation of the developed PLS calibration models was not performed due to the lack of an external test set, this study presents very promising results for real-time monitoring of a photo-BNR reactor using Raman spectroscopy, being the first to report this specific application. Overall, the application of Raman-based monitoring in a photo-BNR reactor offers a fast, simple, non-destructive, eco-friendly and holistic alternative to laborious standard analytical and expensive methods, enabling the quantification of various parameters within a single Raman measurement. Once robust and reliable PLS calibration models have been developed, Raman spectroscopy can be used online to provide real-time process information, facilitating decision-making during wastewater treatment. Nevertheless, regular reference analytical data will always be needed in order to guarantee the long-term validity of the PLS models.

REFERENCES

Barra, I., Haefele, S.M., Sakrabani, R., Kebede, F., 2021. Soil spectroscopy with the use of chemometrics, machine learning and pre-processing techniques in soil diagnosis: Recent advances–A review. Trends Analyt. Chem. 116166, 10.1016/j.trac.2020.116166

Capson-Tojo, G., Batstone, D.J., Grassino, M., Vlaeminck, S.E., Puyol, D., Verstraete, W., Kleerebezem, R., Oehmen, A., Ghimire, A., Pikaar, I., et al., 2020. Purple phototrophic bacteria for resource recovery: Challenges and opportunities. Biotechnol. Adv. 43. 107567, 10.1016/j.biotechadv.2020.107567

Carvalheira, Mónica, Oehmen, A., Carvalho, G., Reis, M.A.M., 2014b. The effect of substrate competition on the metabolism of polyphosphate accumulating organisms (PAOs). Water Res. 64, 149–159. https://doi.org/10.1016/j.watres.2014.07.004

Carvalho, V.C.F., Freitas, E.B., Fradinho, J.C., Reis, M.A.M., Oehmen, A., 2019. The effect of seed sludge on the selection of a photo-EBPR system. N. Biotechnol. 49, 112–119. https://doi.org/10.1016/j.nbt.2018.10.003

Carvalho, V.C.F., Kessler, M., Fradinho, J.C., Oehmen, A., Reis, M.A.M., 2021. Achieving nitrogen and phosphorus removal at low C/N ratios without aeration through a novel phototrophic process, Science of The Total Environment. https://doi.org/10.1016/j.scitotenv.2021.148501

Carvalho, V.C.F., Freitas, E.B., Silva, P.J., Fradinho, J.C., Reis, M.A.M., Oehmen, A., 2018. The impact of operational strategies on the performance of a photo-EBPR system. Water Res. 129, 190–198. 10.1016/j.watres.2017.11.010

Claßen, J., Aupert, F., Reardon, K.F., Solle, D., Scheper, T., 2016. Spectroscopic sensors for in-line bioprocess monitoring in re-search and pharmaceutical industrial application. Anal. Bioanal. Chem. 409, 1–16. 10.1007/s00216-016-0068-x

De Gelder, J., Willemse-Erix, D., Scholtes, M.J., Sanchez, J.I., Maquelin, K., Vandenabeele, P., De Boever, P., Puppels, G.J., Moens, L., De Vos, P., 2008. Monitoring poly(3-hydroxybutyrate) production in Cupriavidus necator DSM 428 (H16) with Raman spectroscopy. Anal. Chem. 80, 2155–2160. 10.1021/ac702185d

Esmonde-White, K.A., Cuellar, M., Uerpmann, C., Lenain, B., Lewis, I.R.,2016. Raman spectroscopy as a process analytical technology for pharmaceutical manufacturing and bioprocessing. Anal. Bioanal. Chem. 409, 1–13. 10.1007/s00216-016-9824-1

Fatemeh, S., Hennige, S., Willoughby, N., Adeloye, A., Gutierrez, T., 2021. Integrating micro-algae into wastewater treatment: A review. Sci. Total Environ. 752, 142168. 10.1016/j.scitotenv.2020.142168

Fernando, E.Y., McIlroy, S.J., Nierychlo, M., Herbst, F.A., Petriglieri, F., Schmid, M.C., Wagner, M., Nielsen, J.L., Nielsen, P.H., 2019. Resolving the individual contribution of key microbial populations to enhanced biological phosphorus removal with Raman–FISH. ISME J. 13, 1933–1946, 10.1038/s41396-019-0399-7

Foladori, P., Petrini, S., Andreottola, G., 2019. How suspended solids concentration affects

nitrification rate in microalgal- bacterial photobioreactors without external aeration. Heliyon. e03088. 10.1016/j.heliyon.2019.e03088

Gschwind, B., Ménard, L., Albuisson, M., Wald, L., 2016. Converting a successful research project into a sustainable service: the case of the SoDa Web service. Environ. Modell. Softw. 21, 1555–1561. 10.1016/j.envsoft.2006.05.002

Guo, G., Wu, D., Ekama, G.A., Ivleva, N.P., Hao, X., Dai, J., Cui, Y., Biswal, B.K., Chen, G., 2019. Investigation of multiple pol-ymers in a denitrifying sulfur conversion-EBPR system: The structural dynamics and storage states. Water Res. 156, 179-187. 10.1016/j.watres.2019.03.025

Hülsen, T., Batstone, D.J., Keller, J. Phototrophic bacteria for nutrient recovery from domestic wastewater., 2013. Water Res. 50, 18–26. doi:10.1016/j.watres.2013.10.051

Ianoul, A., Coleman, T., Asher, SA., 2002. UV resonance Raman spectroscopic detection of nitrate and nitrite in wastewater treatment processes. Anal Chem. 74, 1458–1461. 10.1021/ac010863q

Izadi, P., Izadi, P., Eldyasti, A., 2020. Design, operation and technology configurations for enhanced biological phosphorus removal (EBPR) process: a review, Springer Netherlands. 19. 10.1007/s11157-020-09538-w

Izumi, C.M.S., Temperini, M.L.A., 2010. FT-Raman investigation of biodegradable polymers: poly(3-hydroxybutyrate) and poly(3-hydroxybutyrate-co-3-hydroxyvalerate). Vib. Spectrosc. 54, 127–132. 10.1016/j.vibspec.2010.07.011

Jost, V., Schwarz, M., Langowski. H.C., 2017. Investigation of the 3-hydroxyvalerate content and degree of crystallinity of P3HB-co-3HV cast films using Raman spectroscopy. Polymer. 133, 160–170. 10.1016/j.polymer.2017.11.026

Kobayashi, T., Yamamoto, J., Hirajima, T., Ishibashi, H., Hirano, N., Lai, Y., Prikhod'ko V.S., Arai, S., 2012. Conformity and Precision of CO2 Densimetry in CO2 Inclusions: Microthermometry Versus Raman Microspectroscopic Densimetry. J. Raman Spectrosc. 43, 1126–1133. 10.1002/jrs.3134

Kozma, B., Hirsch, E., Gergely, S., Párta, L., Pataki, H., Salgó, A., 2017. On-line prediction of the glucose concentration of CHO cell cultivations by NIR and Raman spectroscopy: comparative scalability test with a shake flask model system. J. Pharm. Biomed. Anal. 145, 346–355. 10.1016/j.jpba.2017.06.070

Li, Y., Cope, H.A., Rahman, S.M., Li, G., Nielsen, P.H., Elfick, A., Gu, A.Z., 2018. Toward better understanding of EBPR systems via linking Raman based phenotypic profiling with phylogenetic diversity. Environ. Sci. Technol. 52, 8596–8606, 10.1021/acs.est.8b01388

Liu, L., Fan, H., Liu, Y., Liu, C., Huang, X., 2017. Development of algae-bacteria granular consortia in photo-sequencing batch reactor. Bioresour. Technol. 232, 64–71. 10.1016/j.biortech.2017.02.025

Lourenço, N.D., Lopes, J.A., Almeida, C.F., Sarraguça, M.C., Pinheiro, H.M., 2012. Bioreactor monitoring with spectroscopy and chemometrics: a review. Anal. Bioanal. Chem. 404, 1211–1237. 10.1007/s00216-012-6073-9

Ludwig, B., Murugan, R., Ramakrishna, P.V.R., Vohland, M., 2019. Accuracy of estimating soil

properties with mid-infrared spectroscopy: implications of different chemometric approaches and software packages related to calibration sample size. Soil Sci. Soc. Am. J. 83, 1542–1552. 10.2136/sssaj2018.11.0413

Luo, L., Dzakpasu, M., Yang, B., Zhang, W., Yang, Y., Wang, X.C., 2019. A novel index of total oxygen demand for the compre-hensive evaluation of energy consumption for urban wastewater treatment. Appl. Energy. 236, 253–261. 10.1016/j.apenergy.2018.11.101

Ma, H., Xue, Y., Zhang, Y., Kobayashi, T., Kubota, K., Li, Y.-Y., 2020. Simultaneous nitrogen removal and phosphorus recovery using an anammox expanded reactor operated at 25 °C. Water Res. 172, 115510. 10.1016/j.watres.2020.115510

Majed, N., Gu, A.Z., 2020. Phenotypic dynamics in polyphosphate and glycogen accumulating organisms in response to varying influent C/P ratios in EBPR systems. Sci Total Environ. 743, 140603. 10.1016/j.scitotenv.2020.140603

Majed, N., Gu, A.Z., 2010. Application of Raman microscopy for simultaneous and quantitative evaluation of multiple intracellular polymers dynamics functionally relevant to enhanced biological phosphorus removal processes. Environ Sci Technol. 15, 8601–8608. 10.1021/es1016526

Mendes, T.O, Rodrigues, B.V.M., Porto, B.L.S., da Rocha R.A., de Oliveira, M.A.L., de Castro, F.K., dos Anjos, V.C., Bell, M.J.V., 2020. Raman Spectroscopy as a fast tool for whey quantification in raw milk. Vib. Spectrosc. 111. 103150, 10.1016/j.vibspec.2020.103150

Moros, J., Garrigues, S., de la Guardia, M., 2007. Evaluation of nutritional parameters in infant formulas and powdered milk by Raman spectroscopy. Analytica Chimica Acta. 593, 30-38. 10.1016/j.aca.2007.04.036

Moudříková, Š., Mojzeš, P., Zachleder, V., Pfaff, C., Behrendt, D., Nedbal, L., 2016. Raman and fluorescence microscopy sensing energy-transducing and energy-storing structures in microalgae. Algal Res. 16, 224–232. 10.1016/j.algal.2016.03.016

Movasaghi, Z., Rehman, S., Rehman, I.U., 2007. Raman Spectroscopy of Biological Tissues. Appl. Spectrosc. Rev. 42, 493–541. 10.1080/05704920701551530

Muñoz, R., Guieysse, B., 2006. Algal-bacterial processes for the treatment of hazardous contaminants: A review. Water Res. 40, 2799–2815. 10.1016/j.watres.2006.06.011

Muñoz, R., Jacinto, M., Guieysse, B., Mattiasson, B., 2005. Combined carbon and nitrogen removal from acetonitrile using al-gal-bacterial bioreactors. Appl. Microbiol. Biotechnol. 67, 699–707. 10.1007/s00253-004-1811-3

Paudel, A., Raijada, D., Rantanen, J., 2015. Raman spectroscopy in pharmaceutical product design, Adv. Drug Deliv. Rev. 89, 3–20. 10.1016/j.addr.2015.04.003

Rosso, D., Larson, L.E., Stenstrom, M.K., 2008. Aeration of large-scale municipal wastewater treatment plants: state of the art. 973–979. 10.2166/wst.2008.218

Samek, O., Obruca, S., Siler, M., Sedlacek, P., Benesova, P., Kucera, D., Márova, I., Jezek, J., Bernatová, S., Zemánek, P., 2016. Quantitative Raman Spectroscopy Analysis of Polyhydroxyalkanoates Produced by Cupriavidus necator H16. Sensors (Ba-sel). 16. 1808, 10.3390/s16111808

Taziki, M., Ahmadzadeh, H., A. Murry, M., R. Lyon, S., 2015. Nitrate and Nitrite Removal

from Wastewater using Algae. Curr. Biotechnol. 4, 426–440. 10.2174/2211550104666150828193607

Toledo-Cervantes, A., Posadas, E., Bertol, I., Turiel, S., Alcoceba, A., Muñoz, R., 2019. Assessing the influence of the hydraulic retention time and carbon/nitrogen ratio on urban wastewater treatment in a new anoxic-aerobic algal-bacterial photobio-reactor configuration. Algal Res. 44, 101672, 10.1016/j.algal.2019.101672

Valverde Perez, B., 2015. Wastewater resource recovery via the Enhanced Biological Phosphorus Removal and Recovery (EBP2R) process coupled with green microalgae cultivation. Ph.D. thesis. Technical University of Denmark, DTU Environment

Veloso, A.C., Ferreira, E.C., 2017. Online Analysis for Industrial Bioprocesses: Broth Analysis. Current Developments in Bio-technology and Bioengineering: Bioprocesses, Bioreactors and Controls. 23, 679-704. 10.1016/B978-0-444-63663-8.00023-9

Winkler, M.K., Straka, L., 2019 New directions in biological nitrogen removal and recovery from wastewater. Curr. Opin. Bio-technol. 57, 50–55. 10.1016/j.copbio.2018.12.007

7.

LONG TERM OPERATION OF A PHOTOSYNTHETIC BIOLOGICAL NUTRIENT REMOVAL SYSTEM: IMPACT OF CO_2 CONCENTRATION AND LIGHT EXPOSURE ON PROCESS PERFORMANCE

SUMMARY: Conventional wastewater treatment technologies for biological nutrient removal (BNR) are highly dependent on aeration for oxygen supply, which represents a major operational cost of the process. Recently, phototrophic biological nutrient removal (photo-BNR) has been suggested as an alternative to conventional BNR, based on a consortium of photosynthetic microorganisms (microalgae or others) and chemotrophic bacteria, eliminating the need for mechanical aeration. The present study evaluates, for the first time, the long-term operation (260 days) of a photo-BNR system, fed with a COD:N:P ratio of 7.5:1:1, to understand its operational limitations. In particular, different CO_2 concentrations and the length of light exposure period were studied and adjusted to allow more oxygen production (enough to reach around 1-2 mg/L) and preventing complete consumption of polyhydroxyalkanoates (PHA) reserves during the light period, permitting nutrient removal by polyphosphate accumulating organisms during the anoxic period. Six different Na_2CO_3 concentrations in the feed, between 3 and 60 mg C/L, were tested. The period of light exposure was varied from 2.75 h to a maximum of 5.25 h per 8h cycle. Results indicated that in stage 3, with a COD:Na_2CO_3 ratio of about 8.3 mg COD/mg C and a light intensity of 5.4 ± 1.3 W.h/g TSS, no PHA limitation was observed, and 95 ± 6.5%, 92 ± 4.2% and 86 ± 4.6% of removal efficiency was achieved for phosphorus, ammonia and total nitrogen, respectively. 19 ± 1.7 % of the influent N was nitrified and denitrification varied between 4 and 43 % due to excessive oxygen concentrations in some operational periods. Overall, the photo-BNR was able to remove 38 ± 3.3 mg P/L and 33 ± 1.7 mg N/L of phosphorus and nitrogen, highlighting its potential for achieving wastewater treatment without the need of aeration.

Keywords: Biological nutrient removal (BNR); Polyphosphate accumulating organisms (PAOs); Photosynthetic microorganisms; Algae for nutrients removal; Microalgae-bacterial systems.

7.1. Introduction

High concentrations of nutrients, mainly in the form of ammonia and phosphorous, are directly responsible for eutrophication of rivers, lakes and seas, representing a challenge for wastewater treatment (WWT). However, this high nutrient load can also be a chance for the simultaneous nutrient recovery and the production of added-value bioproducts as, for example, biofertilizers (Mulbry et al., 2006, 2005; Ramanan et al., 2016; Torres-Franco et al., 2021). Presently, the WWT industry uses several physical/chemical or biological methods to remove nutrients. Conventional technology, such as biological nutrient removal (BNR) and phosphate/ammonia precipitation are well established. Yet, these processes are highly chemical and energy dependent, becoming non-environmentally sustainable (Rosso et al., 2008; Torres-Franco et al., 2021). Nutrient removal in conventional BNR systems is normally performed by polyphosphate accumulating organisms (PAOs), ammonia oxidizing bacteria (AOBs) and nitrite oxidizing bacteria (NOBs). Nutrient removal is favored by higher COD:P ratios (Kuba et al., 1996; Wang et al., 2009), which normally requires extra COD addition.

Thereupon, algal based technology has been investigated for WWT, using single microalgae technology (De-Bashan and Bashan, 2004) or through consortia of microalgae and bacteria (Carvalho et al., 2021) (Alcántara et al., 2015b; de Godos et al., 2014; Torres-Franco et al., 2021).

As an alternative, microalgae – bacterial consortiums for wastewater treatment have a great potential for nutrient removal and are considered an environmentally friendly technology (Toledo-Cervantes et al., 2019; Young et al., 2017). These consortia require less COD, when compared with conventional BNR systems, since CO_2 is used by microalgae as carbon source, thereby lowering the COD:Nutrient ratio needed for an efficient nutrient removal (Fatemeh et al., 2021; Judd et al., 2015; Wang et al., 2018). For phototrophic growth, microalgae use nutrients and CO_2 as their main source of inorganic carbon (Fatemeh et al., 2021) and produce high amounts of photosynthetic O_2 through solar energy capture. Heterotrophic bacteria consume O_2 and remove organic carbon and nutrients, producing CO_2 that is used for microalgae proliferation (Boelee et al., 2012; Zhang et al., 2018). Algae and bacteria can form granular biomass, (Zhang et al., 2018) improving settling and overcoming the problem of solids and treated water separation that occur in WWT with single algae systems treating.

One of the main advantages of microalgal - bacterial technology is the reduction of greenhouse gas emissions (de Godos et al., 2014). Besides CO_2 fixation by algae that reduce CO_2 emissions, photosynthetic oxygenation also reduces the need of mechanical aeration, decreasing the energy demands of the process (Fatemeh et al., 2021). Higher ammonia assimilation into the microalgal biomass, instead of the dominance of nitrification-denitrification processes, may also decrease the emissions of N_2O, a gas which presents a greenhouse gas 300 times stronger than CO_2 (Alcántara et al., 2015b; Plouviez and Guieysse, 2020).

Microalgal-bacterial photobioreactors performance, when fully optimized, are expected to be comparable with the classical BNR process in terms of nutrient removal but with less energy requirements (de Godos et al., 2014). Whilst parameters such as C:N:P ratios, dissolved

oxygen, pH and temperature have been widely studied for the conventional BNR process, the impact of key parameters in photosynthetic biological nutrient removal (Photo-BNR) systems, like nutrient balancing and light exposure period, still requires further evaluation. Previous studies indicated that the availability of CO_2 is one of the principal limiting factors for microalgae growth (Arias et al., 2017) and for microalgal-bacteria consortiums nutrient removal capacity, since nitrifying bacteria also compete with microalgae for the CO_2 (Choi et al., 2010; de Godos et al., 2014; García et al., 2017). CO_2 sequestration is influenced by light intensity, solution pH and temperature and CO_2 loading biomass concentration and volume (Judd et al., 2015). Algal activity increases with light intensity, until a threshold value where the photosynthetic apparatus is saturated. Indeed, light availability will not only influence the nutrient removal capacity of microalgae and other photosynthetic organisms but will also influence the photosynthetic oxygen production. This oxygen production will influence the growth and nutrient removal capacity of heterotrophic bacteria (PAOs, AOBs, NOBs and others) (Carvalho et al., 2021).

Carvalho et al. (2021) (**chapter 5**) developed an algal-bacterial consortium with the aim to reduce the COD needs in wastewater treatment and allow the treatment of WW with low COD:P and COD:N ratios, and particularly, wastewaters with high P concentrations, with no need of mechanical aeration. This system operates in dark (anaerobic)/light(aerobic)/dark (anoxic) cycles, where a culture composed by microalgae, PAOs, AOB and NOBs were selected. During the dark (anaerobic) VFAs were consumed, while during light period nutrients were removed. P was removed mainly by Poly-P accumulation by PAOs and ammonia was mainly removed by biomass assimilation. 33 ± 5% of ammonia was nitrified and the nitrates produced during light, where removed by denitrification (Carvalho et al., 2021). The goal of the present study is to understand the impact of CO_2 concentration and the length of light/dark phases on the long-term operation of the photo-BNR system, particularly on O_2 production, nitrification, denitrification and phosphorus removal.

7.2. Materials and Methods

7.2.1. Photo-BNR reactor

A sequencing batch reactor (SBR), with a working volume of 3.8 L was inoculated with sludge from a photo-BNR reactor already enriched in PAOs (*Accumulibacter* phosphatis), algae, cyanobacteria and *Thiocapsa*, amongst other microorganisms (Carvalho et al., 2021). The reactor was continuously operated for 260 days, subjected to transient illumination provided by an internal halogen lamp (200 W), with a light intensity of 532 W/m^2 (similar to the average light intensity in Portugal during summer days) (Gschwind et al., 2006), which corresponds to a volumetric light intensity of 4.6 W/L (Carvalho et al., 2021). The sludge retention time (SRT) was 19 ± 1 day to guarantee proliferation of nitrifiers, and the HRT was 16 hours. The photo-BNR reactor was operated in 8 h cycles with sequential dark (anaerobic), light (aerobic) and dark (anoxic) periods, and continuously mixed through magnetic stirring (~700 rpm). In

the end of the anoxic phase, there was a 15 min settling period, followed by a 30 min idle period. The idle period included the removal of supernatant and the beginning of argon sparging before the beginning of the next cycle. Argon was continuously sparged during the dark (anaerobic) phase to assure anaerobic conditions. The reactor was fed in the beginning of the dark (anaerobic) phase with 1.9 L of synthetic medium, where the carbon source was a mixture of acetate and propionate (75% / 25% of COD) to guarantee the proliferation of PAOs over GAOs (Lopez-Vazquez et al., 2009). The synthetic medium fed to the reactor was composed of 75 % (v/v) of a phosphate solution (168 mg/L of K_2HPO_4 and 103 mg/L of KH_2PO_4) and 25 % (v/v) of carbon medium with a concentration per liter of: 0.26 g $C_2H_3O_2Na.3H_2O$; 27 µL $C_3H_6O_2$ (99.5%); 0.59 g NH_4Cl; 0.95 g $MgSO_4.7H_2O$; 0.44 g $CaCl_2.2H_2O$; 31.7 mg ethylenediaminetetraacetic (EDTA) and 3.17 mL of a micronutrients solution, with a concentration per litre of: 1.5 g $FeCl_3.6H_2O$; 0.15 g H_3BO_3; 0.03 g $CuSO_4.5H_2O$; 0.18 g KI; 0.12 g $MnCl_2.4H_2O$; 0.06 g $Na_2MoO.2H_2O$; 0.12 g $ZnSO_4.7H_2O$ and 0.15 g $CoCl_2.6H_2O$. EDTA was used to prevent the precipitation of salts, like Ca^{2+} and PO_4^{3-} present in the media. These concentrations corresponded to a phosphorus and ammonia concentration in the feed of 40 mg P/L and 40 mg N/L, respectively.

7.2.2. Evaluation of operational conditions

Throughout the photo-BNR operation, light intensity, phosphorus and ammonia concentration in the feed remained unchanged. To improve the reactor nutrient removal efficiency and evaluate the impact of CO_2 concentration and illumination periods on the culture's performance, the length of the different phases was adjusted during the photo-BNR operation, as well as the COD and Na_2CO_3 concentration in the feed (**Figure 7.1**). The length of the dark (anaerobic) phase and COD concentration was adjusted to guarantee total volatile fatty acids (VFAs) consumption in the dark phase, preventing the growth of heterotrophic organisms during the light aerobic phase that do not contribute for nutrient removal. The length of the light phase and concentration of Na_2CO_3 was adjusted to guarantee sufficient oxygen production for system oxygenation and allow oxygen measurement by the sensor (> 1 mg O_2/L). The length of the dark (anoxic) phase was modified to guarantee that, after light being turned off, oxygen could be depleted, achieving anoxic conditions and thus, denitrification could occur (**Figure 7.1**). The reactor operation was divided in 4 stages: Stage 1 (104 days) was the start-up period, where COD was increased from 40 to 300 mg COD/L; Stage 2 (86 days) corresponds to the period that the CO_2 concentration, fed to the reactor as Na_2CO_3, was increased from 22 to 36 mg C/L (2a) and to 60 mg C/L (2b) and the light exposure time was increased (2c); Stage 3 (30 days) corresponds to the period with good capacity of nutrients removal, with a COD:Na_2CO_3:N:P: ratio of 7.5:0.9:1:1 (mg basis), while stage 4 (39 days) corresponds to the period where NO_3 leaked to the dark-anaerobic period of the following cycle (**Figure 7.1**).

7.2.3. Chlorophyll and bacteriochlorophyll quantification

The chlorophyll and bacteriochlorophyll concentration were calculated according to Ritchie (2018) using the equations for pigments extraction with 100% ethanol.

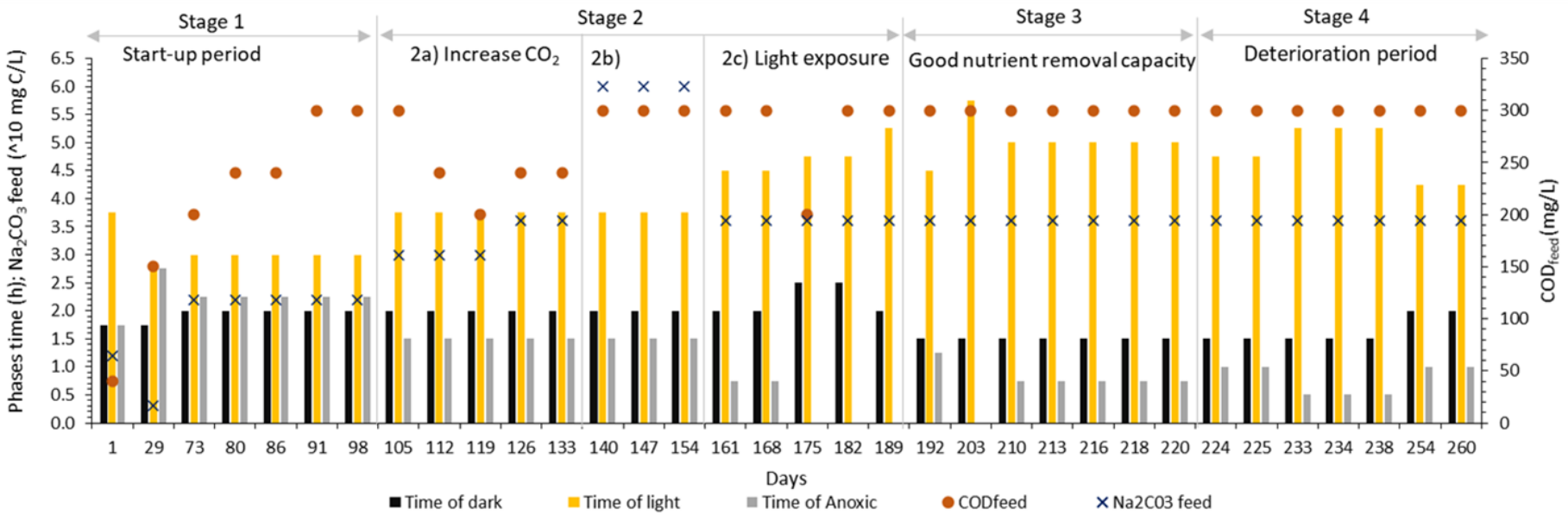

Figure 7.1 - Operational adaptations of the photo-BNR operation.

Stage 1: start-up period; Stage 2: increase auto oxygenation of photo-BNR (2a: increase of CO_2 and adjustment of COD concentration; 2b: increase of CO_2 and COD concentration; 2c: increase the length of the light phase) Stage 3: Photo-BNR operation with good nutrient removal capacity; Stage 4: deterioration of photo-BNR performance. Settling and idle period was 15 and 30 minutes, respectively, during all the period of the photo-BNR operation.

7.3. Results and discussion

7.3.1. Photo-BNR start-up and operation

The photo-BNR reactor was operated for 260 days. During the start-up period (stage 1) COD and Na_2CO_3 in the feed were increased until 300 mg /L and 22 mg C/L, respectively, which corresponds to a COD:CO_2:N:P ratio of 15:1.1:2:2 on a mass basis (**Figure 7.1**). The increase of COD concentration resulted in higher biomass concentration, consequently, resulting in higher oxygen necessities for heterotrophic biomass respiration and growth (**Figure 7.2 - A**, Stage 1), meaning that all the oxygen photosynthetically produced was used by the photo-BNR microorganisms. As PAOs were oxygen limited during the aerobic light phase, they had reduced energy for P uptake and polyphosphate formation, showing low phosphorus content in the biomass (**Figure 7.2 -B,** Stage 1), which gradually decreased PAOs' capability to perform VFAs consumption and P release during the anaerobic phase. Since low nutrients removal was obtained (< 70% for phosphorus and ammonia) and O_2 was barely measured during the start-up period, it can be concluded that nutrients removal was limited by oxygen availability. For that reason, the aim of stage 2 was to increase oxygen production by microalgae/cyanobacteria by means of adjusting CO_2 concentration and illumination length. In stage 2a, when oxygen was limited, the culture was not able to fully consume the 300 mg COD/L fed to the reactor during the dark phase, so, COD was decreased to guarantee full VFAs consumption during the dark period. However, the increase of Na_2CO_3 concentration in the feed from 30 to 36 mg C/L in stage 2a, and later to 60 mg C/L in stage 2b led to an increase of photosynthetic microorganisms concentration (**Figure 7.2**) and, probably, from photosynthetic oxygen production, allowing an increase in the COD concentration in the feed, back to 300 mg COD/L. Along stage 2a and 2b, the DO concentration was routinely limited prompting the increase of the light period in stage 2c from 3.75 h to 5.25h. After around 30 days with higher light exposition time, oxygen production increased (**Figure 7.2**), allowing full removal of phosphorus and around 90 % of ammonia removal in stage 3. When oxygen concentration inside the reactor exceeded a concentration of ~ 2 mg O_2/L at the end of the illuminated phase, subsequent anoxic conditions were hard to achieve and, consequently, denitrification during anoxic period was reduced, which decreased total N removal to around 80%. Overall, these results show how oxygen concentration is a key parameter to control. O_2 production by microalgae/cyanobacteria is dependent on CO_2 availability and light intensity and exposition period (Fatemeh et al., 2021; Judd et al., 2015; Luo et al., 2017; Muñoz and Guieysse, 2006; Razzak et al., 2017). As already indicated, illumination period and intensity have a strong influence on algal-bacteria consortia dynamics and, thus, influence nutrient removal efficiency (Fatemeh et al., 2021). For this reason, the CO_2 concentration and the length of the light phase were the two key parameters explored in the present work, to understand its impact on photo-BNR performance when operated in dark (anaerobic)/light (aerobic)/ dark (anoxic) phases.

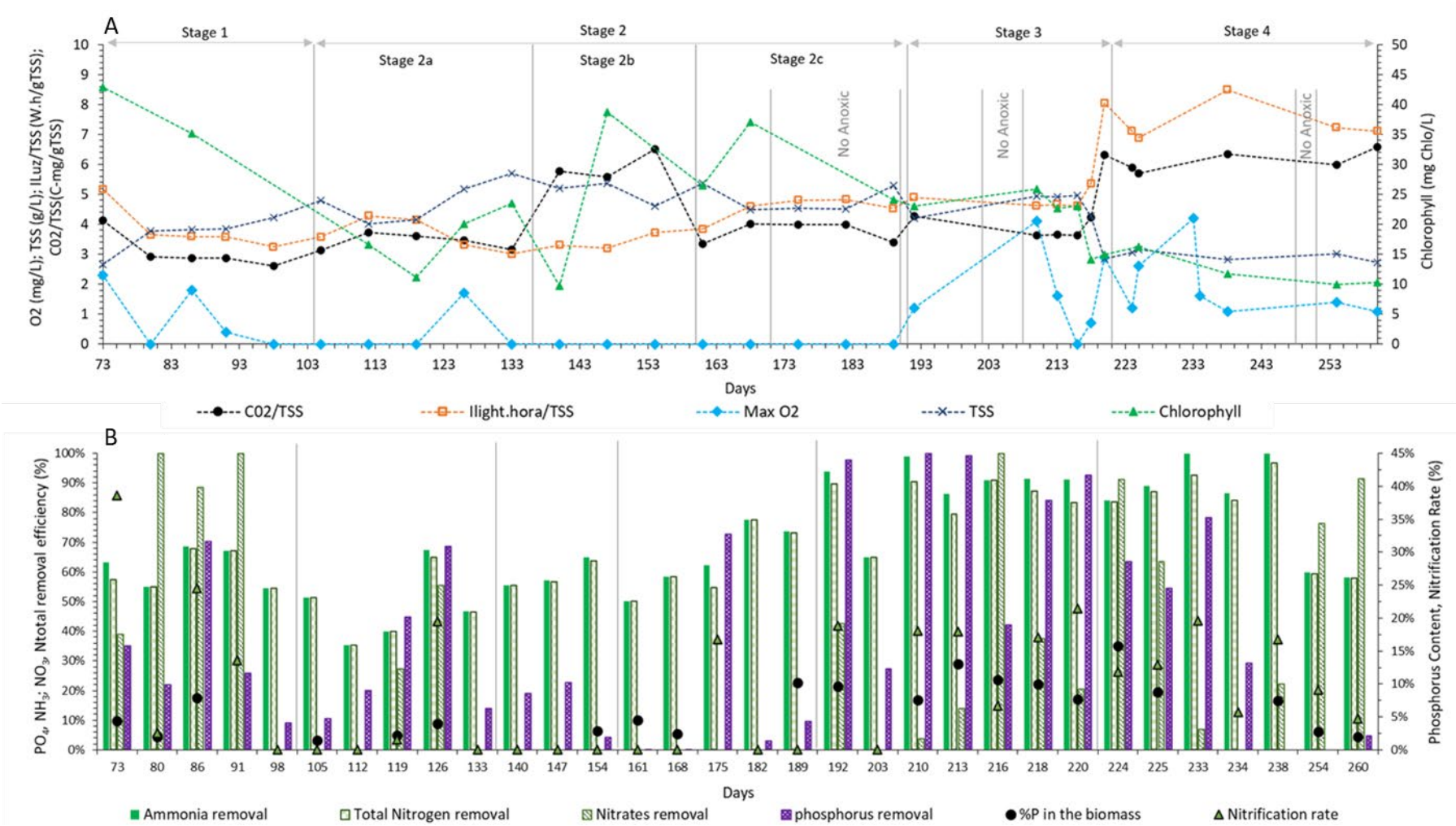

Figure 7.2 - Photo-BNR performance during the 260 days of operation.
TSS value corresponded to the average value of TSS during a daily cycle and Max O_2 corresponds to the oxygen concentration reached in the end of light phase. Stage 1 (until day 104): start-up period; Stage 2: (from day 105 to 191) increase auto oxygenation of photo-BNR; Stage 3 (from day 192 to 221): good capacity of nutrient removal and stage 4 (from day 222 to 260): deterioration of photo-BNR performance. No anoxic phase corresponds to the period when the anoxic phase was removed to allow more time of light exposure.

7.3.2. Impact of CO_2 concentration

Changes in Na_2CO_3 concentration were made to adapt the photosynthetic oxygen production to the photo-BNR necessities. In stage 2a, O_2 was still not measured in the reactor (**Figure 7.2**) even with higher Na_2CO_3 concentrations fed to the reactor. The increase of the TSS concentration was not accompanied by an increase of chlorophyll concentration. In fact, chlorophyll decreased on stage 2a when compared with stage 1, indicating the growth of other autotrophic microorganisms, rather than microalgae. The increase of Na_2CO_3 in the feed from 30 mg C/L to 36mg C/L (during stage 2a) and later to 60 mg C/L (stage 2b) (**Figure 7.1**) led to an increase of chlorophyll concentration (**Figure 7.2**), indicating higher microalgae growth and, thus, higher O_2 production and better nutrients removal was expected. In reality, neither higher oxygen concentrations inside the reactor were achieved, nor a higher P removal was obtained. Only ammonia removal slightly increased to 59 % ± 5 on stage 2b (**Figure 7.2**). The fact that dissolved oxygen could not be detected in the reactor bulk does not necessarily mean that O_2 production was unaffected by the CO_2, since the oxygen measured in the sensor is the extra oxygen that is not consumed by bacteria. With more CO_2 being consumed for autotrophic microorganisms' growth (bacteria or microalgae), higher oxygen is required to support this growth, increasing the global O_2 necessities of the photo-BNR. Nitrification process is both dependent of CO_2 and O_2 availability and during stage 2b, even with an increase of the Na_2CO_3 concentration fed, no nitrification was observed. These results indicate that photosynthetic O_2 production was not enough to fulfil all the microorganisms' requirements.

Fatemeh et al. (2021) and Singh and Singh (2014) reported that low availability of inorganic carbon can limit the microalgae growth and consequently oxygen production, directly affecting the amount of nitrogen and phosphorus assimilated into the biomass. On the other hand, Razzak et al. (2017) and Singh and Singh (2014) also observed that increasing the CO_2 concentration in microalgae systems increased the amount of biomass, however from them results, it is difficult to understand which was the optimal CO_2 concentration for microalgal growth.

A CO_2/TSS ratio of 4.3 ± 1.04 mg C/g TSS (stage 3) and 6.1 ± 0.36 mg C/g TSS (stage 4) allowed enough photosynthetic oxygen production, more than the needs for microorganism's respiration, since O_2 could be measured. During stage 3 (**Figure 7.2**, day 192 to 221, Fig. 4a), higher oxygen availability, that reached 3.8 mg O_2/L, resulted in good nutrient removal efficiency, achieving 100% of P and 90% of total N removal on day 210. Excess O_2 measurement was also observed in Carvalho et al, (2021) (**chapter 5**), with a ratio of 3.1 ± 0.83 mg C CO_2/g TSS. However, in the present study, with a ratio of 3.4 ± 0.27 mg C CO_2/g TSS (stage 2a) and 6.0 ± 0.48 mg C CO_2/g TSS (stage 2b), all the oxygen produced was consumed, probably due to the shadow effect that occurred due to the higher TSS concentration (4.8 ± 0.71 g/L on stage 2a and 5.1 ± 0.40 g/L on stage 2b), or because the period of illumination was not enough, limiting oxygen production (**Figure 7.2**). Anbalagan et al. (2017) found that for higher TSS concentrations, higher light intensities are needed to reach higher oxygen production, since

in microalgae-bacteria consortium, an excessive solids concentration may reduce light penetration, causing self-shading and resulting in oxygen consumption by microalgae dark respiration, which results in lower oxygen availability for bacteria respiration. Literature is unanimous about recommending to maintain biomass concentration not relatively high to avoid self-shading problems (Luo et al., 2017; Muñoz and Guieysse, 2006). Foladori et al (2020) found that the best TSS values for maximum ammonia removal in microalgal-bacterial reactors (light intensity = 45 $\mu mol/m^2s^{-1}$) without external aeration was between 0.7 and 2.6 g/L, depending on the flocs structure. Most of the published studies, either from microalgae or microalgal-bacterial consortiums, used biomass concentrations between 0.35 and 2.8 g/L (García et al., 2017; Judd et al., 2015), which are much lower values than the ones obtained in the present study (from 2.7 g/L (stage 4) to 5.7 g/L (stage 2a) (**Figure 7.2**).

Overall, the obtained results indicate that, increases of the Na_2CO_3 concentration, per se, will not increase photosynthetic oxygen production, since the biomass concentration inside the reactor will affect light penetration and microalgae growth. Higher biomass concentration and associated self-shading appears to be limiting the photosynthetic O_2 production. Nevertheless, with a CO_2/TSS ratio of 4.3 ± 1.0 mg C CO_2/g TSS, the O_2 produced via photosynthesis allowed to achieve higher than 90 % of nutrient removal in most of the days during stage 3. These results indicate that O_2 production could be more dependent on the time of light exposition than on the concentration of CO_2 available.

7.3.3. The impact of the duration of light phase on oxygen concentration and, consequently, on nutrient removal efficiency

Several factors, such as the light exposure time, density of the culture and the cell pigmentation influence the efficiency of light utilization (Razzak et al., 2017). Since the light intensity which the culture was exposed (532 W/m^2) was high, in order to improve photosynthesis efficiency, and consequently allow more oxygen production (Judd et al., 2015; Muñoz and Guieysse, 2006), the period of light exposure was increased (stage 2c –**Figure 7.2**). To achieve longer light exposure periods over the 8h cycle, the anoxic phase length was reduced or even removed. In fact, when oxygen was limited, the culture did not produce nitrate and, consequently, no anoxic phase was needed.

The results obtained during the reactor operation allow to conclude that the length of light phase is very important, since the light time exposure will impact the oxygen photosynthetically produced (**Figure 7.2**). Higher oxygen production permitted higher phosphorus and ammonia removal efficiency during the illuminated period on stage 3 (**Figure 7.2**). The higher oxygen concentrations available increased nitrification rate since it is an oxygen dependent process (**Figure 7.2**). Nevertheless, no more than 21% of the ammonia consumed was nitrified during stage 2, 3 and 4, which was lower than reported in **Chapter 5** (33±5 %) (Carvalho et al.,2021). Lower nitrates concentration measured during the light phase could occur for, at least, 2 reasons: the lower O_2 concentrations achieved promote simultaneous nitrification and

denitrification and leads to underestimated nitrate concentration (Foladori et al., 2020); inhibition of AOB microorganisms by the lower oxygen production caused by the increased shadow effect and/or reduced light penetration (Mohd Udaiyappan et al., 2017). Due to the diversity of the photo-BNR sludge, further research is needed to understand who is performing nitrification (see **section 7.3.4**).

Along Stage 3, from day 191 to day 220 (**Figure 7.2**; **Figure 7.3**), the implemented period of illumination (5 h) resulted in a light availability per TSS of 5.4 ± 1.3 W.h/g TSS and allowed the production of oxygen in excess to the culture needs. The higher oxygen availability at this stage allowed good nutrient removal, with an average removal of 95±7%, 92±5% and 86±5% for PO_4, NH_4 and total N (**Figure 7.3**). P removal during stage 3 (38 ± 3.3 mg P/L) was 1.5 times higher than in Carvalho et al. (2021) (25 ± 9.2 mg P/L) (**chapter 5**), while ammonia removal was similar (33 ± 1.7 mg N/L in the present work, against 38 ± 0.94 mg N/L in Carvalho et al. (2021)). PHA was always available during the light phase, contrary to what happened in Carvalho et al. (2021), showing that phosphorus removal by *Accumulibacter* is dependent of the PHA availability, leading to near full P removal (**Figure 7.4**). Higher PHA availability during the photo-BNR cycles in the present study could be explained by the combination of two factors: 1) the P feed concentration in the present study was 40 mg P/L, lower than the 60 mg P/L fed by Carvalho et al. (2021) (**chapter 5**) and less P uptake by PAOs decreased the PHA needs during light period; 2) ammonia assimilation into the microbial biomass was higher (81 ± 1.7 %, against the 67 ± 5% in Carvalho et al. (2021) and, consequently, higher P would also be assimilated to sustain biomass growth.

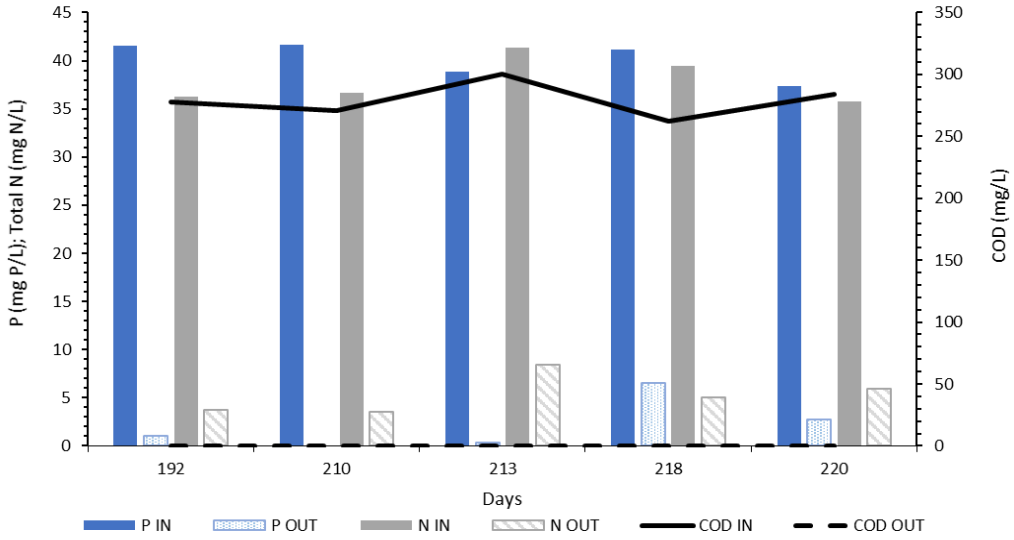

Figure 7.3 - Value of total nitrogen, phosphorus and COD in the influent and effluent during the period of good performance of photo-BNR (stage 3).

Considering that algal organic matter contains on average 1.5% of chlorophyll *a* (Kang et al., 2018), the algal biomass concentration during stage 2c was 1.9 ± 0.5 g/L (44 ± 12% of the VSS) and in stage 3 was 1.3 ± 0.4 g/L, which corresponds to 42 ± 8 % of the total organic biomass (VSS) inside the reactor. These results indicates that photosynthesis efficiency was

limited by the time of light exposition and not by the amount of photosynthetic microorganisms.

Anoxic conditions were difficult to maintain, due to a combination of higher oxygen concentration (> 2mg/L) in the end of the light period and the short period of dark anoxic phase (**Figure 7.4**-a). Denitrification efficiency was generally poor (**Figure 7.2**) and nitrate was consequently present in the next cycle during VFA feeding, resulting in reactor destabilization (**Figure 7.2**). The proliferation of heterotrophic denitrifiers is known for leading to the failure of EBPR systems (Izadi et al., 2020; Valverde, 2015) and likewise, to the failure of the photo-BNR system, since those microorganisms compete with PAOs for the organic carbon. It is important to note that ,when oxygen concentration reached around 1.5 - 2 mg/L in the end of light period, anoxic conditions were achieved (e.g. **Figure 7.4**-b), and denitrification could attain higher than 90 % efficiency (**Figure 7.2**, days 80, 91, 216, 224, 260).

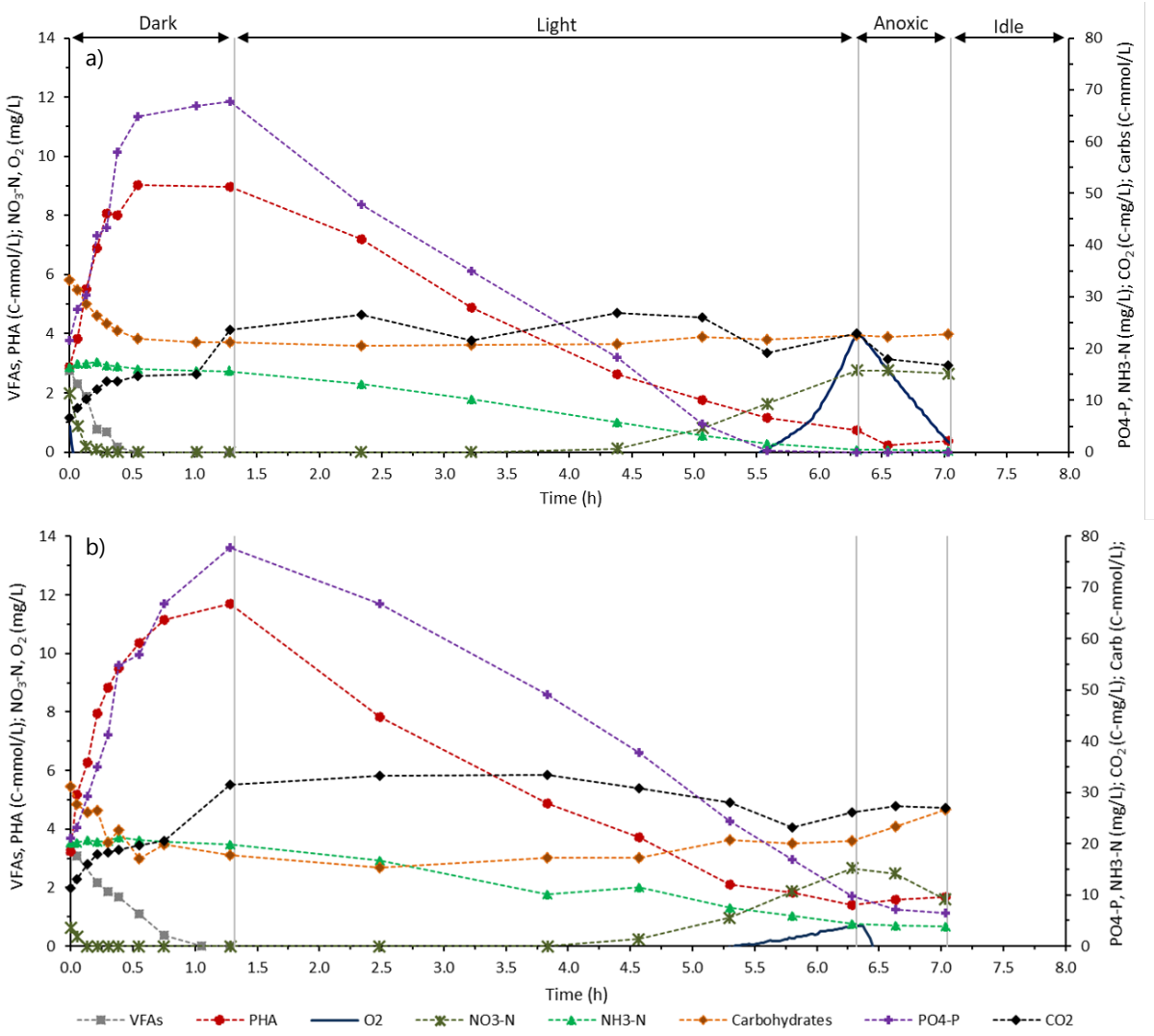

Figure 7.4 - photo-BNR cycle performance over stage 3.
a) day 210; b) day 218.

These results show how important is to control dissolved oxygen concentration across each period of the photo-BNR (Foladori et al., 2018; Torres-Franco et al., 2020). When the photo-BNR culture is exposed to enough light period and CO_2 concentration to overcome oxygen limitation, the increase of N:P ratio favors nutrient assimilation into microalgae biomass and prevents the complete exhaustion of PHA reserves during the light, which are necessary for dark denitrification by PAOs. Phosphorus content in the biomass ranged between 8 and 13% (**Figure 7.2**, stage 3), values that are comparable to conventional EBPR processes (Carvalheira et al., 2014a).

7.3.4. Microbial population of the photo-BNR and nutrient removal mechanisms

The photoperiod may be a key parameter in photo-BNR process, not only because of oxygen production, but also because the microbial consortia respond to different photoperiod conditions with changes in the algal and bacteria population since the time of light exposure also promote the growth of photosynthetic microorganisms.

Whilst FISH results showed *Accumulibacter* as the most abundant microorganism present in photo-BNR between day 192 and 210 (**Table 7.1**), this genus was not detected by sequencing analysis, as already mentioned in previous works (Carvalho et al., 2021; Albertsen et al., 2016; Rubio-Rincón et al., 2019; Valverde-Pérez et al., 2016). During stage 3, the presence of PAOs microorganisms in the biomass increased from abundant to dominant, and clade II started to be the dominant type (**Table 7.1**), which justify the higher P removal, mainly by Poly-P accumulation.

Table 7.1 - FISH results during photo-BNR operation.

		PAOS			GAOS	AOBs	NOBs	
Stage	FISH PROBE	PAOMIX	ACC444-I	ACC444-II	CPB 654	NSO 1225	NIT 3	NTSPA 662
1	Day 73	++	++	+-	++	-	-	-
2	Day 154	++	++	++	++	+-	-	-
3	Day 192	+++	+	+++	++	-	-	-
	Day 210	+++	+	+++	++	+-	-	-
	Day 216	++	++	+++	++	-	-	-
	Day 220	++	++	+++	+	-	-	-

(-) non-existent; (+-) almost non-existent; (+) present; (++) abundant; (+++) dominant. Probes: PAOmix *for Candidatus* Accumulibacter phosphatis; Acc-I-444 which targets type I *Accumulibacter* PAOs and Acc-II-444 for *Accumulibacter* PAOs type II; CPB_654 for *Candidatus* Competibacter phosphatis; Nso1225 and NSO 190 for AOBs; NIT3 and Ntspa662 for NOBs.

Sequencing results (**Table 7.2**) indicates that cyanobacteria species (Chloroplast_OTU_4) were present in high abundance in the photo-BNR. The same trend was observed in **chapter 5** (Carvalho et al., 2021). Cyanobacteria from genus *Calothrix*, that was not present in **chapter 5**, appears in this work as a microorganism with relevant abundancy (**Table**

7.2), which presence increased with the increase of light time exposure and the successive presence of nitrates together with organic carbon. *Calothrix* is also known to form microalgal blooms (Bischoff et al., 2019). The photo-BNR system show, during all operation time, good settling capacity (**Figure 7.5**), however SVI increased, from 42 mL/g TSS on day 86 to 61 mL/g TSS on day 213 and to 123 mL/g TSS on day 260, coinciding with the increase of this filamentous cyanobacteria. It is important to note that settling time was short, only 15 minutes, indicating fast and good settling properties (Pierce et al., 1998) of the microalgal-bacterial granules both on day 86 and 213. This is an extremely important aspect for a cost-efficient microalgae biomass separation by gravity sedimentation (Foladori et al., 2020), since no extra separation steps and, thus, no more energy consumption is necessary to efficiently separate the biomass from the treated liquid before dischargement. *Candidatus* Chloroploca, an anoxygenic phototrophic bacteria capable of storing polyphosphate and PHB (Gorlenko et al., 2014; Grouzdev et al., 2018), appears in the 10 most abundant species in the photo-BNR (**Table 7.2**), whereas in **chapter 5** it could be detected in very low abundance and not within the most abundant species. In the present work, *Candidatus* Chloroploca was found in higher amount between day 154 and 210 (**Table 7.2**) suggesting the contribution of this microorganisms to P removal.

Both FISH (**Table 7.1**) and sequencing results (**Table 7.2**) indicate that AOBs were not abundant in the photo-BNR, so, it can be hypothesized that nitrification from NH_3 to Nitrite could be performed by a side-population, as for example, *Limnohabitans* species (Baskaran et al., 2020). Although these microorganisms were not amongst the 10 most abundant species, they were present in the photo-BNR community. Nitrification from nitrite to nitrate could be performed by photosynthetic microorganisms, as *Thiocapsa* and *Rhodobacter*, (**Table 7.2**) (Levy-Booth et al., 2014).

Since no carbon was fed during the anoxic period, denitrification could be mainly attributed to dPAOs (*Accumulibacter*) and dGAOs (*Competibacter*) (**Table 7.2**). It cannot be ignored the possibility of microalgae starch fermentation during the dark could contribute towards fulfilling the COD demand of denitrification by heterotrophic denitrifying microorganisms. However, PHA consumption and P removal also accompanied denitrification, supporting PAOs activity.

In terms of microalgae composition (**Table 7.3**), the organisms with more relative abundance were from the class Chlorophyceae, followed by the class *Trebouxiophyceae*, both from the phylum *Chlorophyta*. Similar results were observed in the previous chapter (Carvalho et al., 2021), and by Zhang et al. (2018) and Jiménez-Bambague et al. (2020) although in the last 2 works the microalgal-bacterial reactor was operated with light and aeration. Members of phylum *Chlorophyta* are reported in various studies as organisms with good capacity for nutrient removal (Abinandan et al., 2018; Cai et al., 2013; Ji et al., 2020b; Toledo-Cervantes et al., 2019). Indeed, although PAOs are the main responsible for phosphorus removal, microalgae role in phosphorus removal by assimilation cannot be ignored (Bunce et al., 2018; Powell et al., 2011; Shilton et al., 2012). In the case of ammonia removal, microalgae biomass accounts for almost 50% of the VSS concentration in photo-BNR, and since microalgae can efficiently compete with nitrifiers for ammonium (microalgae have higher N uptake and growth rates

(Torres-Franco et al., 2021)), ammonia assimilation could be mainly attributed to microalgae. So far, the results are in accordance with **chapter 5**, that described biomass assimilation (near 70%) as the main mechanism of nitrogen removal in algae-bacteria consortium (Su et al., 2011; Wágner et al., 2021). Full ammonia removal together with high concentrations of P removal (> 10 mg P/L) were not normally found in microalgae-bacteria consortium (Guo et al., 2021; Lima et al., 2020; Posadas et al., 2015b; Torres-Franco et al., 2021). However, high concentrations of P removal, up to 40mg P/L, could be achieved if the biomass is enriched in PAOs microorganisms that accumulate P as poly-P.

Figure 7.5 - Picture of photo-BNR reactor after 15 minutes of settling.
Pictures were taken after a full cycle sampling on day 86 and day 213 of the photo-BNR operation.

Table 7.2 - 10 most abundant prokaryotic species, obtained from DNA sequencing, in the photo-BNR process.

Stage 1	Stage 2b	Stage 3				Stage 4	
Day 73	Day 154	Day 192	Day 210	Day 216	Day 220	Day 260	
37.4	28.3	21.8	30.8	23.2	16.7	2.4	(C) Gammaproteobacteria; (G) Thiocapsa
19.0	24.5	20.9	17.2	15.9	17.3	0.0	(P) Cyanobacteria; (C) Chloroplast_OTU_4
6.3	14.5	25.6	19.6	22.1	21.3	0.7	(C) Gammaproteobacteria; (F) Competibacteraceae; (G) CPB_S18
0.5	2.4	6.8	7.8	13.9	23.3	56.1	(C) Cyanobacteria; (G) Calothrix
0.1	1.9	3.3	3.1	2.2	2.0	3.4	(C) Gammaproteobacteria; (F) Competibacteraceae; (G) CPB_C22&F32
2.4	1.4	1.6	1.7	1.7	1.7	0.0	(P) Cyanobacteria; (C) Chloroplast_OTU_19
1.0	2.7	2.2	2.2	1.3	1.0	1.5	(C) Chloroflexia (F) Chloroflexaceae; (G) Candidatus Chloroploca
0.4	4.4	1.0	1.3	1.3	1.4	0.8	(C) Gammaproteobacteria; (F) Competibacteraceae; (G) CPB_P15
1.7	4.5	2.0	0.6	0.5	0.2	0.0	(C) Chloroflexia (F) Chloroflexaceae; (G)Chloronema
2.8	0.8	0.9	1.0	1.2	1.2	0.5	(C) Alphaproteobacteria; (F) Rhodobacteraceae; (G)Rhodobacter

(K – Kingdom; P – Phylum; C – Class; O – Order; F – Family; G- Genus).

Table 7.3 - 9 most abundant Archaea species, obtained from DNA sequencing, in the photo-BNR process.

Stage 2	Stage 3				
Day 154	**Day 192**	**Day 210**	Day 216	Day 220	
93.2	**93.8**	**88.0**	90.4	89.9	(P) Chlorophyta; (C) Chlorophyceae_OTU_1
4.7	**3.1**	**6.4**	5.1	6.7	(P) Chlorophyta; (C) Trebouxiophyceae_OTU2
0.1	**1.1**	**3.4**	2.3	1.4	(P) Chlorophyta; (C) Chlorophyceae; (G) Uronema
1.3	**0.8**	**1.0**	0.8	0.8	(P) Chlorophyta; (C) Chlorophyceae_OTU_4
0.2	**0.8**	**0.3**	0.8	0.6	(P) Cercozoa; (C) Thecofilosea; (F) Rhizaspididae
0.2	**0.2**	**0.5**	0.3	0.3	(P) Unassigned
0.2	**0.2**	**0.3**	0.2	0.2	(K) Fungi; (P)Ascomycota_Saccharomycotina

(K – Kingdom; P – Phylum; C – Class).

7.3.5. Key parameters to control for the achievement of a stable photo-BNR

The photo-BNR was operated with a SRT of 19 ± 1 days and an HRT of 16 hours. Near full nutrient removal was obtained with a COD:CO_2:N:P ratio of 7.5:0.9:1:1 (mg basis), when the culture was exposed to 5.4 ± 1.3 W.h/g TSS.

The results obtained during the reactor operation allow to conclude that, in particular, the period of light, probably because of the TSS concentration achieved, and dark anoxic period used were not enough to achieve a stable photo-BNR. –The length of these phases was constrained by the reactor laboratorial operation under 8h cycles. However, when operating the photo-BNR in a daily cycle of 12h light/12 dark, this problem could be overcome, since more time of light exposure, and consequently higher oxygen production by microalgae, and a longer anoxic phase for denitrification, could be obtained. Nevertheless, the increase of cycle time, would also increase the HRT and, thus, decrease the amount of wastewater treated per day. Still, if HRT are maintained shorter than 24 h, it is lower than the 10 days HRT used, for example, by Torres-Franco et al. (2021) or the 4 and 4.5 days HRT of Anbalagan et al (2017) and de Godos et al. (2014), respectively, for nutrient removal by microalgal- bacterial consortia. Judd et al. (2015) concluded that HRT between 2 and 5 days are needed to obtain up to 80% nutrient removal in HRAPs, when compared to around 12h found in conventional BNR.

The different climatic conditions during the year affect the sun radiation that reaches the Earth, altering the light availability for microalgae and other phototrophic microorganisms' growth. For this reason, variable light intensities should be tested to understand the impact of light intensity on oxygen production, nutrients removal and CO_2 fixation.

Biomass concentration is also a key parameter to control on photo-BNR process. If for one hand low biomass concentration could reduce O_2 production by algae and decrease nutrient removal capacity, on the other hand, high biomass concentration can lead to a shadow effect and reduce photosynthesis efficiency. The impact of biomass concentration on microalgae light absorbance capacity should be studied as an adequate TSS concentration could lead to a more stable and efficient photo-BNR operation. TSS concentration could be controlled by decreasing the SRT, for example, however, more investigation is needed to understand the impact of reducing this parameter on microorganism's selection and thus, on nutrient removal efficiency.

Furthermore, in situations where the system's oxygen production is lower than required for efficient nutrient removal (e.g. e outdoor system operation using natural sunlight, low inorganic carbon availability), an auxiliary air pump could be temporarily used for oxygen supply. Oxygen concentrations should be controlled at low values (~2 mg O_2/L) to enable nutrients removal whilst not compromising the fast achievement of the subsequent anoxic phase.

Also, the air flow should be rigorously controlled, since some studies indicate that the CO_2 striping caused by high aeration could overcome the benefits of aeration, since less inorganic carbon could be available for both microalgae and nitrifiers (Zhang et al., 2020a, 2020b).

7.4. Conclusions

The results obtained during the 260 days of the photo-BNR operation indicate that the proposed photo-BNR system does not require mechanical aeration, since the oxygen necessary could be photosynthetically produced. Higher photosynthetic oxygen production was obtained when the photo-BNR culture was exposed to longer periods of light, rather than to higher concentrations of Na_2CO_3. Best results for nutrient removal were obtained with a COD:CO_2:N:P ratio of 7.5:0.9:1:1, and a CO_2/TSS ratio of 4.3 ± 1.04 mg C/ g TSS, when the culture received 5.4 ± 1.3 W.h/g TSS. In this case, it was possible to achieve removal efficiencies higher than 90% for phosphorus and ammonia and higher than 85 % for total nitrogen, originating an effluent with 2.1 ± 2.7 mg P/L and 5.3 ± 2.0 mg N/L. The stability of the photo-BNR system with good nutrient removal efficiency is closely related with oxygen concentration, which needs to be strictly controlled to values < 2 mg O_2/L, allowing PAOs respiration but without compromising the transition to the anoxic phase. The present study provides insight on the key parameters that must be tuned and controlled for stable photo-BNR operation and future technology deployment into outdoor applications.

REFERENCES

Abinandan, S., Subashchandrabose, S.R., Venkateswarlu, K., Megharaj, M., 2018. Nutrient removal and biomass production: advances in microalgal biotechnology for wastewater treatment. Crit. Rev. Biotechnol. https://doi.org/10.1080/07388551.2018.1472066

Albertsen, M., McIlroy, S.J., Stokholm-Bjerregaard, M., Karst, S.M., Nielsen, P.H., 2016. "Candidatus Propionivibrio aalborgensis": A novel glycogen accumulating organism abundant in full-scale enhanced biological phosphorus removal plants. Front. Microbiol. 7, 1–17. https://doi.org/10.3389/fmicb.2016.01033

Alcántara, C., Domínguez, J.M., García, D., Blanco, S., Pérez, R., García-Encina, P.A., Muñoz, R., 2015. Evaluation of wastewater treatment in a novel anoxic-aerobic algal-bacterial photobioreactor with biomass recycling through carbon and nitrogen mass balances. Bioresour. Technol. https://doi.org/10.1016/j.biortech.2015.04.125

Anbalagan, A., Schwede, S., Lindberg, C.F., Nehrenheim, E., 2017. Influence of iron precipitated condition and light intensity on microalgae activated sludge based wastewater remediation. Chemosphere 168, 1523–1530. https://doi.org/10.1016/j.chemosphere.2016.11.161

Arias, D.M., Uggetti, E., García-Galán, M.J., García, J., 2017. Cultivation and selection of cyanobacteria in a closed photobioreactor used for secondary effluent and digestate treatment. Sci. Total Environ. 587–588, 157–167. https://doi.org/10.1016/j.scitotenv.2017.02.097

Baskaran, V., Patil, P.K., Antony, M.L., Avunje, S., Nagaraju, V.T., Ghate, S.D., Nathamuni, S., Dineshkumar, N., Alavandi, S. V., Vijayan, K.K., 2020. Microbial community profiling of ammonia and nitrite oxidizing bacterial enrichments from brackishwater ecosystems for mitigating nitrogen species. Sci. Rep. 10, 1–11. https://doi.org/10.1038/s41598-020-62183-9

Bischoff, V., Zucker, F., Moraru, C., 2019. Marine Bacteriophages. Ref. Modul. Life Sci. https://doi.org/10.1016/b978-0-12-809633-8.20988-6

Boelee, N.C., Temmink, H., Janssen, M., Buisman, C.J.N., Wijffels, R.H., 2012. Scenario analysis of nutrient removal from municipal wastewater by microalgal biofilms. Water (Switzerland) 4, 460–473. https://doi.org/10.3390/w4020460

Bothe, H., Jost, G., Schloter, M., Ward, B.B., Witzel, K.P., 2000. Molecular analysis of ammonia oxidation and denitrification in natural environments. FEMS Microbiol. Rev. 24, 673–690. https://doi.org/10.1016/S0168-6445(00)00053-X

Bunce, J.T., Ndam, E., Ofiteru, I.D., Moore, A., Graham, D.W., 2018. A review of phosphorus removal technologies and their applicability to small-scale domestic wastewater treatment systems. Front. Environ. Sci. https://doi.org/10.3389/fenvs.2018.00008

Cai, T., Park, S.Y., Li, Y., 2013. Nutrient recovery from wastewater streams by microalgae: Status and prospects. Renew. Sustain. Energy Rev. 19, 360–369. https://doi.org/10.1016/j.rser.2012.11.030

Carvalheira, M., Oehmen, A., Carvalho, G., Eusébio, M., Reis, M.A.M., 2014. The impact of aeration on the competition between polyphosphate accumulating organisms and glycogen accumulating organisms. Water Res. 66, 296–307. https://doi.org/10.1016/j.watres.2014.08.033

Carvalho, V.C.F., Freitas, E.B., Silva, P.J., Fradinho, J.C., Reis, M.A.M., Oehmen, A., 2018. The impact of operational strategies on the performance of a photo-EBPR system. Water Res. 129, 190–198. https://doi.org/10.1016/j.watres.2017.11.010

Carvalho, V.C.F., Kessler, M., Fradinho, J.C., Oehmen, A., Reis, M.A.M., 2021. Achieving nitrogen and phosphorus removal at low C / N ratios without aeration through a novel phototrophic process. Sci. Total Environ. 793, 148501. https://doi.org/10.1016/j.scitotenv.2021.148501

Choi, O., Das, A., Yu, C.P., Hu, Z., 2010. Nitrifying bacterial growth inhibition in the presence of algae and cyanobacteria. Biotechnol. Bioeng. 107, 1004–1011. https://doi.org/10.1002/bit.22860

De-Bashan, L.E., Bashan, Y., 2004. Recent advances in removing phosphorus from wastewater and its future use as fertilizer (1997-2003). Water Res. 38, 4222–4246. https://doi.org/10.1016/j.watres.2004.07.014

de Godos, I., Vargas, V.A., Guzmán, H.O., Soto, R., García, B., García, P.A., Muñoz, R., 2014. Assessing carbon and nitrogen removal in a novel anoxic-aerobic cyanobacterial-bacterial photobioreactor configuration with enhanced biomass sedimentation. Water Res. 61, 77–85. https://doi.org/10.1016/j.watres.2014.04.050

Fatemeh, S., Hennige, S., Willoughby, N., Adeloye, A., Gutierrez, T., 2021. Integrating micro-algae into wastewater treatment : A review. Sci. Total Environ. 752, 142168. https://doi.org/10.1016/j.scitotenv.2020.142168

Foladori, P., Petrini, S., Andreottola, G., 2020. How suspended solids concentration affects nitrification rate in microalgal- bacterial photobioreactors without external aeration Heliyon How suspended solids concentration affects nitri fi cation rate in microalgal-bacterial photobioreactors without exte. Heliyon e03088. https://doi.org/10.1016/j.heliyon.2019.e03088

Foladori, P., Petrini, S., Andreottola, G., 2018. Evolution of real municipal wastewater treatment in photobioreactors and microalgae-bacteria consortia using real-time parameters. Chem. Eng. J. 345, 507–516. https://doi.org/10.1016/j.cej.2018.03.178

García, D., Alcántara, C., Blanco, S., Pérez, R., Bolado, S., Muñoz, R., 2017. Enhanced carbon, nitrogen and phosphorus removal from domestic wastewater in a novel anoxic-aerobic photobioreactor coupled with biogas upgrading. Chem. Eng. J. 313, 424–434. https://doi.org/10.1016/j.cej.2016.12.054

Gorlenko, V.M., Bryantseva, I.A., Kalashnikov, A.M., Gaisin, V.A., Sukhacheva, M. V., Gruzdev, D.S., Kuznetsov, B.B., 2014. Candidatus "Chloroploca asiatica" gen. nov., sp nov., a New Mesophilic Filamentous Anoxygenic Phototrophic Bacterium. Microbiology 83, 838–848. https://doi.org/10.1134/S0026261714060083

Grouzdev, D.S., Rysina, M.S., Bryantseva, I.A., Gorlenko, V.M., Gaisin, V.A., 2018. Draft

genome sequences of ' Candidatus Chloroploca asiatica ' and ' Candidatus Viridilinea mediisalina ' , candidate representatives of the Chloroflexales order : phylogenetic and taxonomic implications 1–9.

Gschwind, B., Ménard, L., Albuisson, M., Wald, L., 2006. Converting a successful research project into a sustainable service: the case of the SoDa Web service. Environ. Modell. Softw. 21, 1555e1561.

Guo, D., Zhang, X., Shi, Y., Cui, B., Fan, J., Ji, B., Yuan, J., 2021. Microalgal-bacterial granular sludge process outperformed aerobic granular sludge process in municipal wastewater treatment with less carbon dioxide emissions. Environ. Sci. Pollut. Res. 28, 13616–13623. https://doi.org/10.1007/s11356-020-11565-7

Izadi, Parnian, Izadi, Parin, Eldyasti, A., 2020. Design, operation and technology configurations for enhanced biological phosphorus removal (EBPR) process: a review, Reviews in Environmental Science and Biotechnology. Springer Netherlands. https://doi.org/10.1007/s11157-020-09538-w

Ji, B., Zhang, M., Wang, L., Wang, S., Liu, Y., 2020. Removal mechanisms of phosphorus in non-aerated microalgal-bacterial granular sludge process. Bioresour. Technol. 312. https://doi.org/10.1016/j.biortech.2020.123531

Jiménez-Bambague, E.M., Madera-Parra, C.A., Ortiz-Escobar, A.C., Morales-Acosta, P.A., Peña-Salamanca, E.J., Machuca-Martínez, F., 2020. High-rate algal pond for removal of pharmaceutical compounds from urban domestic wastewater under tropical conditions. Case study: Santiago de Cali, Colombia. Water Sci. Technol. 82, 1031–1043. https://doi.org/10.2166/wst.2020.362

Judd, S., van den Broeke, L.J.P., Shurair, M., Kuti, Y., Znad, H., 2015. Algal remediation of CO2 and nutrient discharges: A review. Water Res. 87, 356–366. https://doi.org/10.1016/j.watres.2015.08.021

Kang, D., Kim, K., Jang, Y., Moon, H., Ju, D., Jahng, D., 2018. Nutrient removal and community structure of wastewater-borne algal-bacterial consortia grown in raw wastewater with various wavelengths of light. Int. Biodeterior. Biodegrad. 126, 10–20. https://doi.org/10.1016/j.ibiod.2017.09.022

Kuba, T., Van Loosdrecht, M.C.M., Heijnen, J.J., 1996. Phosphorus and nitrogen removal with minimal COD requirement by integration of denitrifying dephosphatation and nitrification in a two-sludge system. Water Res. 30, 1702–1710. https://doi.org/10.1016/0043-1354(96)00050-4

Levy-Booth, D.J., Prescott, C.E., Grayston, S.J., 2014. Microbial functional genes involved in nitrogen fixation, nitrification and denitrification in forest ecosystems. Soil Biol. Biochem. 75, 11–25. https://doi.org/10.1016/j.soilbio.2014.03.021

Lima, S., Villanova, V., Grisafi, F., Caputo, G., Brucato, A., Scargiali, F., 2020. Autochthonous microalgae grown in municipal wastewaters as a tool for effectively removing nitrogen and phosphorous. J. Water Process Eng. 38, 101647. https://doi.org/10.1016/j.jwpe.2020.101647

Lopez-Vazquez, C.M., Oehmen, A., Hooijmans, C.M., Brdjanovic, D., Gijzen, H.J., Yuan, Z.,

van Loosdrecht, M.C.M., 2009. Modeling the PAO-GAO competition: Effects of carbon source, pH and temperature. Water Res. 43, 450–462. https://doi.org/10.1016/j.watres.2008.10.032

Luo, Y., Le-Clech, P., Henderson, R.K., 2017. Simultaneous microalgae cultivation and wastewater treatment in submerged membrane photobioreactors: A review. Algal Res. 24, 425–437. https://doi.org/10.1016/j.algal.2016.10.026

Mohd Udaiyappan, A.F., Abu Hasan, H., Takriff, M.S., Sheikh Abdullah, S.R., 2017. A review of the potentials, challenges and current status of microalgae biomass applications in industrial wastewater treatment. J. Water Process Eng. 20, 8–21. https://doi.org/10.1016/j.jwpe.2017.09.006

Mulbry, W., Kondrad, S., Pizarro, C., 2006. Biofertilizers from algal treatment of dairy and swine manure effluents: Characterization of algal biomass as a slow release fertilizer. J. Veg. Sci. 12, 107–125. https://doi.org/10.1300/J484v12n04_08

Mulbry, W., Westhead, E.K., Pizarro, C., Sikora, L., 2005. Recycling of manure nutrients: Use of algal biomass from dairy manure treatment as a slow release fertilizer. Bioresour. Technol. 96, 451–458. https://doi.org/10.1016/j.biortech.2004.05.026

Muñoz, R., Guieysse, B., 2006. Algal-bacterial processes for the treatment of hazardous contaminants: A review. Water Res. 40, 2799–2815. https://doi.org/10.1016/j.watres.2006.06.011

Pierce, J.J., Weiner, R.F., Vesilind, P.A., 1998. Environmental Pollution and Control, 4th ed. Butterworth-Heinamann.

Plouviez, M., Guieysse, B., 2020. Nitrous oxide emissions during microalgae-based wastewater treatment: Current state of the art and implication for greenhouse gases budgeting. Water Sci. Technol. 82, 1025–1030. https://doi.org/10.2166/wst.2020.304

Posadas, E., Muñoz, A., García-González, M.C., Muñoz, R., García-Encina, P.A., 2015. A case study of a pilot high rate algal pond for the treatment of fish farm and domestic wastewaters. J. Chem. Technol. Biotechnol. 90, 1094–1101. https://doi.org/10.1002/jctb.4417

Powell, N., Shilton, A.N., Pratt, S., Chisti, Y., 2011. Luxury uptake of phosphorus by microalgae in waste stabilization ponds. Environ. Sci. Technol. 63, 704–709. https://doi.org/10.1021/es703118s

Ramanan, R., Kim, B.H., Cho, D.H., Oh, H.M., Kim, H.S., 2016. Algae-bacteria interactions: Evolution, ecology and emerging applications. Biotechnol. Adv. 34, 14–29. https://doi.org/10.1016/j.biotechadv.2015.12.003

Razzak, S.A., Ali, S.A.M., Hossain, M.M., deLasa, H., 2017. Biological CO2 fixation with production of microalgae in wastewater – A review. Renew. Sustain. Energy Rev. 76, 379–390. https://doi.org/10.1016/j.rser.2017.02.038

Ritchie, R.J., 2018. Measurement of chlorophylls a and b and bacteriochlorophyll a in organisms from hypereutrophic auxinic waters. J. Appl. Phycol. 30, 3075–3087. https://doi.org/10.1007/s10811-018-1431-4

Rosso, D., Larson, L.E., Stenstrom, M.K., 2008. Aeration of large-scale municipal wastewater

treatment plants : state of the art 973–979. https://doi.org/10.2166/wst.2008.218

Rubio-Rincón, F.J., Welles, L., Lopez-Vazquez, C.M., Abbas, B., Van Loosdrecht, M.C.M., Brdjanovic, D., 2019. Effect of lactate on the microbial community and process performance of an EBPR system. Front. Microbiol. 10, 1–11. https://doi.org/10.3389/fmicb.2019.00125

Shilton, A.N., Powell, N., Guieysse, B., 2012. Plant based phosphorus recovery from wastewater via algae and macrophytes. Curr. Opin. Biotechnol. 23, 884–889. https://doi.org/10.1016/j.copbio.2012.07.002

Singh, S.P., Singh, P., 2014. Effect of CO2 concentration on algal growth: A review. Renew. Sustain. Energy Rev. 38, 172–179. https://doi.org/10.1016/j.rser.2014.05.043

Su, Y., Mennerich, A., Urban, B., 2011. Municipal wastewater treatment and biomass accumulation with a wastewater-born and settleable algal-bacterial culture. Water Res. 45, 3351–3358. https://doi.org/10.1016/j.watres.2011.03.046

Toledo-Cervantes, A., Posadas, E., Bertol, I., Turiel, S., Alcoceba, A., Muñoz, R., 2019. Assessing the influence of the hydraulic retention time and carbon/nitrogen ratio on urban wastewater treatment in a new anoxic-aerobic algal-bacterial photobioreactor configuration. Algal Res. 44, 101672. https://doi.org/10.1016/j.algal.2019.101672

Torres-Franco, A., Passos, F., Figueredo, C., Mota, C., Muñoz, R., 2020. Current advances in microalgae-based treatment of high-strength wastewaters: challenges and opportunities to enhance wastewater treatment performance. Rev. Environ. Sci. Biotechnol. 8. https://doi.org/10.1007/s11157-020-09556-8

Torres-Franco, A.F., Zuluaga, M., Hernández-Roldán, D., Leroy-Freitas, D., Sepúlveda-Muñoz, C.A., Blanco, S., Mota, C.R., Muñoz, R., 2021. Assessment of the performance of an anoxic-aerobic microalgal-bacterial system treating digestate. Chemosphere 270. https://doi.org/10.1016/j.chemosphere.2020.129437

Valverde-Pérez, B., Wágner, D.S., Lóránt, B., Gülay, A., Smets, B.F., Plósz, B.G., 2016. Short-sludge age EBPR process – Microbial and biochemical process characterisation during reactor start-up and operation. Water Res. 104, 320–329. https://doi.org/10.1016/j.watres.2016.08.026

Valverde, B., 2015. Wastewater resource recovery via the Enhanced Biological Phosphorus Removal and Recovery (EBP2R) process coupled with green microalgae cultivation.

Wágner, D.S., Cazzaniga, C., Steidl, M., Dechesne, A., Valverde-Pérez, B., Plósz, B.G., 2021. Optimal influent N-to-P ratio for stable microalgal cultivation in water treatment and nutrient recovery. Chemosphere 262. https://doi.org/10.1016/j.chemosphere.2020.127939

Wang, M., Keeley, R., Zalivina, N., Halfhide, T., Scott, K., Zhang, Q., van der Steen, P., Ergas, S.J., 2018. Advances in algal-prokaryotic wastewater treatment: A review of nitrogen transformations, reactor configurations and molecular tools. J. Environ. Manage. 217, 845–857. https://doi.org/10.1016/j.jenvman.2018.04.021

Wang, Y., Peng, Y., Stephenson, T., 2009. Effect of influent nutrient ratios and hydraulic retention time (HRT) on simultaneous phosphorus and nitrogen removal in a two-sludge sequencing batch reactor process. Bioresour. Technol. 100, 3506–3512.

https://doi.org/10.1016/j.biortech.2009.02.026

Young, P., Taylor, M., Fallowfield, H.J., 2017. Mini-review: high rate algal ponds, flexible systems for sustainable wastewater treatment. World J. Microbiol. Biotechnol. 33, 0. https://doi.org/10.1007/s11274-017-2282-x

Zhang, B., Lens, P.N.L., Shi, W., Zhang, R., Zhang, Z., Guo, Y., Bao, X., Cui, F., 2018. Enhancement of aerobic granulation and nutrient removal by an algal–bacterial consortium in a lab-scale photobioreactor. Chem. Eng. J. 334, 2373–2382. https://doi.org/10.1016/j.cej.2017.11.151

Zhang, H., Gong, W., Bai, L., Chen, R., Zeng, W., Yan, Z., Li, G., Liang, H., 2020a. Aeration-induced CO2 stripping, instead of high dissolved oxygen, have a negative impact on algae–bacteria symbiosis (ABS) system stability and wastewater treatment efficiency. Chem. Eng. J. 382, 122957. https://doi.org/10.1016/j.cej.2019.122957

Zhang, H., Gong, W., Jia, B., Zeng, W., Li, G., Liang, H., 2020b. Nighttime aeration mode enhanced the microalgae-bacteria symbiosis (ABS) system stability and pollutants removal efficiencies. Sci. Total Environ. 743, 140607. https://doi.org/10.1016/j.scitotenv.2020.140607

8. CONCLUSIONS AND FUTURE WORK

8.1. Conclusions

The discharge of effluents with high concentration of P and N contributes do the increase of pollution and decrease water quality, unbalancing the ecosystems. Biological wastewater treatment is highly oxygen dependent to allow efficient nutrient removal, increasing the operational costs and the ecological footprint of wastewater treatment, since the energy used is normally derived from fossil fuel sources.

In this work a novel microalgae-bacterial system, cable of removing high amounts of nutrients at low HRT (16h) and COD: P ratio (200:60), with no need of mechanical aeration nor additional organic carbon supplementation, was developed. First, a phototrophic EBPR process was developed by subjecting an *Accumulibacter* enriched sludge to dark – light cycles. It was concluded that a microalgae-bacterial consortium with high capacity of phosphate removal (up to 64 mg/L) could be selected in sequential dark (anaerobic) – light (aerobic) cycles, only using the oxygen photosynthetically produced.

Secondly, the impact of the seed sludge was assessed by using activated sludge as inoculum to select a photo-EBPR system. The obtained results indicated that a higher enrichment of PAO microorganisms in the seed sludge yielded a faster Photo-EBPR selection phase: 29 days when WWTP sludge was as compared to 14 days when the seed sludge was already enriched in PAOs. This strategy allows to facilitate the implementation of photo-EBPR systems in WWTPs that currently do not perform EBPR. Due to the low VSS/TSS ratio and high intracellular poly-P content, obtained in both enrichment strategies, P accumulation by the biomass as poly-P was the main mechanism of P removal, however, the role of microalgae on direct P uptake was also significant, in addition to providing oxygenation to PAO bacteria. The results of these two studies showed for the first time that up to 64 mg P/L could be removed without the need of external aeration in photo-EBPR systems at low COD:P, which opens the possibility towards a reduction in the costs of wastewater treatment that contain high concentrations of P and low organic carbon availability.

Furthermore, to achieve an efficient nutrient removal process, nitrogen removal must be coupled with phosphorus removal. Therefore, in the third study, it was possible to achieve simultaneous N and P removal with no need of mechanical aeration by a microalgal-bacterial

consortium operated in dark (anaerobic)–light (aerobic)–dark (anoxic) cycles. Approximately 30% of the nitrogen removal occurred by nitrification/denitrification, while around 70% of the nitrogen was assimilated into the biomass. During light phase, ammonia assimilation was accomplished by microalgae (and other microorganisms), while nitrification was performed by ammonia and nitrite oxidizing bacteria (AOBS and NOBS). Denitrification was likely performed by denitrifying PAOs during dark anoxic phase. Similarly, to what was observed in the photo-EBPR system, the main mechanism of P removal in the photo-BNR process was also Poly-P accumulation in the biomass. The photo-BNR process can potentially reduce the costs of wastewater treatment, especially for nutrient removal processes, not only by reducing the aeration but also by eliminating the extra COD addition that is often needed for heterotrophic denitrification.

A fourth study focused on the online control of the Photo-BNR system, where models were evaluated by full cross-validation. Results indicated that Raman spectrometry, allied with PLS, is a very promising tool for monitoring the concentration of TOC, VFA, CO_2, NO_3, total P, PHA, TSS and VSS.

In order to achieve a fully stable photo BNR-system, several factors must be controlled. Oxygen concentration is one of the key parameters, where its concentration inside the reactor should be high enough to allow P uptake and nitrification, but also should not be present in excessive amounts that would carry over to the subsequent anoxic phase and impede the denitrification by dPAOs. This was further assessed in a fifth study, where photosynthetic oxygen production by algae could be controlled by the culture light exposition period, rather than by the increase of the CO_2 fed to the reactor. The biomass TSS was also found to influence nutrient removal capacity, since at high cell concentration the shadow effect is higher, reducing the photosynthetic efficiency.

Overall, the use of photo-BNR systems, operated in dark(anaerobic)–light (aerobic)–dark (anoxic) cycles, could potentially be a more sustainable and cost-effective alternative when compared with conventional BNR systems. Furthermore, it could also be a more feasible technology for nutrient removal as compared with other photosynthetic systems, since good nutrient removal capacity was observed at lower HRT as compared to the typical values attained in conventional photosynthetic technologies for nutrient removal (e.g. WSPs, HRAPs).

8.2. Future Work

This study clear demonstrated the possibility of removing nutrients from wastewaters by a microalgal-bacterial consortium under dark-light conditions. Since this novel process is still in its early stages of development, several questions remain open concerning the impact of operational conditions on the mechanisms and nutrient removal capacity. Suggestions for future work are listed below:

- The Photo-BNR system should be tested to work in cycles mimicking the length of day and night periods encountered along the seasons. The cycle time should be increased

to 24 hours and the length of each phase should be adapted to the real conditions found in the field. In addition, the light intensities should also be adjusted to values that can be obtained during winter, spring, summer, and autumn. A progressive increase of the light intensity during the light period should also be tested;

- Evaluate the temperature influence on nutrient removal mechanisms and process efficiency, considering its variability in real outdoor conditions. It is known that P and N removal mechanisms, principally PAOs/GAOs selection and nitrification/denitrification processes (Dobbeleers et al., 2020), are dependent on the operating temperature and it is important to understand how seasonal temperature fluctuations will influence the photo-BNR performance;
- Oxygen concentration reached during the light phase is one of the most important parameters to control. If on one hand, high oxygen concentration guarantees good phosphorus and ammonia removal, on the other hand it could limit denitrification efficiency if anoxic conditions are not achieved. A strategy to control dissolved oxygen levels should be studied, as for example the presence of an auxiliary pump to provide oxygen to the system when light is not sufficient, or the use of a cover that could be opened and closed to control the light reaching the tank.
- Test the SRT impact on biomass concentration and on nutrient removal capacity of the photo-BNR. The biomass concentration influences the light driven reactions. Higher biomass concentration increases the shadow effect and could reduce the efficiency of photosynthesis, while low biomass concentrations could favor oxygen production by the higher availability of light. Besides that, the SRT would also influence the growth of different microorganisms with different capacities of P and N removal that could influence the mechanisms involved in the nutrient removal process.
- Measure the photo-BNR system greenhouse gas emission potential. The interaction of algae and bacteria decrease the CO_2 emissions, since algae consume CO_2 for O_2 and carbohydrate production. However, the potential of N_2O emissions of the photo-BNR was not evaluated and it would be of great interest to conclude the environmental impact of photo-BNR when compared with conventional BNR systems;
- Test the system with real wastewater and understand the impact of different carbon sources on the microbial growth and on the mechanisms involved in nutrient removal;
- Evaluate the biomass composition from recovered sludge and understand its potential use as a fertilizer by quantifying its P, N and composition of other nutrients. The nutrient release capacity of this biofertilizer when in contact with the soil should also be studied. The microbial composition needs to be evaluated in order to understand if the presence of any pathogenic microorganisms could limit the direct sludge reuse in agricultural crops, while heavy metals, organic micropollutants and coliforms also need to be assessed.

A. APPENDIX

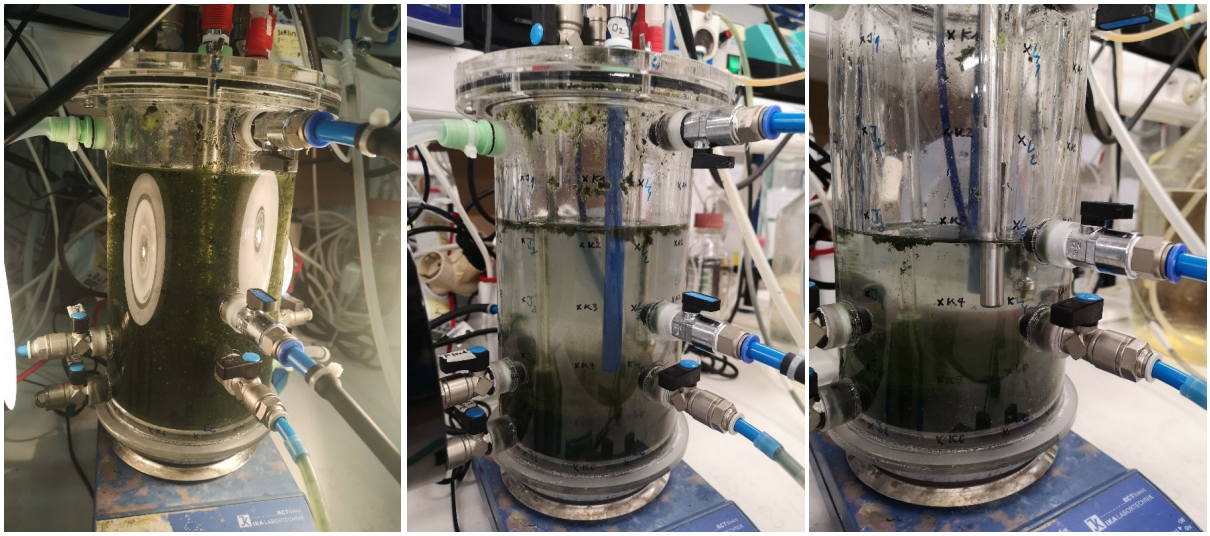

Figure A.1 - Picture of the reactor during stirring and after 15 minutes of settling.

B. APPENDIX

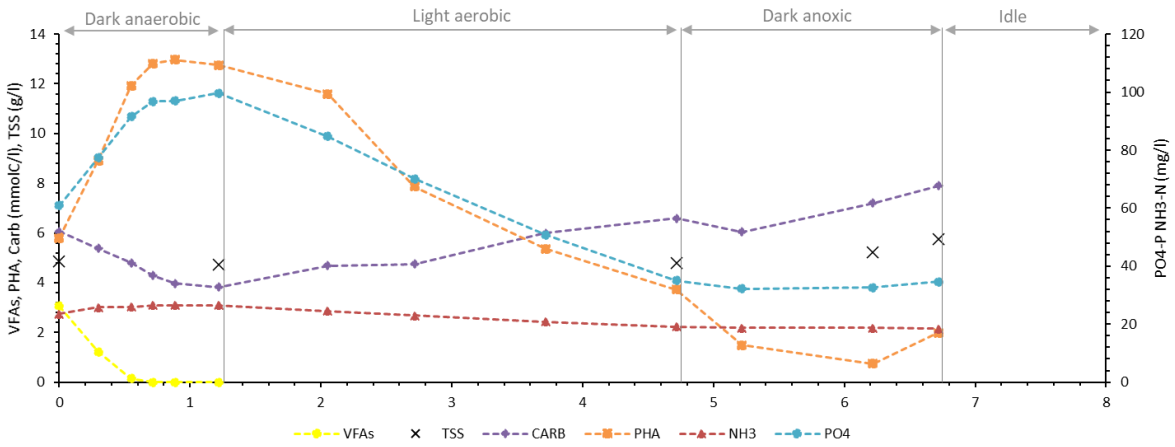

Figure B.1 - Full cycle of the photo-BNR reactor on day 85 of system operation.
Carbohydrates correspond to the sum of bacterial intracellular glycogen and microalgae starch. For details on system operation, please see **chapter 5**.

VIRGÍNIA DA CONCEIÇÃO
FERNANDES DE CARVALHO

NUTRIENT REMOVAL BY A MICROALGAL-BACTERIAL CONSORTIUM AS A MEANS TO REDUCE THE AERATION DEMAND IN WASTEWATER TREATMENT

〈2021〉